

Application of Carbon Dioxide in Reaction Work-up and Purification Procedures

Balazs Kulik

Submitted in accordance with the requirements for the degree of
Doctor of Philosophy

The University of Leeds
School of Chemistry

September, 2013

The candidate confirms that the work submitted is his own and that appropriate credit has been given where reference has been made to the work of others.

This copy has been supplied on the understanding that it is copyright material and that no quotation from the thesis may be published without proper acknowledgement.

The right of Balazs Kulik to be identified as Author of this work has been asserted by him in accordance with the Copyright, Designs and Patents Act 1988.

© 2013 The University of Leeds and Balazs Kulik

Acknowledgements

I would like to thank to all the people who contributed to this research in their ways.

Firstly, distinguished thanks go to my supervisor, Prof. Dr. Christopher M. Rayner, for his enthusiastic support and persistence.

Thanks goes to AstraZeneca for funding this research, and to Dr. Andrew Wells who represented the company.

I would also like to thank the members of the Rayner Group, current and former. A thank goes to Drs. Douglas Barnes, Guillaume Raynel, Chris Pask, Paul Rose, Fiona Kinross, Shasi Bala, Jessica Breen, David O'Brien and Gergely Jakab for their valuable advices and support. Thanks goes to Judith, Lissie, Henry, Rob, and Liam as well. Special thanks goes to Adeyinka Olushola, who contributed to this work during his final master's project.

Acknowledgement goes also to the Chemistry Staff, to Martin Huscroft in the analytical lab, Dr. Colin Kilner at crystallography, John Spence and Resham Bhogal in the electronic workshop, Mat Broadbent in the mechanical workshop and Francis Billingham at stores.

Outside the walls of Chemistry, but still on campus, thanks go to Jacqui, David and Simon, fellow members of the warden team of the Charles Morris Halls, which was my residence during most of my time in Leeds. Together with the Halls staff, Tony, Trevor and Colin, they were a really cheerful company.

Finally, thanks goes to my grandparents, parents and brother for their belief and support from the distance.

Abstract

The production of fine chemicals, including active pharmaceutical ingredients, can lead to large amounts of waste, including by-products and contaminated solvents. In many cases, it is actually the work-up of the reaction and purification, rather than the reaction itself, which is responsible. CO₂-based procedures have been developed, which can potentially alleviate some of these problems. They can be summarised as follows:

- I. The distribution of certain organic bases/acids between organic and aqueous phases could be tuned by exposing the two phases to CO₂, exploiting a *pH* change due to the acidic character of CO₂. The induced change could be reversible by physical decarboxylation.

Numerous amines and other organic bases were tested for CO₂ aided aqueous extraction. Connection between their *pK_a* and *logP* was found, and an empirical formula was proposed to predict the possibility of extraction.

Concentration dependence of the CO₂ aided aqueous extraction and rate of the chemical free neutralisation were also investigated for benzyl amines and drug molecules with amine functions.

- II. CO₂ can enhance the ability to precipitate of certain amines, exploiting a carbamate formation reaction. This would dramatically reduce the amount of acid and base required for preparation of amine salt derivatives and neutralisation.

Tendencies of several secondary amines for CO₂ adduct formation were tested, and detailed analysis of these often labile compounds was discussed. Possibility of carbamate formation based separation was demonstrated.

- III. CO₂ could be used to induce precipitation of polar compounds from their solution at elevated pressures when utilised as an antisolvent, exploiting its nonpolar character and its solubility in organic solvents.

Numerous solute-solvent systems were exposed to pressurised CO₂, either above or under its critical temperature. High pressures can often be a limitation for industrial procedures. Operation at lower temperatures allowed the application of lower pressures, because of the decreased vapour pressure of liquid CO₂. Possibility to separate solute mixtures was also demonstrated.

Table of Contents

| | |
|--|-------------|
| Acknowledgements | ii |
| Abstract | iii |
| Table of Contents | iv |
| Abbreviations | viii |
| Chapter - 1 Introduction | 1 |
| 1.1 Environmental feasibility of fine chemical and pharmaceutical syntheses..... | 2 |
| 1.2 Goals of this project..... | 3 |
| 1.3 General introduction on physical and chemical properties of carbon dioxide | 4 |
| 1.4 Thesis outline..... | 7 |
| Chapter - 2 Carbon dioxide aided aqueous extractions | 8 |
| 2.1 Introduction to liquid-liquid extractions | 9 |
| 2.2 Kinetics of extraction – mass-transfer coefficient | 10 |
| 2.3 Thermodynamics of extractions – chemical potential | 12 |
| 2.4 Extraction as an alternative to distillation | 14 |
| 2.5 Acidic extractions | 15 |
| 2.6 Acidity of CO ₂ | 17 |
| 2.7 Preliminary experiments of CO ₂ aided aqueous extractions..... | 18 |
| 2.8 Screening of amines for CO ₂ aided aqueous extractions..... | 20 |
| 2.8.1 Goal of screening experiments | 20 |
| 2.8.2 Screening procedure | 20 |
| 2.8.3 Range of tested bases | 22 |
| 2.8.4 Discussion of screening experiments | 27 |
| 2.8.5 Possibilities to predict extraction into water + CO ₂ | 30 |
| 2.8.6 Summary | 38 |
| 2.9 Detailed studies of CO ₂ aided aqueous extractions | 38 |
| 2.9.1 The goal of detailed studies of distribution | 38 |
| 2.9.2 Experimental set-up..... | 39 |
| 2.9.3 Investigation of concentration dependence of distribution | 40 |
| 2.9.4 Discussion of distribution tests before and after CO ₂ saturation | 43 |
| 2.9.5 Detailed studies of CO ₂ uptake | 45 |
| 2.9.6 Detailed studies of N ₂ gas induced neutralisation | 46 |
| 2.9.7 Investigation of the effect of the base..... | 47 |
| 2.9.8 Investigation of the effect of nominal amine concentration | 52 |
| 2.9.9 Investigation of the effect of N ₂ gas flowrate | 52 |
| 2.9.10 Investigation of <i>pH</i> during the course of decarboxylation..... | 54 |
| 2.9.11 Discussion of phenomena during N ₂ gas induced decarboxylation | 54 |
| 2.9.12 Summary of N ₂ gas induced decarboxylation | 57 |
| 2.10 Optimised preparative procedure for the purification of <i>o</i> -nitrobenzyl methylamine 2 via CO ₂ aided aqueous extraction combined with N ₂ gas induced neutralisation | 58 |
| 2.11 Summary..... | 59 |
| Chapter - 3 Carbon dioxide based approach to new crystallisation procedures | 61 |
| 3.1 Introduction to crystallisations..... | 62 |
| 3.2 Chemically induced crystallisation | 62 |
| 3.2.1 Crystallisation in industry..... | 63 |
| 3.3 Carbamates..... | 63 |
| 3.4 Amine-CO ₂ reactions | 65 |
| 3.5 Analysis of amine - CO ₂ adducts | 68 |
| 3.5.1 ¹ H- and ¹³ C-NMR spectroscopy | 68 |
| 3.5.2 FTIR Spectroscopy | 72 |
| 3.5.3 Elemental analysis..... | 73 |
| 3.5.4 Melting point..... | 73 |
| 3.5.5 X-Ray crystallography..... | 73 |
| 3.5.6 Mass Spectrometry | 74 |

| | | |
|--|--|------------|
| 3.6 | Goals | 74 |
| 3.7 | Qualitative CO ₂ adduct formation experiments | 75 |
| 3.8 | Analysis of amine - CO ₂ adducts | 77 |
| 3.8.1 | Analysis of <i>o</i> -nitrobenzyl methylamine - CO ₂ adduct 27 | 77 |
| 3.8.2 | Analysis of the benzyl methylamine - CO ₂ adduct | 79 |
| 3.8.3 | Analysis of <i>o</i> -aminobenzyl methylamine - CO ₂ adduct 28 | 79 |
| 3.8.4 | Analysis of CO ₂ adducts of propylamine derivatives | 82 |
| 3.8.5 | Analysis of the bipiperidine - CO ₂ adduct | 84 |
| 3.9 | Preparative carbamate separations | 86 |
| 3.10 | Investigation of the carbamate formation reaction by solubility tests | 87 |
| 3.11 | Stability of carbamate salts | 89 |
| 3.11.1 | Qualitative observations of carbamate stability | 89 |
| 3.11.2 | Quantitative investigation of carbamate decomposition rate by thermogravimetric measurements | 90 |
| 3.11.3 | Accuracy of thermogravimetric measurements | 93 |
| 3.12 | Conclusions of amine - CO ₂ adduct formation tests | 93 |
| 3.13 | Optimised preparative procedures | 96 |
| 3.14 | Amine regeneration experiments | 97 |
| 3.14.1 | Thermal decarboxylation | 97 |
| 3.14.2 | Concentration of alcoholic carbamate solution | 97 |
| 3.14.3 | Boiling of carbamate solution | 97 |
| 3.14.4 | Driving nitrogen gas through carbamate solution | 98 |
| 3.15 | Carbamate salt as starting material | 99 |
| 3.15.1 | Carbamate salt as feedstock for <i>o</i> -aminobenzyl methylamine 3 synthesis <i>via</i> catalytic hydrogenation | 99 |
| 3.15.2 | Application of <i>o</i> -aminobenzyl methylamine carbamate 28 starting material for the synthesis benzodiazepine 4 | 102 |
| 3.16 | Summary | 103 |
| Chapter - 4 Application of carbon dioxide as antisolvent for crystallisation procedures | | 105 |
| 4.1 | Introduction to high pressure CO ₂ based procedures | 106 |
| 4.2 | Measurement methods to acquire high pressure phase equilibria | 106 |
| 4.3 | Obtaining phase equilibria <i>via</i> analytical methods | 106 |
| 4.4 | Obtaining phase equilibria <i>via</i> synthetic methods | 107 |
| 4.5 | Phase behaviour of various binary organic solvent – carbon dioxide systems | 108 |
| 4.6 | Modelling phase equilibria | 110 |
| 4.7 | Gas expanded liquids | 111 |
| 4.7.1 | Introduction to gas expanded liquids (GXLs) | 111 |
| 4.7.2 | Measurement methods of GXLs | 112 |
| 4.7.3 | Volumetric expansion of various organic solvents under pressure of CO ₂ | 113 |
| 4.7.4 | Physical properties of gas expanded liquids | 116 |
| 4.7.5 | Solubility of solids in gas expanded liquids | 118 |
| 4.8 | Particle formation | 121 |
| 4.8.1 | Introduction to particle formation using CO ₂ antisolvent | 121 |
| 4.8.2 | Particle formation with CO ₂ antisolvent in practice | 121 |
| 4.9 | Lowering melting point of solids with CO ₂ | 122 |
| 4.10 | Use of conventional antisolvents in practice | 123 |
| 4.11 | Disadvantages of purifications using antisolvents | 124 |
| 4.12 | Ideal antisolvents and alleviating the disadvantages | 125 |
| 4.13 | Miscibility behaviour of CO ₂ and solvents | 126 |
| 4.14 | Application of pressurised carbon dioxide as an antisolvent | 128 |
| 4.15 | Goal of CO ₂ induced precipitations | 129 |
| 4.16 | Screening of solute-solvent combinations for CO ₂ induced precipitation | 129 |
| 4.16.1 | Goals of CO ₂ antisolvent screening experiments | 129 |
| 4.16.2 | Chosen solvent-solute combinations for CO ₂ induced antisolvent precipitations | 130 |
| 4.17 | Discussion of high pressure CO ₂ antisolvent induced precipitations | 131 |
| 4.17.1 | Experimental set-up | 131 |
| 4.17.2 | Investigation of CO ₂ as antisolvent for DMSO based systems | 132 |

| | | |
|--|---|------------|
| 4.17.3 | Investigation of CO ₂ as antisolvent for ethanol based systems | 134 |
| 4.17.4 | Investigation of CO ₂ as antisolvent for TMU based systems..... | 135 |
| 4.17.5 | Investigation of CO ₂ as antisolvent for DMF based systems..... | 138 |
| 4.17.6 | Investigation of CO ₂ as antisolvent for Quinine solutions | 138 |
| 4.17.7 | Investigation of the effect of temperature for CO ₂ antisolvent induced precipitations | 139 |
| 4.17.8 | Summary of the qualitative CO ₂ antisolvent induced precipitation experiments | 140 |
| 4.18 | Separation of solids in pressurised systems | 141 |
| 4.19 | Antisolvent precipitation at elevated pressures with isolation | 143 |
| 4.20 | CO ₂ antisolvent based separation | 146 |
| 4.21 | Summary of the experiments with CO ₂ antisolvent | 147 |
| Chapter - 5 Conclusions and future work | | 148 |
| 5.1 | CO ₂ aided aqueous extractions | 149 |
| 5.1.1 | Screening experiments - conclusions..... | 149 |
| 5.1.2 | Detailed investigation of distribution - conclusions..... | 150 |
| 5.1.3 | Possibilities for further research | 150 |
| 5.2 | CO ₂ based approach to new crystallisation procedures..... | 152 |
| 5.2.1 | Conclusions | 152 |
| 5.2.2 | Possibilities for further research | 152 |
| 5.3 | Application of CO ₂ as antisolvent for crystallisation procedures | 153 |
| 5.3.1 | Conclusions | 153 |
| 5.3.2 | Potential upgrade of visual phase behaviour investigations | 154 |
| 5.3.3 | Potential upgrades of the solid separation experiments | 154 |
| Chapter - 6 Experimental | | 156 |
| 6.1 | Instrumentation..... | 157 |
| 6.2 | Materials..... | 157 |
| 6.3 | Organic syntheses..... | 158 |
| 6.3.1 | <i>O</i> -Nitrobenzyl methylamine 2 | 158 |
| 6.3.2 | <i>O</i> -Nitrobenzyl <i>n</i> -propylamine 14 | 158 |
| 6.3.3 | Benzyl <i>n</i> -propylamine 32 | 159 |
| 6.3.4 | Synthesis of <i>o</i> -aminobenzyl methylamine 3 by the reduction of <i>o</i> -nitrobenzyl methylamine 2 | 159 |
| 6.3.5 | <i>O</i> -Aminobenzyl <i>n</i> -propylamine hydrochloride 24 | 160 |
| 6.3.6 | Synthesis of benzodiazepine 4 from free amine 3 starting material | 161 |
| 6.4 | UV/Vis spectroscopy and HPLC calibrations | 161 |
| 6.5 | Experiments with CO ₂ adducts | 165 |
| 6.5.1 | Qualitative carbamate formation tests of benzylamines at ambient pressure | 165 |
| 6.5.2 | Qualitative carbamate formation tests of benzylamines at elevated pressures | 167 |
| 6.5.3 | <i>O</i> -Nitrobenzyl methylamine carbamate salt 27 ; Synthesis by exposure to continuous flow of CO ₂ | 167 |
| 6.5.4 | <i>O</i> -Nitrobenzyl methylamine carbamate salt 27 ; Synthesis by stirring in CO ₂ atmosphere | 168 |
| 6.5.5 | Synthesis of <i>o</i> -aminobenzyl methylamine 3 by the reduction of <i>o</i> -nitrobenzyl methylamine carbamate salt 27 starting material..... | 169 |
| 6.5.6 | <i>O</i> -Aminobenzyl methylamine carbamate 28 | 169 |
| 6.5.7 | Bipiperidine bicarbonate 30 | 170 |
| 6.5.8 | Quantitative solubility test of <i>o</i> -nitrobenzyl methylamine 2 in MTBE + CO ₂ | 171 |
| 6.5.9 | Synthesis of benzodiazepine 4 from carbamate salt 28 starting material..... | 172 |
| 6.5.10 | Synthesis of the mixture of anilines 38 and 39 using <i>o</i> -aminobenzyl methylamine 3 starting material..... | 173 |
| 6.5.11 | Synthesis of the mixture of anilines 38 and 39 using <i>o</i> -aminobenzyl methylamine carbamate salt 28 starting material, in CO ₂ atmosphere..... | 173 |
| 6.6 | Carbamate stability tests | 173 |
| 6.6.1 | Qualitative stability experiments | 173 |
| 6.6.2 | Quantitative stability tests of <i>o</i> -nitrobenzyl methylamine carbamate salt 27 | 174 |
| 6.7 | Distribution tests of bases between organic and aqueous phases by preparative procedures - Screening | 176 |

| | | |
|---------|---|------------|
| 6.8 | Distribution tests of bases between organic and aqueous phases under ambient conditions – Detailed studies..... | 183 |
| 6.8.1 | Distribution before CO ₂ exposure..... | 183 |
| 6.8.2 | Distribution after CO ₂ exposure..... | 185 |
| 6.9 | Distribution tests of bases between aqueous and organic phases during the course of N ₂ gas induced decarboxylation | 188 |
| 6.10 | Monitoring of <i>pH</i> | 195 |
| 6.10.1 | Monitoring of <i>pH</i> during the CO ₂ saturation of the <i>o</i> -nitrobenzyl methylamine 2 + water + MTBE system | 195 |
| 6.10.2 | Monitoring of <i>pH</i> during the N ₂ gas induced decarboxylation of the CO ₂ saturated <i>o</i> -nitrobenzyl methylamine 2 + water + MTBE system | 196 |
| 6.11 | Application of CO ₂ as antisolvent at elevated pressures..... | 197 |
| 6.11.1 | Qualitative precipitation tests at room temperature or above | 197 |
| 6.11.2 | Qualitative precipitation tests below room temperature..... | 206 |
| 6.12 | Antisolvent precipitation tests at elevated pressure with solid isolation | 207 |
| 6.12.1 | Experiments above the critical temperature of CO ₂ | 207 |
| 6.12.2 | Experiments below the critical temperature of CO ₂ | 209 |
| 6.13 | Application of CO ₂ antisolvent induced precipitation for separation of solutes | 211 |
| | References | 212 |
| | Appendix - I Description of the high pressure equipment..... | A1 |
| A-1.1 | High pressure CO ₂ supply system | A2 |
| A-1.2 | High pressure view cells | A5 |
| A-1.2.1 | General design of high pressure cells | A5 |
| A-1.2.2 | High pressure cell, modified for isolation of solid under pressure | A5 |
| A-1.3 | Qualitative determination of volumetric expansion in view cell..... | A8 |
| | Appendix - II X-ray crystallographic data tables and structure refinement | A9 |

Abbreviations

| | |
|-----------|----------------------------------|
| " | inch |
| ∞ | infinite; bulk |
| A | absorption; area |
| API | active pharmaceutical ingredient |
| aq. | aqueous |
| b.p. | boiling point |
| BPR | back pressure regulator |
| <i>Bu</i> | butyl |
| CP | cross peak |
| D | dipole |
| <i>d</i> | doublet; differential |
| D | diffusion coefficient |
| DAD | diode array detector |
| DAS | dipolar aprotic solvent |
| DCM | dichloromethane |
| diff. | diffusion |
| DMAD | dimethyl acetylenedicarboxylate |
| DMF | dimethylformamide |
| DMSO | dimethyl sulfoxide |
| <i>e</i> | Euler's number |
| EoS | equation of state |
| Eq. | equation |
| equiv. | equivalent |
| <i>Et</i> | ethyl |
| <i>f</i> | fugacity |
| FT | Fourier transformation |
| g | gas |

| | |
|-----------------------|---|
| G | Gibbs free energy |
| GXL | gas expanded liquids |
| <i>H</i> | Henry's constant; enthalpy |
| HMBC | heteronuclear multiple-bond correlation |
| HPLC | high pressure liquid chromatography |
| <i>i</i> | interphase |
| i.d. | inside diameter |
| IR | infrared |
| <i>J</i> | coupling constant |
| <i>K</i> | equilibrium coefficient; modified Nernst distribution coefficient |
| <i>logP</i> | logarithm (to base 10) of P distribution coefficient |
| <i>l_q</i> | liquid |
| <i>l_{qh}</i> | heavy liquid |
| <i>l_{ql}</i> | light liquid |
| <i>m</i> | mass; multiplet |
| <i>m</i> | <i>meta</i> |
| m.p. | melting point |
| <i>Me</i> | methyl |
| MTBE | methyl <i>tert</i> -butyl ether |
| <i>n</i> | molar amount |
| <i>ṅ</i> | flow; molar amount |
| <i>n</i> - | normal |
| n.a. | not acquired |
| n.t. | not tested |
| NMP | <i>N</i> -methyl pyrrolidone |
| NMR | nuclear magnetic resonance |
| NPT | national pipe thread |
| <i>o</i> | <i>ortho</i> |
| o.d. | outside diameter |

| | |
|------------------------------|---|
| org. | organic |
| <i>p</i> | <i>para</i> |
| P | pressure |
| PABA | <i>para</i> -amino benzoic acid |
| pK_a | negative logarithm (to base 10) of K_a acid distribution constant |
| ppm | parts per million |
| <i>Pr</i> | propyl |
| precip. | precipitation |
| q | quartet |
| r.t. | room temperature |
| SBW | spectral bandwidth |
| sc | supercritical |
| SCF | supercritical fluid |
| sex | sextet |
| S_NX | nucleophilic substitution |
| sol | solid |
| t | time; triplet |
| T | temperature |
| <i>t</i> -; (<i>tert</i> -) | tertiary |
| TGA | thermogravimetric analysis |
| TMU | tetramethyl urea |
| UV | ultraviolet |
| V; vol. | volume |
| \dot{V} | flow; volume |
| Vis | visible |
| wt% | weight percentage |
| x | molar fraction, in liquid phase |
| y | molar fraction, in gas/supercritical phase |
| Z | compressibility |

| | |
|-------------------------|--|
| β | mass transport coefficient |
| δ | chemical shift |
| δ_+ ; δ_- | positive/negative electrostatic polarisation |
| η | dynamic viscosity |
| λ | wavelength |
| μ | chemical potential |
| ν | wavenumber |
| π^* | polarity parameter |
| ρ | density |
| τ | time constant of exponential decay |
| ϕ | fugacity coefficient; diameter |

Chapter - 1

Introduction

1.1 Environmental feasibility of fine chemical and pharmaceutical syntheses

At the end of the last century, the public became more and more environmentally conscious. This subsequently pushed the general development into a more environmentally feasible direction, and the concept of green chemistry was born. Green chemistry is a set of principles that are required from industrial procedures with an intention to reduce their environmental impact. The 12 principles, summarised by Anastas, promote process designs that maximise the product output using the same amount of raw material. The energy consumption and waste production should be kept minimal, and the preference of safe materials is promoted.^[1]

The E-factor, which is the ratio of produced waste and product, generally depends on the value of the product.^[2] Pharmaceutical industry, for instance, could afford to produce more waste, relative to petrochemical industry (Table 1.1).

Table 1.1. Scale, product value and E-factor of chemical industries.

| Industry | Scale t/year | Value of product £/kg | E-factor Kg waste/Kg product |
|----------------|-----------------------------------|--------------------------|------------------------------------|
| Petrochemical | 10 ⁶ - 10 ⁸ | lowest | ~ 0.1 |
| Bulk chemical | 10 ⁴ - 10 ⁶ | low | < 1 - 5 |
| Fine chemical | 10 ² - 10 ⁴ | intermediate | 5 - 50 |
| Pharmaceutical | 10 - 10 ³ | high | 25 - 100 |

Synthesis of chemicals such as pharmaceuticals or pesticides are typically carried out in solution.^[3] On one hand presence of solvent has numerous benefits, such as control over reaction rate,^[4] or heat sink for the reaction enthalpy. These together allow a controlled course of the reaction, which could otherwise be unrealisable. Application of a solvent can also bring otherwise immiscible reactants together into one mutual fluid phase. The solvent may have a preference for the reaction pathway, for instance, preference of S_N1 or S_N2.^[5] On the other hand, application of solvents inevitably lead to a production of waste solvents, decreasing the greenness of the procedure. Other factors, such as solvent volatility and possible escape to the environment, fire hazard because of flammability, risk of solvent residues in product are further complications. Efforts were made to alleviate the problems of solvents, such as solvent free synthesis,^[6] and alternative reaction media such as supercritical solvents^[7] and ionic liquids were also investigated.^[8] The pharmaceutical industry was rather conservative for these new approaches, and the vast majority of their products are synthesised using conventional solvents, however, steps towards sustainable solvents were made.^[9] Recycling of the waste solvents could lessen the waste production, but the necessary separation

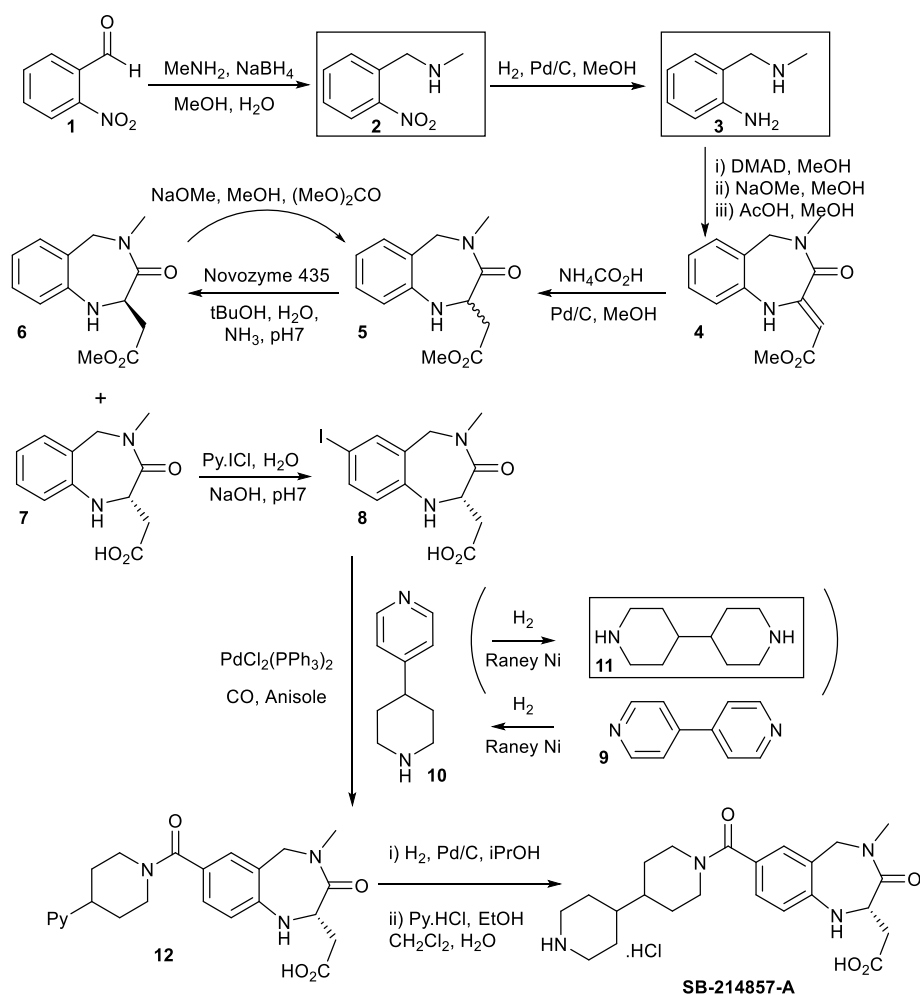
procedures could be energy intensive, especially for the mixture of solvents with a high affinity to each other combined with high boiling points.

Certain, otherwise fairly efficient chemical reactions, such as the Mitsunobu^[10] or Wittig^[11] reaction, cannot be considered green, because of the significant by-product formation, ruining the E-factor.^[2] In these cases the solution could be an alternative reaction for the alkylation or alkene formation. In other cases, the E-factor is affected badly because of a neutralisation procedure forming a salt by product. This is very common in aqueous extractions and crystallisations in salt form.^[3]

1.2 Goals of this project

The goal was to alleviate some of these problems summarised in the former section, concentrating on the problem of waste solvents and salt by-product formation after neutralisation. Methods were pursued that do not need extreme investment into either equipment or chemicals, and could be retrofitted to already existing procedures. Therefore, proposed procedures may find application in the pharmaceutical industry without a reluctance that was witnessed for solvent free procedures, supercritical media or ionic liquids.

The developed novel procedures are based on carbon dioxide, using it either as a reagent or as an inert solvent. The chosen synthesis to demonstrate the potential of the developed procedures was primarily, but not exclusively, the formation of AstraZeneca's drug candidate, SB-214857-A. The synthetic route seemed ideal for investigation as it contained widely used, common synthetic steps like homo- and heterogeneous catalysis for hydrogenation and cross-coupling, reductive amination, cyclization and enzymatic resolution. The intermediate products are also varied in terms of chemical character, with different molecule sizes and various functional groups like halogens, aldehydes, amides, amines, and anilines (Scheme 1.1). *O*-Nitrobenzyl methylamine **2**, *o*-aminobenzyl methylamine **3** and bipyridine derivatives **10** and **11** were particularly interesting, because they were suspected to react with CO₂.

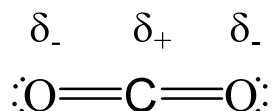


Scheme 1.1. Proposed synthesis of drug candidate SB-214857-A.^[12-13]

1.3 General introduction on physical and chemical properties of carbon dioxide

Carbon dioxide is a colourless gas with a weak acidic smell in high concentrations. It has low price and low toxicity, however it is an asphyxiant. It occurs in nature, being the fourth most abundant gas in air after nitrogen, oxygen and argon. Its concentration in air at the time of this work was 398 ppm, although this is slowly increasing.^[14] It also occurs in natural gas to a varying level and is dissolved in some mineral waters.^[15] Carbon dioxide plays an important role in the natural carbon cycle, being constantly emitted by living organisms by breathing and absorbed by plants through photosynthesis. Anthropogenic CO₂ emissions are significant at about 48 Gt per annum,^[16] and are causing increasing CO₂ levels in the atmosphere.^[17] The connection between increasing CO₂ levels and global climate change has been recognised, and governments are trying to reduce their countries emissions.^[18]

The carbon atom of the CO₂ molecule is between two highly electronegative oxygen atoms. The molecule is linear and highly symmetric, therefore apolar, however, there is a significant quadrupole moment because of the high electron negativity difference (Scheme 1.2)^[19].



Scheme 1.2. The carbon dioxide molecule.

The quadrupole moment can allow a molecule to be polarised by external electrostatic fields. The importance of the quadrupole for solvation can be demonstrated well by comparing benzene and cyclohexane. Both molecules are completely apolar because of their symmetry. Benzene, however, possesses a quadrupole moment but cyclohexane does not. Because of this benzene can be polarised easier, and consequently it is a significantly better solvent of polar molecules compared to cyclohexane.

CO₂ is a low energy molecule, with the carbon atom in its most oxidized state, therefore not expected to be very reactive. Indeed, CO₂ will not react with oxidizing agents, and can be used in fire extinguishers. However, CO₂ is not always inert, the carbon atom is electrophilic and can be attacked by nucleophiles.^[20] Sometimes this can be exploited: For instance, CO₂ may form carbamates with amines.^[21] Carbon dioxide is soluble in water,^[22] and its solution is acidic.^[23] It combines with water to form carbonic acid.

From the process chemist's point of view, CO₂ is an environmentally benign compound. Its favourable properties have drawn the interest of researchers, and numerous applications of pressurised carbon dioxide as a solvent are now well established.^[24] CO₂, which is a gas at atmospheric pressure and room temperature, liquefies around 5.5 MPa if compressed. Above its critical pressure and temperature (7.4 MPa and 304 K) it is a supercritical fluid (Figure 1.1). The properties of supercritical carbon dioxide, scCO₂, can be varied over a wide range by changing pressure and temperature, allowing tuning of its solvent power. This makes it versatile compared to conventional solvents.^[25] Moreover, in the supercritical state the density of CO₂ is of a similar magnitude to conventional liquids, but also, the diffusivity coefficient and the viscosity are closer to gases. This is very important as it greatly enhances mass transport. An equilibrium concentration of phases can be reached in a considerably shorter period of time with scCO₂ solvent compared to conventional solvents, potentially accelerating the procedure.^[25]

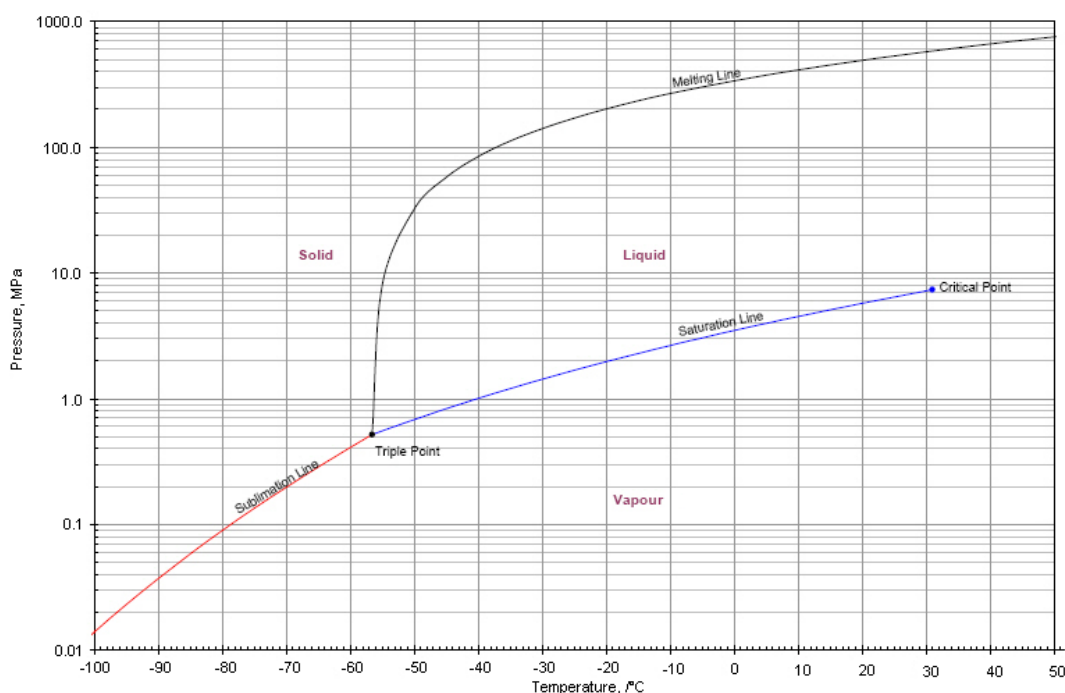


Figure 1.1. Pressure-temperature phase diagram of CO₂.^[26]

Pressurised CO₂ has found application as a solvent in extractions. The earlier mentioned “tunable” solvent power allowed novel separation processes to be developed, such as tea or coffee decaffeination.^[27] CO₂ can be used as an eluent in chromatography.^[28] In polymer processing CO₂ could replace freons in the production of foamy materials, and could be used as a plasticiser. Similarly, CO₂ is useful in the formation of ceramic aerogels,^[29] and for atomization processes in nanotechnology.^[30] As green chemistry has become more popular, researchers have studied reactions using CO₂ as a reaction medium. Mass transport limited reactions, such as heterogeneous catalytic reactions, particularly benefited from the increased diffusivity and decreased viscosity.^[31] The generally poor solvent power of scCO₂ for polar molecules later moved the attention of researchers onto a combination of traditional solvents and carbon dioxide, often referred as gas expanded liquids, GXs.^[32] The synthetic potential of the combination of ionic liquids and carbon dioxide was also investigated.^[33]

Working with supercritical carbon dioxide often involves high pressure operation. This greatly increases the investment costs because high pressure equipment has to be used for the industrial implementation, and there are also significant safety issues. Application of expanded liquids can help to alleviate these problems until a certain extend.^[32]

A more detailed review of the relevant areas will be discussed before each chapter.

1.4 Thesis outline

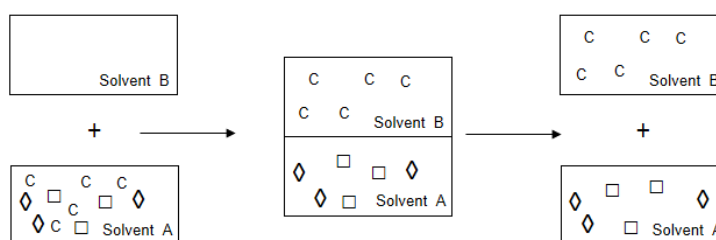
The second chapter is dedicated to the results and discussion of the CO₂ aided aqueous extraction experiments. The third and fourth chapters summarise the results and discussion of crystallisation experiments, using CO₂ either as a reagent or as an inert antisolvent. These are followed by the chapter summarising the results, and outlining possibilities for future research. The chapter of experimental follows, and literature references. The appendices include details of the used high pressure experimental setup and summarise x-ray crystallography data.

Chapter - 2

Carbon dioxide aided aqueous extractions

2.1 Introduction to liquid-liquid extractions

Solvent extractions, occasionally referred as liquid-liquid extractions or partitioning, are common separation procedures in organic laboratories and industry.^[3] A mother liquor is a solution of compound *C* in solvent *A*. The goal of the procedure is to selectively separate compound *C* from the mother liquor with a preferably completely immiscible or at least only partly miscible solvent *B*. The mother liquor may also contain various contaminants dissolved in solvent *A* (Scheme 2.1).



Scheme 2.1. Separation of valuable compound *C* from solvent *A* and contaminants (\diamond, \square) *via* extraction with solvent *B*.

Extractions can be represented on triangle diagrams (Figure 2.1).^[34] The composition of the mother liquor, what is a solution of compound *C* in solvent *A*, is represented by point *F* on the figure. The gross composition of the mixture after the addition of solvent *B* is represented by point *M*. The ratio of mother liquor *F* and solvent *B* determines the location of point *M* on the *FB* line. Point *M* falls on the two phase region of the triangle diagram, therefore the mixture will split into two phases. The composition of these phases is determined by the tie-line at which point *M* falls. After phase split, the composition of the raffinate, that is the phase rich in solvent *A*, is represented by *R* and the composition of the extract is represented by *E*.

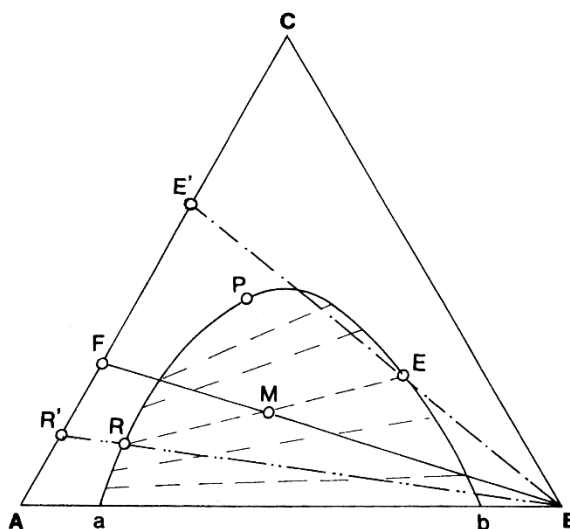


Figure 2.1. Triangle diagram of a solvent extraction. Two phase region is between *a R P E* and *b* points. The dashed tie-lines indicate the composition of co-existing phases in equilibrium.^[34]

2.2 Kinetics of extraction – mass-transfer coefficient

The kinetics of extraction give information about the time needed to reach equilibrium. The migration of solute within a phase during the course of extraction is diffusion, if agitation is not taking place. The rate of this migration could be featured by the flux, that is to amount of compound (*mol*) migrating through an area (m^2) within a period of time (*s*). The flux of a compound into the *x* direction in an ideal solution is given by Fick's law (Eq.1).^[35]

$$j_x = -D \frac{dc}{dx}$$

j_x: flux of compound into the *x* direction
D: diffusion coefficient
 $\frac{dc}{dx}$: concentration gradient, *x* direction

Eq.1

The driving force of the extraction is the dc/dx concentration gradient.

In agitated systems, where a convective flow within the phase is taking place, the transport phenomenon is more complex. A single phase could be divided into a *bulk phase*, in which agitation is effective, and to a *phase boundary layer* or film in the vicinity of the *interphase* (Figure 2.2). The composition of the bulk is quickly homogenised by macroscopic agitation. The amount of solute will be always the same in any dV volume of the bulk in one fraction of time. A fraction of time later the measured amount of solute in a same dV volume may be different compared to the amount that had been measured earlier because of a composition change caused by component transport, but will still be the same in any dV volume of the bulk in the moment of time of sampling. In contrast, the composition in the phase boundary layer or film will not be homogeneous. There is a concentration gradient providing a driving force for the solute to diffuse from the bulk phase to the interphase. Transport of solute in the bulk phase *via* convection is significantly faster compared to its transport in the boundary layer *via* diffusion. The stages of the extraction of solute *C* from solvent *A* into solvent *B* could therefore be divided into three major parts. Firstly, solute *C* migrates from the bulk of solvent *A* to the interphase of solvents *A* and *B*. This migration is mostly by convection in the bulk and by diffusion in the phase boundary layer. Secondly, solute *C* passes the interphase of solvents *A* and *B*. Thirdly, solute *C* migrates within solvent *B* from the interphase to the bulk. Similarly to the migration in solvent *A*, the migration is dominantly convection in the bulk, and diffusion in the boundary layer.^[34]

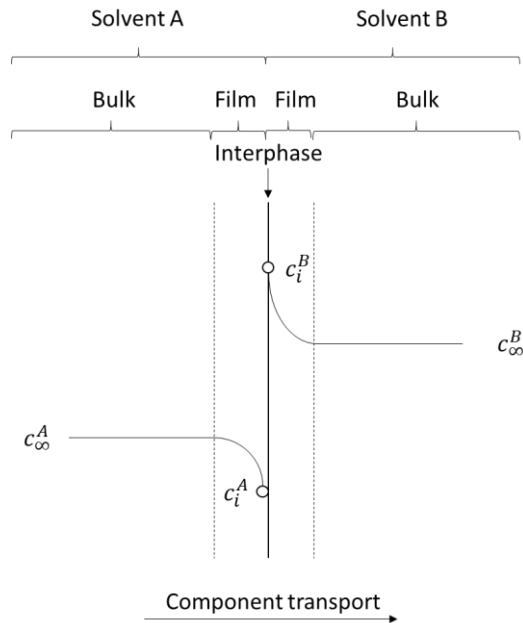


Figure 2.2. Concentration profile of a liquid-liquid extraction before reaching equilibrium. The component migrates from the bulk of solvent A through a phase boundary film in solvent A, the interphase and the phase boundary film in solvent B into the bulk of solvent B.^[34]

The flux of a compound into the x direction (j_x), within one phase, from the bulk to the interphase in an ideal solution is given by (Eq.2), which is the modification of Fick's law (Eq.1).

$$j_x = -(D_i + D_b) \frac{dc}{dx} \quad \begin{array}{l} D_i: \text{effective diff. coefficient in the interphase film} \\ D_b: \text{effective diff. coefficient in the bulk phase} \end{array} \quad \text{Eq.2}$$

The above differential equation (Eq.2) could be integrated between the interphase (i) and the bulk phase (∞) (Eq.3).

$$j_x = \frac{D_i + D_b}{Z} (c_i - c_\infty) \quad \begin{array}{l} Z: \text{distance between the interphase and bulk} \\ c_i: \text{concentration at the interphase} \\ c_\infty: \text{concentration in the bulk} \end{array} \quad \text{Eq.3}$$

The first part of the product in (Eq.3) is β mass-transfer coefficient (Eq.4).^[34]

$$\beta = \frac{D_i + D_b}{Z} = \frac{D_{eff}}{Z} \quad \begin{array}{l} \beta: \text{mass transfer coefficient} \\ D_{eff}: \text{overall effective diffusion coefficient} \end{array} \quad \text{Eq.4}$$

There is a number of difficulties using Fick type equations to calculate mass transport between two liquid layers. Both the effective diffusivity coefficient (D_{eff}) and length to the interface (Z) depend on the flow, *i.e.* the intensity of stirring. Also, concentration on the interface (c_i) cannot be determined in either of the phases. The actual material transport (\dot{n}), that is the amount of material being transported from one phase to the other within a period of time, is calculated according to the equation below (Eq.5).

$$\dot{n}_x = A j_x \quad \begin{array}{l} \dot{n}_x: \text{mass flow} \\ A: \text{surface area} \end{array} \quad \text{Eq.5}$$

The surface area (A) is needed for the calculations, but it is problematic to determine it in a stirred system.

The above equations qualitatively imply how a transport phenomenon could be enhanced. Considering a simple extraction in a separation funnel. Higher surface area enhances the rate of mass transport (Eq.5), which could be achieved by more intense stirring and forming an emulsion, with a significantly larger surface area. More intense stirring also enhances the effective diffusion coefficient (D_{eff}) and reduces the thickness of the phase boundary layer (Z). Both of these will boost β (Eq.4). The mass transport is higher between solvents with higher diffusion coefficients.^[34]

2.3 Thermodynamics of extractions – chemical potential

The composition of co-existing phases in equilibrium is controlled by chemical potentials. Compound C is in equilibrium in two completely immiscible solvents A and B if its chemical potentials are the same in both solvents (Eq.6).

$$\mu_C^A = \mu_C^B \quad \mu_C^A, \mu_C^B: \text{chemical potential of compound } C \text{ in phases } A \text{ and } B \quad \text{Eq.6}$$

If the chemical potential of compound C is higher in the phase of solvent A than in solvent B , compound C will migrate from solvent A to solvent B (Eq.7).

$$\mu_C^A > \mu_C^B \quad \text{Eq.7}$$

The chemical potential of compound C is the partial molar Gibbs energy, provided the pressure, temperature and composition are constant (Eq.8).^[36]

$$\mu_C = \left(\frac{\partial G}{\partial n_C} \right)_{P,T,n_i} \quad G: \text{Gibbs free energy} \quad \text{Eq.8}$$

The Gibbs energy, or free energy, is the amount of energy that can be extracted from a closed system in the form of work, other than work of expansion.^[36]

Chemical potential and Gibbs energy are rather abstract physicochemical values and it is demanding to measure them. Also, chemical potential does not have an absolute value, only the difference between two potentials could be construed. This is similar to other potential type values. The electric potential in a cable is compared to the potential of the ground. The potential energy of a floating object is compared against the ground level. Prausnitz suggested workarounds to overcome the difficulties of abstractness and lack of absolute value of chemical potential.^[37] Fugacity, for instance, is related to the chemical potential. The absolute chemical potential of compound C could be calculated from its fugacity (Eq.9), provided its chemical potential and fugacity are known under the same conditions. For instance, fugacity of compound C is f_C^0 , and its chemical potential is μ_C^0 under standard conditions.

$$\mu_C = \mu_C^0 + RT \ln \frac{f_C}{f_C^0} \quad \begin{array}{l} \mu_C^0: \text{standard chemical potential} \\ f_C^0: \text{fugacity under standard conditions} \end{array} \quad \text{Eq.9}$$

Fugacity is much less abstract compared to chemical potential. Fugacity is the partial pressure in a mixture of ideal gases. In many cases, equilibrium could be assumed in a system if fugacities are equal in the phases. Prausnitz summarised various methods to calculate fugacities of compounds or mixture of compounds in condensed phases, and practices to handle non-ideality. These practises are based on Equation of State, activity coefficients or various empirical models.^[37]

In a real, but dilute solution of compound C in solvent A, fugacity of compound C (f_C^A) could be calculated from its Henry constant in solvent A ($H_{C,A}$) by multiplying it with the mole fraction of C in solvent A (x_C^A) (Eq.10).

$$f_C^A = H_{C,A} x_C^A \quad \begin{array}{l} f_C^A: \text{fugacity of compound C in solvent A} \\ H_{C,A}: \text{Henry constant} \\ x_C^A: \text{molar fraction} \end{array} \quad \text{Eq.10}$$

The fugacity in solvent B can be calculated similarly (Eq.11).

$$f_C^B = H_{C,B} x_C^B \quad \text{Eq.11}$$

There is equilibrium if fugacities in both phases (f_C^A and f_C^B) are equal. The right hand side of (Eq.10) and (Eq.11) must be also equal in equilibrium (Eq.12).

$$H_{C,A} x_C^A = H_{C,B} x_C^B \quad \text{Eq.12}$$

Consequently, a partitioning coefficient could be obtained (Eq.13). This relation (Eq.13) is known as the Nernst equation.^[38]

$$K' = \frac{x_C^A}{x_C^B} = \frac{H_{C,B}}{H_{C,A}} \quad K': \text{Nernst distribution coefficient} \quad \text{Eq.13}$$

In dilute solutions x mole fractions are almost proportional to concentrations (c), therefore mole fractions could be replaced (Eq.14).

$$K = \frac{c_C^A}{c_C^B} \quad K: \text{distribution coefficient} \quad \text{Eq.14}$$

In solutions that follow Henry's law, K' or K distribution coefficients are independent of the overall composition: the ratio of solute mole fractions or ratio of concentrations in a system with two condensed phases will be independent of the overall amount of the solute, as long as the pressure and temperature are the same.

In some cases the non-ideal behaviour of K , that is K' 's concentration dependence, may give implications about phenomena in the system. Aveyard and Mitchell investigated the distribution of alkyl acids between water and n -dodecane.^[39] Utilising the concentration dependency of the distribution coefficient, the authors could prove that

carboxylic acid molecules were predominantly dimers in the organic phase, and predominantly monomers in the aqueous phase, possibly because of solvation.

The distribution coefficient can be manipulated through the manipulation of chemical potential. Chemical potential of weak organic acids and bases in aqueous phases can be manipulated by changing pH . Consider an example of an aqueous solution of weak base B in equilibrium with its organic solution (Figure 2.3). If the pH is lowered by addition of a strong acid, effectively increasing the concentration of hydronium ions (H_3O^+), the acid/base equilibrium is pushed to the left side, into the direction of protonated base (B^+H). Effectively, the concentration of free base B will drop, therefore its fugacity will also drop (Eq.10), as will its chemical potential (Eq.9). Consequently, migration of B from the organic phase to aqueous phase will occur because the chemical potential of free base B decreased in the aqueous phase, compared to the organic phase.

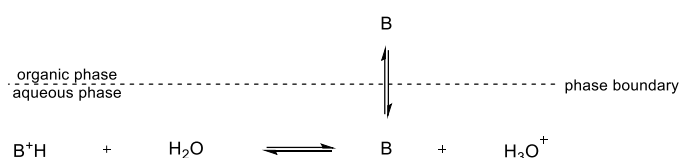


Figure 2.3. Equilibrium relationship in a two phase system containing organic solvent, water, a weak base (B) and a strong acid.^[36]

This manipulation, when an acid or base is extracted into water in its salt form, is a very common separation procedure in chemical laboratories and industry.^[3]

2.4 Extraction as an alternative to distillation

Extraction can remove the desired compound from a solution in solvent A , but it creates a solution of the desired compound in solvent B instead. However, the contaminants may remain in solvent A . Unless the solution of the purified compound in solvent B is used directly in the following step of the technology, it has to be concentrated *via* distillation, a thermal procedure. In such a case one could consider using distillation straight away, using the initial solution in solvent A as feed. However, distillation may not be possible in some cases, and alternative separation must to be used, such as extraction. Assuming solvent A has a high boiling point and the desired compound is heat sensitive, distillation may be problematic because of high temperatures. If either solvent A or any of the non-desired compounds form an azeotrope with the desired compound, distillation cannot be a considered option. Simple energy efficiency considerations may also lead to a preference of extraction over distillation. Consider a fermentation or enzymatic transformation, which are very often carried out in dilute aqueous solutions. If the desired compound was to be isolated by distillation, an enormous amount of water may be needed to be evaporated at high energy costs.

Water has a relatively high boiling point and high enthalpy of evaporation compared to most organic solvents. However, if the broth is extracted into a suitable organic solvent first, such as petrol, ether or ethyl acetate, the obtained organic solution could not only be concentrated at lower energy costs because it is a smaller amount, but also because these solvents have lower boiling point and enthalpy of evaporation compared to water (Table 2.1).

Table 2.1. Evaporation enthalpies of solvents at their boiling points under atmospheric pressure.^[40]

| Entry | Solvent | Boiling point / °C | Enthalpy of evaporation KJ/l |
|-------|---------------|--------------------|------------------------------|
| 1 | Diethyl ether | 35 | 262 |
| 2 | Petrol | 40-60 | ~230 |
| 3 | Ethyl acetate | 77 | 358 |
| 4 | Water | 100 | 2260 |

2.5 Acidic extractions

Greatly different solubility properties of amine-acid salts and their free amine equivalents have long been recognised and exploited for purification procedures.^[3] The free amine, which is typically lipophilic, prefers dissolution in an organic solvent, whereas the hydrophilic protonated form can be extracted into the aqueous phase. In other words, the distribution of an amine between organic and aqueous phases can be tuned by varying *pH*. The tunability of distribution does not exclusively apply for basic amines, but also for acidic species, neat acids being lipophilic and salts being hydrophilic. These phenomena are often exploited in separation procedures in chemical laboratories and industry.^[3] The purification is effective as long as the distribution of contaminants do not change significantly on the applied *pH* range. Jha demonstrated separation of propargyl amines with different basicities by sodium phosphate buffers.^[41]

Consider an organic solution of crude amine with contaminants, such as excess starting materials, by-products or homogeneous catalysts. By decreasing the *pH* with a suitable acid, such as HCl, the amine reacts and forms a water soluble hydrochloric salt, which can be extracted into the aqueous phase. The by-products, ideally, do not react with the used acid in any way, therefore their chemical potential does not change significantly by changing *pH*. The by-products remain in the organic phase after the extraction. The extraction of the mother liquor may be repeated to enhance recovery, and an organic wash of the isolated aqueous can be carried out to enhance purity. The purified amine has to be isolated as a free base eventually. The aqueous solution of its salt therefore has to be neutralised, typically by the addition of base (Figure 2.4). The neutralised organic solution can then be extracted back into an organic solvent, dried and concentrated to give the purified amine.

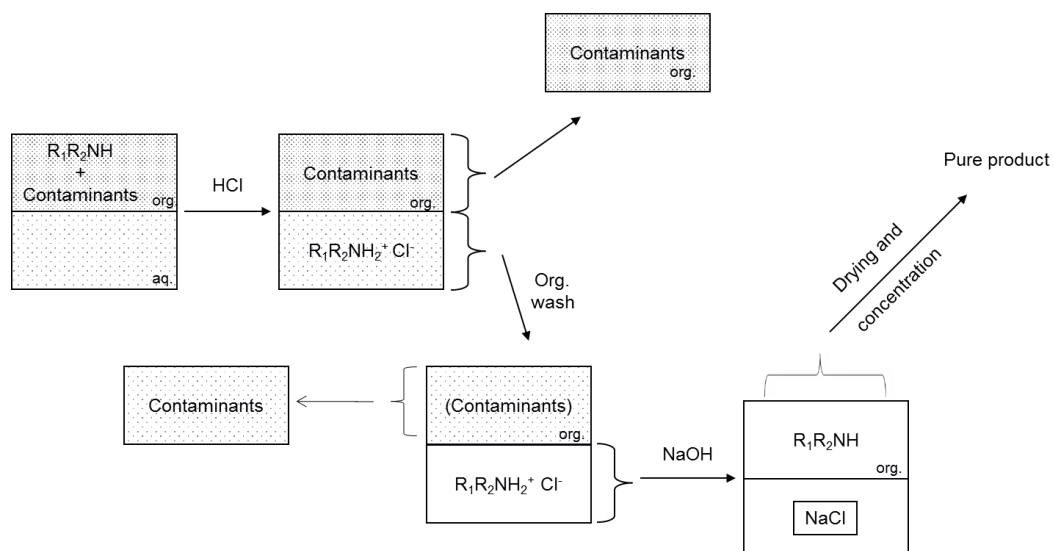


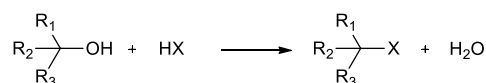
Figure 2.4. Separation of a basic amine from non-basic contaminants *via* aqueous extraction exploiting salt formation. After extraction with aqueous HCl, a wash with organic solvent was applied to remove the remaining contaminants from the aqueous phase. Eventually, the aqueous phase was neutralised with NaOH, and extracted into an organic phase, dried and concentrated to yield the pure product. Note, NaCl by-product was formed as a result of neutralisation.

Conventional aqueous extractions based on acid/base chemistry are typically carried out under ambient conditions. Consequently, they are less energy intensive compared to thermal procedures, such as distillation. Heat sensitive compounds can be purified because of the gentle operating conditions. The target compounds must readily and exclusively participate in the acid/base reaction and there must be significantly different solubility characteristics between free form and salt. Reactions other than acid/base, such as acid or base catalysed hydrolysis may be detrimental. The importance of susceptibility to hydrolysis is more pronounced compared to acid/base aided crystallisation because water is more available.^[42] A further disadvantage of the procedure is chemical consumption, both for salt formation and neutralisation. The neutralisation procedure also forms inorganic salts as by-products in equimolar amount. Aqueous waste water streams are also produced.

A goal of this project was to alleviate some of these difficulties of aqueous extractions by replacing inorganic acids with carbon dioxide. One of the obvious advantages of switching from a conventional acid, such as HCl, to CO_2 would be the replacement of the acid itself. CO_2 is the by-product of the power generation and other industries. Carbon capture and storage technologies have recently become a focus of research, and even wider and cheaper availability of CO_2 can be assumed in the future, therefore costs could be saved.^[43] Another substantial advantage of the replacement is the neutralisation. The salts formed with CO_2 may decompose under controlled conditions because of the reversible character of the reaction, and use of base may not be needed. This would not

only save the costs of the base, but the formation of salt by-products of neutralisation could be avoided.

Further requirements of the auxiliary acids and bases in the procedure, used either for salt formation or for neutralisation, are availability, low price, safety, *i.e.* their corrosive or harmful character must be limited. The used auxiliary acid/base must exclusively react with the target organic in a reversible acid/base reaction at the base/acid functional group of the target. The target organic acid/base may be susceptible to base/acid catalysed hydrolysis. In this case hydrolysis may diminish recoveries. Such functions susceptible to hydrolysis could be esters, amides, imines or nitriles.^[5] Reaction of the target molecule with an auxiliary acid/base may not only reduce recoveries, but could potentially contaminate the product. Hydrogen halides are cheap and available inorganic acids, but may react in a Lucas type reaction with alcohols to form alkyl halides, which are potentially genotoxic impurities^[44] (Scheme 2.2).^[42]



Scheme 2.2. Formation of alkyl halide, a potentially genotoxic impurity, under conditions of crystallisation in a Lucas type reaction.^[42]

Carbon dioxide do not participate in Lucas type reactions. Hence the risk of forming potentially genotoxic impurities can be eliminated. Lower acidity of CO₂ vs. other acids potentially has a favourable effect on hydrolysis as well.

2.6 Acidity of CO₂

Carbon dioxide is soluble in water, and its solubility is relatively high compared to other gases. Henry constants of CO₂ and other gases are summarised in Table 2.2. Henry constants can be used to correlate the concentration of dissolved gas and partial pressure above the solution (Eq.10.) The pressure necessary to reach the same mole fraction in aqueous solution for oxygen is more than 50 times higher compared to CO₂.

Table 2.2. Henry constants of some gases in water at 298 K.^[22]

| Entry | gas | Henry constant /MPa |
|-------|-----------------|-----------------------|
| 1 | CO ₂ | 0.163×10 ³ |
| 2 | CO | 5.828×10 ³ |
| 3 | N ₂ | 9.077×10 ³ |
| 4 | O ₂ | 4.259×10 ³ |
| 5 | H ₂ | 7.099×10 ³ |

The physically dissolved CO₂ undergoes a chemical reaction, a hydration and forms carbonic acid (Figure 2.5, Equilibrium 2). The equilibrium of this reaction is rather pushed into the direction of physically dissolved CO₂ because of the small *K_h* hydration

equilibrium constant ($1.7 \times 10^{-3} \text{ l/mol}\cdot\text{l}^{-1}$). Only about 1 in 600 CO_2 molecules forms H_2CO_3 at equilibrium under ambient conditions.

The formed carbonic acid is fairly acidic. Its pK_{a1} is reported to be 3.60, showing it to be a stronger acid than formic (pK_a 3.74) or acetic acid (pK_a 4.76).^[23] The pK_{a2} is significantly higher, above 10, therefore carbonic acid may lose its second proton only in the presence of strong bases.

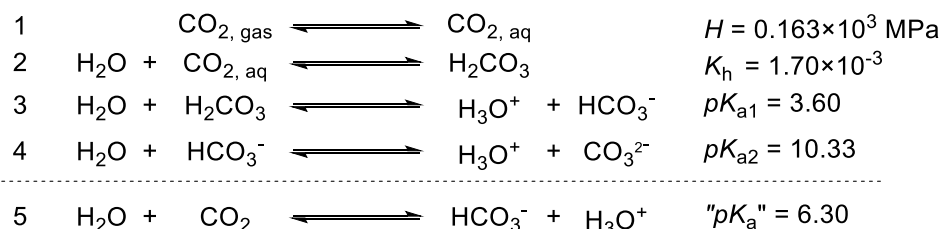
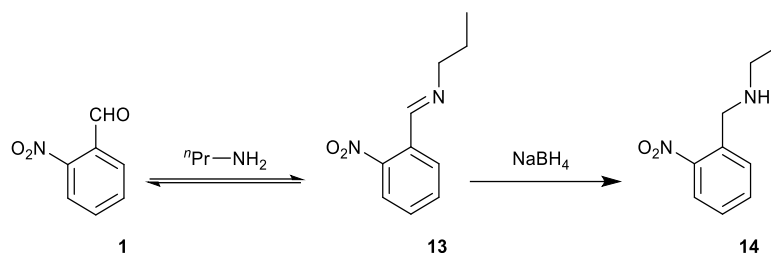


Figure 2.5. CO_2 + water equilibrium at room temperature. Formation of carbonic acid, bicarbonate and carbonate anions.^[23]

If K_h hydration equilibrium constant and pK_{a1} of carbonic acid is taken into account, the pK_a of the $\text{H}_2\text{O}/\text{CO}_2$ system is 6.3 at atmospheric pressure (Figure 2.5, Equilibrium 5). This acidity is comparable to dinitro phenols. The pH of water saturated with CO_2 at atmospheric pressure and room temperature is about 3.9. Carbon dioxide can be used for pH control within a limited range.^[45] The concentration of hydronium ions can be manipulated by CO_2 pressure. At higher pressures CO_2 becomes more soluble, and this pushes the chain of equilibria towards H_3O^+ . The pressurised $\text{CO}_2 + \text{H}_2\text{O}$ system was investigated *via* spectroscopic methods, and a pH of 2.84 was reported at 40 °C and 7.1 MPa. The pH did not decrease significantly even if the pressures were increased to 20 MPa.^[32, 46-47] This is most probably because the $\text{CO}_2 + \text{H}_2\text{O}$ system stopped following Henry's law at high pressures, and the solubility in water did not increase significantly even if the pressure was rising. Formation of acidic species has also been reported in CO_2 + alcohol systems.^[48]

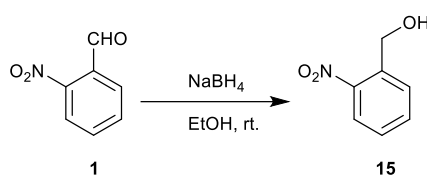
2.7 Preliminary experiments of CO_2 aided aqueous extractions

The synthesis of SB-214857-A was chosen to demonstrate the potential of novel CO_2 based reaction work-ups and purification procedures (1.2). The first reaction of the synthesis was a reductive amination furnishing *o*-nitrobenzyl methylamine **2**. For preliminary experiments the synthesis of propyl derivative **14** was also investigated because of better availability of starting materials (Scheme 2.3).



Scheme 2.3. Synthesis of *o*-nitrobenzyl propylamine **14** via a reductive amination.

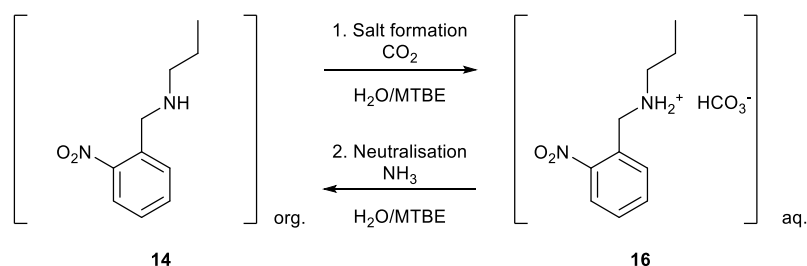
The main by-product of the procedure was benzylalcohol **15** (Scheme 2.4). NaBH₄ apparently reduced some of the starting aldehyde **1**, which was in equilibrium with the imine. The molar ratio of benzylalcohol **15** by-product and propylamine **14** was typically around 1:40 in crude product mixtures, determined by ¹H-NMR spectra integration.



Scheme 2.4. A potential side reaction of the reductive amination: Reduction of aldehyde **1** to by-product benzylalcohol **15**.

Sophisticated reductions that exclusively reduce imines in the presence of aldehydes may be available.^[49] However, this research focused on the separation of these by-products rather than avoiding their production *via* a more advanced synthesis.

An aqueous extraction of crude propylamine **14** exploiting salt formation with CO₂ was carried out on a 2 g scale (Scheme 2.5, Equation 1). An MTBE solution of the amine was extracted into water by bubbling CO₂ through the two phase system. The extraction was repeated two more times, and the combined aqueous phase was neutralized using a base, aqueous NH₃, then extracted into organic solvent, dried and concentrated (Scheme 2.5, Equation 2).



Scheme 2.5. Formation of propylamine bicarbonate **16**, intermediate of aqueous extraction and a subsequent neutralisation using a base.

The recovery of the procedure, 72%, showed the principle was working, and the acidity of CO₂/H₂O was sufficient to extract propylamine **14** into the aqueous phase. Moreover, the concentration of benzylalcohol **15** by-product was reduced to below detection limit of ¹H-NMR spectroscopy.

2.8 Screening of amines for CO₂ aided aqueous extractions

2.8.1 Goal of screening experiments

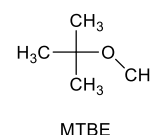
After the successful CO₂ aided aqueous extraction of *o*-nitrobenzyl propylamine **14**, other organic bases were tested in order to investigate the range of chemicals that the procedure can be applied. Ideal candidates for the tests were relatively strong organic bases, with pK_a of conjugated acids being ideally above at least 6 or 7, determined by the acidity of aqueous CO₂ (Figure 2.5). However, carbonic acid could be considered as a strong acid with a pK_a of 3.6, therefore weaker bases with conjugated pK_a s down to 3.6 were also tested. The tested bases were primary, secondary and tertiary amines, anilines, pyridines and basic heterocycles. If the basicity of the used amines was not available in the literature, pK_a values were calculated by the Marvin software package.^[50]

2.8.2 Screening procedure

The preferred organic solvent for the procedure was MTBE. This ether type solvent was chosen because it is fairly apolar, therefore solution characteristics of organic bases vs. their salt counterparts were expected to be significant. It is a recommended solvent for consideration to replace chlorinated solvents, because of its more favourable environmental impact and LCA.^[9] Its boiling point is relatively low, therefore concentration by evaporation is not problematic. Many properties of MTBE are comparable to diethyl ether. However, the higher boiling and flash point of MTBE makes it safer choice in terms of flammability. Peroxide formation tendency is also less pronounced for MTBE compared to diethyl ether.

Table 2.3. Properties of methyl tert-butyl ether, MTBE.

| Entry | Property | Value |
|-------|---------------------|--|
| 1 | b.p. | 55 °C ^[9] |
| 2 | m.p. | -109 °C ^[9] |
| 3 | ρ | 0.734 g/cm ³ ^[51] |
| 4 | P_{vapor} | 30 kPa (22.5 °C) ^[51] |
| 5 | H_{evap} | 30.4 kJ/mol (1 atm, 25 °C) ^[52] |
| 6 | η | 0.333 mPa·s (20.15 °C) ^[51] |
| 7 | $\log P$ | 1.43 ^[53] |
| 8 | Solubility in water | 51.3 g/l (20 °C) ^[54] |
| 9 | Dipole moment | 1.23 D ^[55] |
| 10 | T_{crit} | 224 °C ^[56] |
| 11 | P_{crit} | 3.43 MPa ^[56] |



A simple, efficient protocol was created to screen numerous bases for aqueous extraction. Firstly, the base was dissolved in MTBE. The chosen concentration of the

tests was between 2.5 and 5wt%. This relatively low concentration range was chosen because of the limited solubility of some of the bases. However, if the solubility of base was under 2wt% in MTBE, other solvents, such as ethyl acetate or chlorinated solvents were used instead.

Three experiments were carried out for each solute under ambient conditions. 10 ml organic solutions with accurately know composition were extracted into water, water + CO₂ and 1 equivalent aqueous HCl. The volume of the extracting solvent was always 10 ml. The organic mother liquors were dried over MgSO₄, filtered and concentrated after each extraction. The mass difference between the recovered concentrate and mass of solute in the starting solution was considered as the extracted mass.

The first experiment, extraction with water, gave information about the hydrophilicity of the base. High solubility in water could result in extraction from organic to water without the acidification effect of CO₂. Low recoveries did not necessary indicate the missing amount was extracted by water, but may have indicated evaporation under the conditions of concentration or loss during the drying procedure because of pronounced adsorption to the drying agent. In an ideal case, most of the organic in the starting solution would be recovered.

The second set of experiments was aqueous extraction of the organic solutions, while CO₂ was bubbled through the system with a flowrate of 0.5 l/min for 15 minutes. The flow of gas caused solvent evaporation, which was compensated by topping up. The amount of CO₂ flowing through was about 300 mmol, at least 60 times in excess.

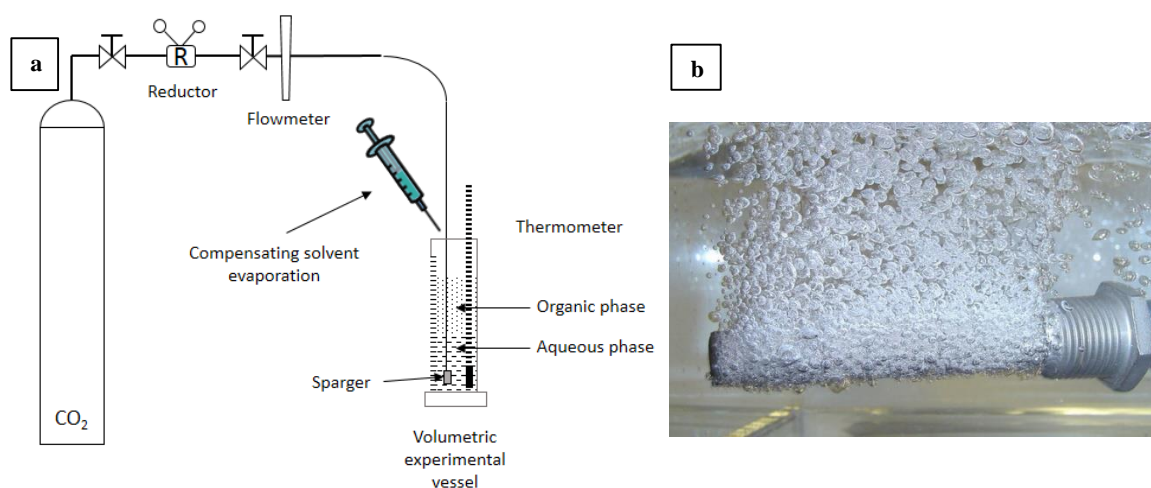


Figure 2.6a-b. Apparatus used for the screening experiments (a). The biphasic system was separated after CO₂ exposure. The organic phase was dried and concentrated. A sparger in operation (b).

After CO₂ saturation the gas stream was stopped allowing separation of layers. After phase separation the organic mother liquor was dried, filtered and concentrated. The mass difference between the recovered concentrate and solute in the starting solution

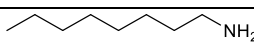
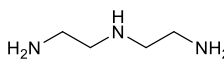
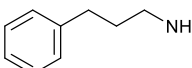
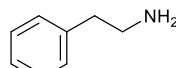
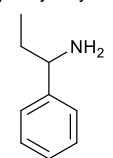
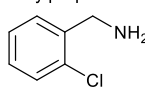
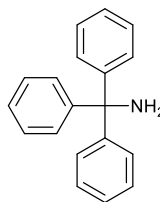
was considered as the mass extracted by water + CO₂. In an ideal case, significant amount of organic base was extracted into the organic phase.

Organic solutions were also extracted with 1 equivalent of aqueous HCl. Successful extraction with HCl, but low extraction with water + CO₂ could indicate either that the solute was possibly not basic enough to form a salt with carbonic acid, or the solubility of the formed carbamate in water was limited.

2.8.3 Range of tested bases

The results of the extraction experiments are summarised below (Table 2.4-2.9).

Table 2.4. Primary amines, extracted from their organic solution with water, water + CO₂ and one equivalent aqueous HCl.

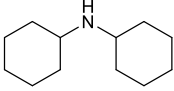
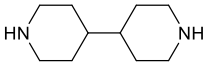
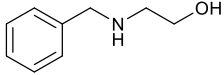
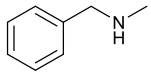
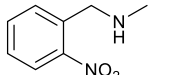
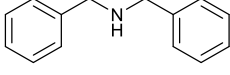
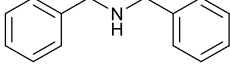
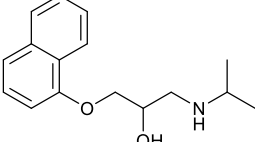
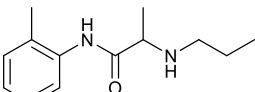
| Entry | Compound | pK_a | $\log P$ | Solvent | Conc. /wt% | Extracted by | | |
|-------|---|-----------------------|----------------------|---------|------------|--------------|-------------------------|--------------------|
| | | | | | | Water | Water + CO ₂ | Aq. HCl (1 equiv.) |
| 1 |  <i>n</i> -octylamine | 10.65 ^[57] | 2.48 | MTBE | 2.5 | 42% | 68% | 68% |
| 2 |  diethylenetriamine | 10.02 ^[23] | -1.79 | MTBE | 2.5 | >95% | n.t. | n.t. |
| 3 |  3-phenylpropylamine | 10.39 ^[23] | 1.83 | MTBE | 2.5 | 30% | >95% | >95% |
| 4 |  2-phenylethylamine | 9.83 ^[23] | 1.41 ^[58] | MTBE | 2.5 | 28% | >95% | >95% |
| 5 |  1-phenylpropan-1-amine | 9.77 | 2.04 | MTBE | 2.5 | 10% | 74% | >95% |
| 6 |  2-chlorobenzylamine | 8.88 ^{a[59]} | 1.70 | MTBE | 2.5 | <5% | 50% | 56% |
| 7 |  tritylamine | 9.2 ^{b[60]} | 4.53 | MTBE | 2.5 | <5% | 6% | >95% |

n.t.: not tested because of too high aqueous solubility

^ain water:methanol 1:1

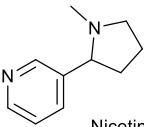
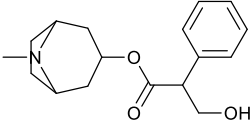
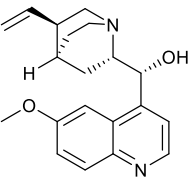
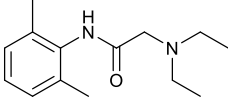
^bin water:acetonitrile 84:16

Table 2.5. Secondary amines, extracted from their organic solution with water, water + CO₂ and one equivalent aqueous HCl.

| Entry | Compound | pK_a | $\log P$ | Solvent | Conc. /wt% | Extracted by | | |
|-------|--|-----------------------|----------------------|-------------------|------------|--------------|-------------------------|--------------------|
| | | | | | | Water | Water + CO ₂ | Aq. HCl (1 equiv.) |
| 1 |  dicyclohexylamine | 11.25 ^[23] | 3.41 | MTBE | 2.5 | 10% | 68% | >95% |
| 2 |  biperidine 11 | 10.88 ^[61] | 0.54 | CHCl ₃ | 3.0 | 33% | >95% | n.t. |
| 3 |  N-benzylethanolamine | 9.18 | 0.84 | MTBE | 2.5 | 37% | >95% | >95% |
| 4 |  methyl benzylamine 17 | 9.71 ^[62] | 1.45 | MTBE | 2.5 | 26% | 74% | 74% |
| 5 |  methyl nitrobenzylamine 2 | 8.89 | 1.47 | MTBE | 5.0 | 36% | 87% | 94% |
| 6 |  dibenzylamine | 8.52 ^[23] | 3.26 | MTBE | 2.5 | <5% | <5% | 53% |
| 7 |  dibenzylamine | 8.52 ^[23] | 3.26 | Hex | 2.5 | <5% | <5% | 67% |
| 8 |  Propranolol 18 | 9.45 ^[63] | 3.37 ^[64] | MTBE | 2.6 | 23% | 84% | >95% |
| 9 |  Prilocaine 19 | 7.32 ^[65] | 2.21 ^[66] | MTBE | 2.6 | 41% | 52% | >95% |

n.t.: not tested because of high extraction with water +CO₂

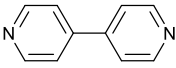
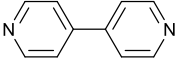
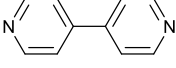
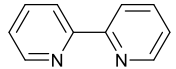
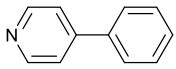
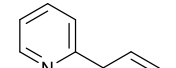
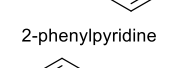
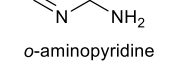
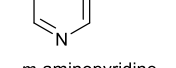
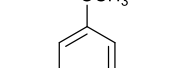
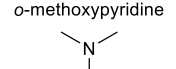
Table 2.6. Tertiary amines, extracted from their organic solution with water, water + CO₂ and one equivalent aqueous HCl.

| Entry | Compound | pK_a | $\log P$ | Solvent | Conc. /wt% | Extracted by | | |
|-------|--|-----------------------|----------------------|---------------------------------|------------|--------------|-------------------------|--------------------|
| | | | | | | Water | Water + CO ₂ | Aq. HCl (1 equiv.) |
| 1 |  Quinuclidine | 11.06 ^[67] | 0.85 | MTBE | 5.0 | 61% | >95% | >95% |
| 2 |  DABCO | 8.70 ^[58] | -0.13 | MTBE | 2.5 | >95% | n.t. | n.t. |
| 3 |  Nicotine | 8.20 ^[68] | 1.20 ^[68] | MTBE | 2.6 | 53% | >95% | >95% |
| 4 |  Atropine | 9.30 ^[69] | 1.81 ^[70] | EtOAc | 2.9 | 28% | >95% | >95% |
| 5 |  Quinine | 8.52 ^[23] | 0.53 ^[71] | CH ₂ Cl ₂ | 5.3 | 12% | precip. | 14% |
| 6 |  Lidocaine 20 | 7.95 ^[72] | 2.44 ^[73] | MTBE | 2.4 | 31% | 60% | >95% |

n.t.: not tested because of too high aqueous solubility

precip.: precipitation of colourless solid was observed; experiment halted

Table 2.7. Pyridines, extracted from their organic solution with water, water + CO₂ and one equivalent aqueous HCl.

| Entry | Compound | pK_a | $\log P$ | Solvent | Conc. /wt% | Extracted by | | |
|-------|--|----------------------|-----------------------|-------------------|------------|--------------|-------------------------|--------------------|
| | | | | | | Water | Water + CO ₂ | Aq. HCl (1 equiv.) |
| 1 |  4,4'-bipyridine 9 | 4.82 ^[23] | 1.19 | MTBE | 2.5 | Precip. | | >95% |
| 2 |  4,4'-bipyridine 9 | 4.82 ^[23] | 1.19 | EtOAc | 2.5 | 17% | 17% | >95% |
| 3 |  4,4'-bipyridine 9 | 4.82 ^[23] | 1.19 | CHCl ₃ | 2.5 | 5% | 27% | >95% |
| 4 |  2,2'-bipyridine | 4.35 ^[23] | 1.96 | MTBE | 2.5 | 16% | 16% | >95% |
| 5 |  4-phenylpyridine | 5.50 ^[74] | 2.59 ^[58] | MTBE | 2.5 | 5% | 5% | >95% |
| 6 |  2-phenylpyridine | 5.30 ^[74] | 2.65 ^[75] | MTBE | 2.5 | 5% | 5% | 74% |
| 7 |  <i>o</i> -aminopyridine | 6.71 ^[23] | -0.54 ^[76] | MTBE | 2.5 | 44% | 55% | >95% |
| 8 |  <i>m</i> -aminopyridine | 6.03 ^[23] | -0.07 | MTBE | 2.5 | 58% | 63% | >95% |
| 9 |  <i>o</i> -methoxypyridine | 6.47 ^[23] | 0.6 | MTBE | 2.6 | 73% | 73% | >95% |
| 10 |  <i>p</i> -dimethylaminopyridine | 9.87 ^[77] | 0.86 | EtOAc | 3.6 | <5% | >95% | 84 |
| 11 |  aminopyridine | 9.42 ^[77] | -0.07 | EtOAc | 0.9 | 76 | >95% | >95% |

precip.: precipitation of colourless solid was observed; experiment halted

Table 2.8. Anilines, extracted from their organic solution with water, water + CO₂ and one equivalent aqueous HCl.

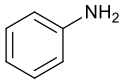
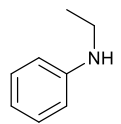
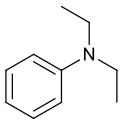
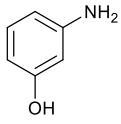
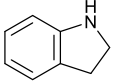
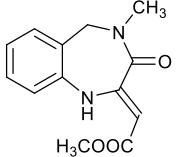
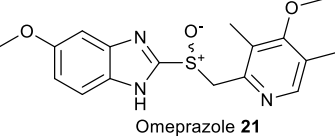
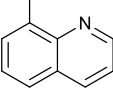
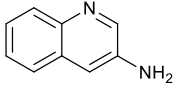
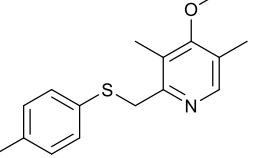
| Entry | Compound | pK_a | $\log P$ | Solvent | Conc. /wt% | Extracted by | | |
|-------|--|----------------------|----------------------|---------|------------|--------------|-------------------------|--------------------|
| | | | | | | Water | Water + CO ₂ | Aq. HCl (1 equiv.) |
| 1 |  aniline | 4.87 ^[58] | 0.90 ^[58] | MTBE | 5.0 | 10% | 10% | >95% |
| 2 |  ethylaniline | 5.11 ^[23] | 1.80 | MTBE | 2.0 | <5% | 13% | 73% |
| 3 |  diethylaniline | 6.56 ^[23] | 1.39 | MTBE | 2.0 | <5% | <5% | 53% |
| 4 |  <i>m</i> -aminophenol | 4.37 ^[58] | 0.84 | MTBE | 2.0 | 47% | 54% | 93% |

Table 2.9. Heterocycles, extracted from their organic solution with water, water + CO₂ and one equivalent aqueous HCl.

| Entry | Compound | pK_a | $\log P$ | Solvent | Conc. /wt% | Extracted by | | |
|-------|---|----------------------|----------|-------------------|------------|--------------|-------------------------|--------------------|
| | | | | | | Water | Water + CO ₂ | Aq. HCl (1 equiv.) |
| 1 |  Indoline | 5.60 ^[78] | 1.49 | MTBE | 10.0 | <5% | <5% | 68% |
| 2 |  benzodiazepine 4 | n.a. | 0.65 | MTBE | 2.3 | 21% | 20% | 26% |
| 3 |  Omeprazole 21 | 4.77 | 2.43 | CHCl ₃ | 2.5 | 9% | 9% | 88% |
| 4 |  8-methylquinoline | 5.67 ^[58] | 2.64 | MTBE | 4.0 | <5% | <5% | >95% |
| 5 |  3-aminoquinoline | 4.91 ^[58] | 1.30 | MTBE | 5.0 | 34% | 21% | >95% |
| 6 |  sulfanylmethylpyridine | 6.69 | 4.26 | MTBE | 2.5 | 10% | 10% | 79% |

2.8.4 Discussion of screening experiments

The main use of the obtained information was to help deciding what range of bases could be suitable for CO₂ aided aqueous extractions, and therefore could be considered for further investigations, and which ones were rather unsuitable. The goal was to quickly screen a large number of bases, therefore time efficiency had priority over accuracy within reason. An ideal candidate for further investigations could be extracted by water + CO₂ in high yields. A further requirement was a relatively low hydrophilicity of the free base. As it was highlighted previously (Figure 2.4), the aqueous extractions are usually followed by neutralisation and an organic extraction. The final organic extraction after neutralisation can be particularly problematic if the base is too hydrophilic. For instance, bases such as Quinuclidine, DABCO and Nicotine (Table 2.6, Entries 1-3) were not ideal candidates for further testing, because they were too hydrophilic and extracted into water without CO₂. This may allow the separation of

these bases from contaminants that are not water soluble. However, the resulting aqueous solutions after separation cannot be extracted back to an organic solvent easily. Bases, such as tritylamine, dibenzylamine or aniline (Table 2.4, Entry 7, Table 2.5, Entry 6, Table 2.8, Entry 1), were not ideal for further investigations either, because their extraction with water + CO₂ apparently did not work. Their extraction with aqueous HCl worked reasonably well, indicating good water solubility of their hydrochloride salts. It could be suspected that poor extractions with water + CO₂ (<30%) combined with good extractions with aqueous HCl (>60%) indicated insufficient basicity of the tested compound to react with water + CO₂. Bases such as *o*-nitrobenzyl methylamine **2**, Propranolol **18** or Lidocaine **20** (Table 2.5, Entries 5 and 8, Table 2.6, Entry 6) were ideal for the further investigation, because water itself did not extract significantly, but water + CO₂ did.

A correlation between physical values of the base and extraction by water + CO₂ would be very useful, because likeliness of successful extraction by water + CO₂ could be predicted without preliminary experimental testing. Correlation between basic strength and CO₂ aided aqueous extraction seemed obvious, therefore connection between pK_a values and the extraction was analysed (Figure 2.7).

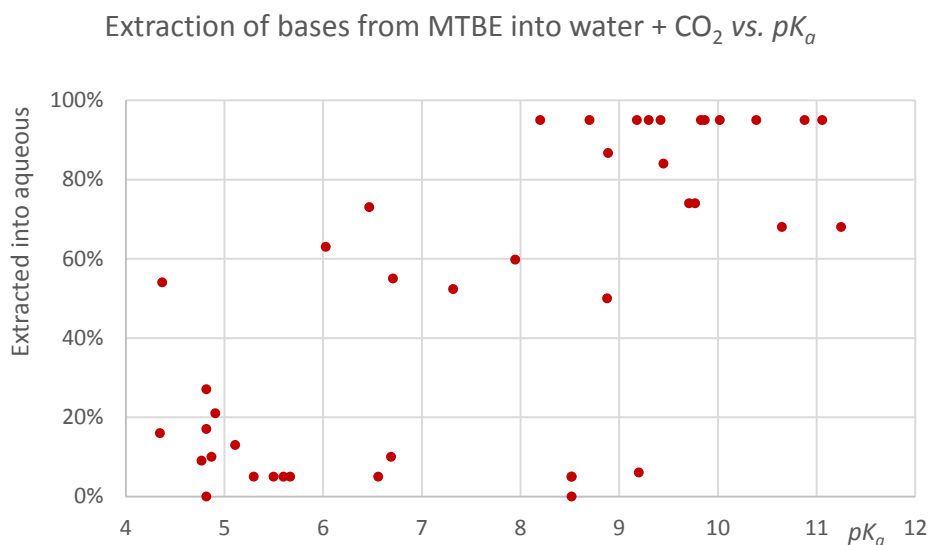


Figure 2.7. Extracted amount by water + CO₂ from organic solutions of bases vs. their pK_a .

Three major zones could be identified on this diagram. At pK_a values under about 6, the extraction was typically below 30%. This pK_a value coincided with the acidity of water + CO₂, which is about 6.3 (Figure 2.5). There is an intermediate zone between pK_a 6 and 8, with typical extractions between 50 and 70%. The highest extractions with water + CO₂ were achieved at pK_a values above 8.

A single extraction with water + CO₂ over 50% efficiency was considered sufficient, because multiple extractions, which are common in laboratory, could enhance the

separation to an acceptable level. For instance, the recovery of a separation that had 50% efficiency after one extraction, could be enhanced up to about 75 or 85.5% efficiency by repeating the extraction one or two more times. Such distribution may also be sufficient for designing a continuous liquid-liquid extraction procedure.

Some bases, such as *o*-aminopyridine (Table 2.7, Entry 8), extracted well with water + CO₂, but this result was rather deceiving, because water on its own also extracted the hydrophilic base well. As was explained before, ideal candidates for purification *via* CO₂ aided aqueous extraction have to be rather lipophilic in free form, but must become significantly hydrophilic after salt formation by exposure to CO₂. If the difference between extraction by water + CO₂ and extraction only by water, from now on referred as *extraction difference*, was plotted against pK_a , the correlation became clearer (Figure 2.8).

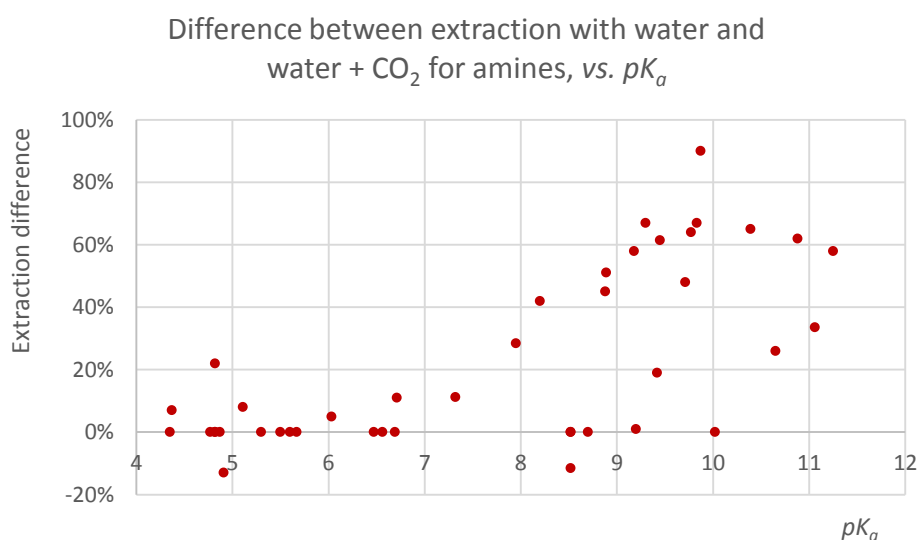


Figure 2.8. *Extraction difference*, that is the difference between the amounts extracted from organic solutions by water + CO₂ and water only vs. pK_a , for various bases.

The use of extraction difference removed the bias of the extracting effect of water. A significantly low extraction difference was found for weak bases with pK_a below 7 but it was high for stronger bases with pK_a above 7, however not consistently. The extraction difference was low with a high overall extraction for strong, but hydrophilic bases such as diethylenetriamine (Table 2.4, Entry 2). This base was very hydrophilic, and could be extracted from organic by water. The presence or absence of CO₂ did not make a difference. The extraction difference was also low with low overall extraction for amines like triethylamine, which is fairly basic primary amine with pK_a over 9. Yet, it could not be extracted well by water + CO₂ (Table 2.4, Entry 7). It could be, however, extracted by aqueous HCl, indicating hydrophilicity of the salt. The significant difference in extraction using H₂CO₃ or HCl as acid was possibly caused by the different hydrophobicity of the

considered for either pesticide or pharmaceutical purposes. $\log P$ values can also be calculated by software, based on group contributions.^[50] Molecules for pharma- or pesticide applications may not even be considered if their calculated $\log P$ (and also pK_a) does not meet certain criteria.

$\log P$ values indicate the distribution between octanol and water. Their application to predict distribution between other solvents may be limited. However, for CO_2 aided aqueous extractions, correlation between $\log P$ and experimental results was investigated, because it is the $\log P$ that is the most common and widely accepted descriptor for hydrophilic/lipophilic character. The extraction by water of the tested bases was plotted against $\log P$ values.

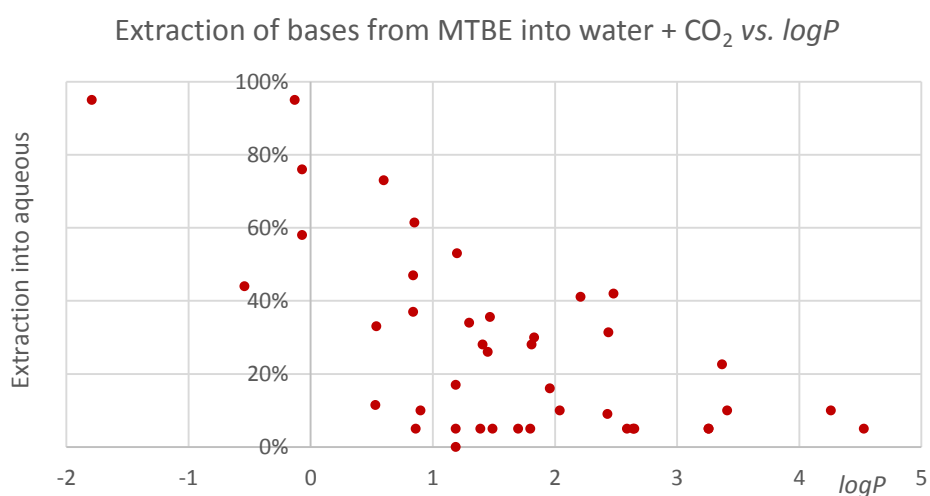


Figure 2.9. Extraction of bases from their organic solutions with water vs. $\log P$.

Bases with low $\log P$ values generally extracted into water better, whereas high $\log P$ s disfavoured extraction. There were numerous exceptions, however. Quinine, for instance had a low $\log P$ value, around 0.5, yet, it could not be extracted into water. One reason for this and for similar cases could be that $\log P$ s apply for octanol-water system, rather than MTBE-water. $\log P$ values are also applied for indefinitely dilute systems. Quinine, for instance, was only sparingly soluble in water. Distortion of $\log P$ at concentrations close to saturation in either of the solvents may be significant.

$\log P$ was chosen to describe the lipophilic character of a compound in this study because this data is well accepted. $\log P$ s of compounds are often measured and published in the literature, but simulation was also possible.^[23, 80] $\log P$, by definition, gives information about the distribution between octanol and water (Eq.15). Experimental aqueous extraction data was available allowing the calculation of data equivalent to $\log P$. This data was plotted against $\log P$ in order to assess its relevancy for MTBE-water systems (Figure 2.10).

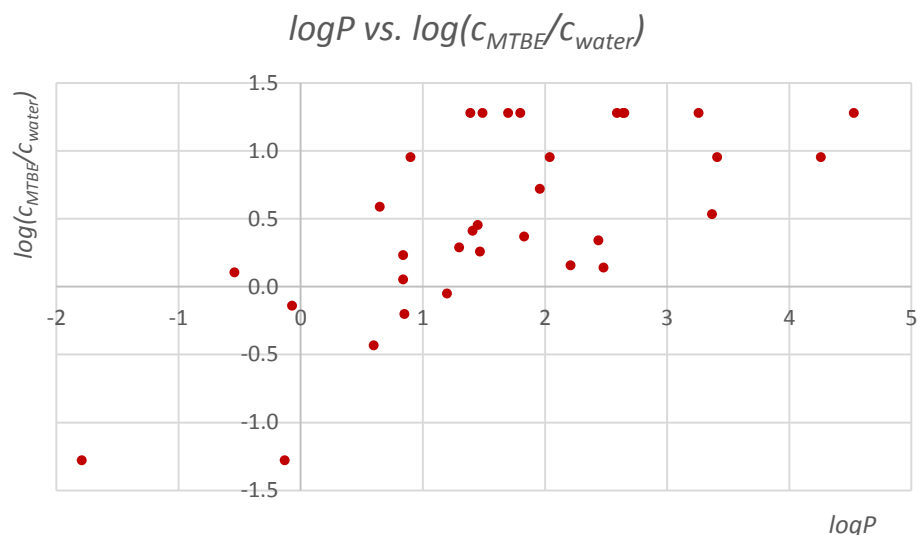


Figure 2.10. The $\log P$, sourced from literature or simulation,^[80] plotted against the equivalent number for the distribution between MTBE and water, calculated from experimental data.

A qualitative analogy between $\log P$ and the equivalent data for the distribution between MTBE ($\log P_{MTBE}$) and water can be observed. The $\log P_{MTBE}$ numbers tended to increase with $\log P$, however, the deviation was significant. Moreover, the $\log P_{MTBE}$ numbers distorted above 1.28, which value was equivalent to 95% solute distributing into the organic phase. The reason for this was the limited accuracy of the preparative measurement method.

It was clear that both pK_a and $\log P$ have an effect on extraction efficiency. Hence, extractions of bases from organic solvent with water + CO₂ was plotted against both pK_a and $\log P$ (Figure 2.11).

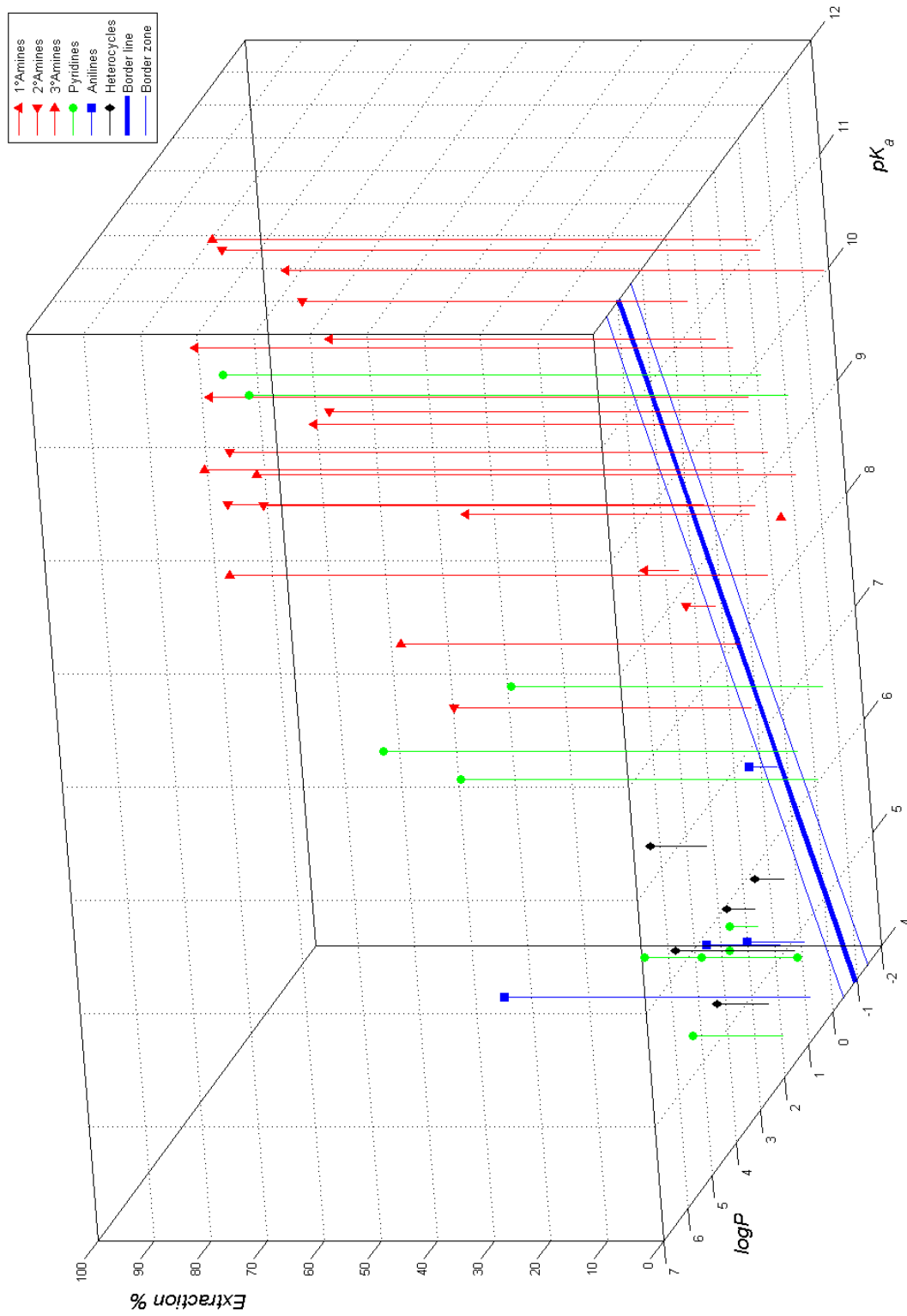


Figure 2.11. Extraction of various bases from organic solvents into water in the presence of CO_2 plotted against pK_a and $\log P$. Two regions could be distinguished. On the left side of the blue border line on the pK_a - $\log P$ plane poor extractions were observed. Extractions were typically above 50% on the right hand side of the border line. There is border zone in the vicinity of border line in which extraction was or was not observed. The blue border line is in the $\log P$ - pK_a plane.

An arbitrary border line was drawn into the $\log P$ - pK_a plane of the diagram (Figure 2.11) to separate two regions. Bases falling into the left hand side region according to their $\log P$ s and pK_a s did not extract well into water + CO₂, with extractions typically below 20%. Extractions of bases over about 50% were however observed on the right hand side. Apparently, it was the combination of $\log P + pK_a$ that determined extraction. This combination was represented by the border line, which could be expressed by Eq.16.

$$\log P = 0.86pK_a - 4.36 \quad \text{Eq.16}$$

Compounds with pK_a s and $\log P$ s that satisfy Eq.17, will fall onto the left hand side of Figure 2.11, therefore it is unlikely that they can be extracted into water + CO₂ (Table 2.10, Entries 2, 12 and 13).

$$\log P - 0.86pK_a + 4.36 > -0.5 \quad \text{Eq.17}$$

In contrast, compounds with pK_a s and $\log P$ s that satisfy Eq.18, will fall onto the right hand side of Figure 2.11, therefore it is likely that they can be extracted into water + CO₂ (Table 2.10, Entries 1, 3, 4, 7, 8, 9 and 11).

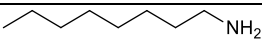
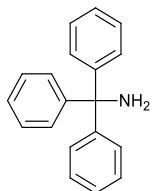
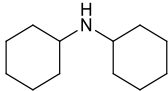
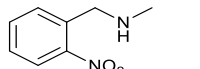
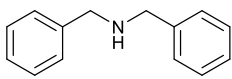
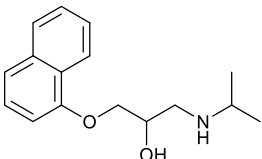
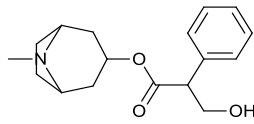
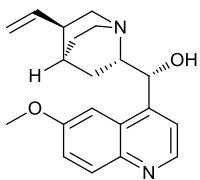
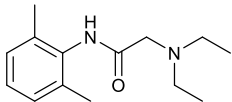
$$\log P - 0.86pK_a + 4.36 < 0.5 \quad \text{Eq.18}$$

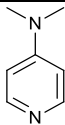
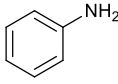
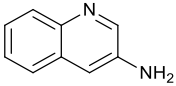
There was an ambiguous intermediate zone in the vicinity of the border line (Figure 2.11), in which extraction may or may not be possible. Compounds satisfying Eq.19 fall into the border zone, in which the prediction is not reliable, and the extraction with water + CO₂ needs to be tested experimentally (Table 2.10, Entries 5, 6 and 10).

$$0.5 \geq \log P - 0.86pK_a + 4.36 \geq -0.5 \quad \text{Eq.19}$$

Extraction with water + CO₂ could be predicted by pK_a and $\log P$ values for numerous bases. However, unexpected results such as precipitation (Quinine, Table 2.10, Entry 9) or hydrolysis or other reactions that do not relate to $\log P$ or pK_a could not be predicted.

Table 2.10. Prediction of extraction (Eq.17, Eq.18) for selected compounds, with the experimental finding.

| Entry | Compound | pK_a | $\log P$ | Formula | Prediction | Extracted by water+ CO ₂ |
|-------|---|-----------------------|----------------------|---------|---------------|-------------------------------------|
| 1 |  <i>n</i> -octylamine | 10.65 ^[57] | 2.48 | -2.32 | Extraction | 68% |
| 2 |  tritylamine | 9.2 ^{a[60]} | 4.53 | 0.98 | No extraction | 6% |
| 3 |  dicyclohexylamine | 11.25 ^[23] | 3.41 | -1.91 | Extraction | 68% |
| 4 |  methyl nitrobenzylamine 2 | 8.89 | 1.47 | -1.82 | Extraction | 86.7% |
| 5 |  dibenzylamine | 8.52 ^[23] | 3.26 | 0.29 | Border case | <5% |
| 6 |  Propranolol 18 | 9.45 ^[63] | 3.37 ^[64] | -0.40 | Border case | 84% |
| 7 |  Nicotine | 8.20 ^[68] | 1.20 ^[68] | -1.49 | Extraction | >95% |
| 8 |  Atropine | 9.30 ^[69] | 1.81 ^[70] | -1.83 | Extraction | >95% |
| 9 |  Quinine | 8.52 ^[23] | 0.53 ^[71] | -2.44 | Extraction | precip. |
| 10 |  Lidocaine 20 | 7.95 ^[72] | 2.44 ^[73] | -0.04 | Border case | 59.8% |

| Entry | Compound | pK_a | $\log P$ | Formula (Eq.17) | Prediction | Extracted by water+ CO ₂ |
|-------|--|----------------------|----------------------|-----------------|---------------|-------------------------------------|
| 11 |  p-dimethylaminopyridine | 9.87 ^[77] | 0.86 | -3.27 | Extraction | >95% |
| 12 |  aniline | 4.87 ^[58] | 0.90 ^[58] | 1.07 | No extraction | 10% |
| 13 |  3-aminoquinoline | 4.91 ^[58] | 1.30 | 1.44 | No extraction | 21% |

^ain water:acetonitrile 84:16

A main disadvantage of prediction according to the diagram (Figure 2.11) or the related equations (Eq.17-Eq.19) was that they did not take extraction by water into account. Extraction by water in the absence of CO₂ could be detrimental, as was discussed. Extraction difference, which was defined earlier as a difference between extraction by water + CO₂ and water only, was plotted against pK_a and $\log P$ (Figure 2.12). The right hand side of Figure 2.11, the area at which extraction with water + CO₂ was possible, was divided into two zones by a new border line on Figure 2.12. Compounds in Zone II could be extracted well by water + CO₂, but also with water only, therefore their extraction difference was low and they were not ideal candidates for further investigations. The borderline between Zone II and Zone III was almost parallel with the pK_a axis. Bases in Zone III had $\log P$ s below 0.8 to 0. The meaning of such shape was in accordance with a practical observation: compounds that have low $\log P$ s are rather hydrophilic. Therefore, these compounds would possibly distribute into water from organic solvents, which may be other than octanol, for which $\log P$ has been defined. Compounds in Zone II were simply too hydrophilic. Compounds in Zone III could be extracted by water + CO₂ because they were basic enough but not too lipophilic. They were however not hydrophilic enough to be extracted by water only. The extraction difference was therefore high in Zone III, and these compounds were ideal candidates for further investigation for CO₂ aided aqueous extractions.

The border line between Zones I and III (Figure 2.12) to predict extraction difference, and the border line to predict extraction by water +CO₂ (Figure 2.11) are identical. Therefore the proposed formulas (Eq.17-Eq.19) can still be used to predict the likeliness of extraction difference, rather than extraction by water + CO₂ with a restriction because of Zone III (Figure 2.12).The border line of Zone III was almost parallel with the pK_a axis. Solutes with $\log P$ below 0.5 were too hydrophilic. The proposed equations cannot be

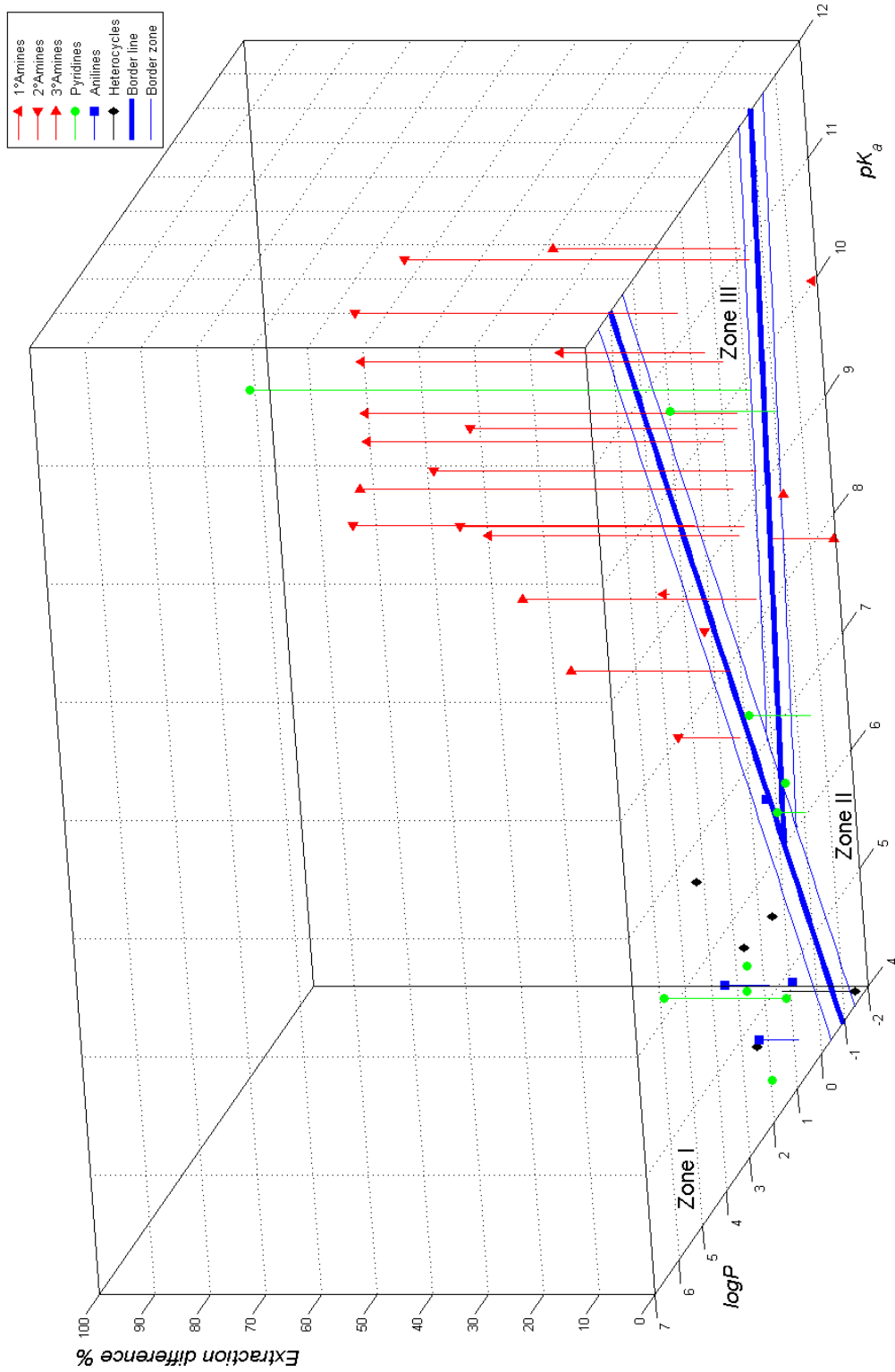


Figure 2.12. Difference between the amount of base extracted from organic solutions by water + CO₂ and water only vs. pK_a and $\log P$ for various bases. Zone I: Low extraction difference; bases were too weak or too lipophilic. Zone II: Low extraction difference; bases were too hydrophilic or too weak. Zone III: High extraction difference; bases were sufficiently basic and lipophilic enough for extraction with water + CO₂, but they were not hydrophilic enough to be extracted by water only. The blue border lines are in the $\log P$ - pK_a plane.

used for compounds with $\log P$ below 0.5. However, these compounds could safely be considered to be part of Zone I.

2.8.6 Summary

Factors that determine the chemical potential in a solution, such as solvation, hydrogen bonding, polarisation etc., can be fairly complex, therefore prediction of solubilities and distribution between solvents are rather challenging, and the reliability of the available *in silico* methods is rather questionable.^[81] However, in case of extraction with water + CO₂, the effect of acid/base reaction was possibly more significant compared to other factors and predictions based on the basic strength, which measured by the pK_a of a conjugate acid, could be relatively reliable. Effects other than acid/base related interactions such as lipophilicity were taken into account using $\log P$.

The intention of these investigations was to help selecting compounds that were likely to be extracted by water + CO₂. Systems of the chosen compounds + water + CO₂ were tested in more detail and will be discussed later (2.9).

The prediction could be useful for those who already operate a conventional aqueous extraction technology based on acids such as HCl. The developed method in this work can help predicting if a conventional aqueous extraction could be switched to the more environmentally feasible CO₂ aided aqueous extraction. Equally, designers of technologies being developed may consider the application of CO₂ to tune distribution by prediction.

2.9 Detailed studies of CO₂ aided aqueous extractions

2.9.1 The goal of detailed studies of distribution

In the last section (2.8) the possibility for CO₂ aided aqueous extraction was investigated for a range of bases. Using this information the likelihood of extraction into water + CO₂ could be predicted for other bases. The main goal of the next sections was to obtain detailed information about kinetics and concentration dependency not only for the CO₂ involved aqueous extraction, but also for the inverse procedure, which is an organic extraction of the aqueous phase, which was neutralised without a reagent (Figure 2.4). Concentration and gas flowrate dependence of carboxylation and N₂ gas induced decarboxylation could be useful for optimising conditions of actual procedures. CO₂ aided aqueous extraction of bases such as *o*-nitrobenzyl- methyl and propylamine **2** and **14**, Lidocaine **20**, Propranolol **18** and Prilocaine **19** was investigated, including details about one of the important advantages, reagent free neutralisation induced by N₂ gas flow.

2.9.2 Experimental set-up

The distribution of bases was measured between organic and aqueous phases with equal volumes. If the system was diluted in order to obtain information about a more dilute system, the volume of added organic solvent and water was the same in order to maintain the equal volume of the phases of the experimental system. The concentrations were measured by either UV/Vis spectroscopy or HPLC after sampling and dilution, which was necessary because the experimental samples were too concentrated for both analytical methods. A modified Nernst distribution coefficient was measured in the investigated two phase systems (Eq.20).

$$K = \frac{c^{Org}}{c^{Aq}} \quad \begin{array}{l} K: \text{modified partitioning coefficient} \\ c^{Org}, c^{Aq}: \text{concentration of compound in organic and aqueous phase} \end{array} \quad \text{Eq.20}$$

The modification was the use of concentration, rather than molar fraction, which was in the original definition by Nernst (Eq.14).^[38] In the following sections often distribution between phases in percentages will be represented rather than the distribution coefficients themselves. Percentages of species distributing between either organic or aqueous phases were considered easier to interpret compared to distribution coefficients.

The distribution was measured before and after CO₂ exposure, and during the course of CO₂ saturation and during the course of N₂ gas induced decarboxylation. All the experiments were conducted under ambient pressure and temperature. The distribution before CO₂ exposure was measured in a separation funnel. When the sample was exposed to gas, either CO₂ or N₂, the setup below was used (Figure 2.13).

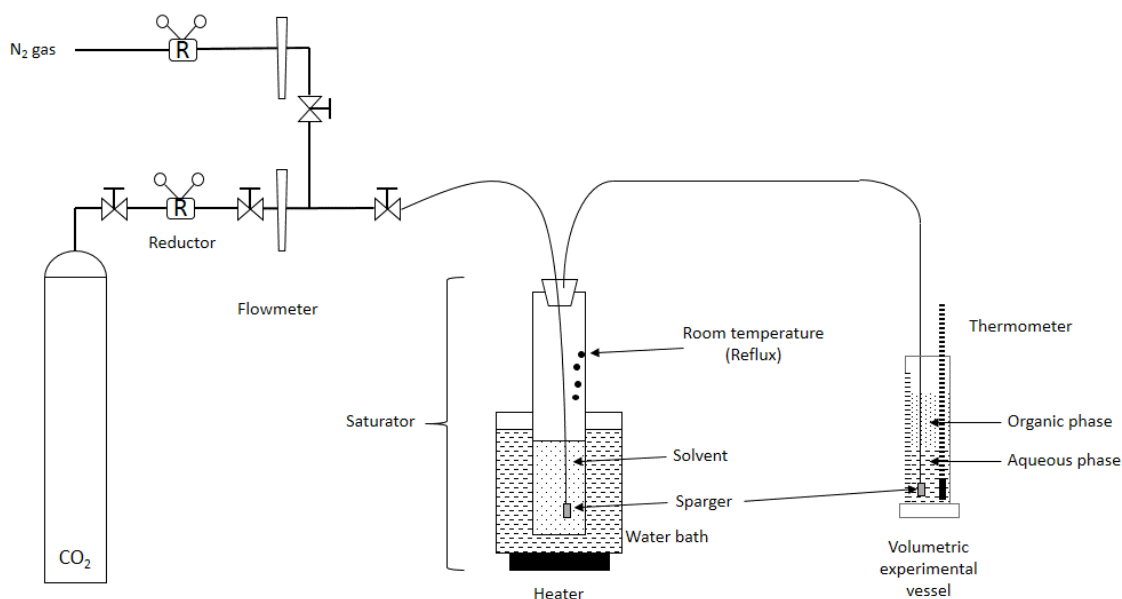


Figure 2.13. Experimental setup for the measurement of phase distribution. The gas supplied into the experimental vessel was saturated with solvent to prevent evaporation from the investigated system.

The CO₂ gas arrived from a cylinder, its pressure was controlled by a reductor. N₂ gas was supplied into the laboratory through pipelines. The stream of gas was streamed through saturator, which was immersed into a heated water-bath at 50 °C. However, the saturator was long enough to allow the gas stream to cool down to room temperature. The condensed excess solvent refluxed back to the saturator. The gas stream entering into the experimental vessel containing the measured system was therefore saturated with solvent at room temperature. The saturation of the gas prevented evaporation, which would not only alter the composition of the experimental system, but the heat effects would cool the system down (Table 2.3). Using solvent saturated gas, the maintenance of temperature and composition was greatly simplified. The temperature of the experimental system was monitored with a thermometer with an accuracy of ± 0.5 °C, and remained at room temperature.

2.9.3 Investigation of concentration dependence of distribution

The distribution of *o*-nitrobenzyl methylamine **2**, *o*-nitrobenzyl propylamine **14**, Lidocaine **20**, Propranolol **18** and Prilocaine **19** was investigated between MTBE and water at various nominal concentrations. The distribution of bases between MTBE and water was measured at the highest nominal concentration first. The aqueous + organic two phase systems were stirred vigorously until equilibrium was assumed. Samples were taken from the co-existing phases, diluted and analysed by UV/Vis spectrometry or HPLC. The two phase systems were diluted to the next nominal concentration by the addition of both water and MTBE, followed by stirring, sampling and analysis. The dilutions were repeated until the lowest nominal concentration was tested. The obtained results were shown with squares on the diagrams below (Figure 2.14a-e).

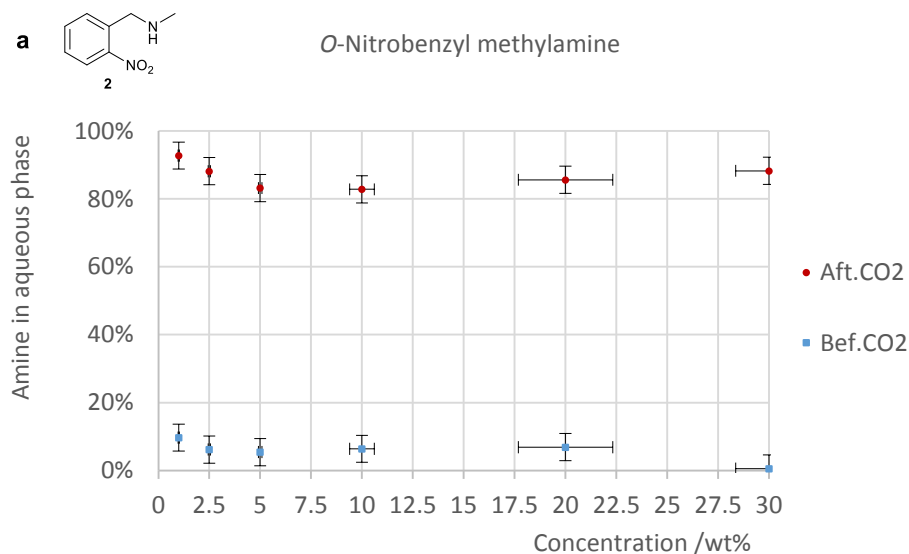
Consider an experimental datum point at $x = 1.0\text{wt}\%$ and $y = 9.6\%$, (Figure 2.14a, leftmost \blacksquare). The meaning of that point is 9.6% of solute distributed into the aqueous phase, compared to all the solute in the system. This also suggests 90.4% remained in the organic phase. The coordinate (x) gives information about the concentration, which is 1.0wt% nominal. "Nominal concentration" means the concentration of the organic phase, assuming all the solute in the system was dissolved only in the organic phase, including the solute actually dissolved in the aqueous phase in equilibrium. After CO₂ exposure, the distribution was significantly different. At the nominal concentration of the example ($x = 1.0\text{wt}\%$), $y = 92.7\%$ of amine was extracted into the aqueous phase (Figure 2.14a, leftmost \bullet).

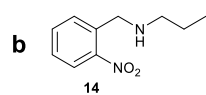
In the very case of the example ($x = 1\text{wt}\%$, Figure 2.14a, leftmost \blacksquare and \bullet), the actual concentration of the starting organic solution was $1.0 \pm 0.03\text{wt}\%$. The precision of solution preparation was dominantly determined by the volumetric measurement of the solvents, for which measuring cylinders were used. The accuracy was lower in

concentrated systems and higher in dilute systems because the solute – solvent ratio increasing with concentration. The accuracy was also influenced by the relative volume of the reaction mixture and the used measuring cylinder.

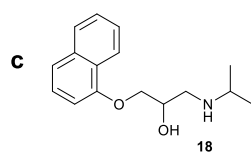
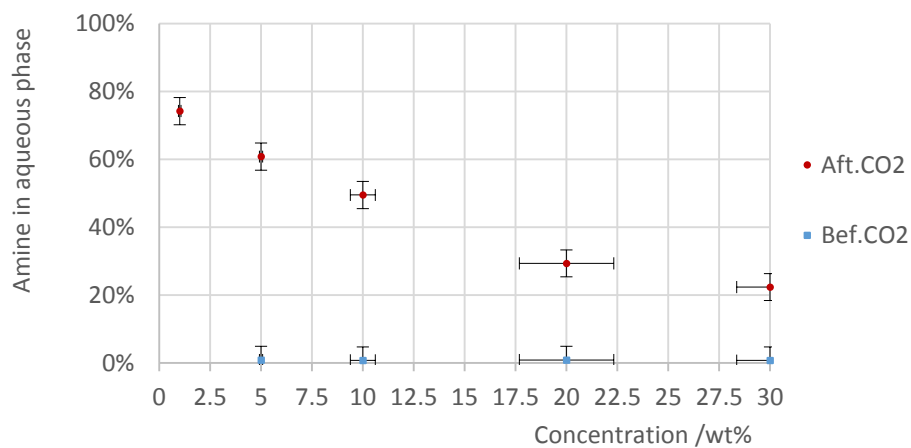
The tested amines predominantly remained in the organic phase before CO₂ exposure, and the distribution was not particularly concentration dependent. The ratio of *o*-nitrobenzyl propylamine **14**, Lidocaine **20**, Propranolol **18** and Prilocaine **19** in the aqueous phase were below 5% at all concentrations (Figure 2.14bde). This ratio was somewhat lower for *o*-nitrobenzyl methylamine **2**, for which a minor concentration dependence was also indicated. The distribution into the aqueous phase was slightly under 10% at the lowest concentration. It decreased to a local minimum with 5% distributing into the aqueous phase at 5wt% concentration. The distribution into the aqueous reached a minimum again in the most concentrated system at 30% (Figure 2.14a). The distribution of Propranolol **18** could not be tested above 10wt% concentration because of limited solubility (Figure 2.14c).

The set of experiments was repeated starting from the highest nominal concentrations again, but this time CO₂ was bubbled through the system for 15 minutes before each sampling.

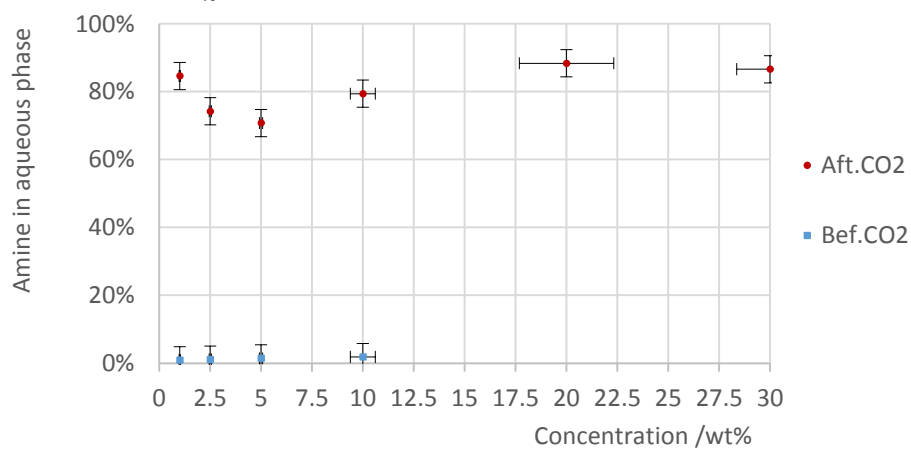




O-Nitrobenzyl propylamine



Propranolol



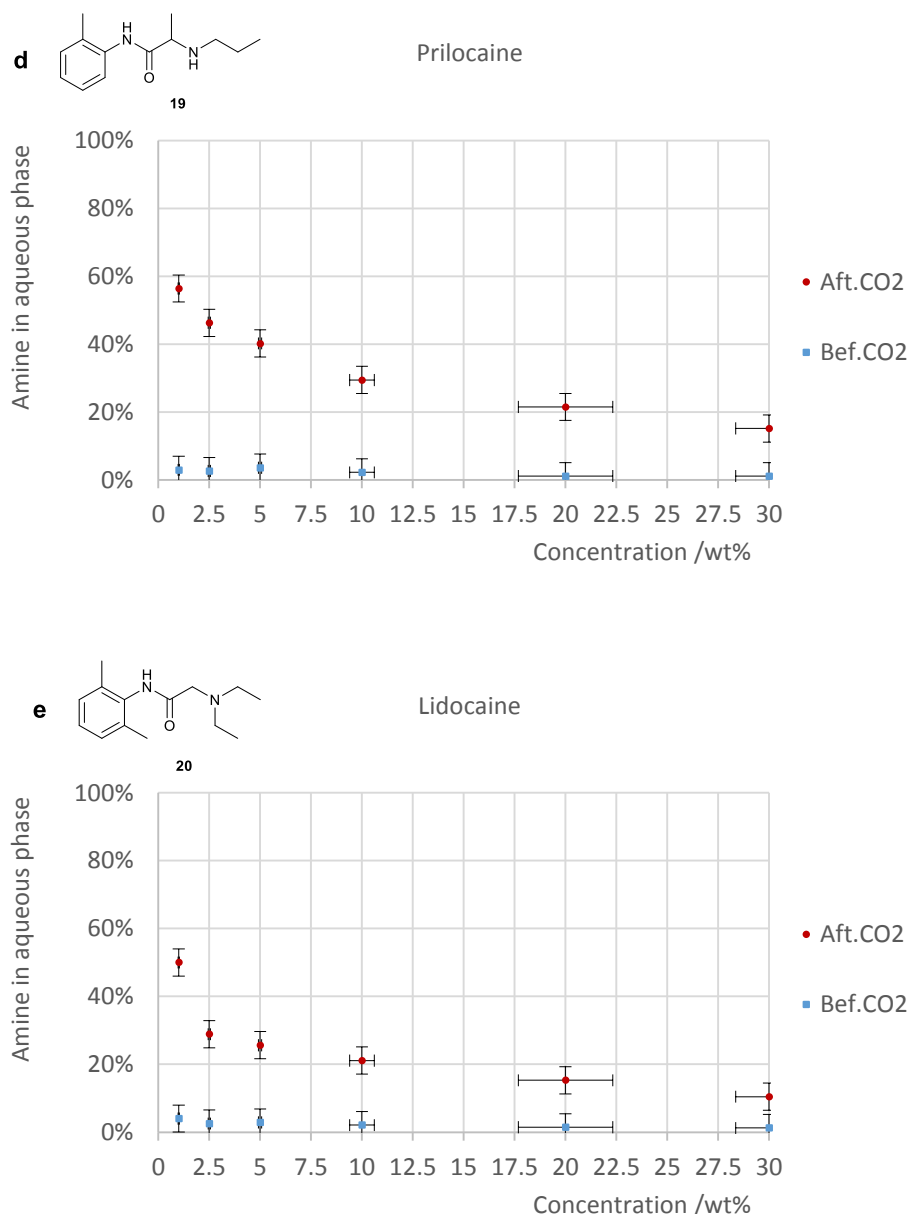


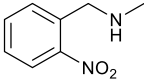
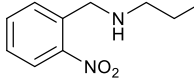
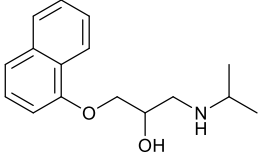
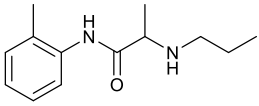
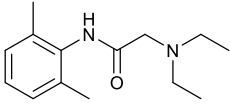
Figure 2.14a-e. Distribution of *o*-nitrobenzyl- methyl **2** (a) and propylamine **14** (b), Propranolol **18** (c), Prilocaine **19** (d), and Lidocaine **20** (e), between MTBE and water before (■) and after (•) CO₂ exposure, under ambient conditions.

2.9.4 Discussion of distribution tests before and after CO₂ saturation

The distribution of the tested bases dramatically changed after CO₂ exposure. A large fraction of base was extracted from the organic into the aqueous phase. A concentration dependency was observed, in general low concentrations favouring aqueous extraction with CO₂. The concentration dependence was significant for *o*-nitrobenzyl propylamine **14**, Prilocaine **19** and Lidocaine **20** (Figure 2.14bde). The amount extracted into the aqueous was about two times more at the lowest concentration compared to the highest concentration. The concentration dependence was the less significant for *o*-nitrobenzyl methylamine **2** and Propranolol **18** (Figure 2.14ac). The

extraction-concentration trace of these two bases exhibited a negative peak, between 5 and 10wt% for methylamine **2** and around 5wt% for Propranolol **18**. At these concentrations a minimal ratio could be extracted into the aqueous phase. Both lower and higher concentrations favoured aqueous extraction, with the highest extractions achieved at extreme low and extreme high concentrations. In case of Propranolol **18** the extraction-concentration trace was possibly affected by the low solubility in the organic solvent. Increasing Propranolol **18** concentrations in the organic phase possibly increased the chemical potential steeply, which could result in precipitation/limited solubility in the absence of CO₂, or pushing the solute into the aqueous phase in the presence of CO₂. Limited solubility was not observed for methylamine **2**, however the underlying reason, steep increase of chemical potential in the organic phase with concentration, relative to the increase in aqueous phase, may have been similar. A steeper increase of chemical potential for methylamine **2** relative to propylamine **14** may be explained by their different structure. Namely, propylamine **14** was more lipophilic because its longer aliphatic chain. As a consequence, dissolution of propylamine **14** could be more energetically favoured compared to the more hydrophilic methyl derivative. The explanation for the different behaviour of methyl and propyl derivatives based on the different lipophilic character seems even more feasible if the basicities are compared because the pK_a of the two amines were almost the same (Table 2.11, Entries 1 and 2), unlikely causing such dramatic change in aqueous extraction behaviour.

Table 2.11. *LogP* and *pK_a* values of the tested amines.

| Entry | Compound | <i>pK_a</i> | <i>logP</i> |
|-------|--|-----------------------|----------------------|
| 1 |  o-nitrobenzyl methylamine 2 | 8.89 ^[50] | 1.47 ^[80] |
| 2 |  o-nitrobenzyl propylamine 14 | 9.13 ^[50] | 2.35 ^[80] |
| 3 |  Propranolol 18 | 9.45 ^[63] | 3.37 ^[64] |
| 4 |  Prilocaine 19 | 7.32 ^[65] | 2.21 ^[66] |
| 5 |  Lidocaine 20 | 7.95 ^[72] | 2.44 ^[73] |

It could be concluded that the aqueous extraction worked better in dilute system. Any obvious pattern of concentration dependence from *pK_a* or *LogP*, was however, not revealed. The extraction efficiency of some bases rapidly decreased with concentration (Figure 2.14bde), other bases (Figure 2.14ac) showed less significant dependence. Low solubility in MTBE (Propranolol **18**), or lower lipophilicity (*o*-nitrobenzyl methylamine **2**) possibly favoured lower concentration dependency of CO₂ aided aqueous extraction.

2.9.5 Detailed studies of CO₂ uptake

The change of phase equilibria that could be achieved by CO₂ saturation of an aqueous-organic two phase system was discussed in the earlier paragraphs (2.9.3). The rate of CO₂ uptake could be also important for a separation procedure, because it could determine how quickly the equilibrium is reached. The phase equilibria of *o*-nitrobenzyl methylamine **2** + water + MTBE system was monitored as CO₂ was bubbled through with a stream of 0.5 l/min under ambient conditions. The *pH* of the aqueous phase was also measured. The nominal concentration of the system was 2.5wt% (Figure 2.15).

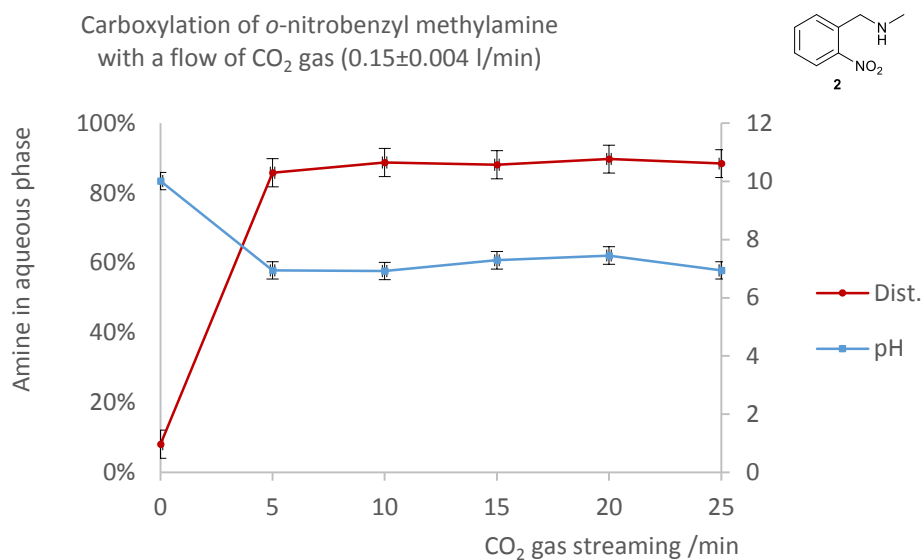


Figure 2.15. Distribution of *o*-nitrobenzyl methylamine **2** between water + MTBE through CO₂ streaming at 0.5 l/min under ambient conditions at 2.5% nominal concentration. The *pH* of the aqueous phase was also represented.

The CO₂ was in a significant excess: an equimolar amount flowed through the system approximately every 14 sec. The amine had a significant affinity for CO₂, and the carboxylation was complete possibly before the first sample was taken after 5 minutes of bubbling. The analysis of the distribution was based on sampling of the co-existing phases, during which the gas flow was suspended to allow the phases to separate. The sampling rate could not be enhanced further, mainly because resuming the flow required time (about 15 sec). Sampling times comparable to the time required for resume the flow could have increased experimental error. The taken samples were later analysed by UV/Vis spectrometry.

The *pH* of the aqueous phase was also measured. It quickly fell from about 10 to 7. The information learned from this experiment was the CO₂ uptake was a fairly rapid, and usually complete, well within the timescale of the experiments.

2.9.6 Detailed studies of N₂ gas induced neutralisation

As was highlighted in the introduction section, a neutralisation has to be subsequently carried out after acid aided aqueous extractions in order to isolate the basic product in a neutral form (2.5, p15; Figure 2.4). A significant disadvantage of using a conventional acid and base was salt formation in equimolar amounts. However, CO₂ aided aqueous extractions may potentially alleviate this disadvantage, and make the procedure greener. Formation of CO₂ adducts, for instance bicarbonate salts, are typically reversible. Simple degasification of the system could yield free amine (Figure 2.16).

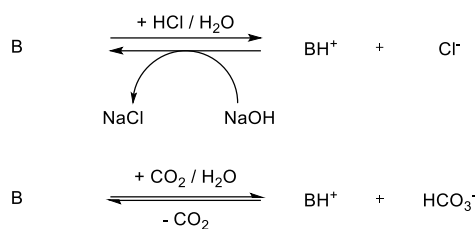


Figure 2.16. Salt formation with HCl and CO₂ and a subsequent neutralisation. Note that a base is needed for neutralising the hydrochloride salt, and a by-product (NaCl) is formed. In contrast, degasification is sufficient to neutralise a CO₂ adduct.

In the former section (2.9.5) CO₂ saturation was discussed and it was found to be rather rapid. The bottleneck of a CO₂ aided aqueous extraction combined with physical neutralisation was the slower neutralisation. In the following sections the neutralisation of CO₂ saturated amine + water + MTBE with N₂ gas sparging will be investigated, including the effects of the kind of the base, of the concentration of the base and of the N₂ gas flowrate.

2.9.7 Investigation of the effect of the base

In this section CO₂ saturated base + water + MTBE systems were decarboxylated by N₂ gas streaming. The decarboxylation was monitored by measuring the distribution of base between the aqueous and organic phase. The effect of the kind of the base was investigated by measuring the distribution of *o*-nitrobenzyl methyl- and propylamine **2** and **14**, Propranolol **18** and Prilocaine **19** during decarboxylation. The experiments were done under atmospheric pressure and temperature. The MTBE solution of these bases was stirred with water first. Samples were taken, which were analysed later by UV/Vis spectroscopy or HPLC. The sample, which was taken from the CO₂ free system, gave information of final distribution that could be expected after a complete decarboxylation. The amine + water + MTBE system was then saturated with a stream of CO₂ of 0.5 l/min for 15 minutes, therefore the excess was significant.[#] The CO₂ saturated systems were then decarboxylated by a stream of N₂ gas. Both N₂ and CO₂ streams were saturated by MTBE previously in order to minimise solvent loss from the experimental systems (Figure 2.13), helping to maintain composition and temperature. Samples were taken throughout the course of decarboxylation, and were analysed later (Figure 2.17-2.20).

[#]Amount of streamed CO₂: $0.5 \frac{\text{l}}{\text{min}} \times 15 \text{ min} \div 24 \frac{\text{l}}{\text{mol}} = 0.31 \text{ mol}$; amount of amine **2** in system: 1.00 g; (6.02 mmol)

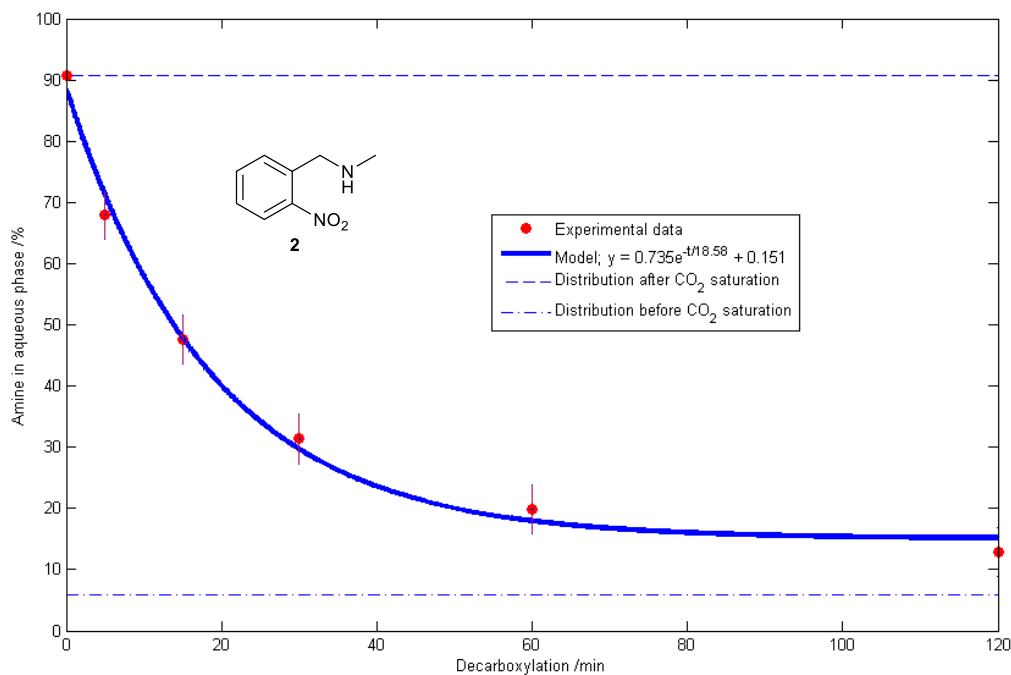


Figure 2.17. Distribution of *o*-nitrobenzyl methylamine **2** between MTBE and water during the course of N₂ gas induced decarboxylation (0.14 l/min) of the CO₂ saturated system at 2.5wt% nominal base concentration. Exponential decay curve was fitted on the experimental results.

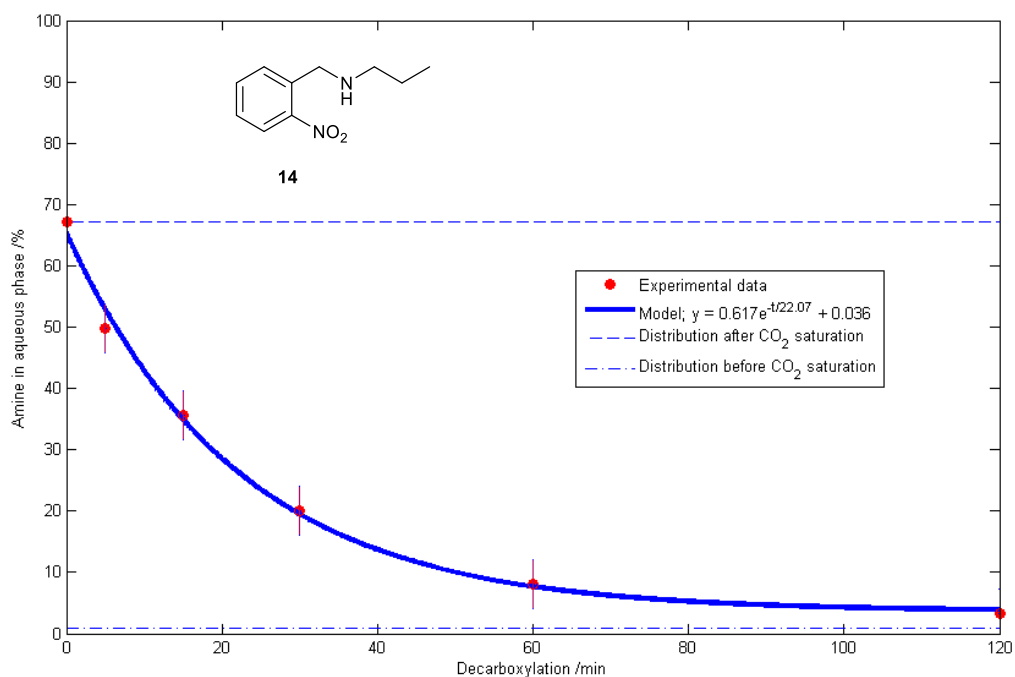


Figure 2.18. Distribution of *o*-nitrobenzyl propylamine **14** between MTBE and water during the course of N₂ gas induced decarboxylation (0.14 l/min) of the CO₂ saturated system at 5wt% nominal base concentration. Exponential decay curve was fitted on the experimental results.

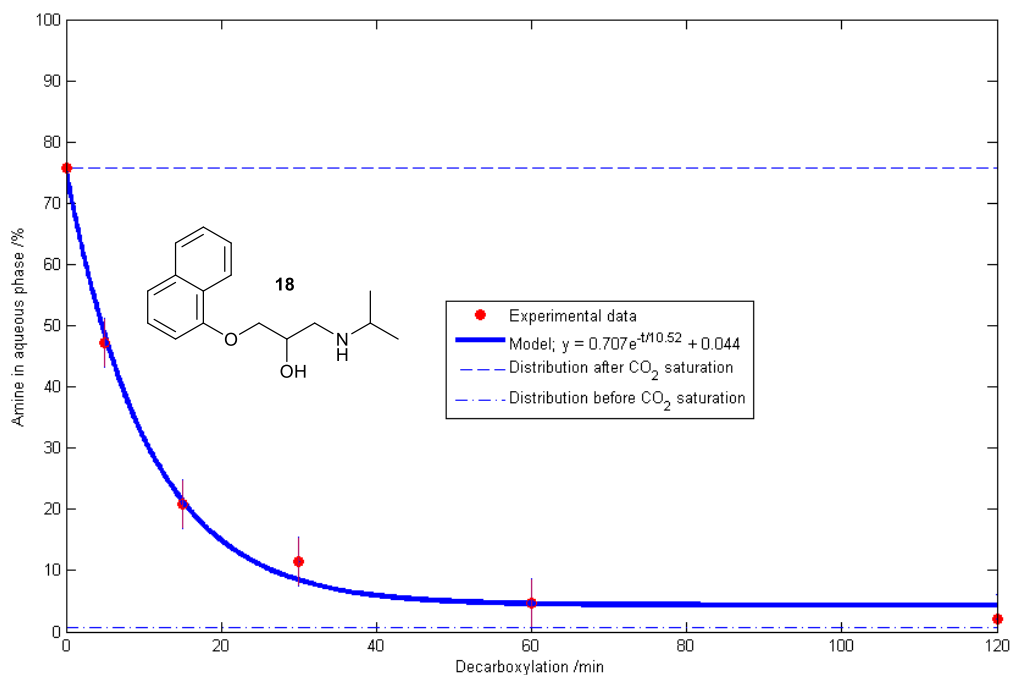


Figure 2.19. Distribution of Propranolol **18** between MTBE and water during the course of N₂ gas induced decarboxylation (0.14 l/min) of the CO₂ saturated system at 2.5wt% nominal base concentration. Exponential decay curve was fitted on the experimental results.

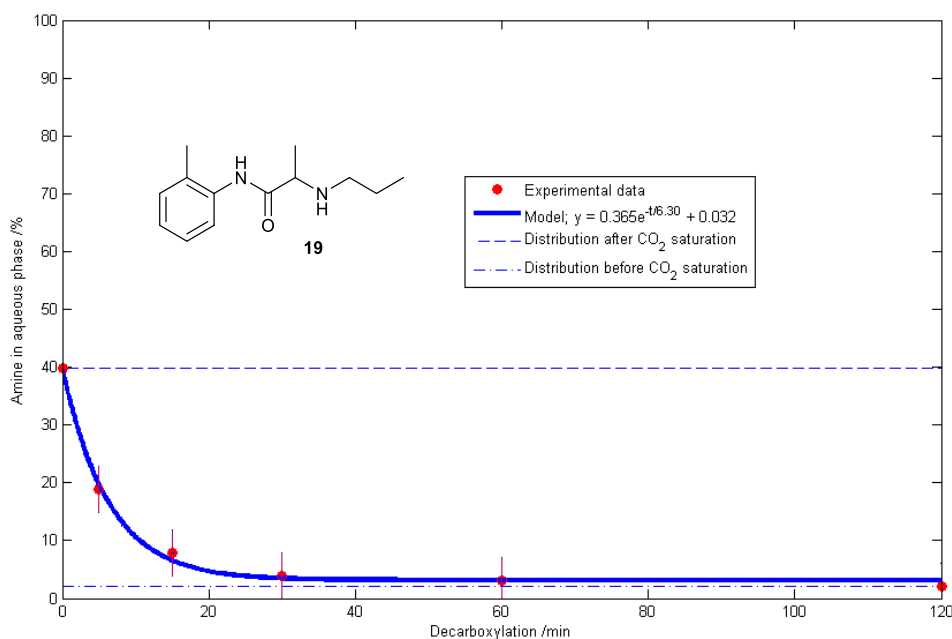


Figure 2.20. Distribution of Prilocaine **19** between MTBE and water during the course of N₂ gas induced decarboxylation (0.14 l/min) of the CO₂ saturated system at 2.5wt% nominal base concentration. Exponential decay curve was fitted on the experimental results.

Bubbling of N₂ gas into the CO₂ saturated systems caused decarboxylation. The distribution change is shown on the above figures by the portion of amine in the aqueous phase (Figure 2.17-2.20). The distributions of CO₂ saturated and CO₂ free systems are also shown. The starting point of the curves was the composition of the CO₂

saturated systems. The portion of amine in the CO₂ saturated aqueous phase before the neutralisation was the highest, nearly 90%, for *o*-nitrobenzyl methylamine **2**, it was intermediate for *o*-nitrobenzyl propylamine **14** and Propranolol **18** with about 67 and 75%, and it was the lowest for Prilocaine **19** with 40% (Table 2.12).

The portion of amine in the aqueous phase decreased continuously for all systems during decarboxylation. A simple model equation according to an exponential decay was fitted on the experimental data. The overall rate of decarboxylation can be described by the time constant of the exponential decay, τ , which is the time needed to carry out a distribution change, which is $1/e$ of the total change (Table 2.12). The τ values were obtained by fitting the equation of the exponential decay on the measurement points (Eq.21).

$$y(t) = A \cdot \exp\left(-\frac{t}{\tau}\right) + b$$

y(t): distribution as a function of time
A: initial distribution
t: time
 τ : time constant of decay
b: offset

Eq.21

The system of Prilocaine **19** exhibited the most rapid decarboxylation with a time constant of 6.3 min (Table 2.12, Entry 4). Decarboxylation of Propranolol **18** was two times slower, with a time constant of about 10.5 min (Table 2.12, Entry 3). Decarboxylation rate of the two nitrobenzyl amines were similar with time constants of about 18.5 min for methyl, and 22 min for propyl derivative (Table 2.12, Entries 1, 2).

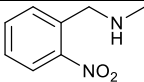
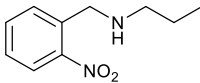
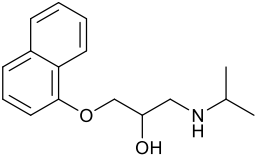
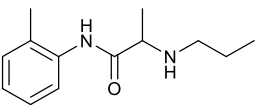
The system of Prilocaine **19** reached complete decarboxylation after about 40 minutes. 120 minutes were necessary for the system of Propranolol **18**. Nitrobenzylamines **2** and **14** did not reach complete decarboxylation even after 120 minutes.

The affinity of the base to CO₂ could relate to the rate of decarboxylation and to the initial ratio of amine in the aqueous phase in the CO₂ saturated system. A correlation between this affinity and basic strength or lipophilicity (pK_a and $\log P$) was expected. Apparently, it was Prilocaine **19** that had the least affinity for CO₂. This was manifested in the poorest ratio of amine in the aqueous phase at starting point (about 40%), and a rapid and complete decomposition (Table 2.11, Entry 4). Prilocaine **19** was the least basic of the tested amines. The affinity of CO₂ and Propranolol **18** was intermediate (Table 2.11, Entry 3). The composition of the CO₂ saturated solution was comparable to *o*-nitrobenzyl propylamine **14**, but the rate of decarboxylation was closer to Prilocaine **19**. Propranolol **18** was the most basic and the most lipophilic substrate in this study. *O*-Nitrobenzyl methylamine **2** had the highest affinity for CO₂ because it had the highest ratio of amine in aqueous in the CO₂ saturated system, and its decarboxylation was the least complete and was slow with a high time constant, second last after *o*-nitrobenzyl propylamine **14** (Table 2.11, Entries 1 and 2). The basicity of the two tested nitrobenzylamines **2** and **14** were very close to each other, around 9. Yet, significant

difference was observed in their affinity to CO₂, which could be explained by their different lipophilic character with about one *logP* difference.

In summary, the ratio of amine extracted into the aqueous phase in the CO₂ saturated systems, and rate of N₂ gas induced decarboxylation were possibly affected by basicity and lipophilicity, determined by *pK_a* and *logP*. The amount of data available were limited because of time consuming experiments and it did not allow detailed investigation of the correlation, such that was completed for screening studies (2.8.5). However, according to the available information, low basicity disfavoured high distribution into aqueous phase (Prilocaine **19**, Table 2.11, Entry 4). The rate of decarboxylation was affected by both *pK_a* and *logP*. Propranolol **18** (Table 2.11, Entry 3) had relatively high initial distribution into the aqueous phase because of its high *pK_a*, but its decarboxylation rate was relatively rapid, possibly because of the high *logP*. In contrast, Prilocaine **19** had the quickest and *o*-nitrobenzyl propylamine **14** had the slowest decarboxylation rates, even though they had very similar *logPs*, but different *pK_as* (Table 2.11, Entries 2 and 4). This indicated the importance of *pK_a* for the decarboxylation rate was also important. The two nitrobenzylamines **2** and **14** had very similar *pK_as* but different *logPs* (Table 2.11, Entries 1 and 2). Slow decarboxylation rates were measured, with methyl derivative having lower *logP* decarboxylating somewhat quicker. Other factors, such as steric hindrance of the basic amines, may be also important.

Table 2.12. Physical values of the tested amines (*pK_a* and *logP*), the ratio of amine in the aqueous phase in the CO₂ saturated system, and the time constant (τ) of N₂ gas induced decarboxylation.

| Entry | Compound | <i>pK_a</i> | <i>logP</i> | Amine ratio (initial, Aq.) /% | τ /min |
|-------|--|-----------------------|----------------------|-------------------------------|-------------|
| 1 |  o-nitrobenzyl methylamine 2 | 8.89 ^[50] | 1.47 ^[80] | 90.7 | 18.58 |
| 2 |  o-nitrobenzyl propylamine 14 | 9.13 ^[50] | 2.35 ^[80] | 67.1 | 22.07 |
| 3 |  Propranolol 18 | 9.45 ^[63] | 3.37 ^[64] | 75.7 | 10.52 |
| 4 |  Prilocaine 19 | 7.32 ^[65] | 2.21 ^[66] | 39.9 | 6.30 |

2.9.8 Investigation of the effect of nominal amine concentration

The effect of nominal amine concentration on the rate of decarboxylation was investigated for the *o*-nitrobenzyl methylamine **2** + water + MTBE system (Figure 2.21). The maximal nominal concentration was not limited by solubility because the amine was miscible in MTBE over the whole concentration range. However, above 30wt% concentration, strong foaming was observed, and the stream of N₂ gas, which was 0.15 l/min, could not be maintained.

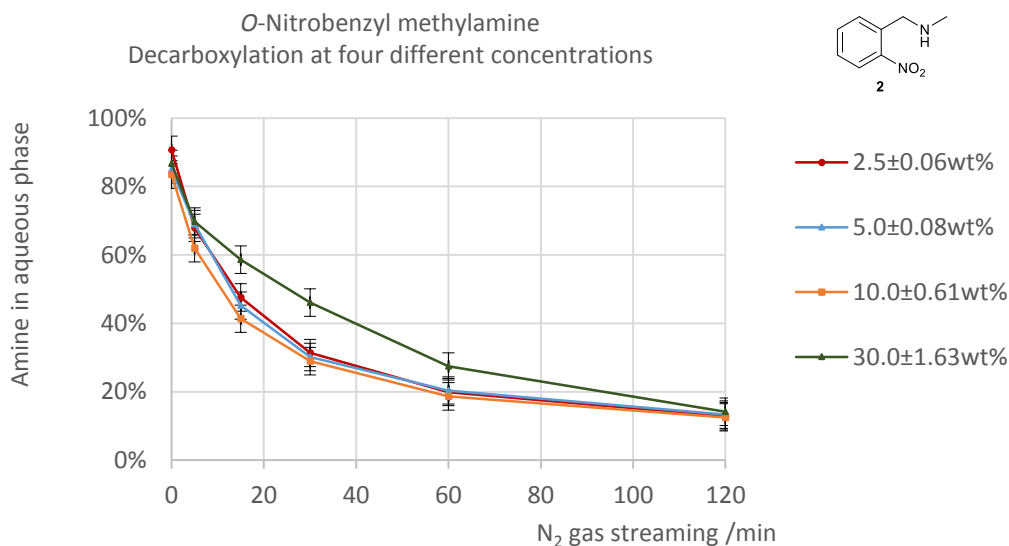


Figure 2.21. Decarboxylation of the CO₂ saturated *o*-nitrobenzyl methylamine **2** + water + MTBE system with a stream of N₂ gas (0.15 l/min) at four different nominal concentrations.

As it could be concluded from the figure, the concentration did not affect the decarboxylation rate at concentrations 2.5 to 10wt%. In fact, the difference between the measured curves in this concentration range was within experimental error. However, the decarboxylation at the highest concentration (30wt%), at which the amount of solute in the system was comparable to the amount of solvent, was somewhat slower, although the shape of the decay was still quite close.

2.9.9 Investigation of the effect of N₂ gas flowrate

The effect of N₂ gas flowrate on the decarboxylation of the *o*-nitrobenzyl methylamine **2** + water + MTBE system was also investigated (Figure 2.22). The gas was introduced into the two phase system through a sparger. The application of the sparger caused certain limitations of the available flowrates. Below a certain flowrate (approximately around 0.1 l/min) the sparging did not function properly, with large bubbles leaving the upper surface of the sparger. The upper flowrate limitation of the experiment was 0.5-0.6 l/min, at which the gas started to discharge the reaction mixture from the experimental vessel. The regime of flow was the same between the low and

high limits by appearance: small bubbles with an approximate diameter below 1 mm entered the aqueous phase, flowed through both phases by vigorously stirring them, and eventually left the system to the atmosphere.

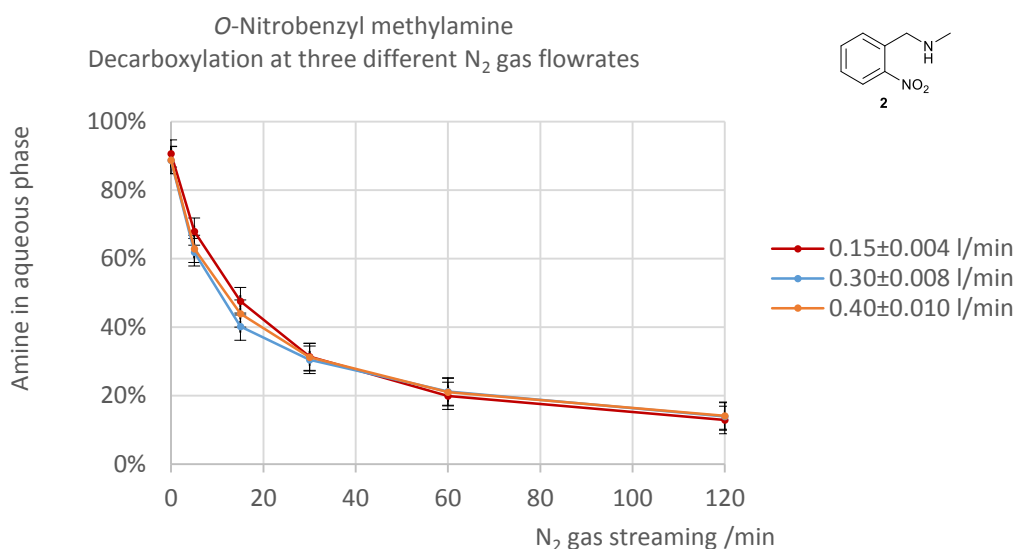


Figure 2.22. Decarboxylation of the CO₂ saturated *o*-nitrobenzyl methylamine **2** + water + MTBE system with a stream of N₂ gas at different flowrates at 2.5wt% nominal concentration.

The measurement of the initial distribution of amine between aqueous and organic phases was also measured with higher sampling rate to obtain more detailed information about this region (Figure 2.23).

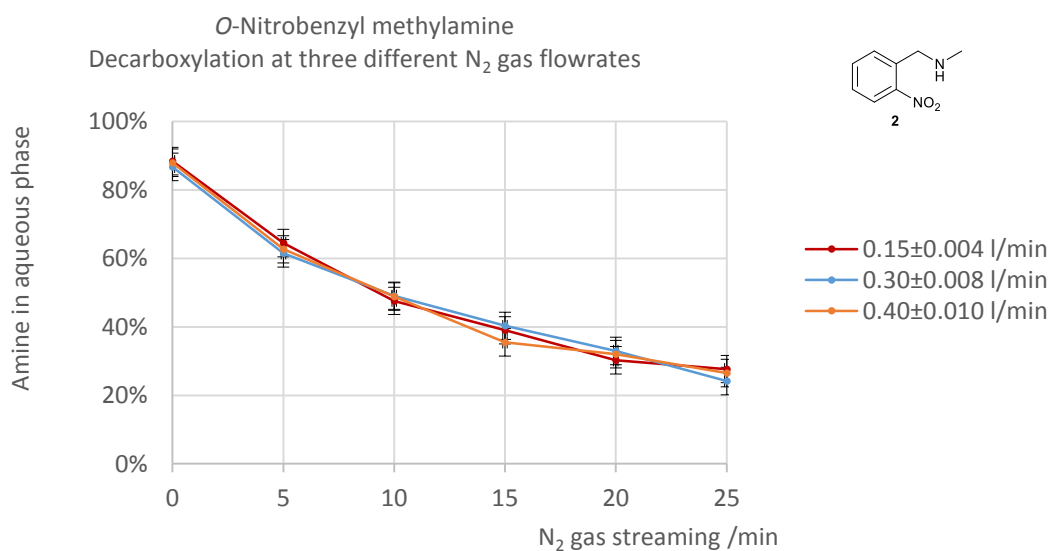


Figure 2.23. Initial stage of the N₂ gas induced decarboxylation of the CO₂ saturated *o*-nitrobenzyl methylamine **2** + water + MTBE system with a stream of N₂ gas at different flowrates at 2.5wt% nominal concentration.

The rate of amine migration from aqueous to organic was apparently independent of the N₂ gas flowrate within the regimes measured. The measured points on the figures

were within the range of experimental deviation. It has to be noted, however, that the concentration of species originated from CO₂, such as physically dissolved CO₂, H₂CO₃ or HCO₃⁻, and the amount of expelled CO₂ were higher at higher nominal base concentrations.

2.9.10 Investigation of *pH* during the course of decarboxylation

The *pH* could be measured much simpler compared to the measurement of distribution by sampling, dilution and spectroscopy or HPLC. Correlation between amine distribution between the phases and *pH* was investigated, with a goal to conclude that this simpler measurement could provide sufficient information about the decarboxylation. A standard glass electrode was immersed into the aqueous part of the two phase system, and *pH* was also measured during decarboxylation (Figure 2.24)

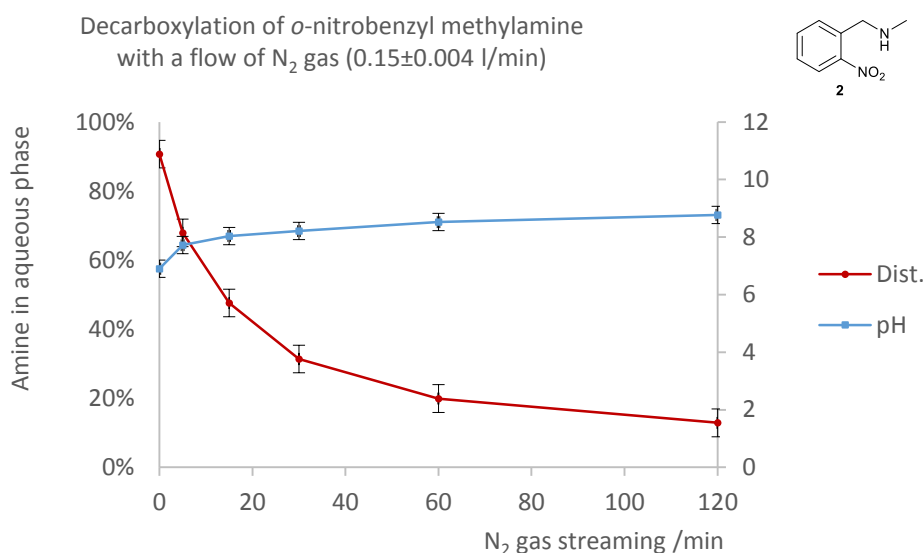


Figure 2.24. Distribution and *pH* trace during the N₂ gas induced decarboxylation of the CO₂ saturated *o*-nitrobenzyl methylamine **2** + water + MTBE system. Nominal concentration: 2.5wt%.

The results of *pH* measurement correlated to the results obtained by sampling and spectrophotometry, however, they were less sensitive to the actual state of the system: the difference between CO₂ saturated (*pH* = 7.0) and CO₂ free system (*pH* = 10.0) was only three units in terms of *pH*. The combined accuracy of *pH* electrode and *pH* meter was around ±0.3 *pH* units. In contrast, amine distributing to the aqueous phase before and after CO₂ saturation was 94.1 and 9.3%, respectively, which were determined by sampling and spectrophotometry with an accuracy of ±4%.

2.9.11 Discussion of phenomena during N₂ gas induced decarboxylation

In the former sections experimental data of the *o*-nitrobenzyl methylamine **2** + water + MTBE system were summarised during the course of N₂ gas induced decarboxylation.

Before the discussion of the obtained data, phenomena during the decarboxylation should be summarised.

The experimental setup was a vessel of cylindrical shape with the heavy phase (aqueous) on the bottom, and the light phase (organic) on the top. A sparger was immersed into the system, through which N_2 gas was streamed. The gas stream was saturated with organic solvent before entering the system to avoid solvent evaporation during the experiment (Figure 2.13). The bubbles of N_2 gas entered into the aqueous layer through the sparger. The mean diameter of the bubbles could not be measured. The mean diameter of the bubbles was below 1 mm between the flowrates of 0.1 and 0.5 l/min, determined by visual observation.

The N_2 gas bubble travelled through the aqueous and then the organic layer. In the aqueous layer it picked up CO_2 gas. The two gases were completely miscible, behaving ideally from this perspective. The bubble, now containing $N_2 + CO_2$ gases, entered the organic phase, and possibly simply travelled through it, because the solubility of CO_2 in the organic phase could be considered minimal at atmospheric pressure, and therefore could be neglected compared to the solubility in water. This is not to be confused with gas expanded liquids. At elevated pressure the solubility of CO_2 is significantly lower in water compared to most of the organic solvents. The residence time of the bubble was determined by the density difference and hydraulic resistance, which was affected by the bubble size. The flow of gas also stirred the system. The efficiency of stirring, by appearance, seemed equally vigorous, regardless the gas flowrate. As the pH of the aqueous phase was increasing because of the expelled CO_2 , free amine was extracted from the aqueous to the organic phase. The gas bubbles containing the CO_2 eventually left the system.

The amount of CO_2 picked up by the bubble could be thermodynamically or kinetically controlled. Under thermodynamic control, the fugacity of CO_2 in the aqueous phase would be equal to the fugacity of CO_2 in the bubble (thermodynamic equilibrium). The fugacity of CO_2 in the aqueous phase was the vapour pressure of dissolved CO_2 , the fugacity of CO_2 in the bubble was the partial pressure. Increasing N_2 gas flow would increase the rate of CO_2 removal, boosting decarboxylation. This was not observed (Figure 2.21).

Kinetic control reigns if the two fugacities were not equal because of any reason. If the residence time of the bubble was too low, or the stirring was not efficient enough, or the chain of chemical reactions forming CO_2 had a rate controlling step, the decarboxylation could be considered kinetically controlled. The independence of decarboxylation rate from N_2 gas flowrate indicated (Figure 2.21 and 2.22), the amount of CO_2 taken from the system into the gas bubble was about the same, regardless of the

flowrate. Increased flowrate would therefore decrease the concentration, or fugacity of CO₂ in the gas stream. Even the lowest N₂ gas flowrate could take away all the CO₂ that was available. Therefore, a kinetic control could be assumed.

The rate of decarboxylation was also independent of the nominal concentration, as far as the distribution of the amine between the phases was concerned. However, the amount of dissolved CO₂ was very different at various nominal concentrations because of the higher amount of base in the system during CO₂ saturation. Increased amount of base in the system would push equilibrium I to the left, which would consume carbonic acid and produce bicarbonate (Figure 2.25). The consumption of carbonic acid would affect equilibria II and III, and consequently more CO₂ would be dissolved in the system. Decreased concentration of free base (B) in the aqueous phase would also affect equilibrium IV: amine would be extracted from the organic phase into the aqueous phase. Direct decarboxylation of bicarbonate into CO₂ and OH⁻ is also possible (equilibrium V). Whether the physically dissolved CO₂ forms HCO₃⁻ directly with OH⁻, or through H₂CO₃ is *pH* dependent, likewise pathway of the opposite reaction, which is decomposition of H₂CO₃ to give dissolved CO₂.^[82]

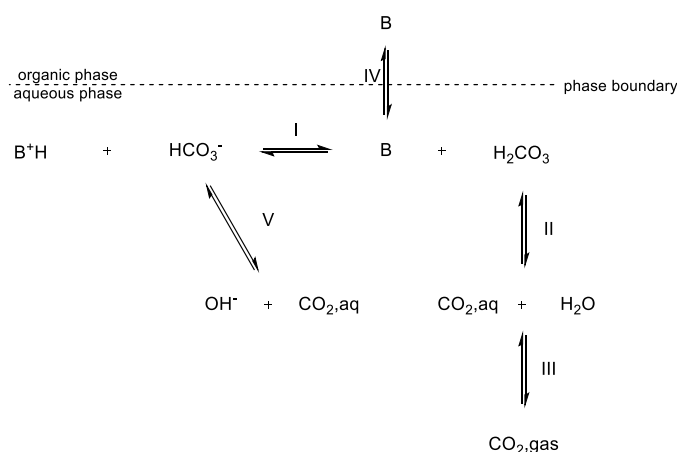


Figure 2.25. Chain of equilibria for an amine + CO₂ + organic solvent +water two phase system.

The decarboxylation experiments at different nominal concentrations (Figure 2.21) can be considered from the perspective of the amount of expelled CO₂. Systems with higher amine concentrations also contained higher overall amount of CO₂, which could result in higher CO₂ fugacity that is higher vapour pressure of CO₂. Therefore, higher amount of CO₂ could be taken away by the steam of N₂ gas. Moreover, the correlation seemed linear: two or three times more concentrated system lost two or three times more CO₂. This would suggest a Henry type concentration-fugacity correlation for the first sight. However, experiments with different N₂ gas flowrates showed kinetic control, because increased N₂ streams did not increase the rate of decarboxylation (2.9.9). The N₂ gas stream took all the available CO₂, of which amount was determined by the fugacity of the physically dissolved CO₂.

The behaviour of the most concentrated system at 30% was somewhat different. It had a slower decarboxylation compared to more dilute systems. The amount of amine in this system was comparable to the amount of solvent. Because of the significantly higher viscosity, possibly kinetic control was obeyed (Figure 2.21). It can be suspected that more efficient stirring or agitation would enhance the decarboxylation rate of the most concentrated system. This could be achieved by higher N₂ gas flowrates.

2.9.12 Summary of N₂ gas induced decarboxylation

The independence of decarboxylation from the flowrate indicated there was possibly no thermodynamic equilibrium between the gas and the liquid phases. Higher flowrates would also enhance the stirring of liquid phases, therefore mass transfer limitations on the interface were not likely rate determining.

The progress of the decarboxylation was monitored by the distribution of amines between the phases, monitored by sampling and analysis. The concentration dependency of decarboxylation was minimal, as long as the ratio of amine between the two phases was used to indicate the progress of decarboxylation. However, the amount of decarboxylated amine in a period of time linearly increased with the overall concentration. However, at very high amine concentration (30wt%), decrease of decarboxylation was observed. Possibly mass transfer limitations emerged as the viscosity of the system increased.

The base had a dramatic effect on the rate of decarboxylation. This also implied, the decarboxylation was possibly not a straightforward first order bicarbonate decomposition, of which rate would depend only on the concentration of dissolved bicarbonate, and the type of base would be indifferent.

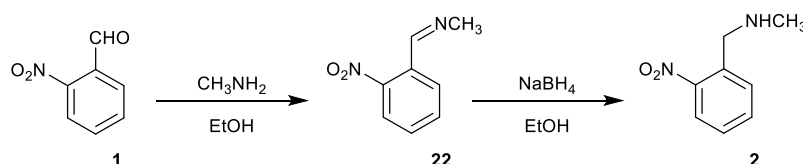
The better understanding of N₂ gas induced decarboxylation requires further research. Acquiring decarboxylation data at different temperatures could indicate whether the rate limitation was mass transport or chemistry related. The base clearly had an effect on the decomposition, therefore the kinetics were not determined solely by the decomposition of bicarbonate. Even though the literature suggests that amine - CO₂ adducts are present as bicarbonates in aqueous solutions,^[83] presence of carbamates, either as intermediates of bicarbonate decomposition, or even as the main species in aqueous solution, cannot be entirely excluded, and should be investigated further.

2.10 Optimised preparative procedure for the purification of *o*-nitrobenzyl methylamine **2** *via* CO₂ aided aqueous extraction combined with N₂ gas induced neutralisation

The preceding studies had provided quantitative information about the extraction/neutralisation processes of base + CO₂ + water + MTBE systems, including numerous amines. In the following sections, this information was used to demonstrate and enhance the effective purification of *o*-nitrobenzyl methylamine **2** *via* CO₂ aided aqueous extraction.

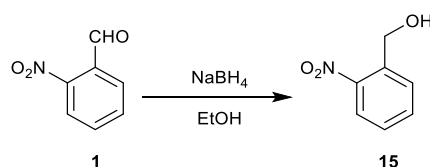
The distribution of *o*-nitrobenzyl methylamine **2** between water and MTBE after CO₂ saturation suggested, it was either a very dilute organic solution that could be extracted well into water + CO₂, or a fairly concentrated. At 1% concentration about 93% was extracted into water + CO₂, but only about 83% at 10wt% concentration (Figure 2.14a). The extraction of amine into aqueous was about 88% at 30wt% nominal concentration. The difference in terms of extraction was not significant between 1 and 30%, therefore the higher concentration was chosen because the amount of solvents could be reduced. This would render the procedure greener and also more effective, because smaller equipment volumes could be used.

O-Nitrobenzyl methylamine **2** is an intermediate of SB-214857-A (Scheme 1.1).^[12-13] It is obtained by the reductive amination of *o*-nitrobenzaldehyde **1** (Scheme 2.7).



Scheme 2.7. Synthesis of methylamine **2** *via* reductive amination.

The main side reaction of the procedure was reduction of starting material *o*-nitrobenzaldehyde **1** to benzylalcohol **15**.



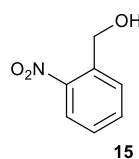
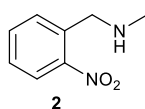
Scheme 2.8. A potential side reaction of reductive amination under the reaction conditions: Reduction of aldehyde **1** to by-product benzylalcohol **15**.

Sophisticated reductions, that exclusively reduce imine **22** in the presence of aldehyde **1**, may be available.^[49] However, this research focuses on the separation of these by-products rather than avoiding their production *via* a more advanced synthesis.

The level of benzylalcohol **15** contamination in the crude of methylamine **2** was between 5 and 10%, determined by $^1\text{H-NMR}$ spectra integration. The initial 60.7% recovery was enhanced to 70.7%, simply by increasing the concentration from 10% to 30% (Table 2.13, Method – I). High concentrations did not favour neutralisation and the subsequent aqueous to organic extraction, therefore the length of neutralisation was extended (Table 2.13, Method – II): Instead of bubbling N_2 gas for only 15 minutes before each organic extraction, the decarboxylation was extended to 15, 30 and 90 minutes before each organic extraction. The aqueous extraction was also divided. The recovery increased further, up to 85%. This recovery was comparable to those expected from acid based aqueous extractions.

Table 2.13. Summary of preparative aqueous extractions of *o*-nitrobenzyl methylamine **2**. The yield was enhanced from 61% to 85% after optimisation.

| Nominal Concentration | | 10% | 30% / Method - I | 30% / Method - II |
|---|--------------------|----------------|---------------------|----------------------|
| Composition (crude) amine 2 - alcohol 15 | | 89.7% - 10.3% | 95.2% - 4.8% | 94.8% - 5.2% |
| Organic to aqueous extraction (CO_2 bubbling) | Bubbling time /min | 1×15 | 1×15 | 2×15 |
| | Volume of water | 1 vol equiv. | 1 vol equiv. | 2×0.5 vol equiv. |
| Aqueous to organic extraction (N_2 gas bubbling) | Bubbling time /min | 3×15 | 3×15 | 1×15, 1×30, 1×90 |
| | Volume of MTBE | 3×1 vol equiv. | 3×1 vol equiv. | 3×1 vol equiv. |
| Composition (purified) amine 2 - alcohol 15 | | 98.86% - 1.14% | 98.68% - 1.32% | 98.11% - 1.89% |
| Yield | | 60.7% | 70.7% | 85.2% |



2.11 Summary

In the former sections the distribution of organic bases between organic solvent and water was investigated, and the effect of CO_2 on this distribution. The results of the screening experiments indicated a pK_a and $\log P$ dependence of the extraction into water + CO_2 . An empiric correlation was proposed, that allowed prediction whether the extraction of a weak organic base from its organic solution into water in the presence of CO_2 is likely (Eq.18), unlikely (Eq.17) or intermediate (Eq.19). This is a great help for designing aqueous extractions, for which the extraction effect of pure water should also be taken into account, with $\log P$ s preferably above 0.5.

The rate of CO₂ intake during aqueous extractions was found to be rapid. However, N₂ gas induced decarboxylation was significantly slower. This reagent-free way of neutralisation prevented the formation of inorganic salt by-products, which are formed in equimolar amount if conventional acids/bases are used affecting the E-factor badly. It was found, at low base concentrations the decarboxylation was apparently independent of N₂ gas streaming as far as the distribution was concerned. At higher concentration, however, more amine could be extracted back to the organic phase, consequently the whole procedure was more efficient. If the concentration increased further, mass transport limitations slowed the decarboxylation possibly because of the higher viscosity. The decarboxylation could potentially be enhanced by more intensive agitation in this concentration range. The decarboxylation could be possibly enhanced by higher operational temperatures.

A green purification procedure based on CO₂ aided aqueous extraction was developed for *o*-nitrobenzyl methylamine **2**, intermediate of AZ drug candidate SB-214857-A. The levels of benzylalcohol **15** contamination were reduced from about 5-10%, typical contamination level in the crude, to below 2%, while the recovery was about 85%, without the formation of inorganic salt by-products. The performance of separation could be better for by-products less hydrophilic than benzylalcohol **15**.

Chapter - 3

Carbon dioxide based approach to new crystallisation procedures

3.1 Introduction to crystallisations

Crystallisation is a preferred separation procedure of chemistry laboratories, chemical and related industries. Crystallisation is a separation procedure that exploits a liquid to solid phase transition. The liquid phase is most commonly a solution, but it could also be a melt.^[3] The thermodynamic driving force that pushes the valuable compound from liquid phase to solid crystalline phase is reduction in the chemical potential.^[37] The chemical potential of the valuable compound therefore must be higher in the liquid phase, than in solid phase. Such a liquid is referred as sub cooled or supersaturated solution, that is a solution holding more solute dissolved than the amount of solute could be dissolved under the same conditions, with equilibrium between solid and liquid phase.^[36] A non-saturated solution can be made supersaturated in many ways. If a portion of solvent is removed from a non-saturated solution *via* evaporation, either at atmospheric pressure or vacuum, it reaches supersaturation. Subject to the temperature dependence of solubility of the solute, cooling could have the same effect. Mixing the solution with a second solvent, a so called antisolvent, can also induce supersaturation. Addition of chemicals to a non-saturated solution could also create a supersaturated solution, by chemically transforming the solute to another chemical entity with different solute characteristics.

A supersaturated solution is an essential thermodynamic requirement of crystal growth. However, it is not sufficient by itself. Solutions, such as honey, can exist in a thermodynamically disfavoured supersaturated state for years. There is a certain kinetic hindrance that the system has to overcome. Once nucleation, the formation of the first crystal, occurs, precipitation starts in the form of crystal growth until thermodynamic equilibrium is reached.^[36] Nucleation could be stimulated by addition of inoculating seed, agitation, sonication, etc.

The relationship between the rate of nucleation and rate of crystal growth can determine a mean crystal size. This could be important in a subsequent step of the procedure, which is typically a filtration. On one hand, too small crystals disfavour filtration because of clogging and high hydraulic resistance of the cake. On the other hand, too large crystals may contain inclusions of the mother liquor reducing the efficacy of the separation and rendering the drying more difficult.

3.2 Chemically induced crystallisation

Chemicals can be used to create a supersaturated solution from a non-saturated solution. These auxiliary chemicals are typically acids or bases. Precipitation of the

desired acidic/basic organic compound in free form may be induced by neutralising a non-saturated aqueous solution of its salt, provided the free base is crystalline. An acid/base is needed to create a water soluble salt of the organic first, and another base/acid is needed for the neutralisation step, in which the used auxiliary chemicals form a soluble salt, while the desired product precipitates in free form.

Alternatively, precipitation of the desired organic compound in salt form may be induced from its non-saturated solution in organic solvent by the addition of base or acid. The formed salt must be a crystalline solid and have low solubility in the organic solvent. Other requirement is that reaction other than acid/base, such as Lucas type alkyl- or benzyl halogenide formation, must not take place under the conditions of the procedure. Production of these species using hydrogen halogenide as an acid may preclude the procedure because they are potentially genotoxic impurities (2.5).^[42, 44]

3.2.1 Crystallisation in industry

Crystallisation, in general, can be a less energy intensive separation procedure compared to distillation, although heat transactions could be involved in the preparation of a supersaturated solutions. The energy needs of producing a supersaturated solution by evaporation is comparable to distillation. However, a procedure of preparing a solution at elevated temperature and cooling it down in a subsequent step to create a supersaturated solution could be significantly less energy intensive. Energy requirements to heat up 1000 ml water from 20 °C to 100 °C is less than sixth of the evaporation enthalpy at boiling point (Table 3.1).

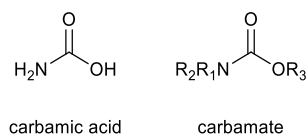
Table 3.1. Energy requirements of heating or evaporating 1000 ml water.^[23]

| | |
|------------------------------|-----------------------|
| Heating from 20 °C to 100 °C | Evaporation at 100 °C |
| 336 KJ | 2270 KJ |

Use of chemicals to form supersaturated solutions could potentially reduce energy consumption further. A disadvantage of using reagents, other than the cost of them, is salt by-product formation in equimolar amount in a final neutralisation, and reduced atom efficiency of the whole procedure.^[2]

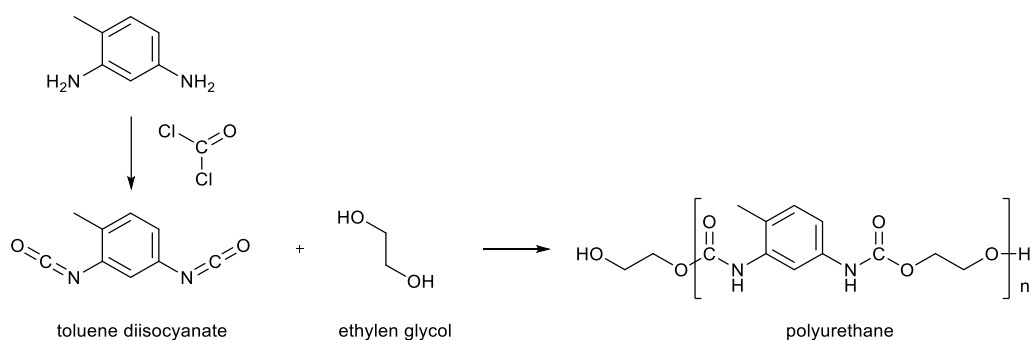
3.3 Carbamates

Carbamates are derivatives of carbamic acid, in which the hydrogen atoms are substituted by alkyl or aryl groups (Scheme 3.1).^[5] Carbamic acid itself is unstable under ambient conditions, therefore its practical use is limited. In contrast, carbamates, which are derivatives of carbamic acid, can be stable, and found numerous applications.



Scheme 3.1. Carbamic acid and carbamates.^[5]

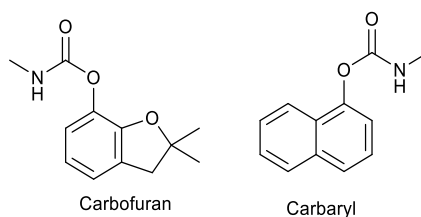
Polycarbamates, also known as polyurethanes, were invented by Bayer in 1937, and they were first synthesised by the polyaddition of diisocyanates and diols (Scheme 3.2).^[84] The unique properties of this high value polymer, such as excellent strength to weight ratio and energy absorbing performance, is exploited in numerous applications, such as the automotive industry. Numerous polyurethane derivatives with different qualities can be produced by using different starting materials. Production of crosslinked polymer chains is also possible by using a triol as starting material.^[85] Polyurethanes are therefore fairly versatile, and could be formulated as soft or rigid foams, elastomers, or as hard or flexible plastics. Polyurethanes had a 7% share of the European polymer market in 2011.^[86]



Scheme 3.2. Synthesis of polyurethane using phosgene.^[84]

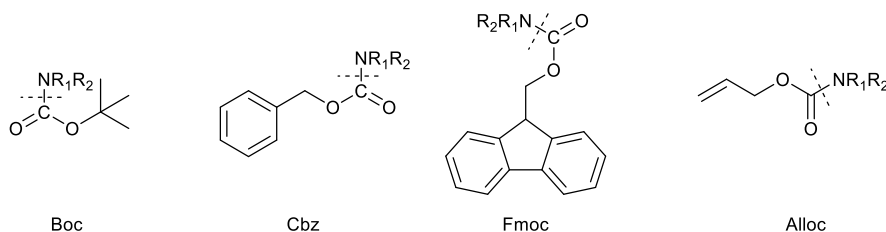
A great disadvantage of this polymer is that its starting monomers, which are isocyanates, are typically produced using phosgene (Scheme 3.2). Alternative sources to replace phosgene, such as carbon dioxide, are currently investigated.^[86]

Carbamate insecticides, such as Carbofuran or Carbaryl (Scheme 3.3), inactivate the enzyme acetylcholinesterase. The inactivation is reversible in contrast to organophosphate ester insecticides. Nevertheless, carbamate insecticides can still be very toxic for humans. Carbamate insecticides are conventionally synthesised using phosgene, similar to polyurethanes.^[87]



Scheme 3.3. Carbamate insecticides.

The carbamate groups are widely used in synthetic organic chemistry for temporary protection of amine or aniline functions. Having protected a reactive amine function, a desired change on the less reactive function can be carried out. This is widely exploited for peptide syntheses.^[5] Some carbamate protecting groups are listed below (Scheme 3.4).



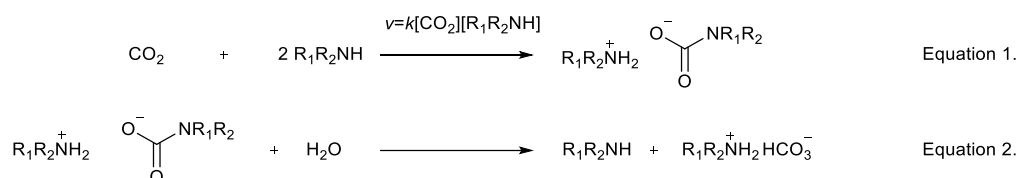
Scheme 3.4. Carbamate protecting groups: *t*-butylcarbonyl (Boc), benzyloxycarbonyl (Cbz), 9-fluorenylmethyl (Fmoc) and allyloxycarbonyl (Alloc) protected amine functions.^[88]

The protection is usually carried out by acylation of the amine function by either acid chloride or anhydride of the corresponding carbonic acid derivative. The amines are typically deprotected by hydrogenolysis or acid catalysed hydrolysis.

3.4 Amine-CO₂ reactions

Amine-CO₂ reactions have long been known. Fichter reported formation of organic carbamates between secondary amines and CO₂ more than hundred years ago.^[89] Wright confirmed the structure of several alkyl- and aryl carbamates by elemental analysis.^[90] The industrial synthesis of urea, which is a more than hundred years old industrial procedure, proceeds through ammonium carbamate.^[91]

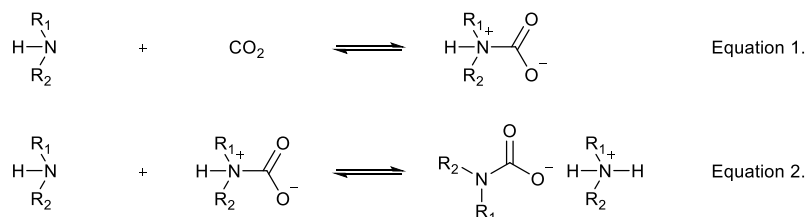
There are number of mechanistic and kinetic studies of amine and CO₂ reactions. Calderazzo summarised works of Faurholt and Jensen concerning reactions of amines with CO₂ reactions in aqueous solutions. They found, the dissolved CO₂ reacted with alkyl amines in a second order reaction (Scheme 3.5, Equation 1) and formed a carbamate salt, which subsequently hydrolysed to form bicarbonate (Scheme 3.5, Equation 2).



Scheme 3.5. Reaction of amines and CO₂ in water. Carbamate was formed first, which then hydrolysed to bicarbonate.^[92]

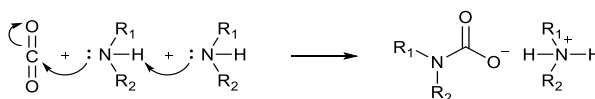
Caplow found that the rate of CO₂ + amine reactions was *pH* dependent. He therefore proposed kinetics that took this dependency into account. His results indicated hydroxide catalysed reaction pathways.^[93]

Dankwerts, who investigated the reaction of CO₂ and ethanolamines in aqueous solutions, proposed a formation of a zwitterion as an immediate product (Scheme 3.6, Equation 1). The reaction of the zwitterion, which was present in very low concentration, and a second molecule of amine produced the final carbamate salt in a rate determining step (Scheme 3.6, Equation 2).^[94]



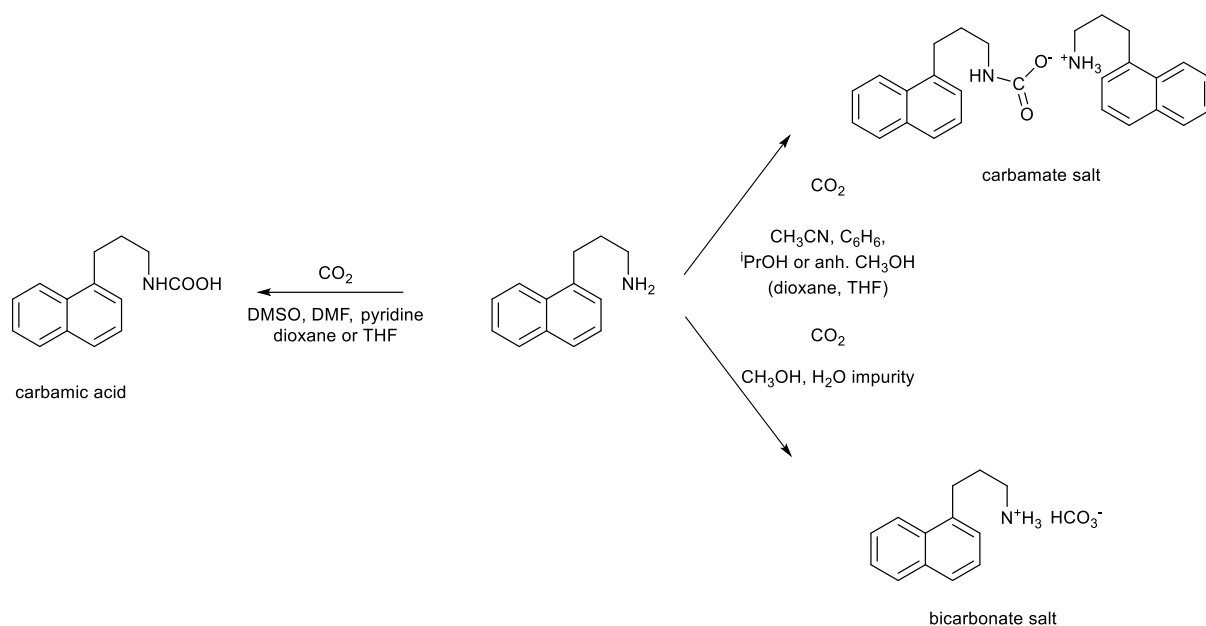
Scheme 3.6. Carbamate formation *via* a zwitterionic Dankwerts mechanism.^[94]

Crooks investigated the reaction of ethanolamine and other amines in water and absolute ethanol. He proposed a one-step termolecular mechanism. According to this, the C-N bond formation and the deprotonation of the amine happened simultaneously.^[95-96]



Scheme 3.7. Carbamate formation *via* a termolecular Crooks mechanism.^[95-96]

Masuda published detailed studies about the solvent dependency of CO₂-amine reactions. He investigated the reaction of naphthylalkylamines and CO₂ under atmospheric conditions (Scheme 3.8).^[83] The reaction products were analysed by FT-IR, ¹H- and ¹³C-NMR spectroscopy.



Scheme 3.8. Reactions of a naphthylpropylamine derivative with CO₂ in various solvents.^[83]

The tested amines quantitatively formed carbamic acids in highly polar aprotic solvents such as DMSO, DMF and pyridine. In the somewhat less polar dioxane carbamic acid was the main product too, but with a minor amount of carbamate salt. In acetonitrile, isopropanol and dry methanol carbamate salts were formed. Apolar solvents, such as benzene or chloroform, promoted carbamate salts were formation. If water was present in the system, even in traces, bicarbonate salts were obtained as main products.^[83]

Masuda reasoned it was always carbamic acid that was formed first when amines were exposed to CO₂. In DMSO, DMF or pyridine, the final product was carbamic acid. However, in acetonitrile, benzene, chloroform, isopropanol or dry methanol, the formed carbamic acid reacted with the starting amine in a rapid acid/base reaction yielding the carbamate salt. The acid was possibly too weak in DMSO, DMF or pyridine to protonate the free amine. In acetonitrile, benzene, chloroform and alcohols, however, the relative acidity of carbamic acid was sufficient to react with the amine, and a carbamate salt was formed. Such solvent effects on acidity were recognised before, and will be discussed later.^[97] In the presence of water, carbonic acid was formed, which was apparently acidic enough to protonate the amine.^[23] Once the amine was protonated, it became less nucleophilic and did not react with CO₂. Therefore the final product was bicarbonate salt.

One of the most promising new fields for CO₂ utilization is the synthesis of carbamates, which are important raw materials for the manufacture of a variety of widely used polymer products or other chemicals. Current commercial processes for carbamate production are aminolysis of chloroformates, or alcoholysis of isocyanates, which are

produced using phosgene. Alternative routes imply the utilization of poisonous carbon monoxide or expensive dialkyl carbonates. Use of CO₂ in carbamate synthesis is particularly attractive since CO₂ could be a non-toxic, non-corrosive, non-flammable, abundant and cheap feedstock.^[98] CO₂ could combine with amines in a reversible reaction to form the corresponding carbamic acids, which could then be alkylated without isolation. Chaturvedi^[21] summarised these efforts (Figure 3.1). The investigated amines were mostly secondary, rarely primary, and never tertiary. The alkylating agents were alkyl halides or tosylates, olefins or epoxides, alkynes, or alcohols under Mitsunobu conditions.^[10] The applied pressures varied from ambient to supercritical and the temperature range was 25 to 150 °C. The yields varied from poor to almost quantitative.

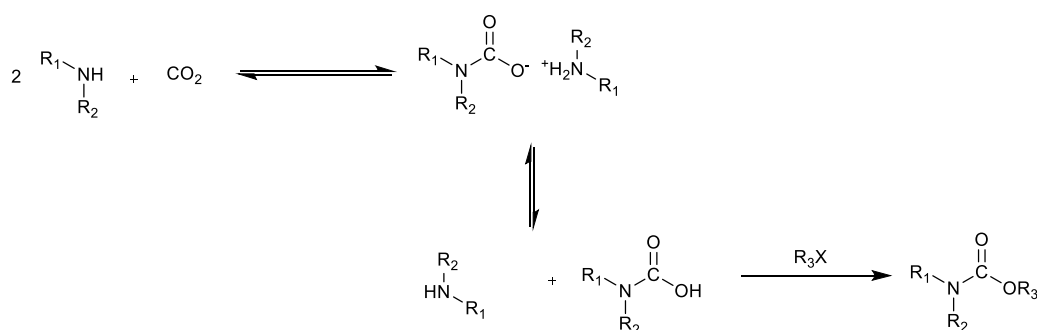


Figure 3.1. Carbamate formation *via* carbamate salt.^[21]

3.5 Analysis of amine - CO₂ adducts

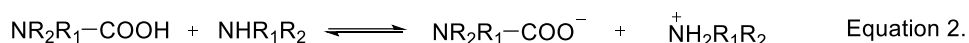
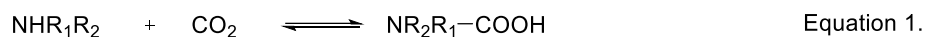
Carbamic acids, carbamate and bicarbonate salts can be unstable compounds. Their analysis, therefore, encounters several difficulties.^[99] Before the discussion of their synthesis, it is expedient to review the available analytical methods for their analysis. These include ¹H- and ¹³C-NMR spectroscopy, FTIR spectroscopy, elemental analysis, melting point, X-ray crystallography and mass spectrometry. For each analytical technique the complications of CO₂ adduct analysis is discussed, along with potential solutions to these problems.

3.5.1 ¹H- and ¹³C-NMR spectroscopy^[83]

The main difficulty of NMR spectroscopy for CO₂ adduct analysis is the sample preparation. Samples have to be dissolved in the deuterated solvent of choice before analysis, and the dissolution can have a dramatic effect on the structure. The solvent dependency of amine + CO₂ reactions has been discussed,^[83] and the reversible character of all reaction steps of carbamate formation, from the dissolution of CO₂ in the solvent to carbamate salt formation, is known.^[89] The new equilibrium of the amine + CO₂ system after dissolution may not reach equilibrium instantly, as kinetic studies indicated.^[100] The rate may depend on other factors such as *pH*.^[93] If the time

needed to reach equilibrium after sample preparation is longer than the NMR timescale, transient stages between two equilibria could be measured, complicating the analysis further.

According to Masuda, if an amine solution is exposed to CO₂ in the absence of water, carbamic acid is formed (Scheme 3.9, Equation 1). The generated carbamic acid may subsequently form a carbamate salt with the free amine in an acid/base reaction (Scheme 3.9, Equation 2).



Scheme 3.9. Amine + CO₂ reactions: Carbamic acid formation in a substitution reaction (Equation 1), and a subsequent carbamate formation in an acid/base reaction (Equation 2).^[83]

The equilibrium concentrations are governed by the acidity of the carbamic acid and basicity of the amine. Acidity and basicity are determined by *pK_a* values. However, *pK_a*s are solvent dependent, and the solvent may have a dramatic effect.^[97] A few *pK_a* values measured in water and DMSO were collected to demonstrate this effect (Table 3.2).^[97, 101]

Table 3.2. The *pK_a* values of various acids/bases in water and DMSO.^[97, 101]

| Acid | <i>pK_a</i> in | | Base | <i>pK_a</i> in | |
|------------------------------------|--------------------------|------|---|--------------------------|-------|
| | H ₂ O | DMSO | | H ₂ O | DMSO |
| HCOOH | 3.6 | 10.3 | NH ₃ | 9.21 | 10.5 |
| CH ₃ COOH | 4.76 | 12.3 | NH ₂ Et | 10.67 | 10.7 |
| C ₆ H ₅ COOH | 4.2 | 11.1 | NH ₂ ⁿ Bu | 10.59 | 11.12 |
| C ₆ H ₅ OH | 10 | 18 | C ₆ H ₅ NH ₂ | 4.85 | 3.82 |

Acetic acid, for instance, has a significantly higher *pK_a* in DMSO compared to water (12.3 vs. 4.76), therefore it is a much weaker acid in DMSO. The *pK_a* of butylammonium ion is somewhat higher in DMSO compared to water (11.12 vs. 10.59), therefore butylamine is somewhat stronger base in DMSO. The acidity of acetic acid is sufficient to protonate butylamine in water, therefore the aqueous solution of butylammonium acetate contains dissolved salt, anions and cations instead of neat acid and neat base. In contrast, acetic acid is not strong enough to protonate butylamine in DMSO, therefore a butylammonium acetate solution in this solvent contains mostly neutral acid and base, instead of anions and cations.

Hence it is easy to understand how the solvent can directly affect the carbamic acid + amine equilibrium (Scheme 3.9, Equation 2). Changing concentrations will also effect the amine + CO₂ equilibrium indirectly (Scheme 3.9, Equation 1). NMR spectroscopy can only give information about the solution of the sample, and this information must be interpreted for the solid sample carefully.

NMR spectroscopic analysis of amine - CO₂ adducts will be discussed using the example of naphthylpropylamine. Masuda reported that this amine may produce carbamic acid, or carbamate or bicarbonate salts with CO₂ depending on the reaction conditions.

Carbamic acid group, formed by carboxylation of the amine, possesses a proton. Similarly to other acidic protons, it is often not visible on ¹H-NMR spectrum because of its mobility and rapid exchange to deuterium in deuterated solvents. Amines behave similarly in terms of proton exchange because of hydrogen atom mobility of their hydrogen atoms.

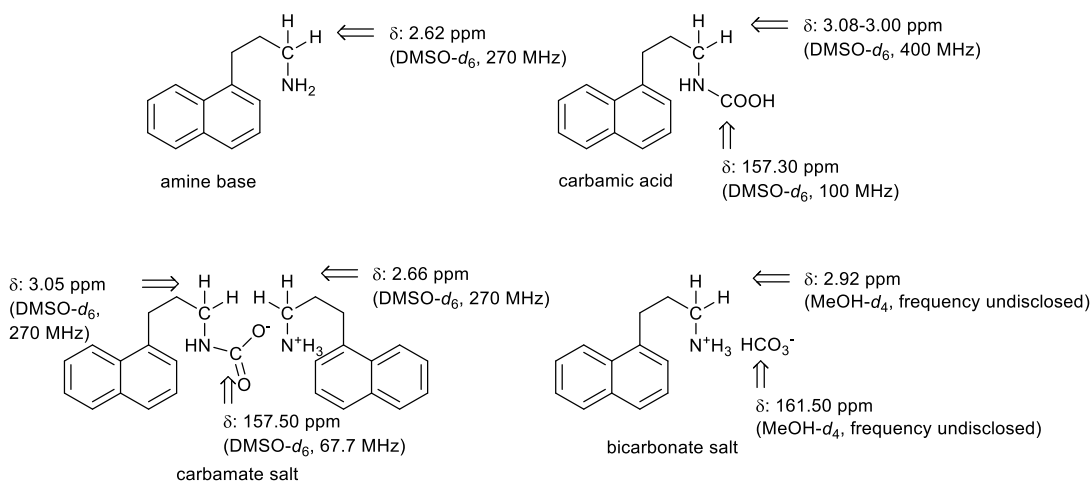
Protons on the carbon in the α position to the carboxylated nitrogen became more deshielded after introduction of the carbamic acid group, with a downfield shift of about 0.4 ppm in DMSO-*d*₆ (Scheme 3.10). Chemical shift of α methylene protons appear indistinguishable in carbamic acids and carbamate anions. The chemical shift was solvent dependent, for instance, it was 0.6 ppm downfield in pyridine-*d*₅ compared to 0.4 ppm in DMSO-*d*₆ (Table 3.3). It should be however noted that Masuda measured spectra of neat amines only in DMSO-*d*₆.

The carbamic acid carbon was visible on the ¹³C-NMR spectrum in a form of a weak peak at low fields, at 157.30 ppm in DMSO-*d*₆. The carbamate anion carbon was very slightly more deshielded at 157.50 ppm, $\Delta\delta$: +0.2 ppm (Scheme 3.10). Significant solvent dependency of the chemical shift of carboxy carbon was observed. For instance, the shift was $\Delta\delta$: +6 ppm in DMF-*d*₅ (Table 3.3).

Ammonium ions in bicarbonate salts have a protonated nitrogen atom. Protons on the carbon in the α position to the protonated nitrogen became deshielded compared to neat amine ($\Delta\delta$: +0.30 ppm), but the deshielding was less significant compared to carbamic acids ($\Delta\delta$: +0.40 ppm). The bicarbonate carbon was visible on the ¹³C spectrum at 161.50 ppm, downfield to carbamic acid or carbamate ion carbons at 157.3 and 157.5 ppm. It shall be, however, pointed out that carbamic acid and carbamate carbons were measured in DMSO-*d*₆ and bicarbonate was measured in MeOH-*d*₄. Solvent dependence, as was mentioned earlier, caused a significant shift of the carbamic acid carbon ($\Delta\delta$: +6 ppm, DMSO-*d*₆ vs. DMF-*d*₅) (Table 3.3).

Signals of the carbon atoms, either in carbamic acid, carbamate or bicarbonate, were very weak, possibly because of slow relaxation.

Masuda also reported that the spectra of ammonium ions, protonated by carbamic acid, were identical to neat amine in terms of chemical shifts. In contrast, he reported a spectroscopic change if the amine was protonated by carbonic acid.

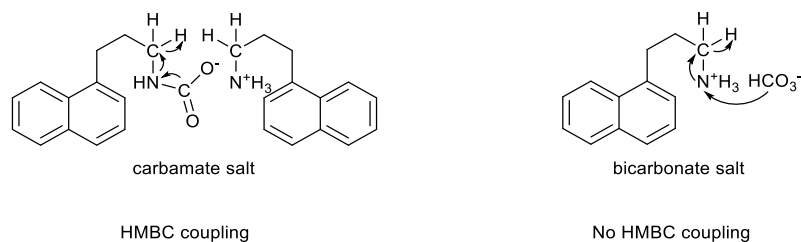


Scheme 3.10. ^1H and ^{13}C -NMR shifts of naphthylpropylamine and its CO_2 adducts. Note spectra were recorded in different solvents, with different spectrometers.^[83]

Table 3.3. Solvent dependence of chemical shifts of naphthylpropylamine - CO_2 adducts. Chemical shifts of protons on the carbon α to nitrogen atom, and carbons in carbamate function are noted.^[83]

| carbamic acid | | | carbamate salt | | |
|-------------------|-------------------------------------|---------------------------------|---------------------|--------------------------------|---------------------------------|
| Solvent | δ_{H} | δ_{C} | Solvent | δ_{H} | δ_{C} |
| DMSO- d_6 | δ_{H} : 3.08-3.00 ppm | δ_{C} : 157.3 ppm | DMSO- d_6 | δ_{H} : 3.05 ppm | δ_{C} : 157.5 ppm |
| DMF- d_5 | δ_{H} : 3.23 ppm | δ_{C} : 163 ppm | 1,4-dioxane- d_8 | δ_{H} : 3.18 ppm | δ_{C} : 160 ppm |
| Pyridine- d_5 | δ_{H} : 3.60 ppm | δ_{C} : 159 ppm | CDCl_3 | δ_{H} : 2.95 ppm | δ_{C} : 163 ppm |
| | | | $i\text{Pr-OH-}d_8$ | δ_{H} : 3.15 ppm | δ_{C} : 162 ppm |

Masuda found coupling between carboxyl carbons and protons on carbon α to the carboxylated nitrogen atom in HMBC[#] spectra.^[83] Coupling was not found between bicarbonate carbons and protons on the carbon α to the protonated nitrogen atom. HMBC NMR spectroscopy could therefore be used to differentiate between carbamates and bicarbonates.



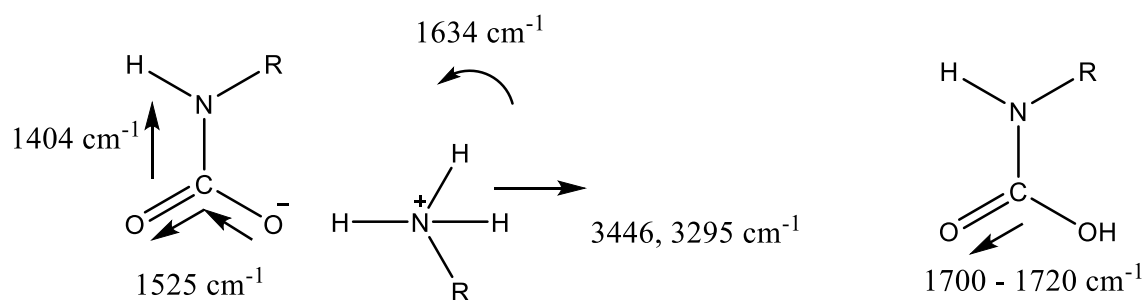
Scheme 3.11. HMBC NMR spectroscopy of naphthylpropylamine - CO_2 adducts. In carbamates there is coupling between the carboxyl carbon and the protons on the carbon α to the carboxylated nitrogen atom. In bicarbonates there is no coupling between the bicarbonate carbon and the protons on the carbon α to the protonated nitrogen atom.^[83]

[#]Heteronuclear multiple-bond correlation

In summary, it is rather challenging to interpret the structure of CO₂ adducts by NMR spectroscopy. Firstly, the sample may undergo decomposition or other change during sample preparation. ¹³C-NMR spectroscopy could indicate CO₂ adduct formation by appearance of a carbon signal at low fields. These signals could be extremely weak and easily overlooked. ¹³C chemical shifts of carbamic acid, carbamate salt and bicarbonate salt signals were not significantly different, and could not be used safely to distinguish between them. ¹H-NMR could clearly show CO₂ adduct formation by chemical shift changes. Difference of chemical shift change could imply whether carbamate or bicarbonate was present. Bigger shifts of proton signals in alpha position typically indicated carbamates, smaller shifts indicated bicarbonates, however, comparison should take solvent dependency into account.

3.5.2 FTIR Spectroscopy^[83]

Detailed analysis of carbamates by FTIR spectroscopy has been published. Absorptions were identified by manipulation with isotope labeling.^[102] According to studies using of ammonium carbamate salt, the asymmetric stretch of the CO₂ moiety absorbs around 1525 cm⁻¹, N-C stretching absorption is around 1404 cm⁻¹. Antisymmetric and symmetric stretching of N-H absorptions are around 3446 and 3295 cm⁻¹, respectively. N-H has another absorption, a bending around 1634 cm⁻¹.^[102] Undissociated carbamic acids have a strong absorption around 1710 cm⁻¹ (Scheme 3.12).^[103] Bicarbonate salts can be identified by bands of HCO₃⁻ around 1625 cm⁻¹, slightly overlapping with carbamate N-H bending, and at 1300 cm⁻¹.^[83]



Scheme 3.12. Typical absorptions of carbamate salts and carbamic acids.^[102-103]

Solid samples can be measured by IR spectrophotometers, therefore dissolution during sample preparation does not cause complications like those seen for NMR spectroscopy. However, even as solids, CO₂ adducts may slowly decarboxylate, forming the corresponding amine starting material and CO₂. The classic sample preparation for solid state IR spectroscopy, forming potassium bromide pellets, is not a favourable option because application of vacuum is involved in the procedure in order to remove traces of

air and water. Application of vacuum would promote decarboxylation by removing CO₂ from the equilibrated amine + CO₂ system. By using a diamond cell, application of vacuum can be eliminated on one hand. On the other hand, the amount of sample used with a diamond cell is very small, only 10-20 µg, with relatively large surface area. The carbamate decomposition rate may increase in the exposed samples because of the increased surface/mass ratio.

3.5.3 Elemental analysis

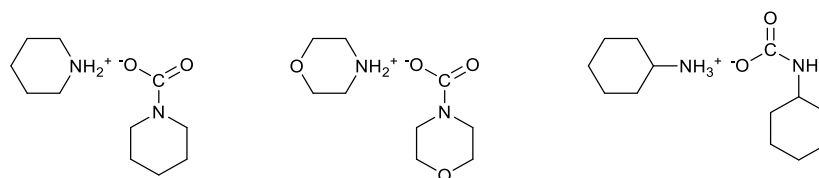
Elemental analysis can be considered as a reliable analytical method for carbamate analysis, because of a relatively large sample size, which increases mass transport limitations to decomposition. Moreover, the sample is exposed to air only during loading into the measuring device. Once the sample is loaded, further decarboxylation will not alter the result. Unfortunately, elemental analysis gives only limited information in a form of an empirical formula. If the sample is dry and clean, possible structures can be speculated from an empirical formula.

3.5.4 Melting point

Carbamate or bicarbonate salts are often unstable and the decomposition rate may depend on temperature. Therefore, the actual, measured melting point may depend on the rate of heating. Slower heating may result in lower experimental melting point. To ensure reproducibility, identical heat profiles must be applied. Also, similar mass transport conditions must be ensured, *i.e.* results of using a glass plate *vs.* capillary method are not interchangeable. The latter is recommended because of more limited exposure to air.

3.5.5 X-Ray crystallography

This measurement method essentially needs a single crystal in adequate size. Crystals are typically grown from solutions, but as discussed earlier, the solvent has an effect on the structure due to the effect on pK_a/pK_b . The structure of carbamate salt formed by crystallization may be therefore solvent dependent. The stability of the single crystal is another issue, with decarboxylation remaining the major complication. However, several carbamate crystal structures were reported by our research group, including piperidinium carbamate, morpholinium carbamate and cyclohexylammonium carbamate.^[104]

Scheme 3.13. Carbamate salts with known crystal structure.^[104]

3.5.6 Mass Spectrometry

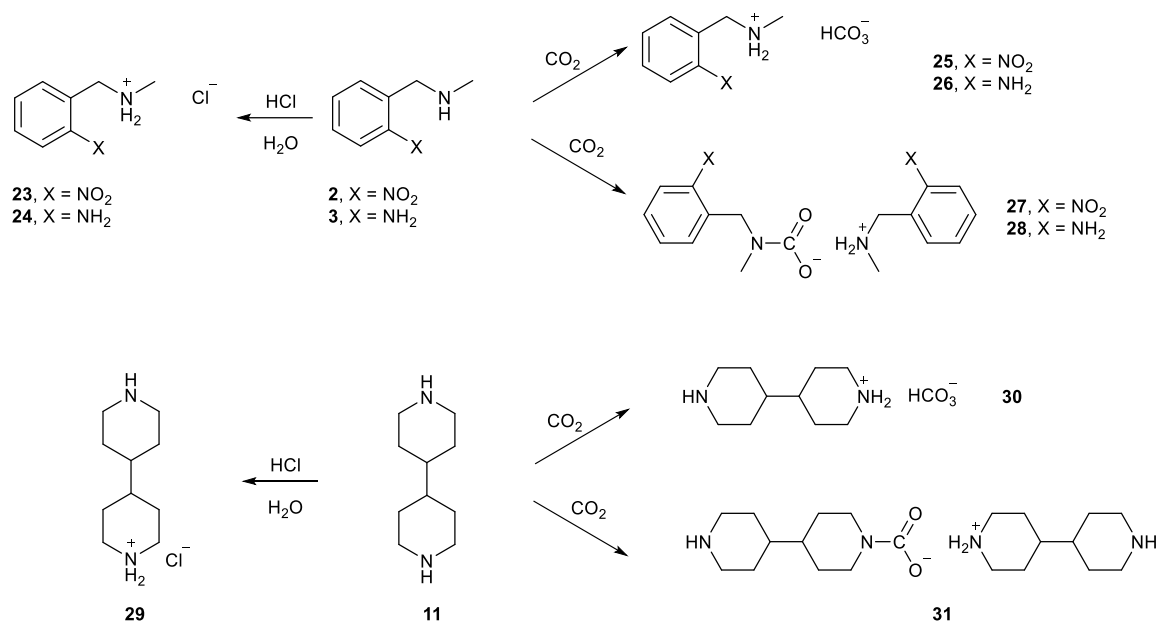
HPLC-MS with electron-spray ionisation was used in our investigations. It uses a highly dilute solution as a sample. According to our experiences, no carbamate salts or carbamic acid fragments could be detected and the main fragment was amine derivative. However, using electron impact ionisation, a peak at 44 m/z (CO_2^+) could indicate a presence of CO_2 adduct.^[105]

3.6 Goals

Difficulties and advantages of chemical induced crystallisations were discussed earlier (3.2). The difficulties, in summary, were chemical consumption for salt formation, chemical consumption for neutralisation, by-product formation in equimolar amounts and undesired reactions of the valuable compound during either salt formation or neutralisation. These reactions could be either because of acid or base catalysed hydrolysis, which may potentially lower the recovery, or other reactions, such as Lucas type halogenation of alcohols, which may contaminate the product.^[42, 44] The advantages of chemical induced crystallisations were, however, rather substantial. Purification of non-crystalline compounds became possible *via* crystallisation, providing high purity products under mild operation conditions at low energy costs. The goal of the project was to alleviate the summarised difficulties by replacing conventional acids by using CO_2 as a reaction partner, and to exploit the formed CO_2 adducts for crystallisation instead of conventional salts, while advantages of chemical induced crystallisation were maintained. The potential of CO_2 based crystallisation procedures was largely, but not exclusively, investigated using the synthesis of AstraZeneca drug candidate SB-214857-A as an example (1.2, Scheme 1.1).^[12-13] It was chosen because the synthesis involved a broad range of chemistries, and involved interesting substrates, many of which would be expected to react with CO_2 .

Considering the synthesis of SB-214857-A, a conventional way of purification of intermediates *o*-nitrobenzyl and *o*-aminobenzyl methylamines **2** and **3** could be distillation, or salt formation based aqueous extraction or crystallisation. In principle, the same procedures could be used to separate biperidine **11** too, which is a by-product of pyridylpiperidine **10** synthesis *via* hydrogenation of bipyridine **9**

(Scheme 1.1). Distillation would be highly energy intensive and aqueous extraction and crystallisation would give inorganic salt by-products in equimolar amount. CO₂ adduct formation of these species was therefore investigated in order to develop greener separations or purifications compared to conventional procedures (Scheme 3.14).



Scheme 3.14. Intermediate formation for crystallisation from *o*-nitrobenzyl and *o*-aminobenzyl methylamines **2** and **3**, and 4-4'-bipiperidine **11** via conventional (HCl) and novel (CO₂) methods, resulting either carbamate or bicarbonate CO₂ adduct.

3.7 Qualitative CO₂ adduct formation experiments

The investigation of CO₂ adduct formation reactions was initiated with simple qualitative tests. The goal of these experiments was to quickly and easily obtain information whether a crystalline product could be isolated after CO₂ exposure. Successful formation of solid would allow the development of separation in adduct form. In contrast, amines that did not form solid carbamate salts were not investigated further. The scale of these tests were up to 1 g amine in 5 ml solvent, and they were carried out under ambient conditions. Benzylamine derivatives *o*-nitrobenzyl- and *o*-aminobenzyl methylamines **2** and **3** were the main interest of this research, but other amines, such as bipiperidine **11**, benzyl methylamine **17**, benzyl- **32**, *o*-nitrobenzyl- **14** and *o*-aminobenzyl propylamine **33** were also tested. The primarily used solvent was MTBE. If precipitation of crystalline solid from the MTBE solution was not detected after CO₂ exposure under ambient conditions, other solvents, such as diethyl ether^[90] and hexane, were used. If precipitation from either solvents did not occur, neat amines were exposed to CO₂ under ambient conditions. If formation of crystalline adduct was not observed, neat amines were also exposed to liquid CO₂ at room temperature and 5.8 MPa, and to supercritical

CO₂ at 10.0 MPa and 40 °C (Figure 3.2). Each case represent a more vigorous exposure method designed to encourage adduct formation.

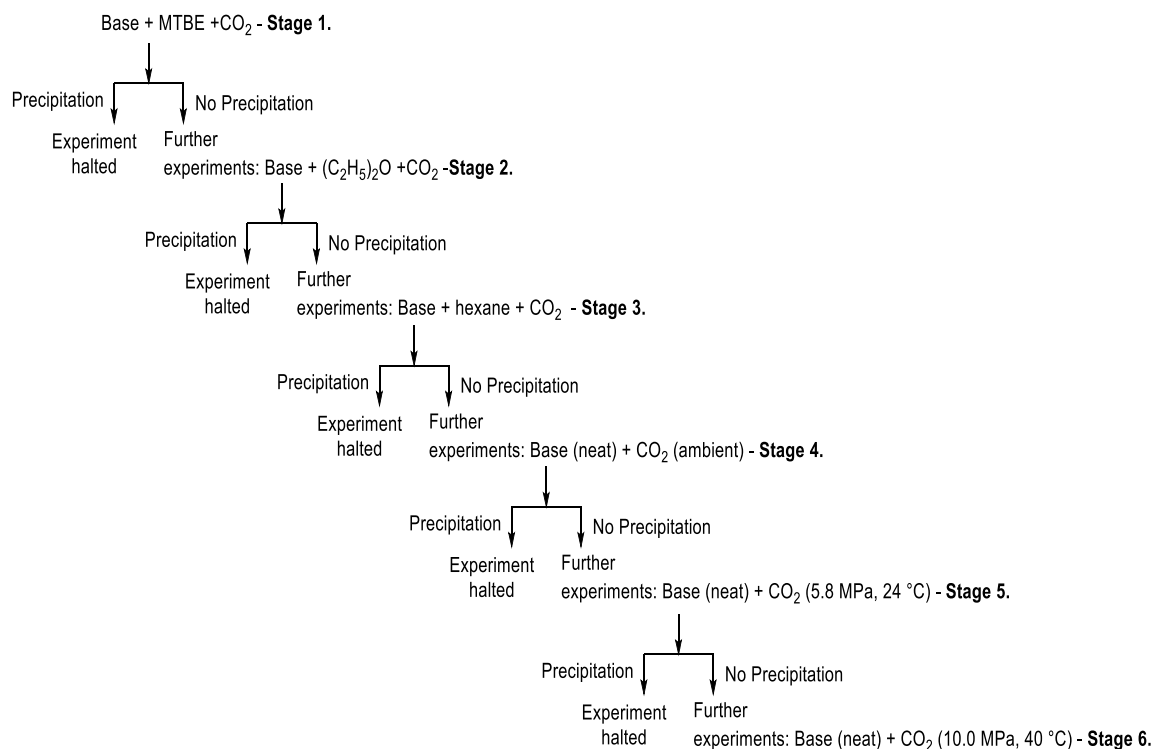
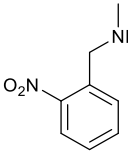
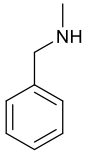
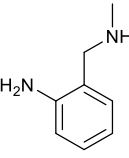
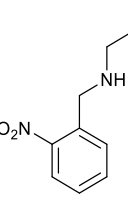
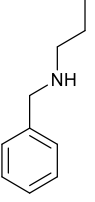
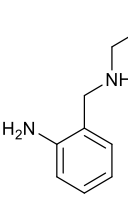


Figure 3.2. Preliminary experiments for amine + CO₂ systems.

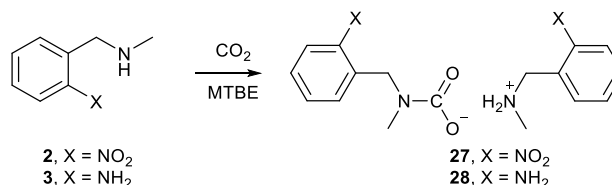
The results of the preliminary tests are summarised in the table below (Table 3.4).

Table 3.4. Summary of preliminary carbamate formation tests of benzyl amines.

| Base: |  |  |  |  |  |  |
|--------------------|---|---|---|--|---|---|
| | 2 | 17 | 3 | 14 | 32 | 33 |
| Experiment halted: | Stage 1 | Stage 6 | Stage 1 | Stage 6 | Stage 6 | Stage 6 |
| Observations: | Pale yellow precipitate | Increase of viscosity | Colourless precipitate | Formation of pale yellow thick gum | Increase of viscosity | Formation of colourless thick gum |

Significant differences were discovered in the affinity of various amines towards CO₂, and tendencies to form crystalline carbamates were also different. Methyl benzyl derivatives **2** and **3** formed crystalline products readily in MTBE under ambient conditions (Scheme 3.15). These reactions and the obtained products were investigated further later. In contrast, nor methyl benzyl derivative **17**, neither propylamines **14**, **32** and **33** formed crystalline solids, therefore they were not suitable to develop

separations based on CO₂ adduct formation. The analysis of the formed CO₂ adducts is discussed in the following sections.



Scheme 3.15. Reaction of *o*-nitro- and *o*-aminobenzyl methylamines **2** and **3** with CO₂ in MTBE under ambient conditions.

3.8 Analysis of amine - CO₂ adducts

3.8.1 Analysis of *o*-nitrobenzyl methylamine - CO₂ adduct **27**

In this section the analysis of the products of the qualitative carbamate formation tests will be discussed. The precipitated solids were isolated from their mother liquors by simple filtration, and washed with a small amount of solvent. The isolated solids were quickly dried in air; the solvent of the mother liquor, MTBE, was fairly volatile.

Elemental analysis, mass spectroscopy and melting point measurement

Elemental analysis confirmed the expected formula of *o*-nitrobenzyl methylamine carbamate **27**. Electron spray ionisation mass spectroscopy did not indicate presence of carbamic acid or carbamate anion, with the peak of amine + 1 H dominating the spectrum.

The melting point of the carbamate salt was 70-73 °C. The sample did not solidify after cooling down to room temperature, therefore possibly decomposed during the measurement. However, obvious evolution of gas was not apparent during the measurement.

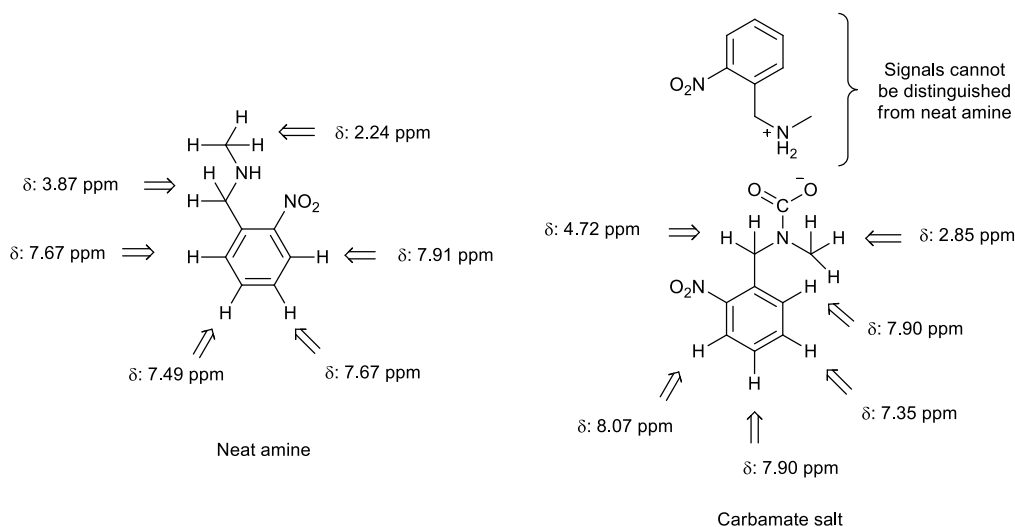
FTIR spectroscopy

The analysis of the FTIR spectrum of the carbamate salt was somewhat problematic, because the characteristic and fairly intensive absorbance peaks of the nitro group (1500 and 1325 cm⁻¹) were in the same region where the appearance of characteristic carbamate resonances were expected (1525 and 1400 cm⁻¹). The first carbamate peak (1525 cm⁻¹), therefore, could not be clearly identified. However, the intensity of a peak at 1400 cm⁻¹, which was present already in the spectra of neat amine, increased indicating carbamate. A characteristic peak at 1650 cm⁻¹ was visible, however, it could either be the N-H bending that is characteristic for carbamates, or a bicarbonate absorbance. The other bicarbonate peak at 1300 cm⁻¹ was in the vicinity of a nitro group at 1325 cm⁻¹ and appeared as a shoulder. Some bicarbonate may have been formed

during the IR measurement itself, because of exposure to moisture. As was discussed earlier, the sample size was very small, and therefore exposed to air (3.5.2).

^1H and ^{13}C -NMR spectroscopy

^1H and ^{13}C -NMR spectra of neat amine and the CO_2 adduct were significantly different. Both carbamate anion and the ammonium cation signals were visible in the ^1H -NMR spectrum of the adduct. Methyl and benzyl proton singlets of the carbamate anion shifted downfield compared to neutral amine, from 3.87 to 4.72 ppm ($\Delta\delta$: +0.85 ppm), and from 2.24 to 2.85 ppm ($\Delta\delta$: +0.61 ppm). The aromatic region was also affected. The chemical shifts of hydrogen atoms in the neat amine, in respect to the nitro function were the following 7.91 (*ortho*), 7.67 (2H; *meta* 1 and 2), and 7.49 (*para*). In the carbamate anion, the doublet ($J = 7.9$ Hz) of the hydrogen atom in *ortho* position to the nitro group shifted downfield, from 7.91 to 8.07 ppm ($\Delta\delta$: +0.16 ppm). The multiplet of the hydrogen atoms in *meta* position to the nitro group shifted downfield, from 7.67 to 7.90 ppm ($\Delta\delta$: +0.23 ppm). Interestingly, the signal of the hydrogen atom in *para* position to the nitro group shifted upfield, from 7.49 to 7.35 ppm ($\Delta\delta$: -0.14 ppm). According to Masuda, ^1H -NMR spectra of neat amine and protonated ammonium ion in the carbamate salt cannot be discriminated.^[83] The ratio of hydrogen atom signals of carbamic anion, compared to the corresponding hydrogen atom signals of neat amine and ammonium ion combined, was consistently about 1 to 2.5. This ratio could be expected to be 1 to 1 for a carbamate salt. However, the ratio of carbamic acid anion was less than expected, possibly because of decarboxylation during sample preparation.



Scheme 3.16. ^1H -NMR shifts of neat *o*-nitrobenzyl methylamine **2** and its carbamate salt.

The signal due to the carbamic carbon was visible in the ^{13}C -NMR spectrum in a form of a weak signal at low field at 157.6 ppm. In the HMBC NMR spectrum cross peaks between the carbamic acid carbon, and the protons in alpha position, on the benzyl and

methyl carbons, were observed. Such cross peaks have been postulated as evidence of carbamate formation.^[83]

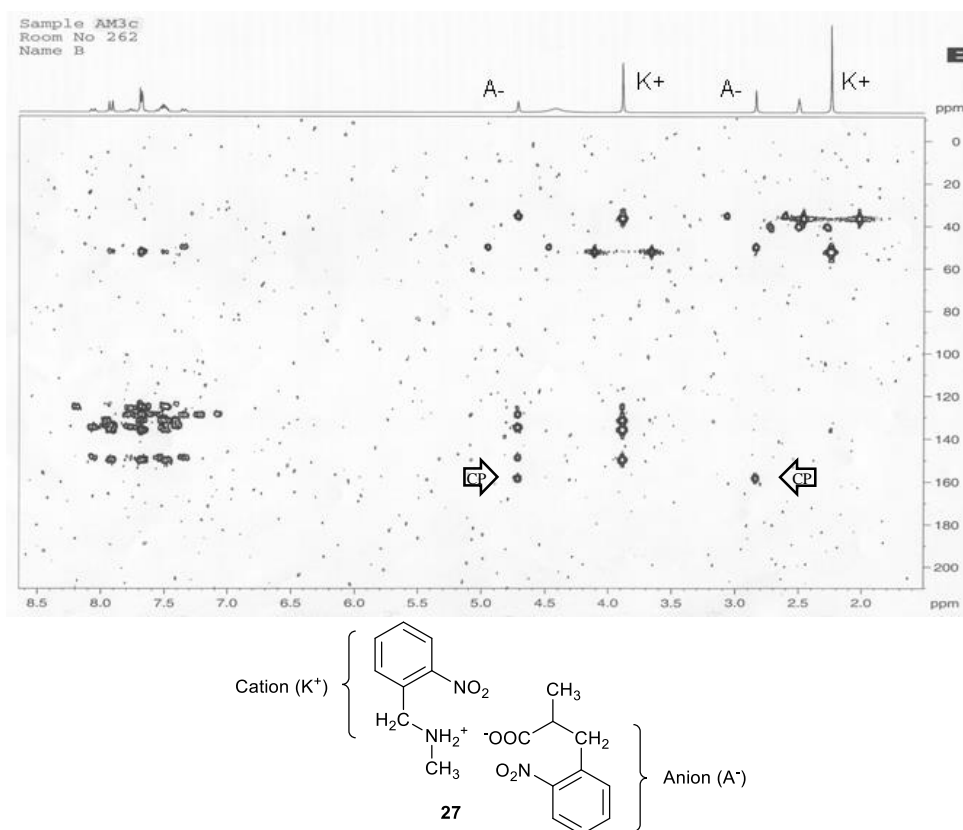


Figure 3.3. HMBC NMR spectrum of *o*-nitrobenzyl methylamine carbamate **27** (300/75 MHz, DMSO-*d*₆). Cross peaks (CP) between carbamic carbon (157.6 ppm), and the benzyl- (4.72 ppm) and methyl protons (2.85 ppm) in carbamic anion (A⁻) indicate the presence of carbamate.

3.8.2 Analysis of the benzyl methylamine - CO₂ adduct

Benzyl methylamine **17** did not form solid crystalline carbamate after CO₂ exposure, either under atmospheric conditions or elevated pressures. Having been exposed to high pressure CO₂, however, the consistency of the starting material changed significantly, indicating reaction with CO₂. The formed viscous gel was measured by FT-IR spectroscopy.

3.8.3 Analysis of *o*-aminobenzyl methylamine - CO₂ adduct **28**

Elemental analysis, mass spectroscopy, melting point measurement and X-ray crystallography

Elemental analysis of suspected aniline carbamate **28** confirmed the structure with one molecule of crystalline water per carbamate salt. Water was not added intentionally to the system, however, starting aniline may have been contaminated by water. Application of CO₂ gas during the precipitation experiment caused solvent evaporation.

The enthalpy of this evaporation cooled down the system, and condensation of water from air may also have happened. The high affinity of the carbamate salt to water may have caused absorption of moisture from air during drying and filtration procedure.

Similarly to the nitro derivative, electron spray ionisation mass spectroscopy did not indicate the presence of carbamic acid or carbamate anion. The peak of amine + 1 H dominated the spectrum.

Melting point of the crystalline sample was 88-92 °C, higher compared to the nitro derivative (70-73 °C), despite lower molecular mass (136 vs. 166 gmol⁻¹). Evolution of gas was not apparent during the measurement, however the sample did not solidify after cooling to room temperature, again indicating decomposition.

The carbamate crystallised out from CO₂ saturated water, and was suitable for X-ray diffraction analysis. The crystal structure revealed that a unit of salt, consisting of one carbamic acid anion and one ammonium cation, bonded to another unit of salt *via* hydrogen bonding and formed a dimer. Two dimers were connected to each other through two molecules of crystalline water with hydrogen bonding (Figure 3.4). This finding was in accordance with the results of elemental analysis, which indicated one molecule of crystalline water per each salt unit.

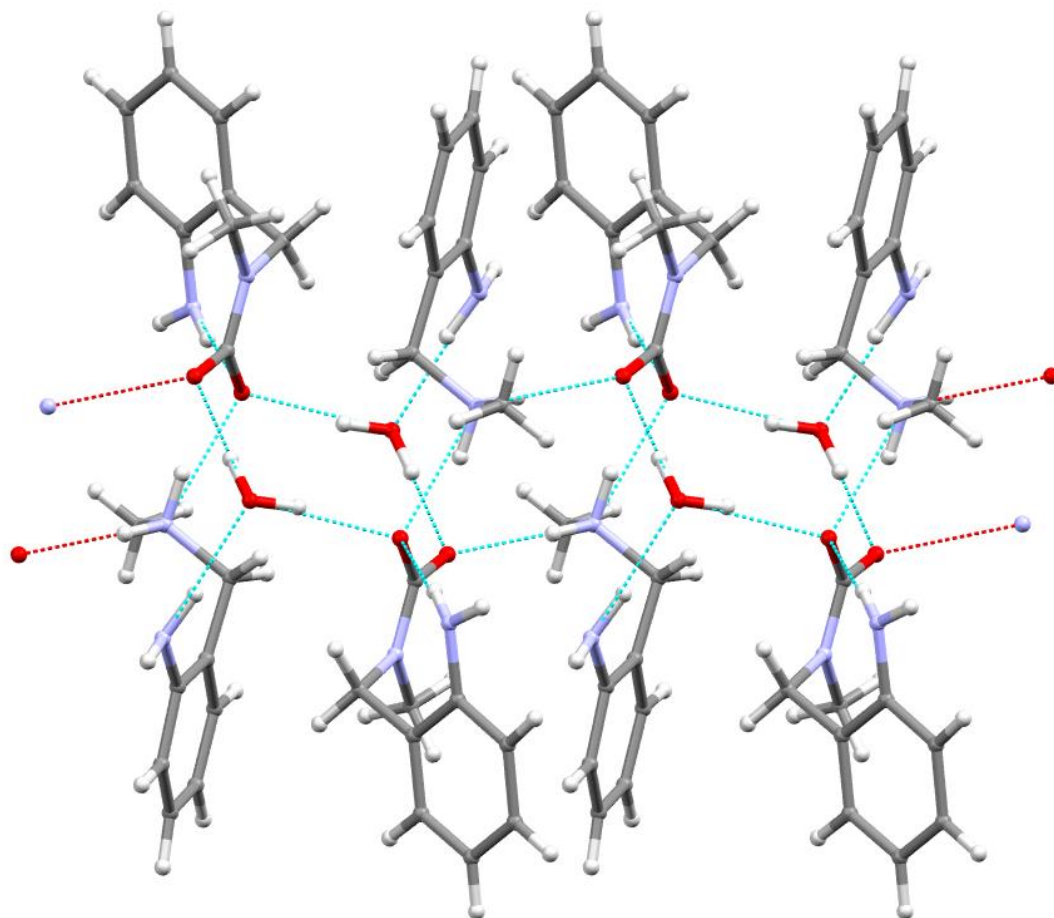


Figure 3.4. Crystal structure of *o*-aminobenzyl methylamine **28**, crystallised from water.

FTIR spectroscopy

FTIR analysis of the CO₂ adduct of aniline **3** indicated the presence of both carbamate and bicarbonate. The peak at 1644 cm⁻¹ could be N-H bending that is characteristic for the ammonium ion in carbamates. Appearance of a strong peak around 1394 cm⁻¹ also indicated carbamate salt (N-C stretching). Observation of the characteristic carbamate peak at 1524 cm⁻¹ was problematic, because peaks in the region were already present on the spectrum of neat aniline. The peak around 1640 cm⁻¹ could also indicate bicarbonate, of which characteristic absorbance around 1300 cm⁻¹ also appeared as a shoulder (Figure 3.5).

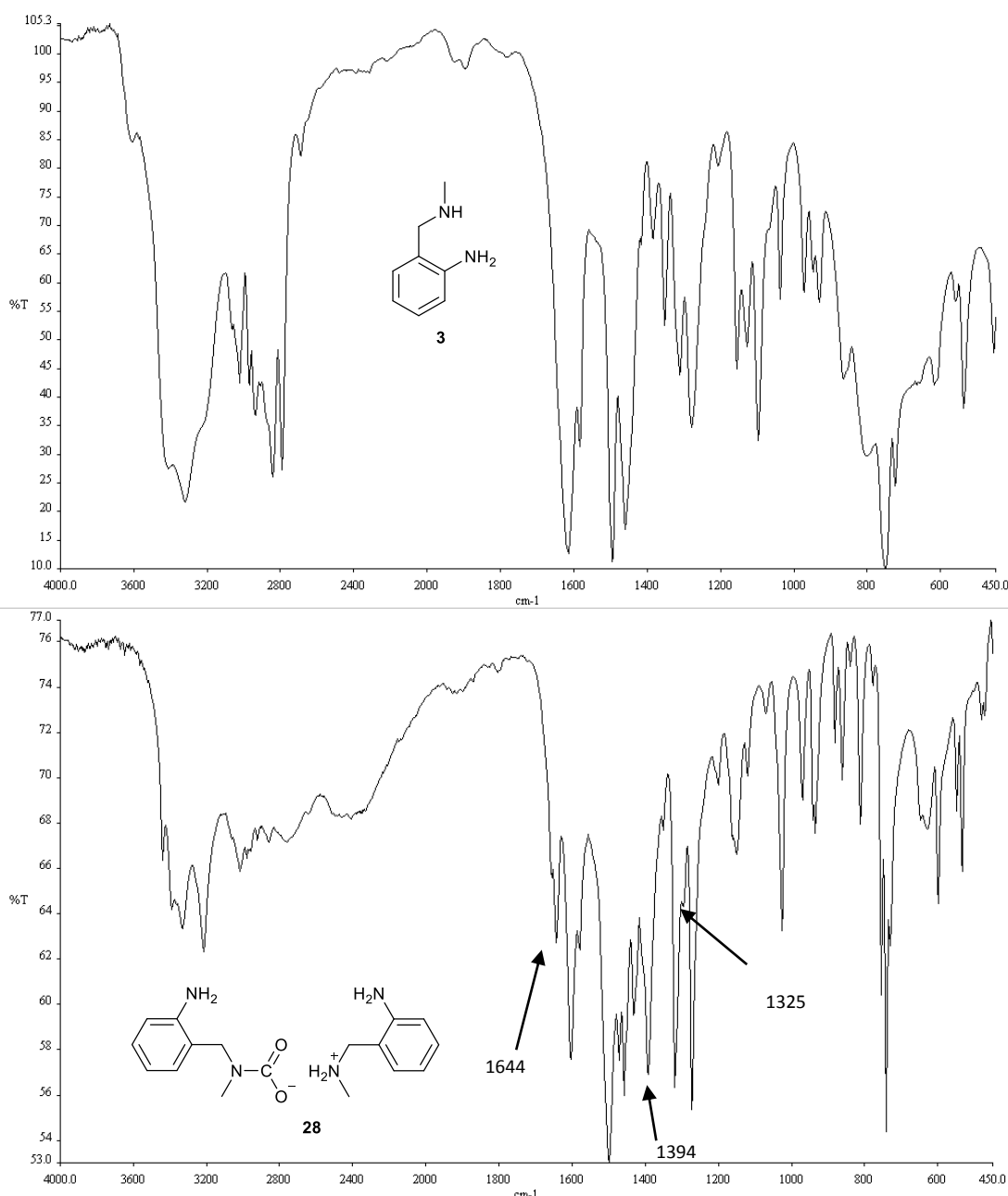


Figure 3.5. FTIR spectra of *o*-aminobenzyl methylamine **3**, and solid adduct **28** that precipitated from MTBE after CO₂ exposure. Appearance of a characteristic carbamate peaks around 1640 cm⁻¹ and 1400 cm⁻¹ indicated carbamate. The shoulder at 1325 cm⁻¹ implied the presence of bicarbonate.

¹H- and ¹³C-NMR spectroscopy

Spectroscopic changes after decarboxylation were similar to that experienced for the nitro derivative. The proton signals of neat amine and ammonium ion were identical.^[83] Benzyl and methyl protons of the carbamic anion significantly shifted downfield, from 3.56 to 4.21 ppm ($\Delta\delta$: +0.65 ppm) and from 2.26 to 2.68 ppm ($\Delta\delta$: +0.42 ppm), respectively. Changes in the aromatic region were not as significant as in the case of nitro derivative. Because of the smaller changes, aromatic signals of the carbamic ion and neat amine overlapped.

A new carbon signal on the ¹³C spectrum of the CO₂ adduct at 159.5 ppm was originated from CO₂. This carbon peak coupled with the protons on the benzyl and on the methyl carbon of the carbamate ion on the HMBC NMR spectrum, proving a presence of carbamate salt, rather than bicarbonate (Figure 3.6).

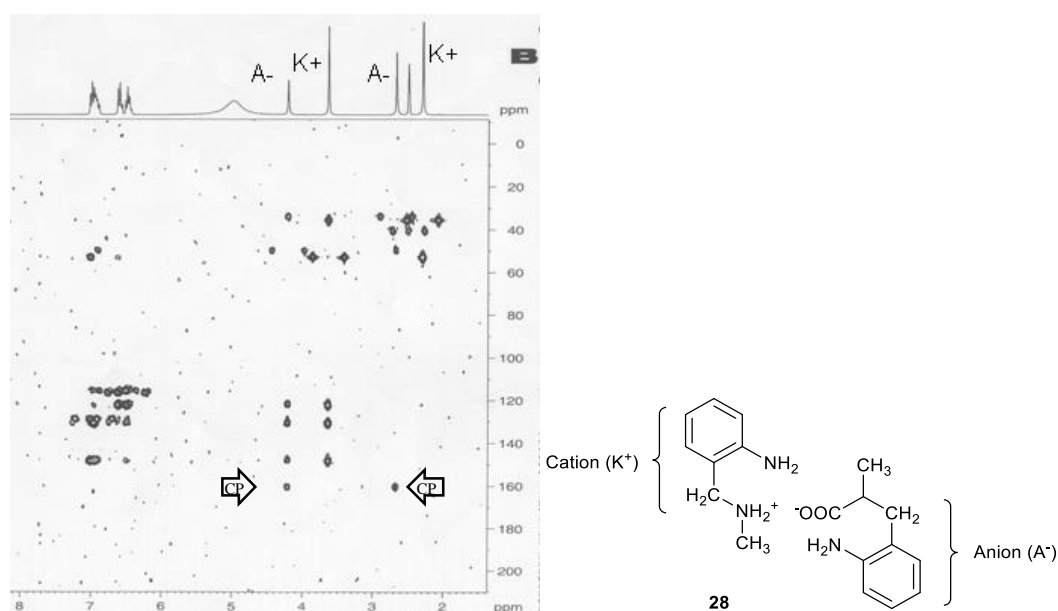


Figure 3.6. HMBC NMR spectrum of aniline carbamate salt **28**. Note the cross peaks between the carbamate carbon (159.5 ppm) and the benzyl protons (4.21 ppm) and methyl protons (2.68 ppm) of the carbamate anion (A⁻) in alpha position.

3.8.4 Analysis of CO₂ adducts of propylamine derivatives

No precipitation of solid was observed after the exposure of methyl derivative **17** or propyl derivatives **14**, **32** and **33**, either MTBE, diethyl ether or hexane was used as solvent. Unfortunately, the lack of crystallinity prevented development of a separation procedure that exploits a CO₂ adduct as an intermediate. During the exposure of propyl derivatives to supercritical CO₂, however, an increase of viscosity was observed indicating a reaction. Having vented the cell, propylamine - CO₂ adducts were recovered

as thick gums, which maintained their consistency for about 30 minutes under ambient conditions in air.

FTIR spectroscopy

A thick gum that was obtained after the exposure of *o*-nitrobenzyl propylamine **14** to supercritical CO₂. The harsher conditions possibly promoted adduct formation (Figure 3.7).

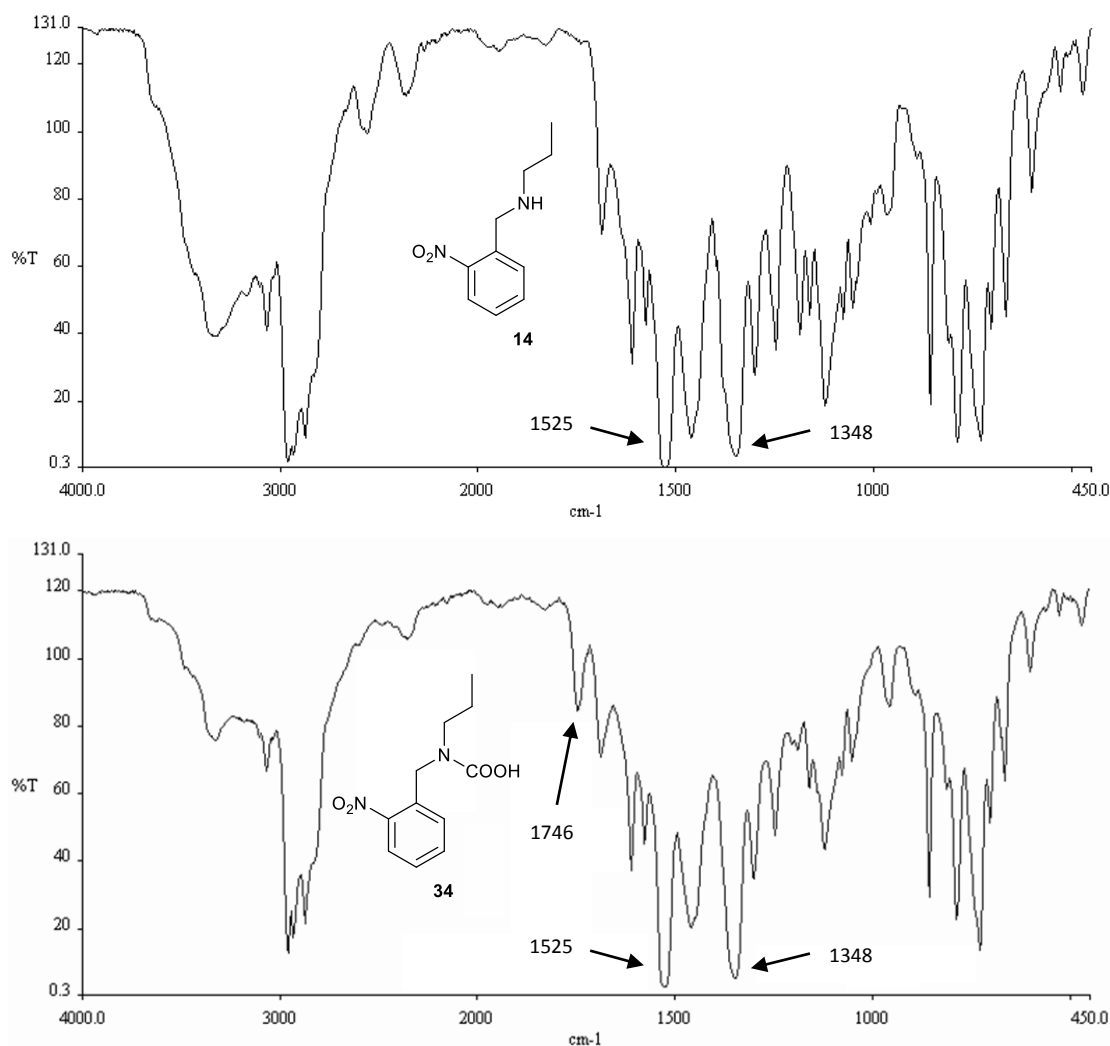


Figure 3.7. FTIR spectra of amine **14** and the resulting thick gum **34** after CO₂ treatment. Peak at 1746 cm⁻¹ implied a presence of carbamic acid. Characteristic absorbance of the nitro group at 1525 and 1348 cm⁻¹ dominate the spectra.

FTIR spectroscopy confirmed that there was a chemical change that caused the viscosity increase. Namely, appearance of a peak at 1746 cm⁻¹ indicated the presence of carbamic acid.

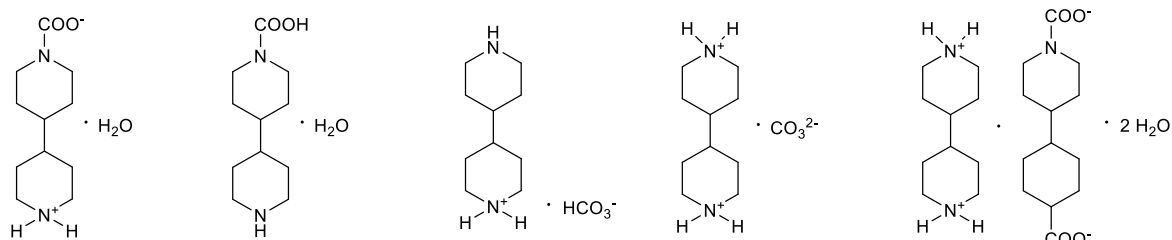
Formation of carbamic acid, rather than carbamate salt could explain the different consistency of CO₂ adduct of propyl derivative **14** compared to methyl derivative **2**. The

different reactivity may have been caused by the longer, and more greasy aliphatic chain.

3.8.5 Analysis of the bipiperidine - CO₂ adduct

Elemental analysis and melting point measurement

Bipiperidine **11** could potentially be a contamination of pyridyl piperidine **10**, which is an intermediate of SB-214857-A and made by hydrogenation of bipyridine **9** (Scheme 1.1).^[13] therefore its affinity to CO₂ was tested. If its solution in chloroform was exposed to CO₂, colourless precipitate was formed. Elemental analysis of CO₂ adduct disproved the formation of carbamate salt, which needed 1 mol carbon and 2 mol oxygen additional to the starting formula. Instead, according to the empirical formula calculated from the results of elemental analysis, 1 mol carbon, 2 mol hydrogen and 3 mol oxygen were added to each mol of neat bipiperidine **10**. Possible products with the empirical formula C₁₁H₂₂N₂O₃, calculated from elemental analysis, could be carbamate salt with one mole of crystalline water. *O*-Aminobenzyl methylamine carbamate salt **28** also crystallised with one mole of water (3.8.3). Other structures for the formula could be carbamic acid with crystalline water. Bicarbonate or carbamate salts also share the same formula. Intra-, or intermolecular formations could also be possible (Scheme 3.17).



Scheme 3.17. Possible carbamate and bicarbonate CO₂ adducts of bipiperidine **11** for the formula C₁₁H₂₂N₂O₃, derived from elemental analysis.

Measured melting point of the CO₂ adduct was identical to bipiperidine, that is 170-172 °C. Thermal decarboxylation during the measurement may have reproduced bipiperidine, although evolution of CO₂ or water vapours were not visually observed during the measurement. Complete decarboxylation likely resulted in the measurement of the melting point of neat bipiperidine.

FTIR spectroscopy

IR spectroscopy indicated considerable difference between bipiperidine **11** starting material and the obtained CO₂ adduct. N-H resonances at 3211 cm⁻¹ were hugely reduced, and new peaks at 1637 and 1266 cm⁻¹ appeared, which are characteristic for

bicarbonate. However, peaks typical for carbamate salts were also visible at 1560 and 1408 cm^{-1} .

NMR spectroscopy

Fine details of the ^1H -NMR spectra of both neat biperidine and its CO_2 adduct could not be recorded, because conformational equilibrium between chair and boat conformations broadened the peaks. Similar phenomena was observed for other cyclohexane derivatives, and usually could be alleviated by spectra collection at low temperatures. However, our spectra were recorded at room temperature.

There were four hydrogen signals on the spectrum of biperidine base. These were, from downfield to upfield, equatorial H atoms alpha to the nitrogen (2.82 ppm), axial H atoms alpha to the nitrogen (2.33 ppm), equatorial H atoms beta to the nitrogen (1.53 ppm), and axial H atoms beta to the nitrogen, combined with H atom on the gamma carbon (0.96 ppm). Duplication of hydrogen peaks, which was observed for benzyl amines, did not occur on the ^1H spectrum of the CO_2 threated product of biperidine. Duplication of hydrogen peaks was typical for carbamate salts, because signals of protonated amines, which were indistinguishable from neat amines present, and signals of carbamic acid were both present. Lack of duplication on the spectra of the biperidine - CO_2 adduct therefore indicated complete product formation, which could be either carbamic acid, bicarbonate or maybe carbonate salt. The main ^1H atom signals on the spectrum of the CO_2 adduct, compared to neat piperidine, from downfield to upfield were equatorial H atoms alpha to the nitrogen (3.18 ppm, $\Delta\delta$: +0.36 ppm), axial H atoms alpha to the nitrogen (2.78 ppm, $\Delta\delta$: +0.45 ppm), equatorial H atoms beta to the nitrogen (1.79 ppm, $\Delta\delta$: +0.26 ppm), axial H atoms beta to the nitrogen and H atom on the gamma carbon (1.20 ppm, $\Delta\delta$: +0.24 ppm). The shifts were smaller to that compared to those observed for carbamic anions, which were up to +0.8-0.6 ppm. This also indicated the product could be other than carbamate salt.

A weak signal on the ^{13}C spectrum appeared at 166.0 ppm, and an even weaker one at 163.2 ppm. Carbamic carbon signals of benzyl amine - CO_2 adducts were at higher fields, below 160 ppm, although they were recorded in $\text{DMSO-}d_6$ rather than $\text{MeOH-}d_4$. Results of Masuda showed, solvent effects could cause a signal shift of this magnitude (Table 3.3). HMBC NMR spectroscopy showed no coupling of the stronger carbon signal at 166.0 ppm, indicating it was a ^{13}C signal of bicarbonate anion. The weaker carbon signal at 163.2 ppm coupled with a minor proton signal at 2.48 ppm. This coupling indicated the presence of carbamate minor product. HMBC NMR spectroscopy also showed coupling of carbons at 171 and 181 ppm, with a sharp minor proton peak at 1.92 ppm, and with a minor signal appearing as a shoulder of a main peak at 1.70 ppm (Figure 3.8). These two couplings indicated a presence of other carbamate type minor

products. These could be either zwitterions, or dicarboxylated species (Scheme 3.17). Multiple carboxylation, and also the stability of the bicarbonate concluded the affinity of this alkyl amine to CO₂ was high.

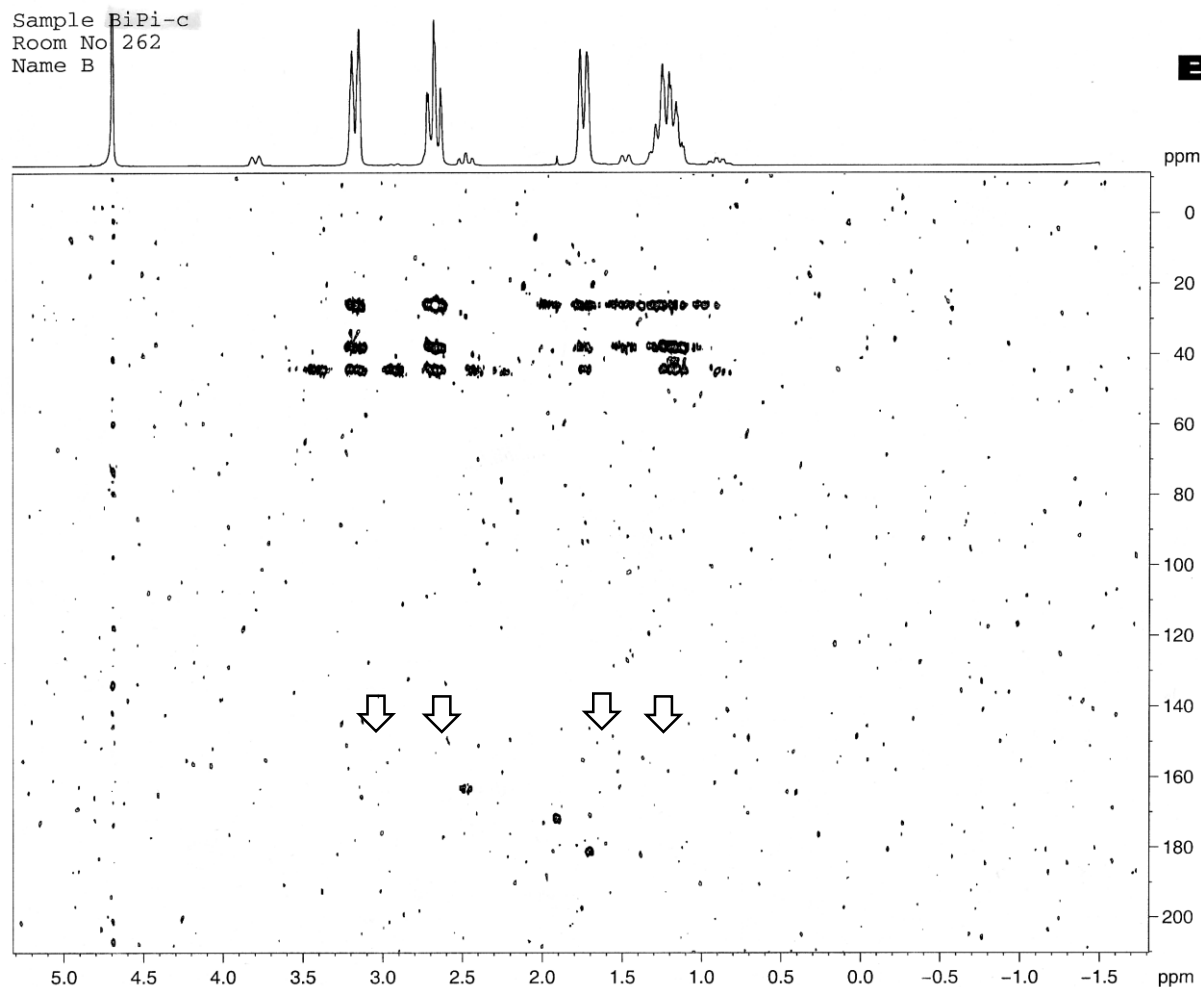


Figure 3.8. HMBC NMR spectrum of bipiperidine - CO₂ adduct. Note there are no cross peaks between the main proton signals and carbons at low field, indicating the main product was bicarbonate salt. A cross peak between a carbon signal at 163.3 ppm and a minor proton signal at (2.48 ppm) indicated carbamate or carbamic acid minor product. Coupling of carbon signals at 171 and 181 ppm, with minor proton peak at 1.92 ppm, and with a minor proton signal appearing as a shoulder of a main peak at 1.70 ppm indicated the presence of other carbamate type minor products.

3.9 Preparative carbamate separations

The main goal of this project was to exploit carbamate salts as intermediates for novel reaction work-up and purification procedures. Namely, if an amine form a crystalline CO₂ adduct that precipitates from a solution, and contaminants remain dissolved in the liquor, the solid can be filtered off, and later converted back to pure amine.

The robustness of carbamate formation reaction was tested for the separation procedure of *o*-nitrobenzyl methylamine **2** from by-product benzylalcohol **15**. The mixture of 0.66 g nitroamine **2** and 0.33 g benzylalcohol **15** was dissolved in MTBE (10 ml), and treated with CO₂. The precipitated pale yellow solid, carbamate salt **27**, was filtered off, washed with MTBE and dried. It was then converted back to free amine **2**, by concentrating its alcoholic solution in vacuum. The recovery of nitroamine **2** was 61%, and the level of contaminant **15** was reduced from 33wt% to below 1wt%, determined by ¹H-NMR integration.

The purification performance of the procedure was impressive, the level of contaminant benzylalcohol **15** significantly decreased. However, the yield was rather moderate for a separation procedure (60%). Efforts were made to identify the reasons of modest yields, and possibilities to enhance were investigated.

Two main reasons that could decrease the yield were speculated. A possibility of loss could be incomplete carbamate formation reaction. This could be either because of kinetic reasons, *i.e.* the carbamate formation reaction was terminated before completion, or because of thermodynamic reasons, *i.e.* the carbamate formation reaction reached an equilibrium rather than proceeding to completion.

Other possibility of loss was a possible decomposition of the CO₂ adduct during the steps of the preparative procedure. These steps were filtration, washing with solvent and drying by driving air through the filter cake by vacuum. Decomposition during filtration, for instance, could significantly decrease the yield. Amine accumulated in the filter cake could be carried away in the next step of the procedure, which was a wash with organic solvent.

Both the completeness of carbamate formation reaction, and the stability of the CO₂ adduct was carefully investigated and will be discussed in the following sections.

3.10 Investigation of the carbamate formation reaction by solubility tests

The yield of separating *o*-nitrobenzyl methylamine **2** in carbamate form was around 60%. In order to obtain more detailed information about CO₂ induced precipitation as purification procedure, further studies were made. Methylamine **2** was miscible with MTBE on the whole concentration range. If CO₂ was bubbled through this solution, a chemical reaction between amine and CO₂ occurred, and the formed CO₂ adduct precipitated from the solution. A portion of amine, however, remained dissolved, and therefore could not be separated in the form of solid CO₂ adduct, and could be considered as a loss of the procedure. The amine + MTBE + solid adduct system could be considered as a saturated solution. The lower the concentration of the saturated

solution, the more amine precipitated in a form of carbamate, and the less amine remained dissolved, determining the yield of isolation.

The solubility of amine **2** in MTBE + CO₂ was tested at 0 °C and at room temperature (24 °C). A solution of 30wt% amine **2** in MTBE (7 ml), was exposed to excess CO₂. After 2 minutes, precipitation occurred, and an increase of temperature was observed, possibly because of the exothermic reaction. After 30 minutes, the bubbling of CO₂ was stopped, and the solid product, carbamate salt **27**, was allowed to sediment. The liquid phase was sampled, diluted and assayed by UV/Vis spectroscopy. Having diluted the reaction mixture with MTBE, the experiment was resumed with further CO₂ bubbling at lower overall concentrations, with 20 and 10wt% amine **2** dissolved in the system (Table 3.5).

Table 3.5. Solubility *o*-nitrobenzyl methylamine **2** carbamate in MTBE at two different temperatures. The concentration of samples was measured by UV/Vis spectroscopy after dilution ($\lambda = 261 \text{ nm}$, SBW = 3 nm).

| Temperature | Composition /wt% | Absorbance | Dilution | C _{sample} /M | C _{solution} /M | g/l | Amine precipitated* |
|-------------|------------------|------------|----------|------------------------|--------------------------|-------|---------------------|
| 0 °C | 10 | 0.456 | 416 | 0.86×10 ⁻⁰⁴ | 0.027 | 4.44 | 95% |
| | 20 | 0.560 | 417 | 1.05×10 ⁻⁰⁴ | 0.033 | 5.46 | 97% |
| | 30 | 0.666 | 417 | 1.25×10 ⁻⁰⁴ | 0.039 | 6.50 | 98% |
| 24 °C | 10 | 1.576 | 315 | 2.97×10 ⁻⁰⁴ | 0.124 | 20.56 | 75% |
| | 20 | 1.668 | 315 | 3.15×10 ⁻⁰⁴ | 0.131 | 21.75 | 88% |
| | 30 | 1.729 | 315 | 3.26×10 ⁻⁰⁴ | 0.136 | 22.54 | 93% |

*: Ratio of the amine precipitated out from the solution after CO₂ exposure, relative to the overall amount of amine in the starting solution. The value was calculated using the amine concentration of the starting solution, and the amine concentration of the CO₂ saturated solution.

The results indicated the solubility of carbamate was rather temperature dependent. The solubility was about 4-5 times higher at room temperature compared to 0 °C. Preparative recovery of amine at room temperature from 8wt% solution was 61% (3.9), which was in accordance with the solubility data, however, somewhat lower. It also has to be emphasised, the preparative purification test was not a clean amine + CO₂ + MTBE system, but benzylalcohol **15** was also present, and it may have acted as a co-solvent. It could be concluded from the solubility tests, that the main reason for the moderate yield of the preparative experiment was incomplete carbamate formation at the temperature of the experiment. The yields to separate *o*-nitrobenzyl methylamine **2** could be expected to increase significantly, up to above 95%, at decreased temperatures, according to the solubility studies.

Solution concentrations, which were essentially the concentration of the saturated carbamate solution, were expected to be independent of amine-solvent ratio at the same temperature. A composition dependence was indicated, however, it was not significant. The difference could be attributed to experimental error. At 30wt%

concentration, for instance, the solid precipitate occupied significant volume of the load of the experimental vessel after sedimentation, about 75%. This figure significantly decreased for the experiment at 20 and 10wt%, as the volume of solvent present increased. The reaction mixtures were always allowed to sediment before the sampling took place. The necessary time for sedimentation was the highest at 30wt% concentration, intermediate at 20wt% and lowest at 10%. Therefore, the higher the experimental concentration was, the more time the system had to decarboxylate, consequently increasing the concentration of amine in the liquid phase.

3.11 Stability of carbamate salts

The yield of recovered *o*-nitrobenzyl methylamine **2** was about 60%, however solubility studies implied, at least about 70% amine could precipitate out from an MTBE if exposed to CO₂ at that concentration. The stability of the carbamate was investigated, whether decomposition during the separation procedure reduced the yield.

The stability of carbamates was also important, because they only serve as intermediate products of purification and work-up procedures rather than final products. Having separated these intermediates, they will have to decompose to neat amine before the next synthetic step.

In the following sections, stability of *o*-nitrobenzyl methylamine **2** carbamate salt was investigated.

3.11.1 Qualitative observations of carbamate stability

Carbamate salt of *o*-nitrobenzyl methylamine **2** did not maintain its solid structure if it was exposed to air in opened vial, but liquefied, and the formation of the corresponding amine was observed. Efforts were made to investigate the possible reasons for this decomposition.

Two reasons for liquefaction were postulated. Hygroscopicity, in which the sample adsorbs water from the air and turns into solution, and instability, in which the sample forms liquid amine as a result of decarboxylation. A simple set of experiments was carried out to investigate the importance of these two factors. Carbamate salt **27** (4×125 mg) was loaded into four sample vials. One was left opened and exposed to air, one closed with air, one closed with a small vial with water inside and one was put into a round bottom flask and evacuated.

The solid carbamate sample decomposed in the open vial in 24 hours into thick oil, free amine **2**. This was caused by either hygroscopicity or decomposition/CO₂ loss. In the closed vial carbamate salt **27** stayed solid at room temperature for weeks, proving

stability if not exposed to the humidity of air, or the escape of CO₂ was prevented. In the closed vial with water inside the carbamate salt stayed solid for several days, suggesting the decomposition was not caused by hygroscopicity. Carbamate in the evacuated vial turned into liquid within few days, suggesting the instability was in connection with the CO₂ escape. This simple set of experiments suggested the instability of carbamates under ambient conditions was caused by the loss of CO₂, rather than hygroscopicity (Table 3.6).

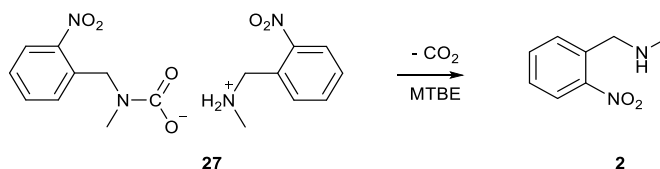
Table 3.6. Summary of qualitative stability tests of *o*-nitrobenzyl methylamine carbamate salt **27**.

| | Vial open to air | Closed vial | Closed vial + water | Evacuated vial |
|-------------|---|---|--|--|
| Observation | Carbamate turned liquid within 24h | Carbamate remained solid for weeks | Carbamate turned liquid within several days | Carbamate turned liquid in few days |
| Deduction: | Hygroscopy or decarboxylation may have caused decomposition | Hygroscopy and decarboxylation were excluded: no decomposition was observed | Decarboxylation excluded; Role of hygroscopy was not significant | Hygroscopy was excluded; Role of decarboxylation was significant |

3.11.2 Quantitative investigation of carbamate decomposition rate by thermogravimetric measurements

Investigation of thermal carbamate stability was very important, because decarboxylation of carbamate, which was an intermediate of the purification procedure, may be essential. In the same time, the carbamate intermediate must be stable enough for preparation.

The decomposition rate of *o*-nitrobenzyl methylamine carbamate **27** was monitored by CO₂ loss, which can be measured by a sensitive scale (Scheme 3.18). A known amount (110 mg) of carbamate **27** was put on a scale in a Petri dish. A data recording system collated on-line continuously recorded the actual weight. A constant flow of dry nitrogen was applied to remove the evolved CO₂, and prevent it affecting the rate of decarboxylation.



Scheme 3.18. Decarboxylation of *o*-nitrobenzyl methylamine **27** carbamate.

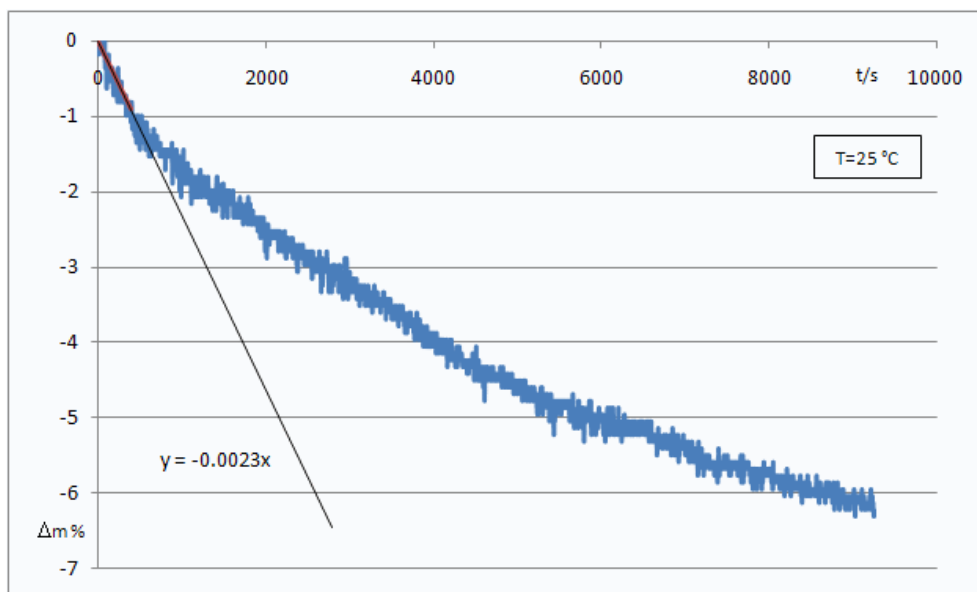


Figure 3.9. Weight trace of *o*-nitrobenzyl methylamine carbamate salt **27** at 25 °C. Weight loss indicated CO₂ loss caused by decarboxylation.

A plot of the collected mass trace was graphically represented (Figure 3.9). The *x* axis shows the time in seconds, the *y* axis shows the weight change in percentage of the initial weight.

Decomposition rate *r* is the time derivative of weight loss Eq.22.

$$r \left[\frac{\Delta m\%}{s} \right] = \frac{d(\Delta m\%)}{dt} \quad r: \text{decomposition rate} \quad \text{Eq.22}$$

Decomposition rate *r* showed the percentage of weight loss caused by the escaped carbon dioxide in one second. The initial decomposition rate was the highest. During the decomposition, amine **2** was expelled from the solid in the form of thick oil and it constrained the further escape of CO₂ by covering the solid. Therefore, at the later parts of the curve, mass transport limitations became rate determining rather than kinetically driven. Consequently, the most descriptive information about the stability of a carbamate was the initial decomposition rate that was the slope of the initial part of the weight-curve. The slope allowed quantifying the decomposition rate of carbamates at the measured temperature. The experimental setup was designed to operate at room temperature, but the rate of decomposition was also measured at 30, 40 and 50 °C by thermogravimetric analysis, TGA. The found results are shown below (Figure 3.10). The initial decomposition rates are also summarised (Table 3.7).

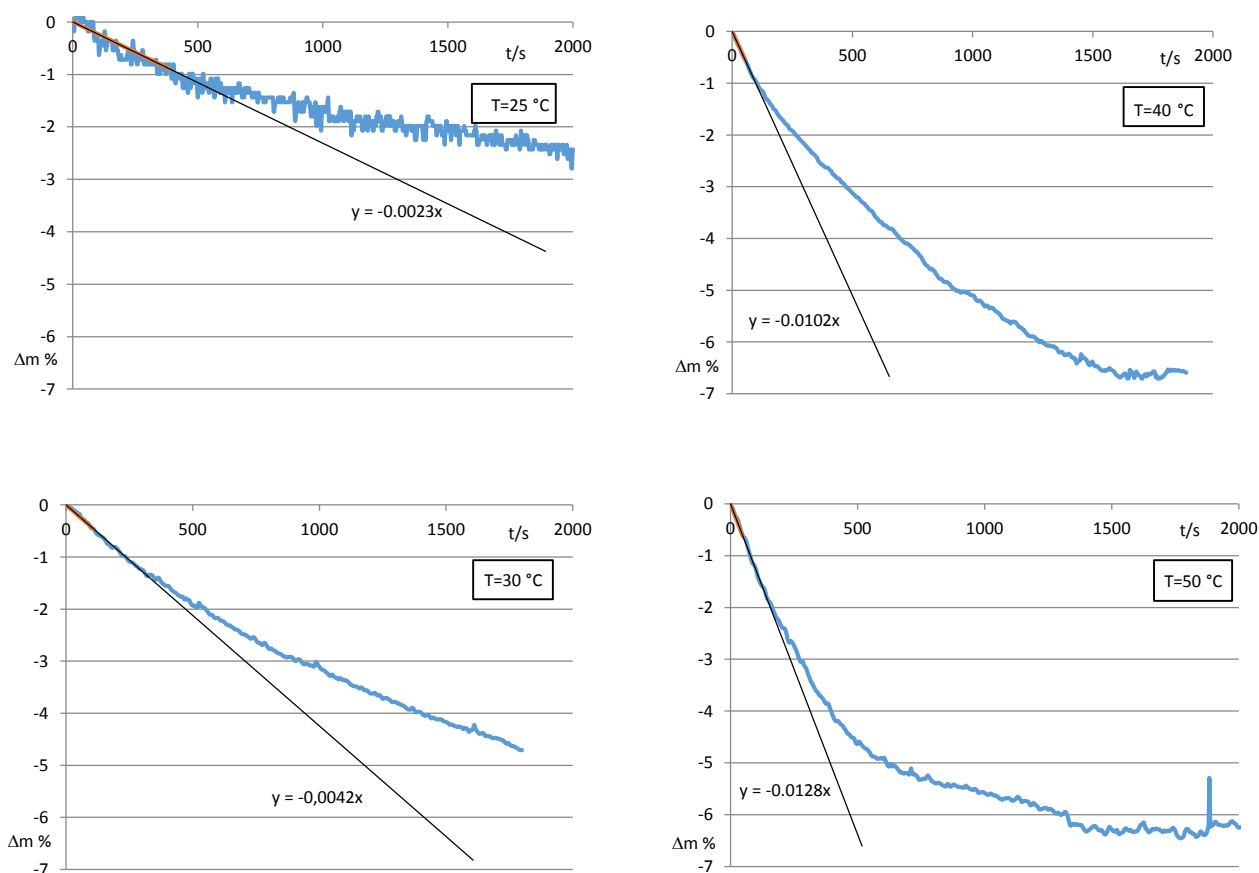


Figure 3.10. Weight trace of *o*-nitrobenzyl methylamine carbamate salt **27** at 25, 30, 40 and 50 °C. Weight loss indicates CO₂ loss caused by decarboxylation.

Table 3.7. Experimental initial decomposition rate at four different temperatures.

| Temperature (°C) | 25 | 30 | 40 | 50 |
|--|---------|---------|---------|---------|
| Decomposition rate ($\frac{\Delta m\%}{\%}$) | -0.0023 | -0.0042 | -0.0102 | -0.0128 |
| Relative rate | 1 | 1.82 | 4.43 | 5.57 |

The decomposition rate consistently slowed with time at all temperatures. This was explained by mass transport limitations earlier. However, the decomposition rate clearly increased with temperature (Table 3.7). The decomposition rate was nearly doubled (82% increase) after the temperature was increased from 25 °C to 30 °C and also a large increase of rate (140%) was observed after a temperature increase from 30 °C to 40 °C. Changing from 40 °C to 50 °C, however, induced the only a considerably lower (30%) rate increase. Temperature dependence of reaction rates could be explained by well-known kinetic rules, such as the Arrhenius equation.^[4] According to this, the rate of a chemical reaction increases with temperature, and the increase depends on the activation energy. Carbamate formation was an exothermic reaction, because increase of temperature was observed during formation (3.9). From the thermodynamic point of view, carbamate formation could be considered as an exothermic reversible reaction.

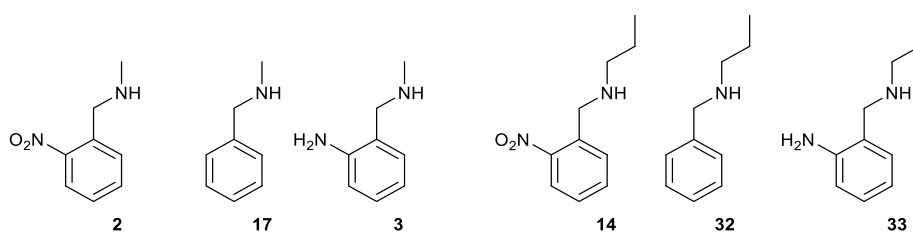
3.11.3 Accuracy of thermogravimetric measurements

The TGA device did not start recording the weight immediately after insertion of the sample, but only after a settling procedure. As the graphs demonstrate, the decomposition rate decreased with time as mass transport limitations became rate determining (Figure 3.10). It could be suspected that an initial decomposition occurred during the settling procedure. This partial decomposition could explain why the rate increase was less significant when the temperature was increased from 40 to 50 °C, compared to rate increases from 30 to 40 and 25 to 30 °C.

According to the proposed molecular formula of carbamate salt **27**, about 11.7% weight loss was expected after total decarboxylation. TGA experiment at 25 and 30 °C were not run until completion, the mass trace did not reach plateau when the experiments were stopped (Figure 3.9, Figure 3.10). Experiments at 40 and 50 °C, however, showed complete decarboxylation with around 6.5% weight loss. The difference between measured (6.5%) the calculated (11.7%) weight loss could be attributed to the decarboxylation during the settling period, which was not monitored. Incomplete CO₂ escape could also explain why the calculated weight loss (11.7%) was not reached. Even though carbamate **27** decomposed completely, a portion of CO₂ may have remained physically dissolved in the sample, and therefore did not cause weight loss.

The stability of *o*-aminobenzyl methylamine carbamate salt **28** was investigated using a laboratory scale at room temperature. In contrast to carbamate salt **27**, no weight loss was observed.

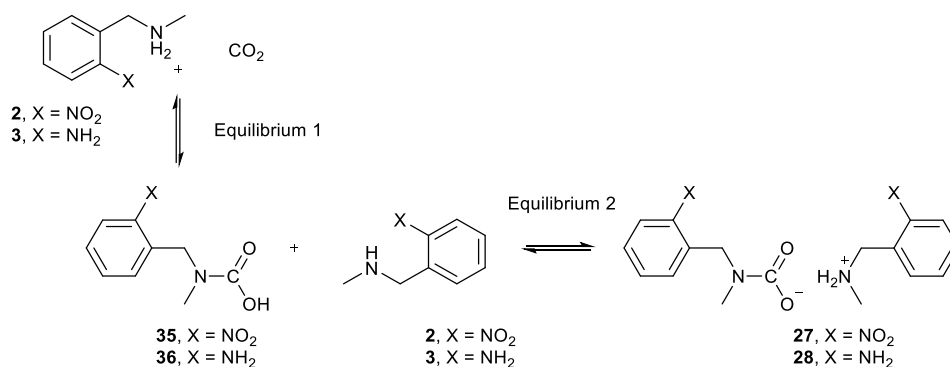
3.12 Conclusions of amine - CO₂ adduct formation tests



Propylamines **14**, **32**, and **33** and methylamine **17** did not form solid carbamate, while methylamines **2** and **3** did. However, reaction between CO₂ and amines **17**, **14**, **32** and **33** was also occurring. Formation of CO₂ adducts could be speculated, but their low crystallinity because of a relatively long, greasy aliphatic chain possibly prevented them assuming a crystalline form.

Stability comparison of CO₂ adducts **27** and **28** showed considerable difference: While nitro derivative **27** slowly decomposed, aniline derivative **28** remained solid at room

temperature if exposed to air. Methylamine **17** did not form a crystalline CO₂ adduct. The group in *ortho* position, in the case of the investigated benzyl amines amino, hydrogen or nitro groups, could possibly affect the stability of the corresponding adduct. Consider the following equilibria between neat amine + CO₂ and carbamate salts, through carbamic acid intermediate (Scheme 3.19).

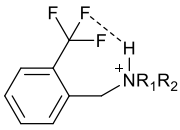
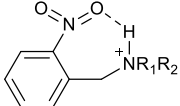
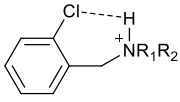
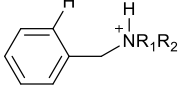
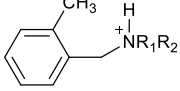
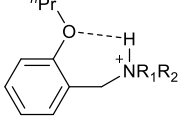
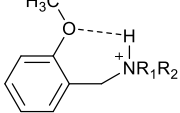


Scheme 3.19. Equilibrium between neat amine + CO₂ and carbamate salt through carbamic acid.

Equilibrium 2 is an acid/base reaction. The ratio of carbamic acid salt and carbamic acid + neat amine, which is in relation with the *K* of Equilibrium 2, is determined by acidic and basic strength of the reactants. Higher acidic/basic strength will push Equilibrium 2 into the direction of carbamic acid. Carbamic acid is in equilibrium with neat amine + CO₂. Increasing free carbamic acid concentration will push Equilibrium 1 to the direction that produces CO₂. The fugacity of CO₂ will therefore increase and it can escape easier. If the sample is exposed to air and the evolved CO₂ could leave the system, and Equilibrium 1 will become quasi irreversible. If CO₂ is free to go, carbamate salt will decarboxylate to neat amine through Equilibria 1 and 2. This theory can also explain why *o*-nitrobenzyl methylamine carbamate salt **27** was stable in a closed vial for several months (3.11.1).

Basicity of *ortho* functionalised benzyl amines was investigated by Bartolini.^[106] He investigated the relation between groups in *ortho* position and basic strength (Table 3.8).

Table 3.8. Effect of the group in *ortho* position on the acidity of conjugate acids of benzylamines.^[106]

| Entry | Acid | pK_a |
|-------|--|--------|
| 1 |  | 6.15 |
| 2 |  | 6.25 |
| 3 |  | 6.92 |
| 4 |  | 7.42 |
| 5 |  | 7.46 |
| 6 |  | 7.75 |
| 7 |  | 7.80 |

Bartolini found, groups that are able to form H bonds, may either stabilise or destabilise the protonated ammonium ion. Benzylamines with strongly electron withdrawing groups, such as $-CF_3$ or $-NO_2$ (Table 3.8, Entries 1 and 2), were weaker bases compared to benzylamines without intramolecular H bonds (Table 3.8, Entries 4 and 5). Groups that could donate electrons (Table 3.8, Entries 6 and 7) could stabilize the cation, and enhance basicity of benzylamine. Unfortunately, he did not test the basicity of the *ortho* amino derivatives. It could be assumed, however, that an amino group in *ortho* position would increase basicity because it is an electron rich H acceptor. The basicities of the benzyl methylamines we investigated were the following in increasing order: *o*-nitrobenzyl methylamine **2**, benzyl methylamine **17** and *o*-aminobenzyl methylamine **3**. *O*-Aminobenzyl methylamine **3** formed the most stable carbamate, which was in accordance of basicity considerations. However, *o*-nitrobenzyl methylamine **2** also formed a relatively stable, crystalline carbamate, while the CO_2 adduct of benzyl methylamine **17** was not solid, and that was less stable. If the stability was determined by the basic strength, the benzyl derivative should be more stable than the nitrobenzyl derivative. Basic strength on its own therefore was not the sole determining factor of carbamate stability.

There is very limited amount of information about the acidity of carbamic acids.^[107] They are fairly instable compounds, especially under aqueous conditions.^[83] Their acidity

therefore cannot be measured in water. The *o*-substituents of *o*-aminobenzyl-, benzyl- and *o*-nitrobenzyl methylamines, however, may have affected the stability of the deprotonated carbamic acid anion, therefore the acidity. Stronger carbamic acidity could increase carbamate stability, similarly to increased basicity. Even though a nitro group decreased basicity of the amine, it may have significantly increased the acidity of the carbamic acid, consequently Equilibrium 2 was pushed into the direction of salt formation (Scheme 3.19). The amino group significantly increased the basicity, and only slightly decreased acidity, consequently the Equilibrium 2 was also pushed into the direction of salt formation. Nor basicity neither acidity was increased when only hydrogen atoms were in *ortho* position, consequently Equilibrium 2 was pushed into the direction of neat amine and neat carbamic acid. It is assumed that the carbamic acid pushed Equilibrium 1 into the direction of neat amine and CO₂, disfavoring carbamate formation of benzyl methylamine.

3.13 Optimised preparative procedures

It is essential that the intermediate product of a separation procedure has very good yields. The preparative yield of *o*-nitrobenzyl methylamine carbamate **27** was rather moderate, only around 60%. Stability tests indicated, *o*-nitrobenzyl methylamine carbamate **27** slowly decomposed in air. To reduce the rate of decomposition, the preparative procedure of carbamate salt synthesis was repeated, but the steps of the work-up procedure, filtration, washing and drying, were carried out in CO₂ enriched atmosphere. The scale of the procedure was 50 g. A crude amine was used as a starting material, with *o*-nitrobenzyl methylamine **2** concentrations about 95%. The MTBE solution of the crude was stirred in CO₂ atmosphere for 16 hours. The concentration of amine in the starting reaction mixture was 20wt%.

Carbamic salt was obtained in 74% yield, which was about 15% increase compared to initial preliminary results. The increase was attributed to reduced loss during the work-up procedure, *i.e.* the decomposition of carbamate salt during filtration, washing and drying was limited thanks to the CO₂ enriched atmosphere.

The obtained yield (74%) was close to the yield that could be calculated from solubility data (Table 3.5, 88%). It has to be highlighted, that the two yields are not necessary comparable. The yield of the preparative procedure was obtained using a crude amine as a starting material, containing about 5wt% by-product, *o*-nitrobenzylalcohol **15**. In contrast, purified amine starting material was used for solubility tests. Co- or antisolvent effects of by-product benzylalcohol **15** in the amine + CO₂ + MTBE system were not investigated, therefore its effect on the yield could not be estimated.

The yields of separating *o*-nitrobenzyl methylamine **2** from its MTBE solution could be potentially increased further by applying decreased temperatures for carbamate formation, as solubility tests indicated. Application of enhanced CO₂ pressure for carbamate formation could also have a positive effect, because it would push the amine + CO₂ equilibrium into the direction of carbamate salt (Scheme 3.19).

3.14 Amine regeneration experiments

A produced carbamate salt would serve only as an intermediate for the purification or work-up procedure. The real target was not the carbamate salt itself, but the purified amine. Carbamates have to be decarboxylated before the following reaction steps. The decomposition of *o*-nitrobenzyl methylamine carbamate salt **27** was tested in order to reproduce amine starting material.

3.14.1 Thermal decarboxylation

Decarboxylation rate of carbamate salt **27** was investigated quantitatively (3.11.2). The decomposition rate increased with temperature. Carbamate salt **27** was heated to 90 °C, to above its melting point (70-73 °C). Evolution of gas was observed indicating decarboxylation. Having cooled down the flask, no solid crystallized out. The product of the decarboxylation was identified as *o*-nitrobenzylamine **2** by ¹H-NMR spectroscopy.

3.14.2 Concentration of alcoholic carbamate solution

Carbamate salt of *o*-nitrobenzyl methylamine **2** was dissolved in ethanol. The solution was concentrated using a rotary evaporator. No solid was observed in the flask after the procedure, only oil, of which ¹H-NMR spectrum was identical to that of neat *o*-nitrobenzyl methylamine **2**.

We concluded that concentration of alcoholic carbamate salt solutions could also lead to free amine.

3.14.3 Boiling of carbamate solution

Boiling the aqueous solution of *o*-nitrobenzyl methylamine carbamate salt **27** was also studied as a procedure for decarboxylation. After 30 minutes of boiling the reproduced amine formed a separate bottom layer. The amine was extracted into ethyl acetate, dried and concentrated to afford purified amine **2**. No signs of thermal decomposition were indicated by ¹H-NMR spectroscopy.

This method gave an alternative to the dissolution and concentration. According to Table 3.1, heating water from ambient temperature to its boiling point and evaporation

requires more the seven times more energy than the energy needed only for heating up. Concentration *via* evaporation after the aqueous extraction may be avoided if the amine can be used in aqueous solution.

3.14.4 Driving nitrogen gas through carbamate solution

Carbamate salt **27** was dissolved in methanol-*d*₄. The carbamate form in the initial solution could be clearly identified by ¹H-NMR spectroscopy as carbamic acid derivative peaks at 4.69 (benzyl, I.) and 2.80 ppm (methyl, II.) (Figure 3.11). These peaks disappeared after no more than 20 minutes of N₂ gas bubbling, after which only neat amine was indicated by ¹H-NMR spectroscopy (Figure 3.12).

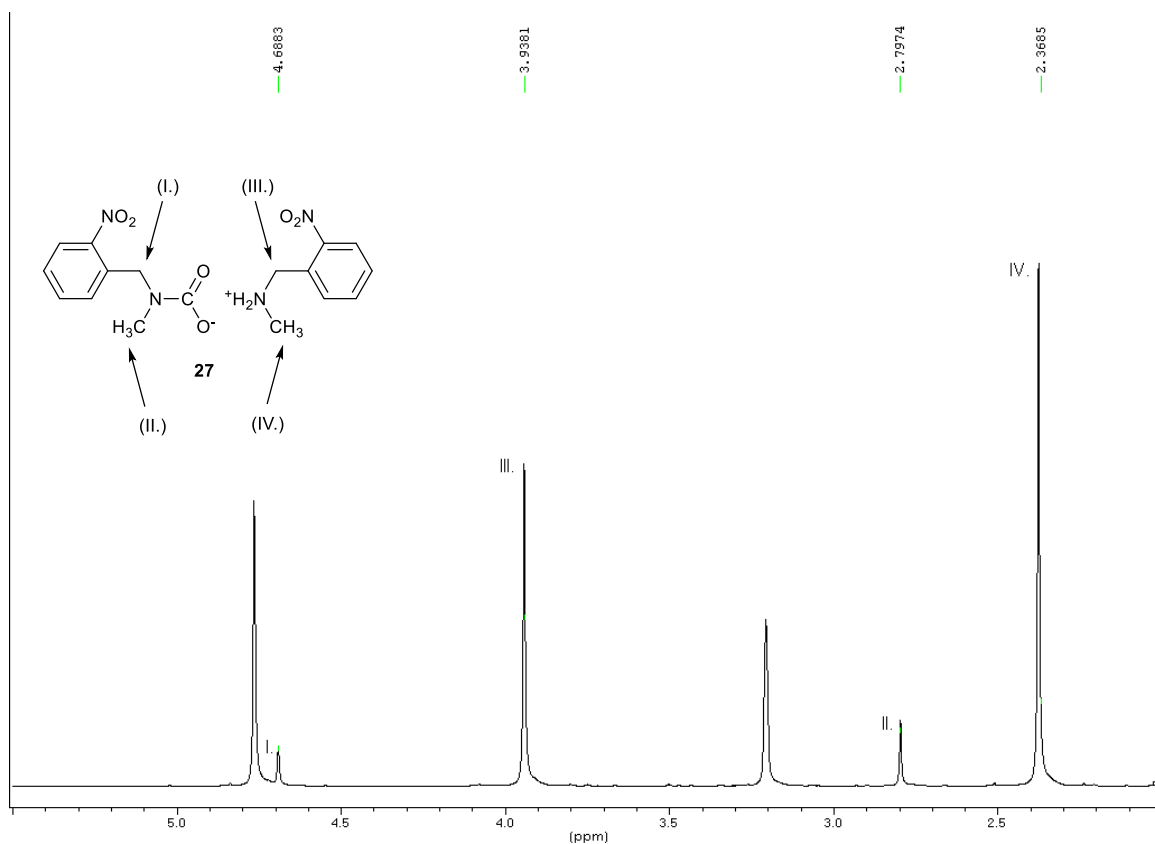


Figure 3.11. Carbamate salt **27** in CD₄OD before N₂ gas bubbling. Aromatic region omitted.

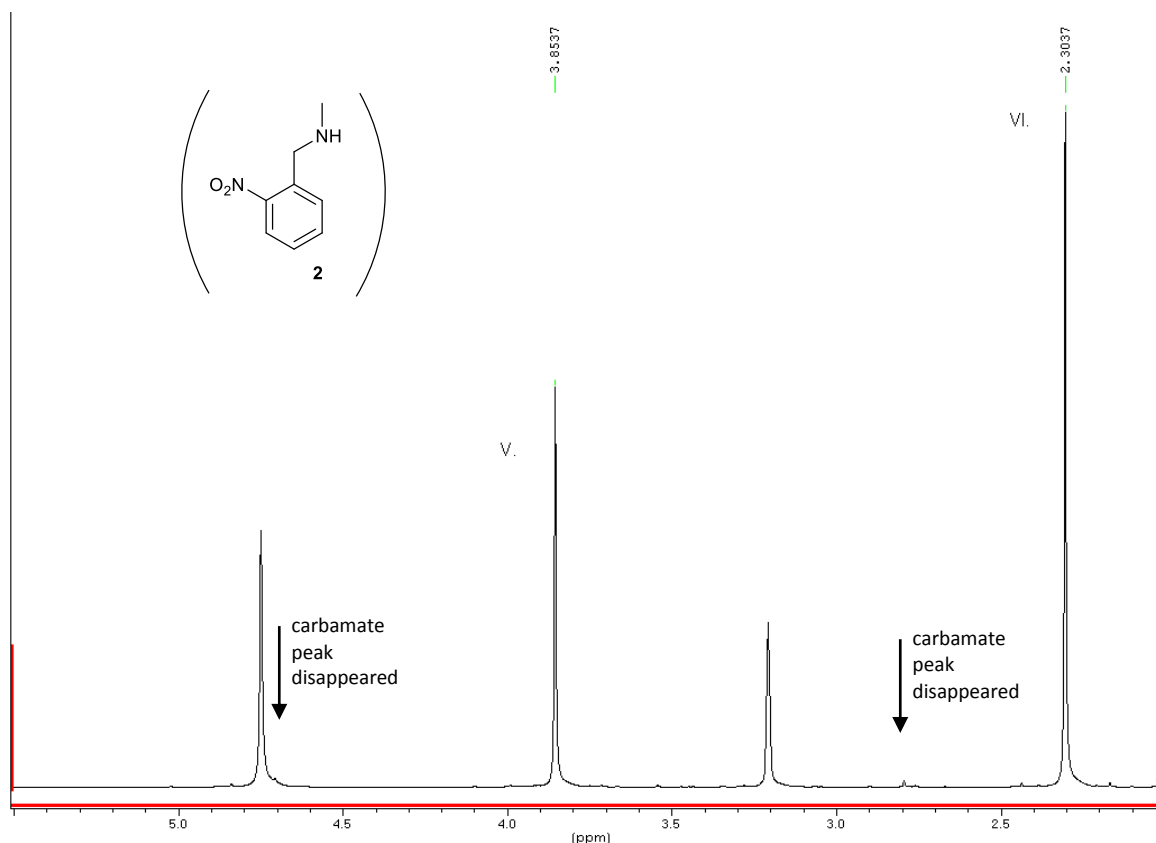


Figure 3.12. Carbamate salt **27** in CD₄OD after N₂ gas bubbling. Aromatic region omitted.

The benzyl protons of the ammonium cation in carbamate salt **27** (III.) were identical to the benzyl protons of amine **2** (V.), likewise methyl protons (IV. and VI.) were.^[83] Peaks at 4.87 and 3.31 ppm were water contamination and solvent residual signals.

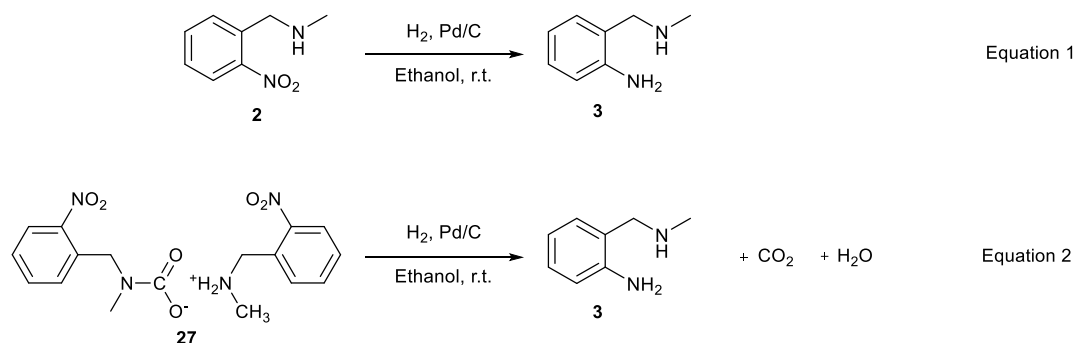
3.15 Carbamate salt as starting material

O-Aminobenzyl methylamine **3** and benzodiazepine **4**, intermediates of SB-214857-A, (Scheme 1.1) were synthesised using the corresponding amine starting materials, *o*-nitrobenzyl methylamine **2** and *o*-aminobenzyl methylamine **3**, as feedstock. However, carbamate salt derivatives **27** and **28** as possible feedstock were also tested. If they could be used as starting material without mayor complications, the procedure of decarboxylation could be skipped.

3.15.1 Carbamate salt as feedstock for *o*-aminobenzyl methylamine **3** synthesis *via* catalytic hydrogenation

The catalytic reduction of *o*-nitrobenzyl methylamine **2** to furnish *o*-aminobenzyl methylamine **3** was quantitative in ethanol at room temperature, (Scheme 3.20, Equation 1) despite worries that the benzylamines, either in nitro or the reduced amino

form, may be susceptible for hydrogenolysis.^[108] The starting nitroamine **2** was replaced with its carbamate salt **27** (Scheme 3.20, Equation 2).

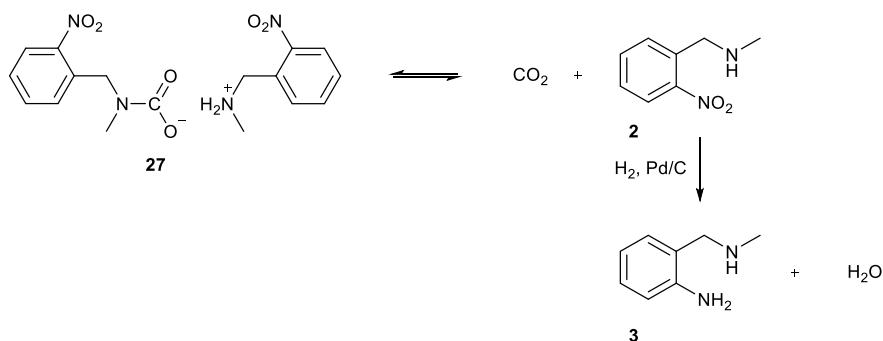


Scheme 3.20. Synthesis of *o*-aminobenzyl methylamine **3** *via* catalytic hydrogenation using either *o*-nitrobenzyl methylamine **2** (Equation 1) or *o*-nitrobenzyl methylamine carbamate **27** (Equation 2) as starting material. Both reactions were quantitative.

Quantitative yield was achieved either free *o*-nitrobenzyl amine **2** or its carbamate salt **27** was used as starting material. It could be therefore concluded, carbamate salt starting materials may not need to be decarboxylated before a next synthetic step, but could be used simply as starting material as a replacement of neat amine.

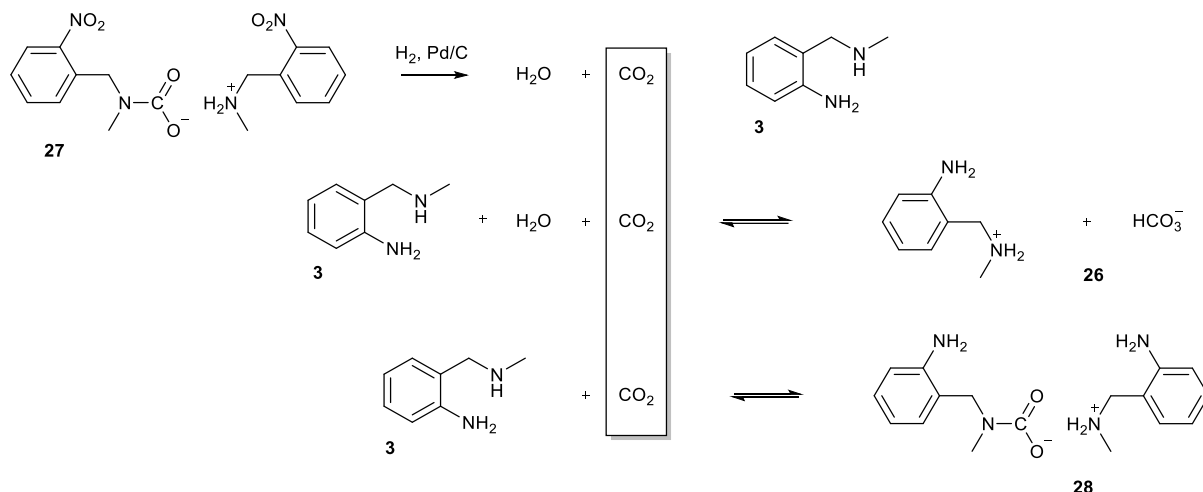
In the very case of the reduction of carbamate derivative, the standard procedure of hydrogenation was followed, including purging to avoid the formation of explosive H₂ gas + air mixture. This involved evacuation of the experimental vessel and filling with hydrogen a number of times. Evacuation of an alcoholic carbamate solution may lead to decarboxylation, as was demonstrated earlier (3.14). The ethanolic carbamate solution possibly underwent a certain degree of decarboxylation *in situ*, during the purging procedure of hydrogenation.

The presence of the remaining CO₂ in the system after *in situ* decarboxylation would possibly not affect the hydrogenation. An equilibrium between carbamic salt and free amine could be assumed. The free amine was reduced, giving the desired aniline and water as by-product. Consumption of nitroamine **2** made the decarboxylation quasi irreversible (Scheme 3.21).



Scheme 3.21. Hydrogenation of *o*-nitrobenzyl methylamine carbamate **27**. The carbamate salt is in equilibrium with free amine **2**, which actually is reduced. The reduction furnished the desired aniline **3**, and gave water as by-product. CO₂ was also liberated from the carbamate.

The accumulation of liberated CO₂ in the system would push the equilibrium into the direction of carbamate formation, and eventually would slow down the hydrogenation because concentration of free nitroamine **2** would decrease. However, aniline **3** product had higher affinity to CO₂ according to earlier observations (3.12), and was explained by its higher basicity. The aniline product would therefore consume the liberated CO₂ either in a bicarbonate or a carbamate formation reaction (Scheme 3.22).

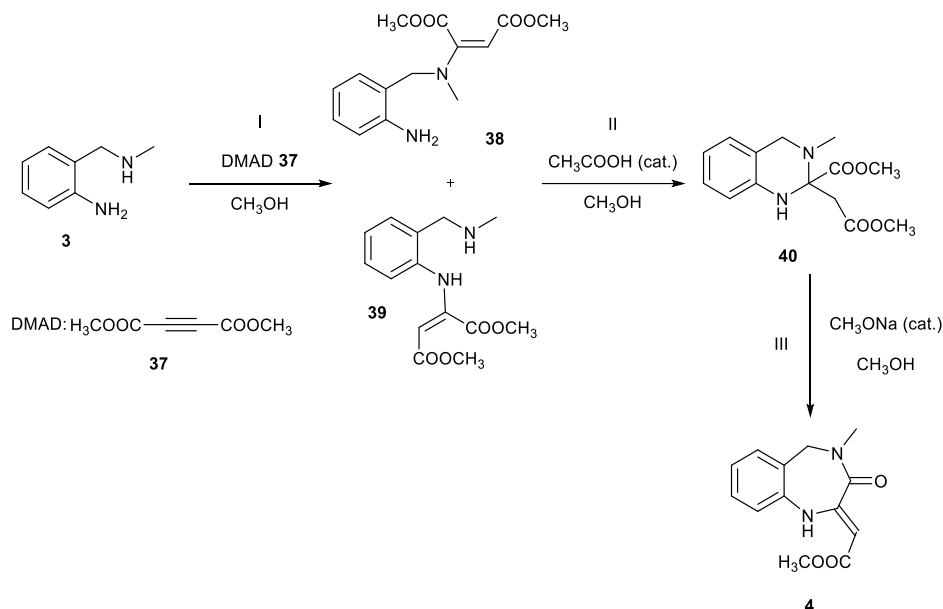


Scheme 3.22. Carbamate or bicarbonate formation reactions of aniline **3** with the CO₂ liberated during the reduction of nitroamine carbamate salt **27**.

Aniline carbamate **28** or bicarbonate **26** may have been formed during the reduction with the remaining CO₂ in the system, but they possibly decomposed during the reaction work up procedure, which involved the concentration of the alcoholic solution of the crude *in vacuo*.

3.15.2 Application of *o*-aminobenzyl methylamine carbamate **28** starting material for the synthesis benzodiazepine **4**

Synthesis of benzodiazepine **4** using *o*-aminobenzyl methylamine **3** starting material was carried out according to the published procedure, and about 51% yield was achieved in the three step one pot synthesis (Scheme 3.23).^[12]



Scheme 3.23. Synthesis of benzodiazepine **4** in a three step one pot procedure. I: alkenylation of aniline **3** with DMAD **37**; II: cyclisation; III: rearrangement.^[12]

When aniline **3** starting material was replaced by its carbamate salt **28**, benzodiazepine **4** was obtained, but the yield dramatically decreased to 16%.

The alkenylation of free aniline and aniline carbamate salt was repeated in $\text{MeOD-}d_4$, and the product, mixture of **38** and **39** alkenylated products, was assayed by $^1\text{H-NMR}$ spectroscopy. $\text{MeOD-}d_4$ was chosen as medium, because this way the reaction mixture could be easily monitored by NMR spectroscopy without removal of MeOH solvent. Solvent removal could be a thermal procedure, such as distillation, which could significantly change the composition of the reaction mixture, which otherwise was proceeding at 0-5 °C. A disadvantage of using $\text{MeOD-}d_4$ reaction medium was a risk of H-D exchange, which was observed; alkene protons did not appear on the spectra. Alkene hydrogen atoms originated from either amine or aniline hydrogen atoms, which were rather mobile, and possibly rapidly exchanged to deuterium after dissolving the starting material in $\text{MeOH-}d_4$ solvent.

The intermediate after addition of DMAD was analysed by $^1\text{H-NMR}$ spectroscopy for both reactions, either aniline **3** or its carbamate salt **28** was the starting material. The analysis indicated the alkenylation was progressing in both cases. The ratio of

intermediates **38** and **39** was determined by integration of benzyl hydrogen atoms at 4.31 ppm (**41**) and 4.25 ppm (**40**). The ratio of isomers **38** and **39** in the first experiment (absence of CO₂, aniline **3** starting material) was 1:0.75. In the second experiment (presence of CO₂, carbamate salt **28** starting material), the ratio of isomers **38** and **39** was 1:0.81, similar to experiment one. Presence of CO₂ did not affect the ratio, therefore was not able to act as a protecting group to control the electrophilic attack of DMAD to either amine or aniline nitrogen atoms.

Peaks of both alkenylated aniline of **38** and **39** doubled in their ¹H-NMR spectra in presence of CO₂, indicating the formation of CO₂ adducts. Duplication of peaks was a typical sign of reaction with CO₂ (3.5.1) either for carbamate (Figure 3.11, Figure 3.12) or bicarbonate formation.

CO₂ possibly remained in the reaction mixture until the third step, which was a base catalysed rearrangement to yield benzodiazepine **4** (Scheme 3.23). Presence of CO₂ became critical at this stage, because it possibly scavenged sodium methanolate, a strong base, which was added in catalytic amount to catalyse the final rearrangement.

3.16 Summary

Crystallisation is a favoured separation and purification procedure of the pharmaceutical industry. The target of the species must, however, be crystalline, and precipitate out from a solution in pure form. Crystallisation could be extended to APIs or their intermediates even if they are not actually crystalline. The most common way of doing this is isolation in a form of salt with a suitable acid or base. Amine functions are common in APIs or in their intermediates. In this research the reactivity of amines with CO₂ was investigated in order to form solids that can replace salts of conventional acids in the purification procedure.

A range of investigated amines were tested for carbamate formations. The available information does not allow predicting which amines are suitable for carbamate formation.

Carbamate formation of *o*-nitrobenzyl methylamine **2**, intermediate of AZ drug candidate SB-214857-A, was observed, however, the yield of purification was only 60% initially. The carbamate formation reaction was investigated in more details in order to improve this. Solubility tests indicated, carrying out the carbamate formation reaction at lower temperatures could potentially increase the overall efficiency of the procedure. TGA measurements showed, the carbamate decomposed if exposed to air. Decomposition during the separation procedure, *i.e.* filtration, washing and drying, could potentially reduce the recovery. By carrying out these steps in CO₂ enriched

atmosphere, the recovery could be increased up to 74%. This example demonstrated the potential and competitiveness of the CO₂ aided crystallisation.

The carbamate salt of *o*-nitrobenzyl methylamine **2** was only exploited as an intermediate of the purification procedure, but it was not the final product. Its decarboxylation that yielded the required free amine was therefore investigated. If the carbamate salt was exposed to air, it slowly decarboxylated. The rate of the decarboxylation increased with temperature, as TGA measurements showed. Decarboxylation could be also carried out by treating the solution of the carbamate salt either by heating or N₂ gas sparging.

Carbamates may be used as starting material to replace their free amine equivalents, therefore the step of decarboxylation can be skipped. This was demonstrated by the hydrogenation of *o*-nitrobenzyl methylamine **2** to yield *o*-aminobenzyl methylamine **3**. Replacement of *o*-aminobenzyl methylamine **3** with its carbamate derivative as starting material for the synthesis of benzodiazepine **4** was, however not successful, the yield decreased from 51 % to 16%. Exploitation of carbamates as protecting group to control the reactivity of amino- and aniline nitrogen atoms was not successful and would need more detailed research.

Chapter - 4

Application of carbon dioxide as antisolvent for crystallisation procedures

4.1 Introduction to high pressure CO₂ based procedures

Liquid or scCO₂ based antisolvent procedures are high pressure applications. Relevant areas, including phase equilibria measurement and modelling will be reviewed in the next sections.

4.2 Measurement methods to acquire high pressure phase equilibria

The phase behaviour of carbon dioxide – organic solute binary systems has been studied extensively. Dohrn reviewed the available experimental techniques.^[109] There are fundamentally two methods for obtaining these measurements, either *analytical* or *synthetic* methods.^[25]

4.3 Obtaining phase equilibria *via* analytical methods

Analytical methods require the measurement of the co-existing phases. The composition of the co-existing phases can be determined under atmospheric conditions after sampling using a conventional analytical procedure, such as chromatography. An important advantage is to apply a highly accurate, reliable, conventional analysis. The disadvantage is disturbing the system with sampling. Alternatively, the compositions could also be determined without sampling within the high pressure cell using methods such as spectroscopy. The advantage is the lack of disturbance because of the lack of sampling. The disadvantage is a complicated calibration of the analysis.

A typical equipment designed for phase equilibria measurements *via* an analytical method is built around a thermostatic high pressure vessel (C) of reasonably large volume, up to 1 litre (Figure 4.1). Mixing is carried out by pumps P1 and P3. Multiple windows allow viewing of the content, and the alignment of piping allows the sampling of all the co-existing phases in equilibrium. The sampling occurs when the temperature and pressure are steady, and the phases settled after the mixing had ceased. The measurement method is usually gas chromatography which could be incorporated into the system, because the sample must be transferred to the GC's evaporator without change. A problem in this method is the disturbance of the system because of sampling: the loss of material changes the pressure and affects the equilibrium. The impact can be minimised by a large vessel volume, but this increases the volume of chemicals required. An important advantage is that the composition of co-existing phases will be available.

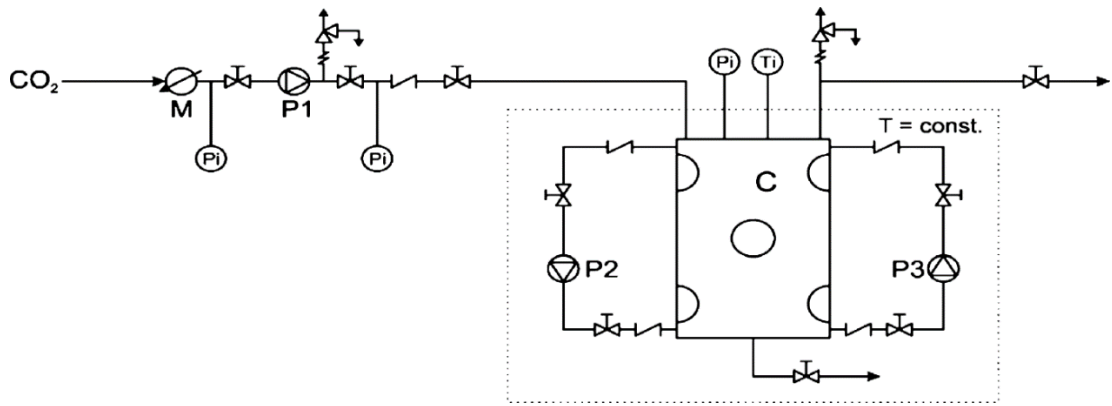


Figure 4.1. Typical set-up for static-analytic method. P_i, T_i: pressure and temperature sensors; P1,P2 P3: pumps; M: mass flow meter.^[110]

4.4 Obtaining phase equilibria *via* synthetic methods

In the case of the “synthetic method” sampling is not needed. A mixture is made, “synthesised”, in a precisely known composition. The mixture is initially single phase, then by varying either pressure or temperature, a formation of a second phase starts. The problem of analysing the composition of co-existing phases is replaced by their synthesis, which may not be obvious in high pressure systems.^[109]

A typical synthetic experimental set-up is built around a thermostatic variable volume view cell (VVVC) (Figure 4.2).^[111] The temperature is controlled by a heating mantle (M) until the desired temperature is reached. The pressure is increased by a piston (P) forestroke until the monophasic region attained using hydraulic pump (HP2). The hydraulic pressure is then decreased slowly, so that the piston (P) starts a backstroke. Upon this isothermal expansion the phase envelope is intersected at a certain pressure, and the mixture becomes cloudy indicating phase separation. This pressure is then noted on a pressure-composition (p-x) diagram. The experiment is repeated on different compositions and the phase diagram at the particular temperature can be obtained. A setback of the method is that the composition of phases in equilibrium is not obtained pairwise, which could be necessary for phase equilibria modelling with Equation of State (EoS), for instance. Therefore, after the whole phase diagram is outlined, the composition of co-existing phases is calculated by interpolation the nearest measurement points. This reduces the accuracy of the method.

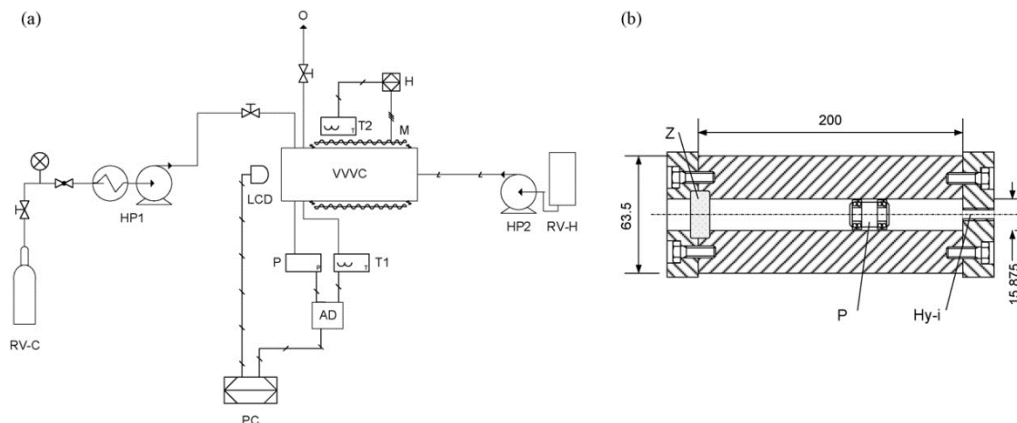


Figure 4.2. Typical set-up for synthetic method. RV-C, RV-H: reservoir for CO₂ and hydraulic oil; HP1, HP2: high pressure pumps; LDC: camera; P, T1, T2: pressure and temperature sensors; AD, PC: analog-digital converter and data acquisition system; H, M: heat control and heating mantle; VVVC: variable volume view cell; P: plunger; Hy-i: hydraulic oil inlet.^[112]

The accuracies of static-analytic and synthetic methods are of a similar order of magnitude. Synthetic methods have a disadvantage if there are more than two components. However, volumes may be small because the lack of sampling. Small volumes allow robust constructions. Smith investigated phase equilibria up to 2.60 GPa and 670 °C.^[113]

Analytical methods may be problematic if phase separation is difficult, because of similar densities, for instance. The density of co-existing phases can often be similar, especially in the vicinity of the critical point. In these cases synthetic methods have an advantage.^[109]

4.5 Phase behaviour of various binary organic solvent – carbon dioxide systems

The experimental results of CO₂ with water,^[114] dimethyl sulfoxide (DMSO),^[115-116] dimethylformamide (DMF),^[117-118] diethylformamide (DEF),^[118] dibutylformamide (DBF),^[118] *N*-methyl-2-pyrrolidone (NMP),^[119] *N*-ethyl-2-pyrrolidone (NEP),^[119] ethyl acetate (EtOAc),^[120] tetrahydrofuran (THF)^[110] ethanol^[110] and methanol^[121] are available in the literature. These diagrams provide the composition of the CO₂ rich and solvent rich phases in equilibrium. They give information about the mutual solubility, and also the critical pressure, above which the miscibility is complete at the whole composition range. These results are not only useful if solubility data are needed at the temperature of an actual experiment. Most authors also provide modelling data with Equation of State and mixing rule parameters. Phase equilibrium data therefore can be interpolated or extrapolated to the temperature of interest.

Phase behaviour of binary systems could be disturbed by a third component. In a practical example, when solvent residues are extracted from a pharmaceutical with supercritical CO₂, the drug may have high affinity to the solvent and could adsorb solvent similarly to a drying agent adsorbing moisture. However, solvent-CO₂ binary data may still give a general idea about the solubility, but its validity and accuracy must not be overestimated.

The phase diagram of the DMF-CO₂ system is shown below (Figure 4.3). Consider the phase equilibrium data at 313.05K (▲curve).

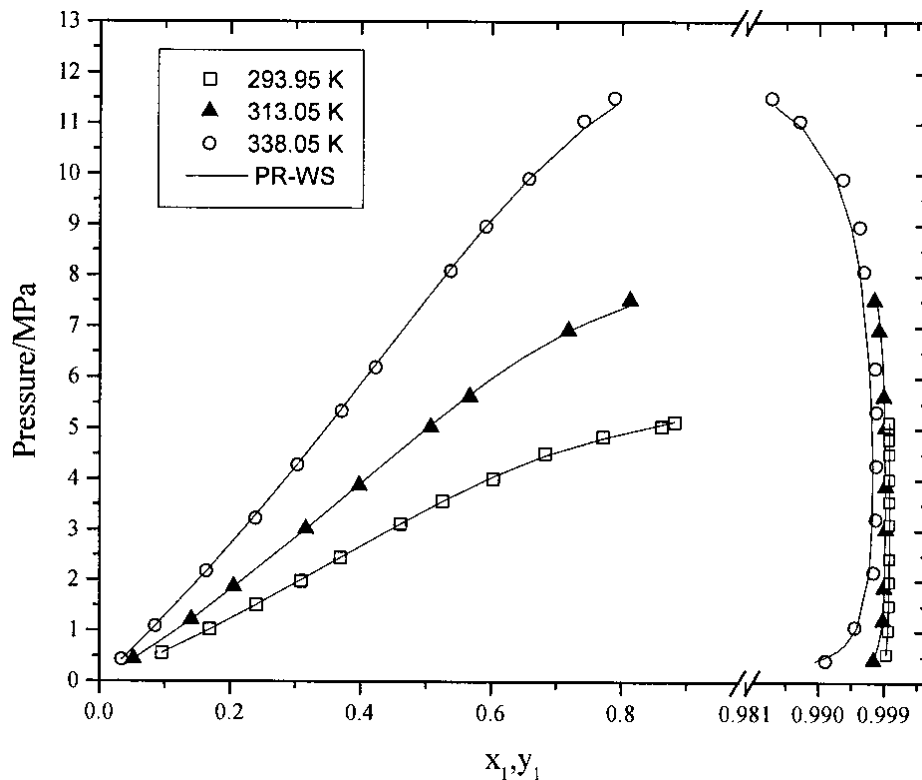


Figure 4.3. DMF – CO₂ binary system. Static method.^[117]

Above the line (▲curve) there is a single phase fluid phase, consisting of DMF and CO₂. Under the line there is the two phase envelope, with liquid + gas co-existence. The composition of the gas and liquid in equilibrium is determined by the tie line, which is perpendicular to the pressure axis, and intersects at the actual pressure of the system. The highest pressure of the phase envelope, above that only one fluid phase exists, is the critical solution pressure. It is about 7.2 MPa at this temperature. Critical solution pressure of some systems are summarised below (Table 4.1).

Table 4.1. Critical solution pressure of various solvent + CO₂ systems at 313 K.

| Entry | Solvent | Critical pressure /MPa |
|-------|---------------|------------------------|
| 1 | DMF | 8 |
| 2 | DMSO | 10 |
| 3 | NMP | 10 |
| 4 | Ethyl acetate | 6 |
| 5 | THF | 7 |
| 6 | Ethanol | 7 |

Above the critical solution pressure only one fluid phase exists, regardless of the concentration. Note that the third chemical (the pharmaceutical to be dried) may impact on the solvent + CO₂ phase behaviour.^[122]

4.6 Modelling phase equilibria^[123]

Binary phase equilibria can be modelled, and the calculation is usually based on fugacity. If the partial fugacities are equal for each component in all the phases, the system is in thermodynamic equilibrium: phases β and γ are in equilibrium, if the fugacities are equal for all i components Eq.23.

$$f_i^\beta = f_i^\gamma \quad f: \text{fugacities of compound } i \text{ in phases } \beta \text{ and } \gamma \quad \text{Eq.23}$$

The fugacity is calculated using fugacity coefficient Eq.24, which can be calculated by Eq.25 if the pressure dependence of the compressibility factor is known and the temperature and composition are constant.

$$f_i = x_i \Phi_i p \quad \begin{array}{l} x: \text{molar fraction} \\ \Phi: \text{fugacity coefficient} \end{array} \quad \text{Eq.24}$$

$$\ln \Phi = \int_0^p (Z - 1) \frac{dp}{p} \quad Z: \text{compressibility} \quad \text{Eq.25}$$

Knowledge of the pressure dependence of the compressibility Z factor is necessary. This can be derived from an equation of state (EoS). The more accurate the EoS is for a given system, the more accurate the fugacity coefficient will be.^[123] Cubic EoSs can be used to calculate liquid-liquid equilibria, although they can describe liquid phases less accurately than gas phases. There are various EoSs published in the literature. None of them have been proved to be superior to the rest. Choosing a proper EoS to describe a particular system is always a trial-and-error procedure.^[37, 123]

An EoS itself describes a single component fluid system. Using a mixing rule to calculate EoS constants, it can be applied on fluid mixtures as well. The mixing rules are empirical relationships, and their parameters are varied by an optimization algorithm like a simplex method to minimize the deviation between calculated and measured data.^[124]

In the case of EoS, there is a wide choice of mixing rules. None of them have been proved superior to the rest.

Having a model for a binary system, interpolation between the collected data points or even careful extrapolation are possible, therefore phase behaviour data can be used at a temperature other than the experimental temperatures. The accuracy depends on how well the EoS and the mixing rule can describe a particular system with the given constants.

4.7 Gas expanded liquids

4.7.1 Introduction to gas expanded liquids (GXLs)

A CO₂ antisolvent procedure relies on the solubility of the gas in the actual solvent. The formed CO₂-solvent mixture is often referred as gas expanded liquid or GXL. GXLs will be reviewed in the next section.

If GXLs are investigated, the focus of interest is on the heavy phase, which is rich in the organic solvent, even though the light phase (vapour) that is in equilibrium with the heavy phase (liquid) is also a mixture of CO₂ and solvent. The light phase is rich in CO₂ and typically poor in solvent, particularly below the critical pressure of the mixture. The composition of the light phase is often not investigated. Investigation of GXLs is therefore less detailed than investigation of full equilibria.

Jessop categorized solvents into three classes according to their expansion under pressure of CO₂ (Table 4.2):^[32]

Class I liquids have insufficient ability to dissolve CO₂, therefore do not expand significantly and, except for *pH*, they have no significant change in their properties. Water is a typical class I liquid.

Class II liquids dissolve large amounts of CO₂, expand greatly and consequently undergo significant changes in virtually every physical property. Class II liquids are methanol, hexane and most other traditional organic solvents.

Class III liquids dissolve only moderate amounts of CO₂ and, therefore, expand only moderately in volume. As a result, some properties such as viscosity, change significantly while others, such as polarity, do not. Class III liquids are ionic liquids, liquid polymers and crude oil.

Table 4.2. Three classes of solvents depending on their expansion with CO₂. The experiments were conducted at 40 °C.^[32]

| Class | Solvent | Pressure | Volumetric expansion | CO ₂ | |
|-------|------------------------------------|----------|----------------------|-----------------|------|
| | | MPa | % | wt% | mol% |
| I | H ₂ O | 7.0 | na. | 4.8 | 2 |
| II | MeCN | 6.9 | 387 | 83 | 82 |
| | 1,4-dioxane | 6.9 | 954 | 79 | 89 |
| | DMF | 6.9 | 281 | 52 | 65 |
| III | [bmim]BF ₄ ^a | 7.0 | 17 | 15 | 47 |
| | PEG-400 | 8.0 | 25 | 16 | 63 |
| | PEG-2700 ^b | 6.0 | 25 | 12 | 89 |

na.: not available

^ainterpolated from literature data

^bAt 35 °C

4.7.2 Measurement methods of GXs

The most common methods for measurement of volumetric expansion are densitometry coupled with sampling,^[116] or the use of a view cell that allows a visual volume measurement (Figure 4.4).^[125] A different experimental device used a fibre-optic probe to read the fluid level in the system.^[126]

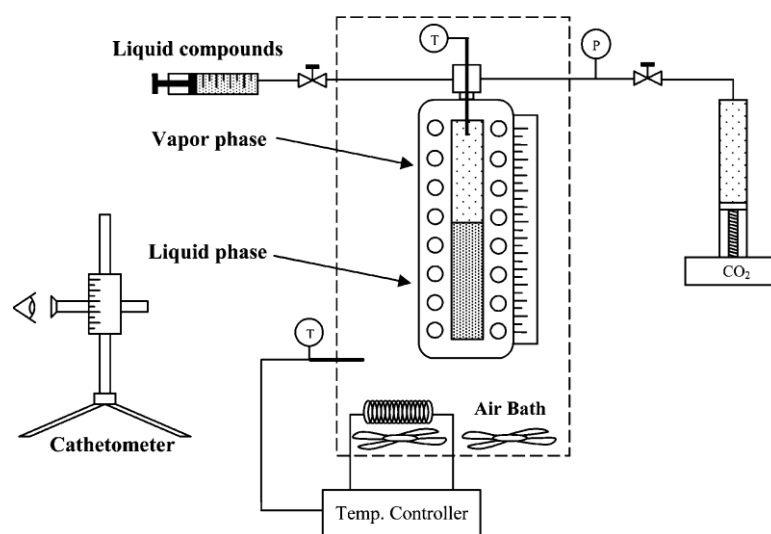


Figure 4.4. Typical Jerguson-type view cell for solvent expansion measurement, used up to 10 MPa.^[125]

These experiments measure only a part of phase equilibria, namely the volumetric expansion and composition of the heavy phase. The composition of the light phase will not be available.

The liquid phase expansion measurements therefore carry a systematic error. The degree of error depends on the amount of organic solvent dissolved in the light phase. In the case of typical, non-volatile ionic liquids, zero solubility can be quite a good approximation and close to the actual value. However, in the case of DMF, for instance,

the concentration of organic solvent in the light phase is around 0.1% at 294 K and it reaches 1.25% at 338 K at pressures around 11.0 MPa (Figure 4.3).

The volume of the light phase depends on the initial load of organic solvent. If the expanded volume is low, a large volume of light phase remains. In an extreme case, when a very small amount of solvent is loaded, it can completely evaporate into the light phase and volumetric contraction could be observed instead of expansion. The problem of initial load could be avoided by using a VVVC, which was described earlier (Figure 4.2). A highly compressed single phase CO₂-organic solution can be expanded by a piston movement until the occurrence of a gas phase is detected optically, by opalescence. A minimal volume of gas phase can be sufficient for this, therefore the composition of the heavy phase is accurately known (same as the initially synthesised mixture). In the case of analytical methods, the light phase has to have a considerable volume, but it is assayed by sampling, and not assumed to have zero concentration. Consequently, either synthetic or analytical methods that are used to study the exact phase behaviour of binary systems, are superior compared to the methods measuring the volumetric expansion of liquids exclusively.

4.7.3 Volumetric expansion of various organic solvents under pressure of CO₂

Volumetric expansion of solvents under CO₂ pressure is well studied. Eckert investigated systems of CO₂ + solvents, such as isopropanol, acetonitrile, dichloromethane, nitromethane, NMP, THF, 2,2,2-trifluoroethanol, perfluorohexane, acetone, toluene, ethanol and DMSO.^[125]

The temperature has a significant effect on volumetric expansion of solvents by gases. Toluene expands 180% in volume at 5.0 MPa at 25 °C, but 7.8 MPa is needed for the same expansion at 50 °C (Figure 4.5).^[126] It is suspected to be possible to achieve the same expansion at significantly lower pressures at about 0 °C easing the equipment design, but no experimental data are available in the literature.

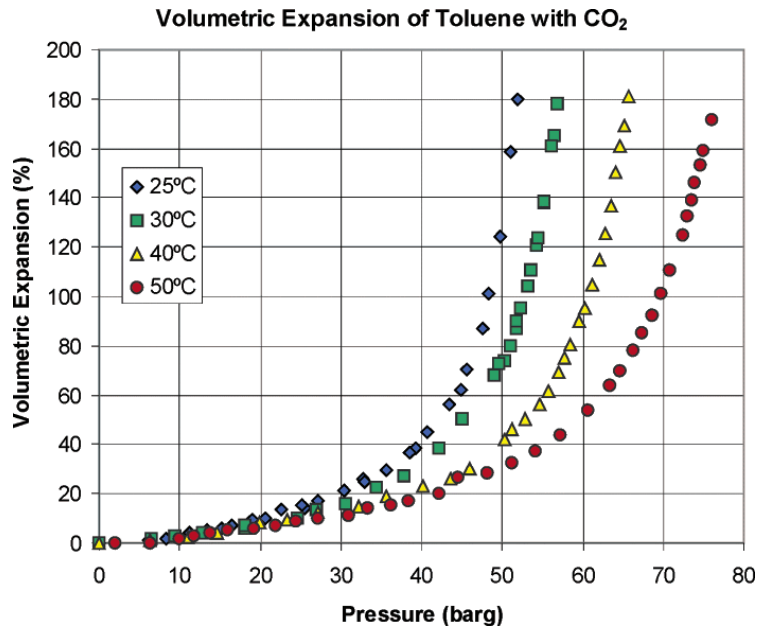


Figure 4.5. Expansion of toluene at four different temperatures. Used method: fibre-optic cell.^[126]

The volumetric expansion tends to increase exponentially with pressure. However, there could be significant differences between the expansions of different solvents at the same pressure. Rajasingam compared the volumetric expansion of acetone, DMSO and NMP (Figure 4.6).^[127] The same expansion (around 100% in volume) could be reached already at 4.0 MPa for acetone, but a significantly higher pressure, about 6.0 MPa was necessary for DMSO or NMP.

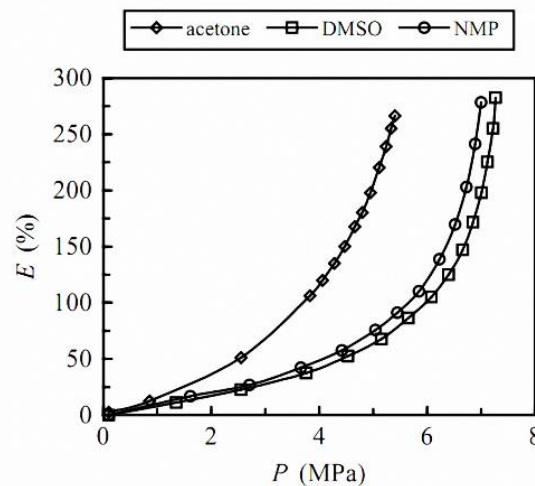


Figure 4.6. Expansion of three organic solvents at 308 K. Used method: view cell.^[127]

Eckert found that NMP expands around 100% at 7.0 MPa, while THF expands around 600% at the same pressure. In the region of moderate pressures, between 2.0 and 4.0 MPa, the expansion is already significant varying from 12 to 30% in the case of NMP, and 24 to 70% for acetonitrile. Considering the solubility of CO₂ in a series of polar organic solvents some interesting behaviour can be seen. The solubility of CO₂ at an

arbitrary pressure of 5.0 MPa in various solvents decreases in the following order: perfluorohexane, tetrahydrofuran, dichloromethane, acetonitrile, *N*-methyl-2-pyrrolidone, nitromethane, 2,2,2-trifluoroethanol, and 2-propanol.^[125] CO₂ has a zero net dipole moment because of its symmetry, therefore it is a highly apolar molecule. However, CO₂ has high affinity towards polar solvents, which could be attributed to its quadrupole moment and the polarising effect of polar solvent.^[37] CO₂ is more soluble in 2,2,2-trifluoroethanol than the less polar ethanol. The mole fraction of CO₂ in saturated trifluoroethanol is 0.517 at 5.5 MPa and 313 K,^[125] significantly more compared to saturated ethanol with 0.366 mole fraction under the same conditions.^[110] CO₂ mole fractions in various solvents were measured by Abbot.^[128] The measured values varied significantly in different solvents 5.0 MPa and 298 K (Figure 4.7). *N*-Propanol and *t*- or *n*-butanol had less affinity compared to others, like cyclohexane, ethanol or DMF. However, as findings of Kordikowski showed (Figure 4.8), similar volumetric expansions could be expected for each solvent by applying higher pressure and increasing CO₂ mole fractions to the same level.

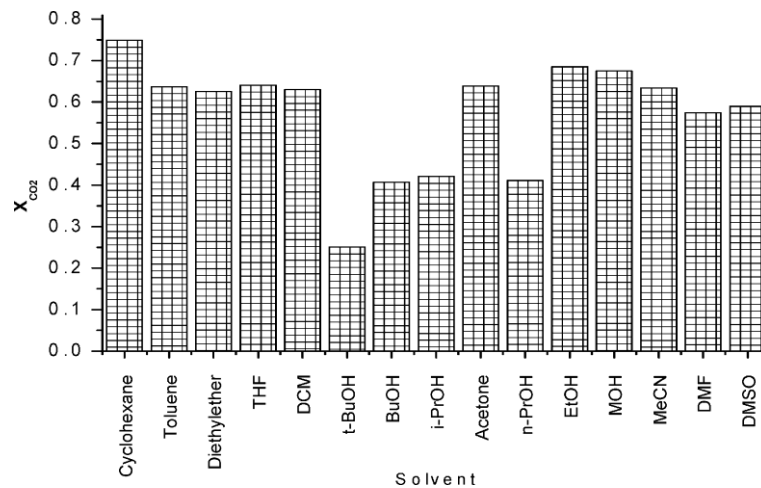


Figure 4.7. Solubility of CO₂ in various solvents at 5.0 MPa and 298 K.^[128]

The volumetric change after CO₂ dissolution is also dependent on solvent density. Volumetric expansion vs. mass fraction of CO₂ in the liquid phase is most rapid with very dense solvents such as perfluorohexane (1.67 g/cm³), less so with dichloromethane (1.29 g/cm³), and least with acetonitrile (0.76 g/cm³).^[125]

Kordikowski plotted the volumetric expansion against the mole fraction of dissolved CO₂ instead of pressure and revealed a striking similarity between the various systems (Figure 4.8).^[116] Not only that the expansion of various solvents coincide, but the expansion curves are also indistinguishable for all temperatures. However, using different gases, like ethane or ethylene, the curves are different. The reason of similar results with C₂H₆ and C₂H₄ was speculated to be their similarity.

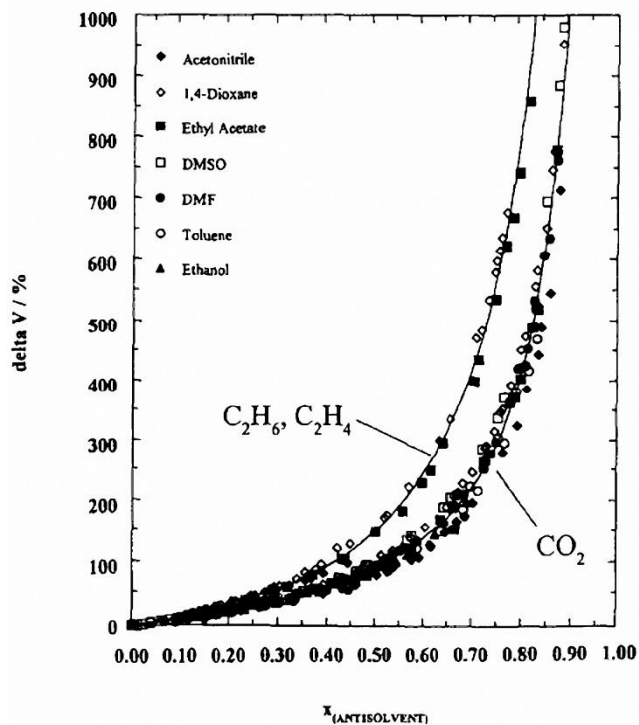


Figure 4.8. Volumetric expansion of acetonitrile, dioxane, ethyl acetate, DMSO, DMF, Toluene and ethanol with ethane, ethylene and CO_2 , plotted against the mole fraction of dissolved gas at 298 to 323 K. Used method: densitometry.^[116]

The necessary pressure to reach the same mole fraction of CO_2 could be of course very different comparing one solvent to other, and it is also pressure dependent.

4.7.4 Physical properties of gas expanded liquids

Gas expanded liquids are CO_2 solutions in solvents. One could therefore expect their physical properties to be somewhere between neat solvents and pure CO_2 , depending on the actual ratio of solvent and CO_2 . To understand the solubility of solids and the change of solvent effects in organic reactions carried out in GXLs, efforts have been made to investigate their physical properties.^[128] Permittivity was investigated using an electrical capacitance measurement between two rectangular plates in a cell lined with teflon and with a known mixture inside. The density was measured *via* a densitometer containing a vibrating U tube. The polarity was measured optically, based on the solvatochromic shift of different indicator dyes in the visible spectrum.

Dipolar aprotic solvents like DMF and DMSO have the highest relative permittivity. Their permittivity was nearly halved upon expansion with CO_2 at 5.0 MPa to a comparable value to those of neat acetone or butanol (Figure 4.9). The relative permittivity of apolar solvents like cyclohexane or toluene also decreased, although the change was not that significant. In the intermediate region, difference can be observed between solvents. In the case of acetone and *n*-butanol the effect of expansion with 5.0 MPa CO_2 is more significant compared to *t*-butanol, for instance.

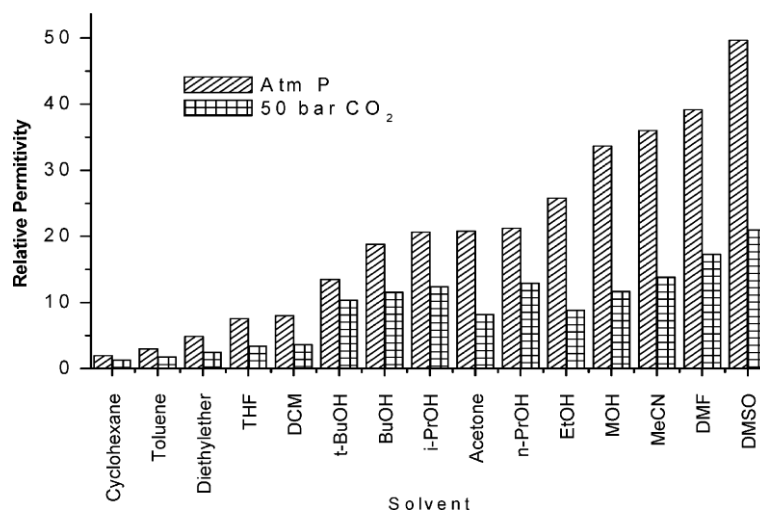


Figure 4.9. Change of relative permittivity of various solvents upon expansion at 298 K.^[128]

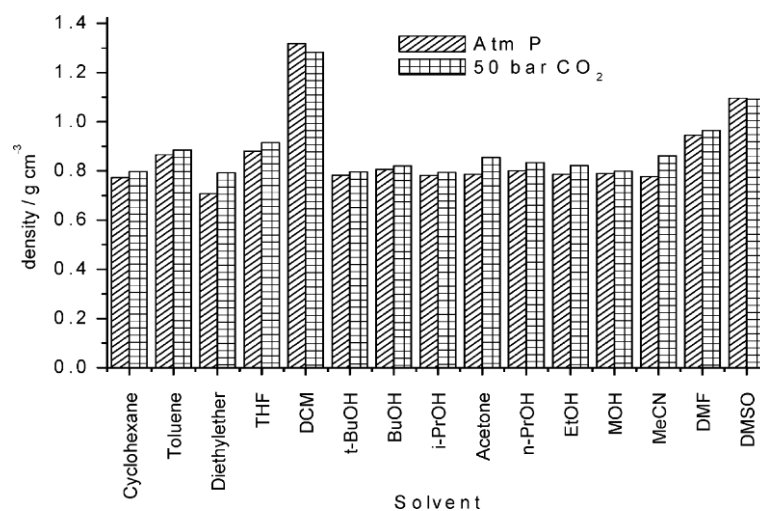


Figure 4.10. Density change of various solvents upon expansion at 298 K.^[128]

The degree of density change (Figure 4.10) may be surprising at first sight, as in the earlier section (4.7.3, Figure 4.5, Figure 4.6) 40-100% volumetric expansion of solvents was reported in the same pressure and temperature range (5.0 MPa and 298 K). However, the amount of dissolved CO₂ is considerable, between mole fractions 0.25 and 0.75 (Figure 4.7), therefore the mass of the solution also increases counteracting the effect of volumetric increase (Eq.26) and roughly maintains the density.

$$\rho = \frac{m \uparrow}{V \uparrow}$$

m: mass of GXL

V: volume of GXL

ρ : density of GXL

Eq.26

Relative permittivity and density data only are insufficient to predict solvent effects on reaction pathway preferences or solubilities.^[129] In contrast, solvatochromic parameters, such as π^* polarity parameters on the Kamlet-Taft scale,^[129] were designed to allow an insight into solvation and local density. Table 4.3 shows π^* parameters for

solvents before and after CO₂ expansion at 5.0 MPa, which were obtained by spectroscopic analysis of Nile red or phenol blue indicators that have different absorption spectra depending on their chemical environment.

Table 4.3. Measured π^* values of various organic solvents at 298 K at atmospheric pressure and after expansion to 5.0 MPa with CO₂.^[128]

| Entry | Solvent | π^* | |
|-------|---|---------|-------|
| | | 0.1 MPa | 5 MPa |
| 1 | Cyclohexane | 0.034 | 0.067 |
| 2 | DMF | 0.880 | 0.841 |
| 3 | DMSO | 1.039 | 0.938 |
| 4 | MeOH | 0.598 | 0.372 |
| 5 | EtOH | 0.537 | 0.291 |
| 6 | DCM | 0.812 | 0.487 |
| 7 | (C ₂ H ₅) ₂ O | 0.266 | 0.043 |
| 8 | Acetone | 0.677 | 0.432 |
| 9 | Toluene | 0.503 | 0.177 |

Expansion with CO₂ caused a polarity decrease of the system in most cases, with the exception of cyclohexane. Significant differences between solvents were found. The change of π^* was minimal if highly polar aprotic solvents were expanded, like, DMF or DMSO. The change was more significant but still moderate for polar aprotic solvents, such as alcohols. A more substantial change of π^* could be observed if weakly polar solvents such as ether, dichloromethane or acetone were expanded. Toluene, which would be classified as apolar solvent because of its low relative permittivity, also showed a significant change.

4.7.5 Solubility of solids in gas expanded liquids

A CO₂ antisolvent procedure manipulates the solubility of solute, decreasing it in ideal case and induce precipitation. Solubility of solutes in gas expanded liquids, which are the mixture of solvent and CO₂, are reviewed in the following section.

At the current stage of overall scientific development there is no accurate way to predict the relationship between solubility and measurable physical parameters, such as density or relative permittivity. Solubility of solids in pure supercritical carbon dioxide has been investigated, particularly with regard to supercritical extractions.^[37] The modelling of such systems is usually based on fugacity calculations, similarly to fluids (4.6). There are various equations to describe fugacities of solids in the function of pressure and temperature; some of them are empirical.^[123] There are methods to estimate the solubilities in the presence of a third component that is often referred to as a co-solvent in the terminology of extractions. These methods are based on the application of EoSs and mixing rules.^[37]

The solubilities of biologically active organic molecules have been measured in GXLs by numerous authors.^[130-132] One of the measurement methods was using vanishing point

detection (Figure 4.11). A known amount of CO₂ was introduced into a thermostated and agitated view cell (1), then compressed up to the pressure of interest using the hydraulic pressure of mercury (2). Syringe pump (5) was loaded with the known solution (solute dissolved in organic solvent) and set to constant pressure mode. The mercury left the cell through a manually controlled valve, and syringe pump (5) maintained the pressure by the continuous introduction of solution. Precipitation of solid occurred immediately. By a continuous withdrawal of mercury and addition of solution, the concentration of CO₂ decreased. At an end point the concentration of CO₂ decreased to below a critical level, and the solid precipitate was no longer visible. These measurements are often referred as “vanishing point measurement”.^[132] The amount of introduced CO₂ and injected solution was precisely known allowing the calculation of composition of saturation. The end point corresponded to the composition of the saturated solute + solvent + CO₂ system.

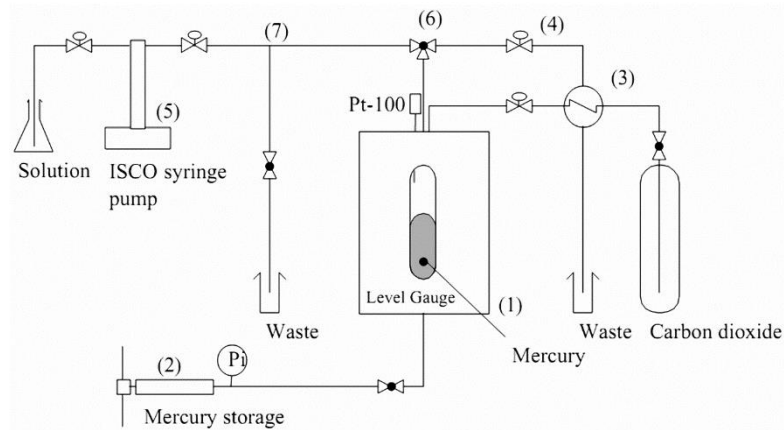
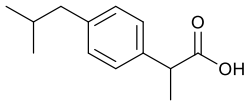
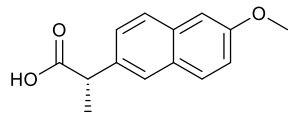


Figure 4.11. Typical equipment to measure solubility of a solid in GXL (vanishing point)^[132]

Authors modelling solubility in gas expanded systems found that empiric equations, like the one proposed by Wubbolts,^[132] often give better results than ones based on fundamental modelling of phase equilibria based on equation of states.

The effect of solvent expansion on solubility cannot be predicted easily. This can be demonstrated on the example of Ibuprofen and Naproxen, which are otherwise similar molecules in terms of structure; some of their properties are summarised below (Table 4.4). Their solution in acetone behaved differently during CO₂ exposure (Figure 4.12).^[131]

Table 4.4. Properties of Ibuprofen and Naproxen.

| Structure | Ibuprofen | Naproxen |
|-------------------------|---|--|
| |  |  |
| MW / gmol ⁻¹ | 206 | 230 |
| m.p. / °C | 73-76 ^[133] | 157-158 ^[133] |
| p <i>K</i> _a | 4.4 ^[134] | 4.01 ^[135] |
| log <i>P</i> | 3.50 ^[136] | 3.18 ^[136] |

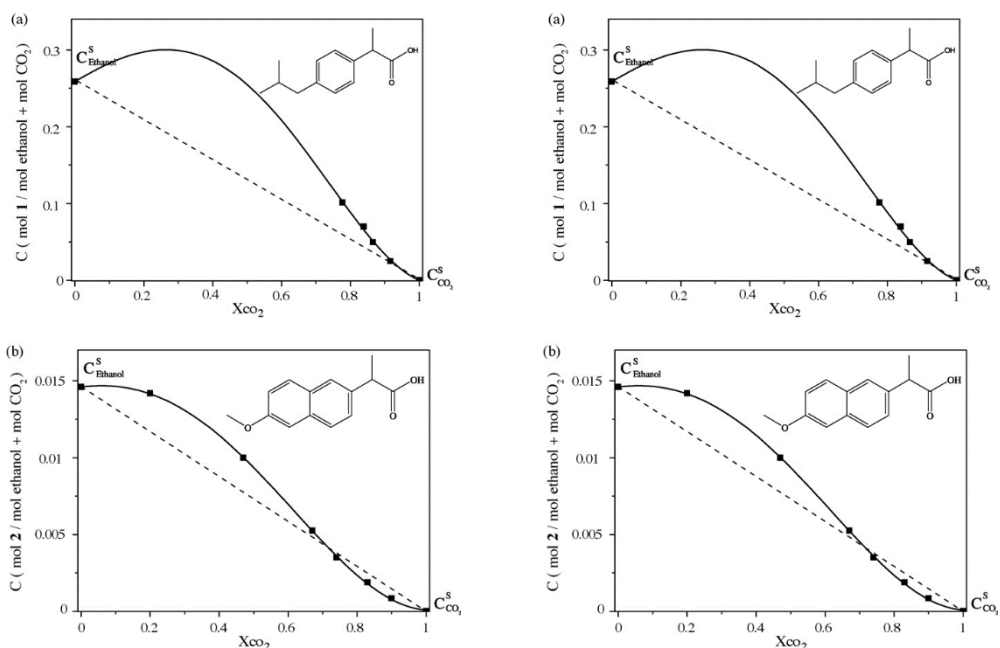


Figure 4.12. Solubility of Ibuprofen and Naproxen in CO₂ expanded acetone at 10.0 MPa and 298 K.^[131]

The molar fraction of saturated solution of Ibuprofen in acetone is about 0.26. If CO₂ was dissolved, that is the solution was expanded, the solubility initially increased and peaked at 0.3 molar fraction; CO₂ acted as a co-solvent, rather than as an antisolvent. The solution of Naproxen behaved differently. The solubility of was the highest in neat acetone (molar fraction about 0.015), and in contrast to Ibuprofen, it decreased as soon as CO₂ was introduced.

This example demonstrates well the difficulties of solubility predictions. The solvent power of CO₂ expanded acetone was compared for Ibuprofen and Naproxen. Consequently, all the physical parameters of the solvent, such as density, relative permittivity, π^* , etc. changed similarly. One could expect that the solubilities of these two similar chemicals exhibit a similar behaviour. Nevertheless, the found tendencies were the opposite. CO₂ enhanced the solubility of Ibuprofen, but reduced the solubility

of Naproxen. Predicting the effect of gas expansion on solubility in CO₂ + solvent systems seems therefore problematic, however, prediction methods exist.^[137-138]

4.8 Particle formation

4.8.1 Introduction to particle formation using CO₂ antisolvent

If CO₂ acts as an antisolvent for an actual solvent-solute system, it could be used to make the solution supersaturated and induce precipitation during expansion. Solubility reduction upon expansion has been recognised, and exploited for particle formation.^[30, 139] The rate of dilution can affect the ratio of rates of nucleation and of crystal growth, and therefore subsequently affect crystal size.^[36] If a supercritical fluid is used as an antisolvent instead of a liquid antisolvent, mass transport, which may limit the rate, can be greatly enhanced because of the lower viscosity and higher diffusion coefficient of a GXL compared to a system of two conventional solvents. Particles with unique properties were formed exploiting supercritical antisolvent crystallisations,^[139] which can be useful for applications such as nanotechnology, catalysts and catalyst supports, column packages for chromatography, plastics with antibiotic character or drugs with controlled release.^[140]

4.8.2 Particle formation with CO₂ antisolvent in practice

Particle formation processes can be operated either in a batch mode or continuously.^[141] Either supercritical CO₂ is introduced into a pressure chamber containing the solution, or the solution is introduced into CO₂. The difference is whether the precipitation occurs in a liquid rich phase or in the supercritical fluid rich phase. The actual construction of the injection nozzle also has an impact. The product quality in terms of mean particle size and size distribution can be controlled by operation parameters and equipment design. Batch procedures are often not productive enough on scale for particle formation. Moreover, it is also difficult to control the process parameters in batch mode because the procedure is not steady state, and there may be problems with reproducibility. In continuous operation the supercritical carbon dioxide and the solvent are introduced simultaneously into a precipitation chamber (CS) (Figure 4.13).

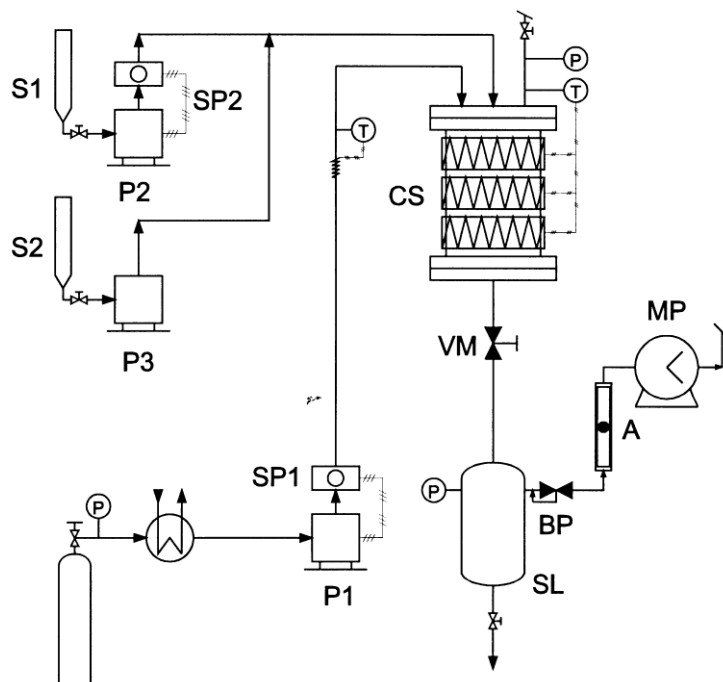


Figure 4.13. Typical set-up for continuous precipitation.^[30] P1, P2 and P3, high pressure pumps; SP1 and SP2, pressure dampeners; S1 and S2, liquid solution supplies; CS, precipitation vessel; VM, micrometering valve; BP, backpressure valve; SL, liquid separator; A, calibrated rota meter; and MP, wet test meter.

Continuous operation is considered to be more productive, although it has to be noted that the solid product, which may contain residues of the solvents and must be dried, is collected in a separator with a fixed volume making this method rather quasi-continuous. However, the operational pressure of the precipitation unit (CS) is significantly higher compared to the separator (SL). The precipitator unit could operate in continuous mode, which makes it productive. Therefore, a small precipitator volume may be sufficient for the actual procedure. The volume of the less effective separator, operating in batch mode, could be increased without raising the investment costs substantially, because it operates at relatively low pressure. An elegant way of drying the precipitated product would be the use of supercritical fluid extraction. It has to be emphasized that the primary goal of these authors was to control particle size and size distribution, and optimising yields was rather secondary. If one used the procedure for separation, the primary target would be a good yield, and particle size and size distribution would be secondary.

4.9 Lowering melting point of solids with CO₂

Precipitation and separation of a product in a solid form is not the only option that could be used in a reaction work-up procedure. Even though there are productive methods to process solid materials,^[34] these are designed for ambient pressures and their upgrade for high pressures may be complicated. It would make actual processes easier to design

if the desired product could be isolated in a fluid form. This is particularly true for continuous procedures. Although the melting points of the majority of materials, with the exception of few examples like water, increases with pressure, hydraulic pressure of some gases like carbon dioxide, ethylene etc. induced melting point decrease, sometimes to a significant degree (Figure 4.14).^[32] This is probably because of the diffusion and solution of gas into the solid and lowering of the melting point.^[27]

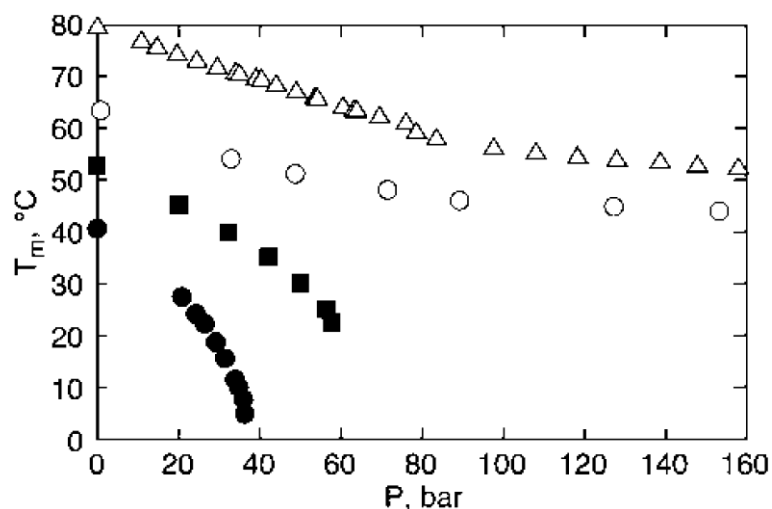
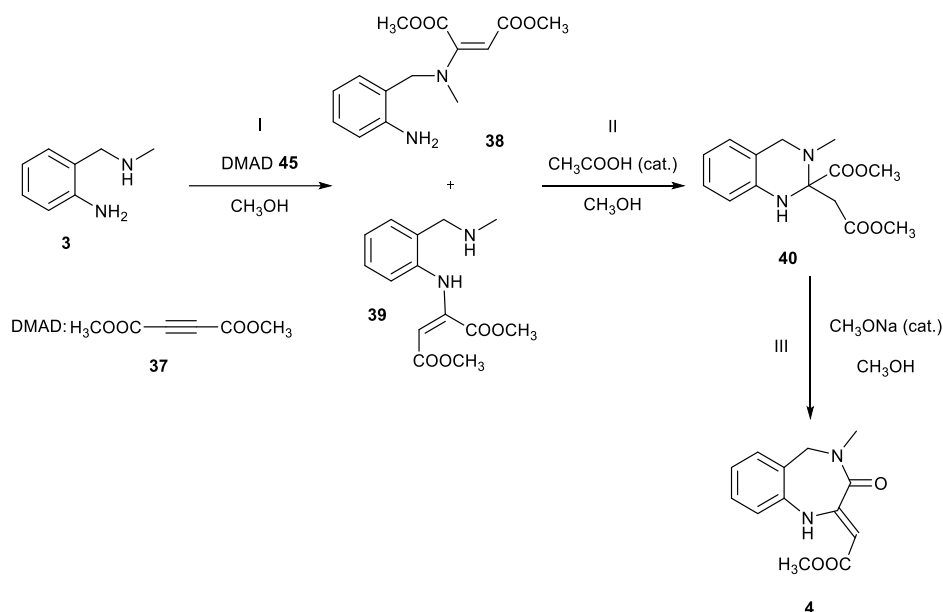


Figure 4.14. Effect of ethylene on the melting point of naphthalene Δ , octacosane \circ , *p*-dichlorobenzene \blacksquare and menthol \bullet .^[32]

If the melting point of an actual pharmaceutical or intermediate product can be varied by supercritical CO₂ or other gas, it is worth considering how the phenomenon could be exploited. For instance, withdrawal of a product in CO₂ induced molten form could potentially eliminate complicated technological steps required for solid products: filtration, centrifugation or transportation of solids could be avoided. Continuous operation is often prevented by a need of solid handling. Finally, the product isolated in fluid form would crystallise back to solid after the pressure decreased CO₂ released. The pressure relief may also be exploited for the formation of fine particles, in the PGSS (particles from gas saturated solutions) procedure.^[142]

4.10 Use of conventional antisolvents in practice

Application of antisolvent is a common procedure for purification and work-up in laboratories and industry.^[3] Consider the following example of furnishing benzodiazepine **4** (Scheme 3.23).^[12]



Scheme 4.1. Synthesis of benzodiazepine **4** in a three step one pot procedure. The final work-up procedure was an addition of water antisolvent into the crude solution of benzodiazepine product. The ideal ratio of water and methanol was about 3:2. Benzodiazepine **4** was obtained in about 51% yield.^[12]

The crude solution of benzodiazepine **4** in methanol was treated with water. The addition of water reduced the solvent power of methanol, which was otherwise a good solvent for the benzodiazepine, and a precipitation of the product occurred and could be isolated after filtration with 51% yield on a 2 g scale. An overall yield of 68% was reported at a 7 times larger scale.^[12] The achieved yield could be considered acceptable for a molecule of such complexity produced in a three step one-pot synthesis. Also, the purity was excellent. However, considering a green approach for this synthesis, the residues, including acetic acid and sodium acetate, unreacted starting materials and by-products, dissolved in aqueous methanol are yet to be separated from each other. The separation of a mixture of such complexity is rather challenging. The most valuable component in this mixture, assuming only a minimal amount of product remained dissolved, is the organic solvent, methanol. Methanol is rather volatile with a low boiling point and does not form an azeotrope with water. Therefore, it could be distilled out from the mixture at certain energy costs and possibly used for another batch.^[143] The residue of the distillation is an aqueous solution or dispersion of by-products, and typically incinerated, which could be problematic because of the water present.

4.11 Disadvantages of purifications using antisolvents

As was shown on the example of benzodiazepine **4**, it is always a mixture of solvents that is created after using an antisolvent for crystallisation. The solvent mixture is then to be separated, possibly by distillation. One may consider using distillation for the

separation of a reaction mixture straight away instead of antisolvent induced crystallisation. However, operational conditions of such a thermal procedure may restrict its application for heat sensitive compounds. Furthermore, consideration of energy costs of separating a crude mixture *via* distillation vs. application of antisolvent with a subsequent separation of the resulting solvent mixture may favour the antisolvent involved procedure. In the example of benzodiazepine a mixture of methanol and water antisolvent was created (Scheme 3.23). Separation of these two solvents is not particularly problematic because of the relatively low boiling point of methanol and lack of azeotrope formation.^[143] Separation of solvents with high boiling points, such as DMF, DMSO or NMP, from their aqueous solutions could be particularly challenging and energy intensive. Separation of water and solvents forming azeotropes, such as ethanol, *i*-propanol or tetrahydrofuran, can also be particularly problematic by distillation.

4.12 Ideal antisolvents and alleviating the disadvantages

The summarised difficulties help suggest the properties of an ideal antisolvent. The first requirement was miscibility with the solvent of the mother liquor. Yet, the antisolvent must be a poor solvent for typical pharmaceutical APIs or their intermediates, which are typically polar molecules. Limited miscibility may be acceptable as long as the antisolvent is effective enough to induce precipitation on the limited miscibility range. Easy separation of the antisolvent from the solvent of the mother liquor is another important requirement. A typical way for separation of solvents is distillation, which is easier to carry out if azeotropes are not formed, and the boiling points of the solvent are low, yet significantly different from each other with high relative volatility.^[144] The solvent of mother liquor is generally restricted by the reaction chemistry, but the antisolvent can be varied more widely.

Choosing carbon dioxide as an antisolvent could meet these criteria. CO₂ is an apolar molecule because of its high symmetry. On one hand CO₂ is a relatively poor solvent for large, polar, drug-like structures because of the apolar character. However, CO₂ is polarisable because of its significant quadrupole moment, which renders it soluble in polar solvents, particularly at elevated pressures. CO₂ is a gas under atmospheric conditions, therefore has a significantly lower boiling point compared to commonly used solvents. CO₂ can simply evaporate out from a solution with a high boiling organic solvent once the pressure is reduced, rendering solvent and antisolvent separation much simpler compared to distillation or rectification. Further advantages of CO₂ are its environmentally benign and non-toxic nature. It is non-flammable, readily available and cheap. Technologies even without CO₂ recycling could be considered environmentally

friendly and economically efficient, depending on the scale. CO₂ is also relatively inert, a broad range of solutes could be exposed to it without reaction, and residues of CO₂ in the recycled solvent are unlikely to disturb the course of reaction. A disadvantage, however, is a need for high pressure operation. The required pressure to create an organic solvent + CO₂ solution with a sufficient composition to induce supersaturation and solute precipitation depend on the combination of the actual solute, the solvent of the mother liquor and the temperature. At 313 K, for instance, the pressure needed to dissolve 50mol% CO₂ in THF, EtOH and DMSO are about 4.0, 6.2 and 6.5 MPa.^[110, 115] Operations with solids such as precipitation, centrifugation and filtration, which are otherwise fairly straightforward under atmospheric conditions, could be rather challenging at such elevated pressures.

4.13 Miscibility behaviour of CO₂ and solvents

As was highlighted in the former paragraphs, miscibility of the solvent of the mother liquor and the antisolvent is required for antisolvent induced separations. The van der Waals equation^[145] can qualitatively predict what kind of phase behaviour may be expected in binary systems in terms of mutual solubility, and these predictions were classified by van Konynenburg and Scott into five types.^[146] From the perspective of liquid-liquid miscibility, these five types are the following:

Type – I: full liquid-liquid solubility exists, regardless of pressure, temperature and composition (Figure 4.15a). Example: toluene + CO₂.^[147]

Type – II: limited liquid-liquid solubility exists under the critical temperature of the more volatile compound. Mutual solubility may be possible above the pressure dependent upper critical solution temperature (Figure 4.15b). Example: *n*-octane + CO₂.^[27]

Type – III: limited liquid-liquid solubility exists under an intermediate temperature between the critical temperatures of the two compounds. Above this temperature mutual solubility may be possible within a limited pressure range (Figure 4.15c). Example: water + CO₂.^[148]

Type – IV: limited liquid-liquid solubility exists well under the critical temperature of the more volatile compound, and at temperatures in the vicinity of the critical temperature of the more volatile compound. Mutual solubility may be possible in a limited temperature window below the critical temperature of the more volatile compound, and above an intermediate temperatures between the critical temperatures of the two components (Figure 4.15d). Example: DMSO + CO₂.^[115]

Type – V: full liquid-liquid solubility exists under the critical temperature of the more volatile compound and above an intermediate temperature between the critical temperature two compounds. Liquid-liquid immiscibility occurs in the vicinity of the critical temperature of the more volatile compound (Figure 4.15e). Example: ethane + ethanol.^[149]

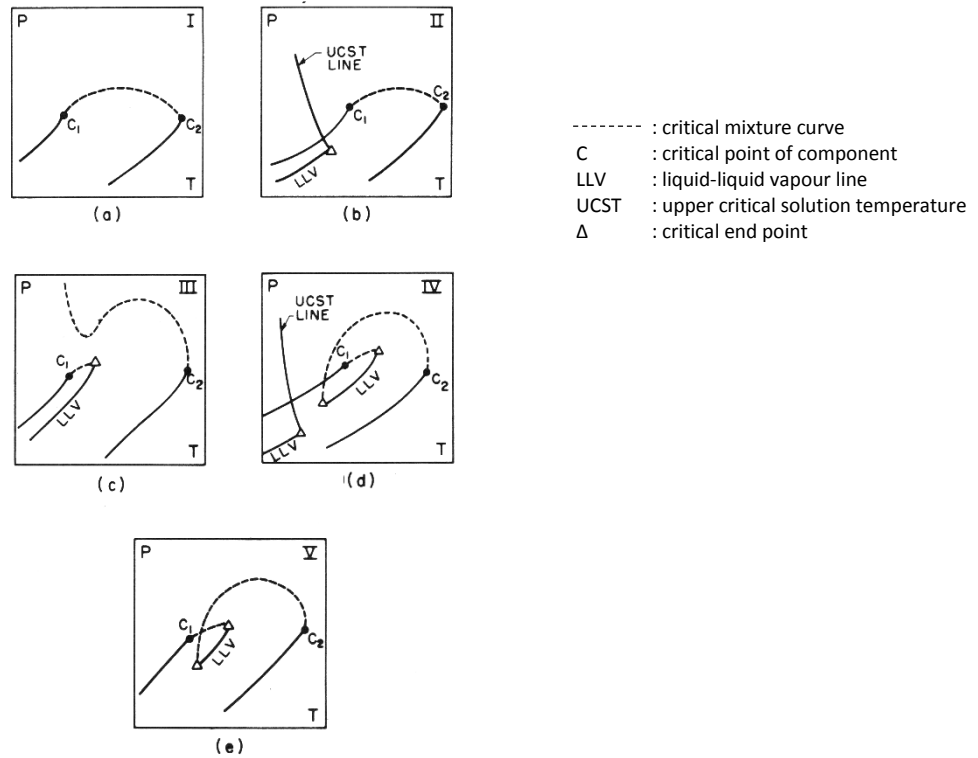


Figure 4.15a-e. Classification of binary systems according to their phase behaviours, according to van Konynenburg and Scott.^[146]

In this work CO₂ was investigated as antisolvent, both below and above its critical temperature. According to the classification of binary solvent systems, Type – I behaviour is ideal to use CO₂ as an antisolvent over the whole temperature range, therefore both below and above the critical temperature of CO₂. Type – II systems are ideal to exploit CO₂ as antisolvent at temperatures in the vicinity or above the critical temperature of CO₂. Type – III binary systems are not ideal for exploiting CO₂ antisolvent procedures because of the limited mutual solubility. Mutual solubility may be possible above an intermediate temperature between the critical temperature of CO₂ and the critical temperature of the other solvent, but pressure and temperature requirements may be too harsh for a feasible application. Type – IV systems have a temperature window in the vicinity of the critical temperature of the more volatile solvent with limited mutual solubility, therefore operation in this window is not ideal. Immiscibility occurs at low temperatures too. CO₂ could be ideally used as antisolvent in the windows of mutual miscibility. Type – V systems have a window of immiscibility in the vicinity of

the critical temperature of CO₂. At other temperatures CO₂ can be ideally used as an antisolvent.

As discussed, operation conditions with full miscibility were ideal for ideal application of CO₂ antisolvent. However, a limited solvent-antisolvent miscibility may be sufficient, provided effective antisolvent behaviour is exhibited on the region of mutual solubility and precipitation of solute occurs before the envelope of mutual solubility is crossed and further addition of more CO₂ leads to formation of a separate liquid phase because of the miscibility limitations. It must also be noted that the presence of a third compound, which is essentially present in a separation procedure, may alter the miscibility behaviour of two solvents, decreasing (known as salting-out) or increasing mutual solubility. In the case of real reaction work-up or purification procedures, the actual composition of the system could be ill-defined. Other species present, such as water, may also have an effect.

4.14 Application of pressurised carbon dioxide as an antisolvent

As discussed, application of a CO₂ antisolvent can be ideal for solvents that are miscible. These systems were Type – I, and V without limitations for operation below, and Type – I and II systems for operations above the critical temperature of CO₂. Below the critical temperature of CO₂, liquid CO₂ can exist. If a solution is exposed to CO₂ pressure, the solvent dissolves the CO₂. The overall amount of solution, now including CO₂, increases resulting in volumetric expansion. If more and more CO₂ is added, the solution becomes progressively weaker in the original solvent. Precipitation of solute can occur at a composition at which the solvent power is reduced to below a certain level. Most importantly, the temperature is below the critical temperature of CO₂. The literature often refers these systems as gas expanded liquids.^[32] This term is rather abstract for those who are not familiar with the phenomena. Solvent + CO₂ systems could also be considered as simple mixture of two liquid solvents, at pressures necessary to keep the more volatile solvent liquid and prevent it from boiling. This pressure is determined by the actual solvent-CO₂ composition, by Henry's law in an ideal case. Unless a positive azeotrope is formed, the ceiling of pressure above the mixture of liquids will be limited by the vapour pressure of CO₂ at the temperature of operation. Further addition of CO₂ (as a liquid) will not increase the pressure significantly.

The situation is somewhat different above the critical temperature of CO₂, because liquid CO₂ in this region cannot exist. This operation is suitable for those solvents that are miscible with CO₂ above its critical temperature, which are Type – I and II. The phenomena of CO₂ addition into the system is initially very similar compared to

sub-critical operation. The system is exposed to CO₂, which is dissolved. The overall amount of solution increases as the ratio of dissolved CO₂ increases, causing volumetric expansion. However, CO₂ does not have a vapour pressure, because it is supercritical. Therefore, a pressure ceiling cannot exist, and CO₂ can be added into the system continuously, increasing the pressure. At a certain composition the liquid phase becomes critically equal to the gas phase, and the whole mixture become supercritical. However, further addition of CO₂ is still possible, resulting further pressure increase.

Phase behaviour of high pressure CO₂ + organic solvent systems is well investigated above the supercritical temperatures of CO₂ because these data were required for the design SCF procedures (4.5). Equilibria of CO₂ + solvents at lower temperatures and pressures is much less studied. Miscibility of liquid CO₂ and many typical organic solvents is not widely available.

4.15 Goal of CO₂ induced precipitations

The goal of this part of the project was to demonstrate that liquid or supercritical CO₂ can be used as an antisolvent for some systems, and practical isolation of a valuable solute in crystalline form from its solution after the induced precipitation can be carried out. Firstly, numerous solute + solvent systems were exposed to CO₂ under various conditions, and the phase behaviour was visually observed. Systems that exhibited precipitation of solid, which was essential for the development of separations, were subsequently tested for preparative experiments.

4.16 Screening of solute-solvent combinations for CO₂ induced precipitation

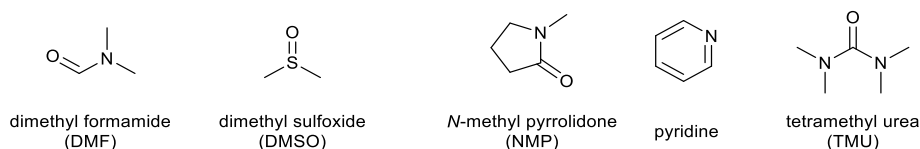
4.16.1 Goals of CO₂ antisolvent screening experiments

Determination of the optimal pressure, temperature and CO₂ concentration for a CO₂ involved antisolvent precipitation procedure would ideally start by obtaining an accurate knowledge of the actual system of solute + solvent + CO₂, in a form of a phase diagram. The yield and purification performance of the design could be calculated from the concentration of phases in equilibrium combined with material balance. Also, sensible compromises between yield, purity and operational conditions could be made. Temperature and particularly the pressure of operation are very important for scale up and actual feasibility. The determination of a complete phase behaviour of such system is rather cumbersome and time consuming, and would require sophisticated equipment that we did not possess. Instead of learning all the details of one particular system and develop a fully optimised procedure, the strategy of this study was to investigate

multiple systems to establish general principles. Instead of acquiring a phase diagram, only a simple visual observation for precipitation was carried out in a view cell for a number of solute-solvent combinations. The goal of the screening experiments was to find suitable solute-solvent combinations, for which CO₂ can act as an antisolvent.

4.16.2 Chosen solvent-solute combinations for CO₂ induced antisolvent precipitations

The main disadvantage of using antisolvents in general was the production of a subsequent solvent mixture by-product. The separation of solutes from their solutions in dipolar aprotic solvents (DAS) is generally carried out by addition of an antisolvent, most typically water.^[3] The added water may not necessary induce a precipitation of solid, but the produced DAS - water mixture typically has a reduced solvent power. More importantly the solvent mixture, depending on the concentration of water, has a limited miscibility with less polar solvents. It can be therefore extracted with solvents such as DCM, ethyl acetate or ether type solvents. The goal of high pressure CO₂ antisolvent induced precipitations was to produce a CO₂ - solvent mixture instead, which could be relatively easily separated. The research primarily focused on systems based on dipolar aprotic solvents because their separation from water is particularly problematic. The commonly used DASs are dimethyl formamide (DMF), dimethyl sulfoxide (DMSO), *N*-methyl pyrrolidone (NMP) and pyridine. Tetramethyl urea (TMU), a novel, and considerably green DAS was also of interest (Scheme 4.2).



Scheme 4.2. Dipolar aprotic solvents (DASs).

The chosen substrates were molecules that were considered “drug-like”, that is their molecule resembles to APIs, in terms of similar size, polarity and functional groups. This was because a CO₂ antisolvent based procedure would be most likely employed for similar molecules that are the targets of the pharmaceutical industry. Antisolvent precipitation has an analogy to SCF extractions. For an antisolvent procedure, the organic solvent is the solvent, and CO₂ is the antisolvent. With the terminology of SCF extractions, CO₂ is the solvent, and the organic solvent is the co-solvent (Table 4.5). Solutes with high solubility are preferred for SCF extractions, but low solubility is better for the antisolvent procedure. Molecules with amine functions were interesting for the antisolvent investigations, because they have low solubility in scCO₂, attributed to their basic character and formation of adducts with CO₂.^[46] The formed adducts are not volatile, and have low solubility in the apolar CO₂ because of their salt like character.

Table 4.5. Terminology of antisolvent precipitations and supercritical fluid extractions.

| Terminology of antisolvent precipitations | ← System → | Terminology of SCF extractions |
|---|-----------------|--------------------------------|
| Solute | Solute | Solute |
| Antisolvent | CO ₂ | Solvent |
| Solvent | Organic solvent | Co-solvent |

4.17 Discussion of high pressure CO₂ antisolvent induced precipitations

As it was mentioned in the former section, the goal of the screening was to find solvent-solute combinations that exhibit solute precipitation if exposed to high pressure CO₂. These systems later could be used to demonstrate the actual separation of solute from the solution.

4.17.1 Experimental set-up[#]

A home built high pressure system was used for the experiments. A detailed description can be found in. The view cell was loaded with the solution of a known composition. The air was removed from the cell by venting with CO₂. The temperature of the view cell was set to a chosen temperature, and once reached CO₂ was introduced into the stirred cell stepwise. Phase behaviour during CO₂ introduction was monitored. As CO₂ was continuously introduced, CO₂ concentration in the fluid phase increased, causing a volumetric expansion of the solution. The volumetric increase, and the amount of injected CO₂ were qualitatively monitored, simply by observing the meniscus of the liquid phase.

During the course of expansion, various phase behaviour were observed, other than volumetric expansion. The desired phase transition that would allow further development of CO₂ antisolvent induced precipitation procedures, was precipitation of solid. Precipitation of liquid, that is formation of two liquid layers, was also observed. Distinguishing between solid or liquid precipitate was rather complicated, because both phase transitions rendered the content of the view cell opaque. Further addition of CO₂, and sedimentation was necessary to determine the actual state of the precipitate. The amount of solid was determined visually at this stage. Some qualitative observations were noted, such as large or small amount of solid. Once the expanded liquid filled the whole cell, further addition of CO₂ resulted in a steep increase of pressure, because

[#]Detailed information can be found about the experimental set-up in Appendix - I.

liquids are largely incompressible. The volume of the view cell was therefore a limitation for the solvent-antisolvent ratio.

4.17.2 Investigation of CO₂ as antisolvent for DMSO based systems

DMSO is a widely used dipolar aprotic solvent. One of its main advantage is that it is relatively harmless for human health, compared to other DASs. Its main disadvantage is its high melting point, which may render its general use, including transportation, difficult (Table 4.6).

Table 4.6. Properties of DMSO.^[23]

|  | m.p./ °C | b.p./ °C | ρ / kg/m ³ | Dielectric constant |
|---|----------|----------|----------------------------|---------------------|
| DMSO | 19 | 189 | 1100 | 47.24 |

Various systems based on DMSO were tested. Rather than the expected precipitation of the solute, often formation of a second liquid layer was formed at pressures around 8 MPa. (Table 4.7). Andreatta published a global phase diagram of the DMSO + CO₂ system (Figure 4.16).^[115] A limited miscibility in a relatively small region, slightly above the critical pressure of CO₂ was reported, based on predictions.^[150] A Type – IV phase behaviour was proposed, however it was not confirmed by low temperature measurements. The temperature of our experiments (313 K) overlapped with the region of immiscibility, which could explain why 7 out of 9 experiments with DMSO based systems resulted in a precipitation of liquid (Table 4.7).

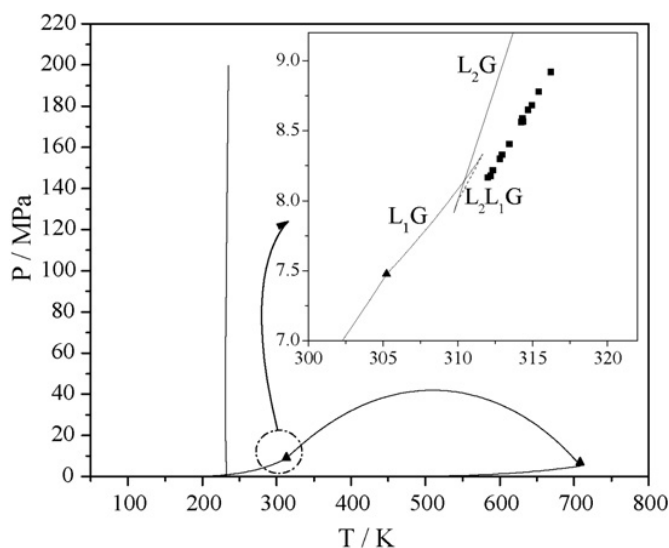


Figure 4.16. Global phase behaviour of the DMSO + CO₂ system.^[115] Can be classified as Type – IV, according to van Konynenburg and Scott.^[146]

Lidocaine **20** and benzodiazepine may have sufficiently affected the mutual solubility of DMSO and CO₂ to avoid phase splitting, however precipitation of solid did not occur (Table 4.8).

Table 4.7. Exposure of various solutes in DMSO to CO₂ at 40 °C. Initial volume of solution: 1 ml. Concentration: 100 g/l. At P pressure formation of two liquid layers was observed. Precipitation of solid was not observed.

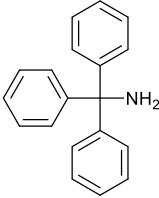
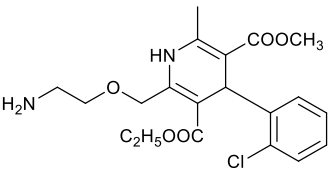
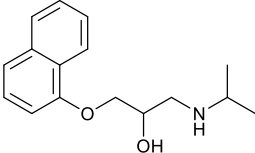
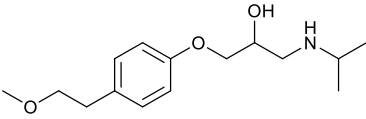
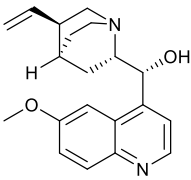
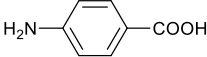
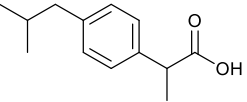
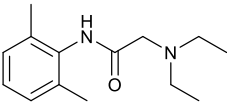
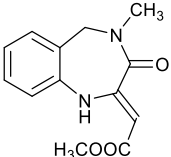
| Entry | Solute | P/MPa | Approximate Expansion |
|-------|---|-------|-----------------------|
| 1 |  tritylamine | 8.2 | 6x |
| 2 |  Amlodipine | 8.1 | 6x |
| 3 |  Propranolol 18 | 7.5 | 6x |
| 4 |  Metoprolol | 8.2 | 6x |
| 5 |  Quinine | 8.2 | 6x |
| 6 |  PABA | 8.2 | 9x |
| 7 |  Ibuprofen | 8.2 | 9x |

Table 4.8. Exposure of various solutes in DMSO to CO₂ at 40 °C. Initial volume of solution: 1 ml. Concentration: 100 g/l. A single liquid phase was in equilibrium with the gas. Precipitation of solid was not observed. P is the maximum pressure to which the system was raised.

| Entry | Solute | P/MPa | Approximate Expansion | Observation |
|-------|---|-------|-----------------------|---|
| 1 |  Lidocaine 20 | 13.2 | 17x | Single liquid phase No precipitation |
| 2 |  benzodiazepine 4 | 12.8 | 17x | Single liquid phase No precipitation |

4.17.3 Investigation of CO₂ as antisolvent for ethanol based systems

Systems based on ethanol were also investigated (Table 4.9). If CO₂ and water are compared as antisolvents for ethanol based systems, CO₂ certainly has some advantages because of the rather complicated separation of water + ethanol mixtures because of azeotrope formation.^[143]

Table 4.9. Properties of ethanol.^[23]

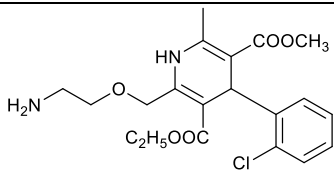
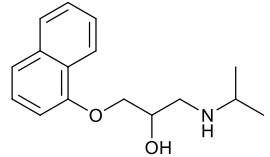
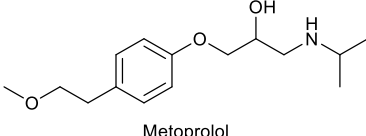
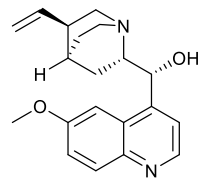
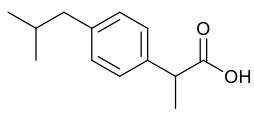
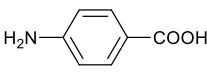
| | | | | |
|---|----------|----------|----------------------------|---------------------|
|  | m.p./ °C | b.p./ °C | ρ / kg/m ³ | Dielectric constant |
| Ethanol | -114 | 78 | 789 | 25.3 |

Formation of a second liquid layer was often observed for ethanol based systems (Table 4.10), similarly to DMSO. Knez investigated the ethanol-CO₂ system above 40 °C.^[110] He reported full liquid-liquid solubility, but did not extrapolate with his model to lower temperatures to predict the type of the system. However, CO₂ and ethanol likely exhibit a Type – I phase behaviour.^[110] Ethanol is often contaminated by water because of its slight hygroscopicity. Presence of water could induce a precipitation of a liquid phase. Water has a poor solubility in CO₂ and exhibits a Type – III behaviour.^[148]

The system of Ibuprofen + ethanol + CO₂ was homogeneous (Table 4.10), which was in accordance with the findings of Munto, who found CO₂ was rather a co-solvent for the ethanol + Ibuprofen system, rather than antisolvent.^[131]

Para-amino benzoic acid, however, precipitated out from its ethanol solution upon CO₂ exposure (Table 4.10). Liu also found rapid decrease of solubility for this solute in the same pressure region, above 6 MPa.^[151]

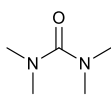
Table 4.10. Exposure of various solutes in ethanol to CO₂ at 40 °C. Initial volume of solution: 1 ml. Concentration: 100 g/l. P is the pressure at which phase transition was observed.

| Entry | Solute | P/MPa | Approximate Expansion | Observation |
|-------|---|-------|-----------------------|---|
| 1 |  <p>Amlodipine</p> | 7.7 | 6× | Two liquids |
| 2 |  <p>Propranolol 18</p> | 7.5 | 6× | Two liquids |
| 3 |  <p>Metoprolol</p> | 7.8 | 9× | Two liquids |
| 4 |  <p>Quinine</p> | 7.8 | 6× | Two liquids |
| 5 |  <p>Ibuprofen</p> | 13.3 | 17× | Single liquid phase No precipitation |
| 6 |  <p>PABA</p> | 6.0 | 1.5× | Precipitation of solid |

4.17.4 Investigation of CO₂ as antisolvent for TMU based systems

TMU is a novel, and relatively green DAS solvent (Table 4.11), often considered as a possible replacement in pharmaceutical applications for other polar solvents,^[152] such as DMF. There is a very limited information available about its phase behaviour with CO₂. The solubility of CO₂ in TMU seemed sufficient for antisolvent application, although detailed phase behaviour studies were not conducted.

Table 4.11. Properties of TMU.^[153]

| | | | | |
|--|----------|----------|----------------------|---------------------|
|  <p>TMU</p> | m.p./ °C | b.p./ °C | ρ/ kg/m ³ | Dielectric constant |
| | -1 | 177 | 968 | 23.10 |

Precipitation of liquid rather than solid was also observed for several TMU based systems (Table 4.12), similarly to DMSO and ethanol. However, Tritylamine, Amlodipine

and Quinine, precipitated out in solid form (Table 4.14). The pressures, at which the precipitation occurred, were slightly milder in TMU compared to the precipitation of liquid from DMSO (8.1, 6.6 and 6.0 MPa vs. 8.2, 8.1 and 8.2 MPa). Presence of CO₂ could decrease melting points of solids, although it is hard to predict the value of the change. In the introduction this phenomenon was discussed in more details (4.9). Melting point of naphthalene and *p*-dichlorobenzene were reduced from about 62 to 48 and 52 to below 20 °C, respectively, if exposed to CO₂ at above 6 MPa.^[32] The higher the pressure the more significant the melting point depression may be,^[32] and this could explain why liquid precipitated out from DMSO and why solid precipitated from TMU. The pressure difference for tritylamine was, however, minimal, making the theory of melting point depression rather less likely. No precipitation of solid was observed for systems containing benzodiazepine **4** and Lidocaine **20** (Table 4.13). Experiments with DMSO based systems with these solutes showed similar results (Table 4.8), indicating these species possibly had a high affinity to CO₂, therefore antisolvent behaviour was not observed.

Table 4.12. Exposure of various solutes in TMU to CO₂. Initial volume of solution: 1 ml. Concentration: 100 g/l. P is the pressure at which formation of two liquid layers was observed. Precipitation of solid was not observed.

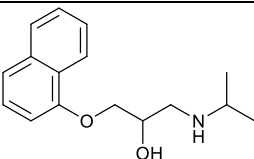
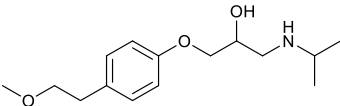
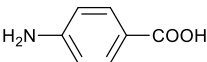
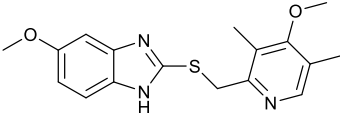
| Entry | Solute | Temperature /°C | P/MPa | Approximate Expansion |
|-------|---|-----------------|-------|-----------------------|
| 1 |  Propranolol 18 | 40 | 7.5 | 6× |
| 2 | | -5 | 3.20 | 8× |
| 3 | | -13 | 2.28 | 8× |
| 4 | | -15 | 2.21 | 6× |
| 5 | | -17 | 1.87 | 6× |
| 6 |  Metoprolol | 40 | 7.9 | 9× |
| 7 |  PABA | 40 | 7.8 | 6× |
| 8 |  Pyrimetazole 41 | 40 | 7.9 | 9× |
| 9 | | 25 | 5.7 | 9× |

Table 4.13. Exposure of various solutes in TMU to CO₂. Initial volume of solution: 1 ml. Concentration: 100 g/l. Formation of a single gas expanded liquid layer was observed. Precipitation of solid was not observed. P is the maximum pressure to which the system was raised.

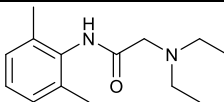
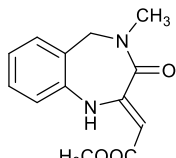
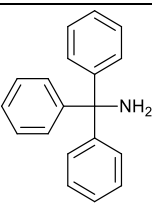
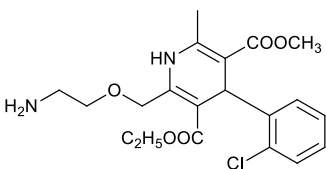
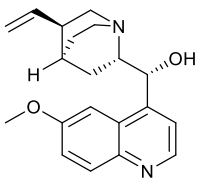
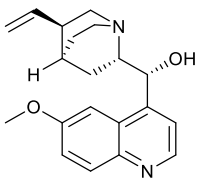
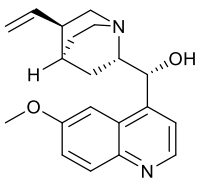
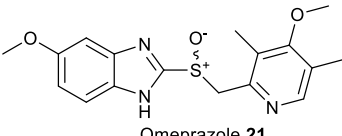
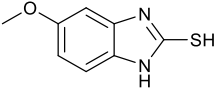
| Entry | Solute | Temperature /°C | P/MPa | Approximate Expansion |
|-------|---|-----------------|-------|-----------------------|
| 1 |  Lidocaine 20 | 40 | 11.8 | 17x |
| 2 |  benzodiazepine 4 | 40 | 12.9 | 17x |

Table 4.14. Exposure of various solutes in TMU to CO₂. Initial volume of solution: 1 ml. Concentration: 100 g/l. Precipitation of solid from the single gas expanded liquid layer was observed at P pressure.

| Entry | Solute | Temperature /°C | P/MPa | Approximate Expansion |
|-------|--|-----------------|-------|-----------------------|
| 1 |  tritylamine | 40 | 8.1 | 11x |
| 2 |  Amlodipine | 40 | 6.6 | 3x |
| 3 |  Quinine | 40 | 6.0 | 2x |
| 4 |  Quinine | -6 | 2.5 | 6x |
| 5 |  Quinine | -16 | 2.1 | 6x |
| 6 |  Omeprazole 21 | 40 | 7.4 | 6x |
| 7 |  benzimidazole | 40 | 7.9 | 9x |

4.17.5 Investigation of CO₂ as antisolvent for DMF based systems

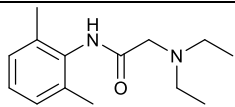
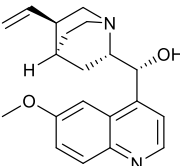
Less data were measured for DMF based systems (Table 4.15).

Table 4.15. Properties of DMF.^[23]

|  | m.p./ °C | b.p./ °C | ρ / kg/m ³ | Dielectric constant |
|---|----------|----------|----------------------------|---------------------|
| DMF | -61 | 153 | 944 | 38.25 |

The DMF + Lidocaine **20** system did not yield precipitate, similarly to DMSO and TMU systems (Table 4.16), confirming the affinity of Lidocaine **20** and CO₂. Quinine precipitated out from DMF, however the amount, determined by visual observation, was significantly lower compared to the TMU system. There was also a significant difference in pressure at which the precipitation started, 7.8 MPa for DMF vs. 6.0 MPa for TMU (Table 4.16, entry 2; Table 4.14 entry 3).

Table 4.16. Exposure of various solutes in DMF to CO₂ at 40 °C. Initial volume of solution: 1 ml. Concentration: 100 g/l. Formation of single gas expanded liquid layer was observed. Precipitation of solid was not observed, or only in very small amount. P is the maximum pressure to which the system was raised.

| Entry | Solute | P/MPa | Approximate Expansion |
|-------|--|-------|-----------------------|
| 1 |  Lidocaine 20 | 10.4 | 17x |
| 2 |  Quinine | 7.8 | 9x |

4.17.6 Investigation of CO₂ as antisolvent for Quinine solutions

In the previous sections the phase behaviour of several solute-solvent pairs during expansion by CO₂ was investigated. Quinine is an interesting, readily available drug-like structure, with an aromatic heterocycle and an amine function. Its CO₂ induced precipitation was already tested from its DMSO, ethanol, TMU and DMF solution. Acetic acid as a solvent was also tested, because it was expected to form a salt with the basic function of the amine function of Quinine. The formed quinine acetate was expected to have a low solubility in CO₂ expanded acetic acid because of its salt character (Table 4.17).

Table 4.17. Expansion of various Quinine solutions with CO₂. Initial volume of solution: 1 ml. Concentration: 100 g/l.

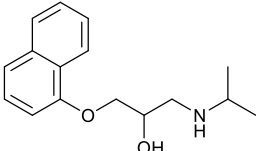
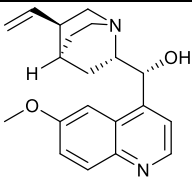
| Entry | Solvent | Temperature /°C | P/MPa | Approximate expansion | Observation |
|-------|----------------------|-----------------|-------|-----------------------|---------------------------------------|
| 1 | DMSO | 40 | 8.2 | 6× | Two liquids |
| 2 | EtOH | 40 | 7.8 | 6× | Two liquids |
| 3 | TMU | 40 | 6.0 | 2× | Precipitation of solid |
| 4 | DMF | 40 | 7.8 | 9× | Precipitation of solid (small amount) |
| 5 | CH ₃ COOH | 40 | 7.6 | 9× | Two liquids |

Precipitation of liquid rather than solid was observed from DMSO, ethanol and acetic acid. Precipitation of solid was observed from DMF and TMU. The amount of precipitate was appeared more from TMU, and the pressure at which the precipitation started was also lower compared to DMF (6 vs. 7.8 MPa). Precipitation of liquid rather than solute was observed for acetic acid, DMSO and ethanol based systems, indicating a strong solute-solvent interaction, which was possibly hydrogen bonding. Formation of insoluble acetate salt, result of an acid-base reaction of Quinine and acetic acid, was not observed. Precipitation of solid was observed from TMU and DMF. This may have occurred because weaker solute-solvent interactions.

4.17.7 Investigation of the effect of temperature for CO₂ antisolvent induced precipitations

The TMU solutions of Quinine and Propranolol **18** were expanded by CO₂ below the critical temperature of CO₂ in order to investigate the effect of temperature (Table 4.18).

Table 4.18. CO₂ antisolvent induced precipitations from TMU at low temperatures. Initial volume of solution: 1 ml. Concentration: 100 g/l. P is the maximum pressure to which the system was raised (**18**), or the pressure at which phase transition occurred (Quinine).

| Entry | Solute | Temperature /°C | P/MPa | Approximate Expansion | Observation |
|-------|--|-----------------|-------|-----------------------|---|
| 1 |  Propranolol 18 | 40 | 7.5 | 6× | Precipitation of solid was not observed |
| 2 | | -5 | 3.2 | 8× | |
| 3 | | -13 | 2.3 | 8× | |
| 4 | | -15 | 2.2 | 6× | |
| 5 | | -17 | 1.9 | 6× | |
| 6 |  Quinine | 40 | 6.0 | 2× | Precipitation of solid |
| 7 | | -6 | 2.5 | 6× | |
| 8 | | -16 | 2.1 | 6× | |

Precipitation of solid was not observed for Propranolol **18** at low temperatures either. Note that the pressure above the mixture of liquid CO₂ + TMU + solute was progressively decreasing as the temperature was decreased.

The decrease of pressure was similar for the system of liquid CO₂ + TMU + Quinine. At the lowest temperature (Table 4.18, entry 6), the pressure was reduced to 2.1 MPa. The amount of CO₂ was also increased in the system, resulting higher expansion, yet the pressure did not increase significantly.

Lower temperatures allowed operation around the vapour pressure of CO₂ at the actual temperature. Pressure necessary to precipitate Quinine from TMU was reduced from 6.0 MPa to 2.5 and 2.1 MPa, at -6 and -16 °C, respectively (Table 4.17), which was a significant decrease compared to experiments conducted at 40 °C (Table 4.14).

4.17.8 Summary of the qualitative CO₂ antisolvent induced precipitation experiments

In summary, CO₂ could be applied as antisolvent with the best results for TMU based systems, which often exhibited precipitation of solid after CO₂ exposure. By appearance, significant amount of tritylamine, Amlodipine, Quinine and Omeprazole (Table 4.14) precipitated out from its TMU solution after CO₂ exposure. The pressure necessary to induce precipitation were 8.1, 6.6, 6.0, 7.4 and 7.9 MPa were, respectively. TMU based systems were the best candidates for the development of antisolvent based preparative separations.

Solutions of DMSO often yielded liquid precipitates, possibly because of a relatively lower DMSO-CO₂ affinity (4.13). Such phase behaviour could be still exploited for separations, provided most of the solute was present in the liquid precipitate, and contaminants would remain in the CO₂ rich phase. This is more like if the contaminants are non-polar. Because the lack of solid precipitate, only methods other than antisolvent induced crystallisation could be used, and these were not in the focus of this research.

Precipitation of liquid from ethanol based solutions was also often observed. Because of the hygroscopy of ethanol, water may have been present in the system, and may have been responsible for the phase behaviour. This was not investigated in details.

Precipitation of liquid, which was also observed for TMU, may have caused by melting point depression of the solute by CO₂. The precipitated liquid may have been rich in the valuable solute, a melt of pure solid + CO₂ in ideal case. This could be exploited for separations other than antisolvent induced crystallisation. More complex phase behaviour resulting a combination of solute + CO₂ + solvent to precipitate was equally

possible. The measurement of composition and accurate amount of the precipitated liquid could not be carried out because of the lack of equipment.

The melting point depressing effect of CO₂ also manifested itself at operations below the normal melting point of TMU, which remained liquid under CO₂ pressure at low temperatures.

4.18 Separation of solids in pressurised systems

The CO₂ antisolvent induced precipitation was fully reversible. Once the pressure of CO₂ was vented, the CO₂ rapidly boiled out from the solution, and the solute redissolved. The precipitated solid therefore had to be isolated while the system was pressurised. To achieve this, a filter compartment, formed by ¼" tubing and a frit, was connected to a high pressure cell with a bottom withdrawal port. The cell was vented through the filter compartment while a continuous stream of CO₂ was pumped through the stirred system, with a back pressure regulator connected after the filter and maintaining the pressure. The cell was behaving like a continuous stirred tank reactor. The sample solution was injected into the cell using a HPLC injector loop online. More information about the setup and the high pressure equipment is summarised in

Under operation at temperatures above the critical temperature of CO₂, the injection occurred when the pressure in the cell was regulated by the back pressure regulator, and the flow of CO₂ and the temperature were steady. Immediately after injection precipitation occurred, while a slight pressure drop was also observed. The flow of CO₂ quickly increased the pressure within the cell to the opening pressure of the back pressure regulator (BPR), and the stream through the cell resumed. The filter on the outlet of the cell collected the solute in a form of solid precipitate, while the solvent + CO₂ mixture left the system through the filter and BPR. The sufficient period of time for CO₂ streaming to completely expel all the organic solvent from a 17 ml reactor was estimated to be 40 minutes, estimated from the response of an ideal continuous stirred tank reactor (CSTR) (Eq.27), (Figure 4.17). The stirring was therefore stopped 40 minutes after sample injection. CO₂ was streamed for further 10 minutes to promote sedimentation, then the cell was vented to atmospheric pressure through the BPR. The precipitate was collected from the filter compartment and from the cell.

$$V_{solvent} = V_{solvent}^0 \cdot \exp\left(-\frac{t}{V_{cell}/\dot{V}}\right)$$

V_{solvent}: normal volume of solvent in cell

V_{solvent}⁰: volume of initially loaded solvent

t: time

V_{cell}: volume of the cell

Ṃ: flow through the cell

Eq.27

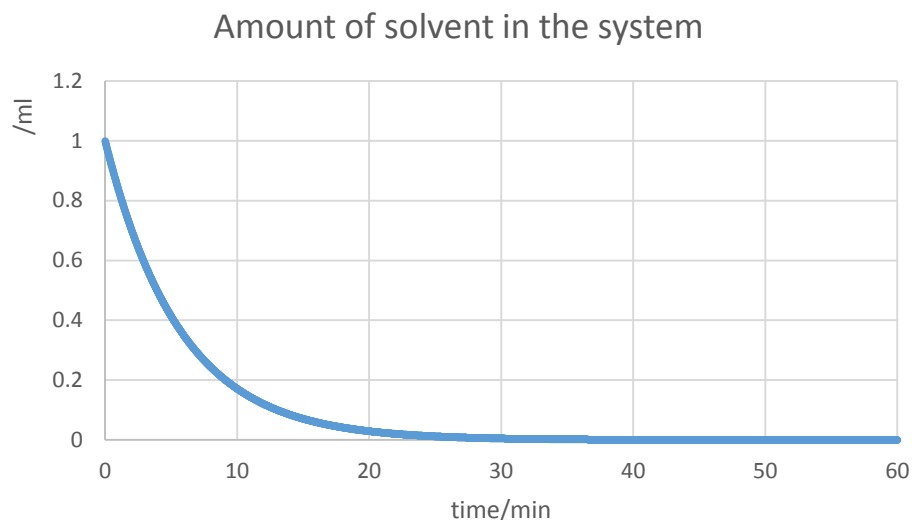


Figure 4.17. Rinsing of solvent from a CSTR, calculated with Eq.27.

$$V_{solvent}^0 = 1 \text{ ml}$$

$$V_{cell} = 17 \text{ ml}$$

$$\dot{V} = 3 \text{ ml/min}$$

Operation at subcritical CO₂ temperatures was slightly different. First the cell (volume about 17 ml) was loaded with liquid CO₂ to about 1/3 volume. The stream of CO₂ was turned on, and the solution was injected. The breaking pressure of the back pressure regulator was set at least about 1 MPa above the vapour pressure of CO₂ at the temperature of the experiment. This was necessary, because the BPR was able to keep the pressure within a certain pressure window, rather than at a very accurate pressure. This operational window had to be significantly above the vapour pressure of the CO₂. Should there be an overlap, the whole liquid phase could have been vented through the BPR because the vapour pressure would push it out. Above the vapour pressure, however, the pressure was hydraulically maintained by a syringe pump, and was controlled by the BPR. After injection of the sample the volume of liquid level started to rise because of the continuous stream of CO₂, meanwhile the pressure in the system was nearly steady. The injected sample, which was about 1 ml, was diluted up to 17 ml with liquid CO₂. At the moment when the cell was fully loaded with liquid, the hydraulic pressure started to rise rapidly until it reached the breaking pressure of the BPR. At this moment the flow through the cell started and the experiment was executed the same way as for temperatures supercritical for CO₂. The amount of solvent in the system was reduced continuously (Figure 4.17).

The stirring during the separation was paramount. Insufficient stirring would have caused dead volumes, through which the stream of CO₂ would not rinse the organic solvent, which would remain in the system after the procedure as contamination.

4.19 Antisolvent precipitation at elevated pressures with isolation

Expansion of solutions by CO₂ could lead to precipitation (4.16). It is, however, important that chemical conversion is not involved in this phenomenon. Moreover, it is completely reversible: if the pressure is reduced, the dissolved CO₂ would boil out from the solution, and the precipitated solute would re-dissolve. To avoid this, the isolation of solid must be carried out under pressure. A semi-continuous approach to achieve this was explained in the last section (4.18). In this section the application this approach in practice will be demonstrated.

Phase diagrams that allow delicate design of a high pressure antisolvent procedure were not available for the compounds we investigated. Rapid, qualitative precipitation tests were carried out instead. These tests confirmed if precipitation of a solid was possible, rather than giving optimal operational conditions, such as pressure, temperature and solvent-CO₂ ratio. Consequently, the results of separation experiments could potentially be increased by further optimisation.

Preparative separation of solutes above (Table 4.19) and below (Table 4.20) the critical temperature of CO₂ are summarised below.

Table 4.19. Preparative isolation of solutes from 1 ml solutions (concentration: 100 g/l), exploiting CO₂ induced precipitation at 40 °C (above the critical temperature of CO₂). A stream of CO₂ (3 ml/min for 40 min) was used at P pressure to remove the traces of remaining organic solvents.

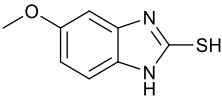
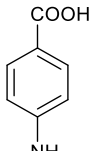
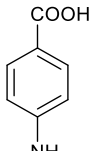
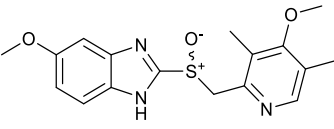
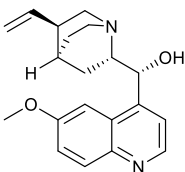
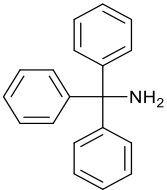
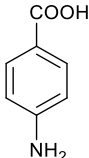
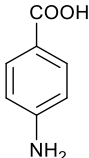
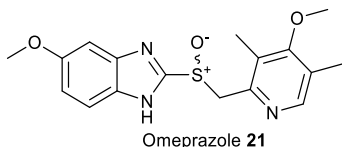
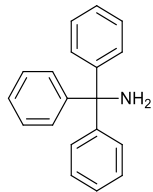
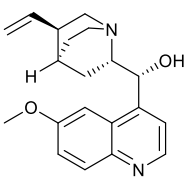
| Entry | Solute | Solvent | P /MPa | Recovery /% |
|-------|--|---------|--------|-------------|
| 1 |  benzimidazole | TMU | 10.0 | 70 |
| 2 |  PABA | EtOH | 10.0 | 53 |
| 3* |  PABA | EtOH | 10.5 | 47 |
| 4 |  Omeprazole 21 | TMU | 8.3 | 22 |
| 5 |  Quinine | TMU | 10.7 | 21 |
| 6 |  tritylamine | TMU | 8.8 | 3 |

Table 4.20. Preparative isolation of solutes from 1 ml solutions (concentration: 100 g/l), exploiting CO₂ induced precipitation at T temperature (below the critical temperature of CO₂). A stream of CO₂ (3 ml/min for 40 min) was used at P pressure to remove the traces of remaining organic solvents.

| Entry | Solute | Solvent | T /°C | P /MPa | Recovery /% |
|-------|--|---------|-------|--------|-------------|
| 1 |  | EtOH | 25 | 8.3 | 54 |
| 2 |  | EtOH | 0 | 7.3 | 46 |
| 3 | PABA | EtOH | -21 | 8.0 | 66 |
| 4 |  Omeprazole 21 | TMU | 25 | 7.0 | 93 |
| 6 |  tritylamine | TMU | 25 | 9.0 | 4 |
| 7 |  Quinine | TMU | 25 | 8.0 | 22.4 |

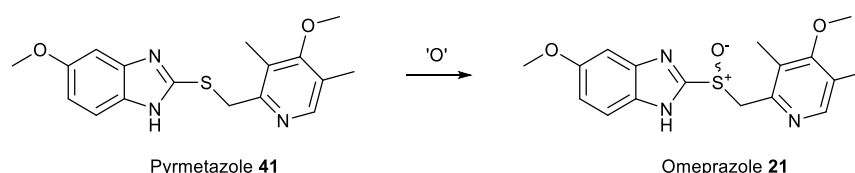
The first thing to note is that the recoveries varied significantly, from over 90% through intermediate and below 5% (Table 4.19, entries 4 and 6, Table 4.20, entry 4). According to earlier precipitation tests (Table 4.12, entries 1 and 15), visual observation of precipitate qualitatively reported the amounts of solid. These visual observations may have therefore had only a fairly limited accuracy.

Separation of PABA from ethanol was carried out at 60, 40, 25, 0 and -21 °C. At the highest temperature, the flowrate of CO₂ had to be reduced from 3 to 0.25 ml/min, because clogging impeded the filter. The pressure drop on the filter decreased at lower flowrates, but the time period of streaming had to be extended accordingly to 6 hours, in order to rinse all the solvents out from the cell thoroughly (Eq.27). The clogging was possibly caused because the temperature within the cell was higher than the temperature of the filter compartment. This was because the cell itself was heated, but the filter compartment was not. Precipitation possibly occurred when the warm, saturated solution arriving from the bulk of the cell entered the filter, and caused clogging. This may be mitigated by ensuring the temperature of the cell and the filter compartment are the same. Efficient heat insulation of the filter compartment may be sufficient to achieve this. The solute recoveries were not significantly different at various

temperatures, varying between 47 and 66%. However, the highest yield was achieved at the lowest temperature. The limitation of pressure was the vapour pressure of CO₂ at temperatures subcritical for CO₂. The actual operational pressures were, however, higher, around 8 MPa (Table 4.20, entries 1-3). These could be potentially reduced, to slightly above the vapour pressure of CO₂ at the temperature of operation (1.9, 3.5 and 6.4 MPa at -21, 0 and 25 °C, respectively). The positive effect of temperature decrease was also demonstrated by the isolation of Omeprazole from TMU. Recoveries increased significantly from 22 to above 90% as the temperature was decreased from 40 °C to room temperature. Further decrease of temperature possibly would not have a dramatic effect on the further increase of recovery, however, operation pressure may be decreased further, allowing easier design.

4.20 CO₂ antisolvent based separation

Omeprazole is synthesised by oxidation of Pymetazole (Scheme 4.3). Production of sulfone, which is the over oxidised by-product, can be avoided if Pymetazole starting material is added in excess. This would, however, result in incomplete conversion with starting material contaminating the product. The separation of the two molecules may be particularly complicated because of their similarity.



Scheme 4.3. Synthesis of Omeprazole by oxidising Pymetazole.

In the screening experiments, precipitation of solid was observed for Omeprazole, but was not observed for Pymetazole when the corresponding solutions were expanded with CO₂ (Table 4.14 entry 6, Table 4.12 entry 8). Isolation of Omeprazole and Pymetazole was attempted on a 100 mg scale. 1 ml TMU solution containing a mixture of Omeprazole (90 mg) and Pymetazole (10 mg) was injected into liquid CO₂ at room temperature. Precipitation occurred immediately. Liquid CO₂ was pumped through the system, and the precipitate was filtered out. About 80 mg Omeprazole was recovered, with Pymetazole concentration reduced to below 1.7wt%, determined by ¹H-NMR spectroscopy. The pressure during CO₂ pumping was about 7 MPa, controlled by a BPR, and could potentially be mitigated to about 2 MPa by decreasing the operational temperature to about -20 °C. However, it is required that Pymetazole does not precipitate at that temperature.

4.21 Summary of the experiments with CO₂ antisolvent

Having recognised the disadvantages of antisolvent induced precipitations, namely production of solvent mixture by-products that are difficult to separate, application of CO₂ antisolvent was considered to alleviate this problem. Numerous solutions were tested for CO₂ induced antisolvent precipitation. The precipitation of solute was found highly solvent dependent. For instance, precipitation from DMSO rarely occurred, while precipitation from TMU was more successful. A noteworthy disadvantage of CO₂ antisolvent is operation at elevated pressures, which industrial applications do not prefer. The effect of temperature was investigated, and pressures at which CO₂ could be used as an antisolvent were found to be as low as 2 MPa at -20 °C; however, operation at low temperatures may badly affect energy efficiency. The CO₂ induced precipitation was fully reversible. Experimental systems were developed that allowed the isolation of the precipitated solid under pressure. The potential of such separation procedure was demonstrated on the separation of Omeprazole and Pyrimetazole.

Chapter - 5

Conclusions and future work

5.1 CO₂ aided aqueous extractions

Separations *via* aqueous extractions are widely used purification procedures of laboratories and the pharmaceutical and fine chemical industry.^[3] Aqueous extractions are based on the different distribution of certain solutes between two non-mixing solvents. Two compounds, for instance a desired product and a by-product could be separated, provided their distribution between two solvents, for instance MTBE and water, are different. If the first compound is hydrophilic, and the second is lipophilic, water will be enriched in the first compound, and MTBE will be enriched in the second compound. The two compounds can be separated by the separation of the two phases.

The distribution of certain solutes could be manipulated by changing *pH*, for which conventional acids and bases are widely used.^[3] The two most important disadvantages of the procedure are by-product formation in equimolar amounts,^[154] and reaction of the solute with the used acid or base.^[42] These two disadvantages could be overcome for the purification of basic compounds, if the used acid is replaced by carbonic acid, and the neutralisation step is replaced by physical decarboxylation.

5.1.1 Screening experiments - conclusions

Several organic bases, including primary, secondary and tertiary amines, pyridines, anilines and heterocycles were assayed for CO₂ aided aqueous extractions (2.8, p20). The investigated bases could be categorised into three main classes, as long the effect of CO₂ is concerned: The first class of bases could not be extracted into an aqueous phase in the presence of CO₂ because they were either too weak bases, or too lipophilic. The second class comprised bases that could be extracted into the aqueous phase from the organic phase even without exposure to CO₂. This was because these species were hydrophilic enough for aqueous extraction even in free base form. Bases of the third class could be extracted into the aqueous phase only after CO₂ exposure. These bases were basic enough to react with CO₂, but were not hydrophilic enough to be extracted in absence of CO₂. They were not too lipophilic either, which would have prevented the extraction even in the presence of CO₂.

The success of the CO₂ aided extraction seemed to be determined by the substrate's basic strength and lipophilic character, which are most commonly measured by the *pK_a* and *logP*. When the extraction difference, that is the difference of solute extracted from the organic phase by water in the presence and absence of CO₂, was plotted against both *pK_a* and *logP*, the zones of the three classes on the *pK_a* - *logP* plane were revealed (Figure 2.8, p29). Simple empiric equations were also proposed to predict which zone a

base may fall (Eq.17, Eq.19, p34). The measures of basicity or lipophilic character are often not available. In this case calculated values could be used.^[50, 80]

The compiled diagram or the proposed empiric equations, combined with predicted pK_a or $\log P$ values, could be powerful tools to predict if an already existing purification procedure of a base *via* aqueous extraction could or could not be replaced by CO₂ aided aqueous extraction.

5.1.2 Detailed investigation of distribution - conclusions

The concentration dependency of distribution in CO₂ saturated systems was also studied on several amines (2.9.3, p40). In general, low concentrations promoted the organic to aqueous extraction in presence of CO₂, however, some of the tested bases did not show strong concentration dependence.

The kinetics of carboxylation by CO₂ streaming, and decarboxylation by N₂ gas streaming were also investigated (2.9.5, p45). The carboxylation was found to be significantly, roughly 25 times faster compared to the decarboxylation.

The slower neutralisations step was investigated in more details. The dependence of the decarboxylation rate from the type of the amine, from the concentration of the system, and from the N₂ gas flowrate was studied (2.9.6, p46).

The N₂ gas flow had negligible effect on the decarboxylation within the investigated flowrate range. The effect of the concentration of the system was also negligible at lower concentrations (<20 wt%), as long as the distribution of base was concerned. At the highest tested concentration, however, the rate of decarboxylation decreased. It should be emphasised that the completeness of decarboxylation was measured by distribution, and the higher the amine concentration was the more CO₂ had to be driven off to achieve the same change in distribution. The type of amine highly influenced the rate and completeness of decarboxylation. Low pK_a and high $\log P$ values enhanced the rate decarboxylation.

5.1.3 Possibilities for further research

The screening experiments focused on the change of distribution caused by CO₂ exposure, rather than studying the actual chemical phenomena in details. However, the chemical change may have an impact on the distribution, particularly in the case of primary and secondary amines. These amines may form both carbamate salts and bicarbonate salts, although the literature suggests the formation of bicarbonates is more likely if water is present.^[83] The ratio of carbamate or bicarbonate salts may affect the amine distribution between organic solvent and water, and the decarboxylation kinetics may also be affected. The determination of the salt or salt mixture in the

aqueous phase is rather challenging. The most feasible approach is by NMR spectroscopy.^[83]

In this research mostly MTBE was used for the screening experiment as the organic solvents. Investigation of a range of organic solvents would give valuable information about the solvent dependency of the procedure.

The acidity of CO₂ at higher pressures increases,^[23] which may allow the extraction of weaker bases. It could be also worthwhile to investigate the phase distribution at pressures above ambient. This may evolve into a fine control of *pH* by variation of CO₂ pressure, which could allow the separation of species with varying basic strength.^[155] The control of *pH* only by CO₂ may be useful for other *pH* sensitive applications, such as biotransformations.^[156]

The detailed phase distribution studies required more time consuming experiments compared to the screening studies, consequently the obtained information is more limited. Extending the investigation of distribution to further organic bases could allow revealing a more detailed connection between carboxylation or decarboxylation rate and the chemical and physical properties of the base, including basicity and lipophilicity. Determination of an empiric equation between the time constant of the decarboxylation and *pK_a* and *logP*, similarly to that found in the screening experiments, may be possible. Presence of both bicarbonates and carbamates in the system may also have an effect on the kinetics of decarboxylation, and yet to be investigated. A chain of chemical reactions, formation of physically dissolved CO₂ all the way from bicarbonate seemed to have an effect on the rate of decarboxylation, in which the type of the base seemed to be important. The rate of chemical reactions typically have a more pronounced temperature dependence compared to mass transport limitation. Investigating the effect of temperature on the decarboxylation rate could potentially help confirming the rate limiting phenomena.

A set-back of CO₂ aided aqueous extractions was concentration dependency. Typically, the more dilute a system was, the more amine could be extracted into the aqueous phase with CO₂. Conventional chemistries are normally carried out at concentrations as high as possible because this way less amount of solvent has to be dealt with for the same product output, and the available reactor volume could be used more efficiently. Moreover, higher concentrations potentially increase reaction rates.^[36] Biotransformations, however, are typically carried out in significantly lower concentrations, mainly because of substrate inhibition or enzyme coagulation.^[156-157] Several biotransformations use amines as either products or starting materials.^[158-160] The manipulations of amine distribution between organic solvents and water could be

therefore a great use to improve either these procedures themselves, or their work-up procedures.

5.2 CO₂ based approach to new crystallisation procedures

Crystallisation is a preferred way of purification in pharmaceutical and fine chemical industry. An inevitable requirement towards the substrate to purify is that it must be crystalline. However, crystallisation can be extended to otherwise non crystalline chemicals. In this case it is not the neat substrate which is isolated, but rather its crystalline derivative.^[3] These crystalline derivatives are often salts if the substrate is an acid or base. After the purification procedure, however, the formed salt need to be neutralised in order to obtain the free base/acid. A main disadvantage of the procedure is that salt by-products are formed.^[154] Strong bases or acids involved in the procedure may also cause undesired reactions.^[42]

5.2.1 Conclusions

Reactions of certain amines with CO₂ were investigated in this research (3.7, p75). Detailed analysis of the formed CO₂ adducts was carried out (3.8, p77), and their stability and reactivity was also investigated (3.10, p87; 3.15, p99). However, the main purpose of the adduct formation was the development of novel crystallisation procedures for separation and purification purposes based on carbamate salt formation rather than salt formation with inorganic acids (3.13, p96). The procedure can potentially alleviate the problems of salt by-product formation and undesired reactions.^[42, 154] However, the range of the suitable substrates for isolation in a form of a carbamate is limited.

5.2.2 Possibilities for further research

At the current stage of research, prediction whether a particular substrates is suitable or unsuitable is not yet possible. Further investigation of carbamate formation reactions on a wider range of amines could potentially lead to a better understanding of the phenomenon, and may allow predictions. In this research ether type solvents were found to be ideal for carbamate formation reactions. Screening of other solvents in further research could also contribute. The CO₂ adduct formation in this project were carried out under ambient pressures; investigation of the effect of pressure may also be worthwhile. Higher pressures, but still in the conveniently attainable region (< 2.0 MPa) may significantly enhance the efficiency of the separation procedure. Operation at lower temperatures may have similar effects. Moreover, amines that did not form crystalline CO₂ adducts at room temperature, may do so at lower temperatures. The adduct formation may be sensitive to certain chemicals, such as water or acids. Better

understanding of the tolerance of carbamate formation by further investigation of amine + CO₂ reactions in the presence of potential by-products and contaminants may help extending the application from purification procedures to actual reaction work-ups.

5.3 Application of CO₂ as antisolvent for crystallisation procedures

Application of conventional antisolvents can induce precipitation by reducing the solvent power in the original solution.^[144] The precipitated solute can then be collected, while the contaminants remain dissolved, therefore an isolation can be realised. However, the procedure will result a solvent mixture that has to be treated, ideally separated, typically by distillation. Distillation of certain pairs of solvents can be particularly problematic, either because of azeotrope formation or simply because of the high energy demand.^[9] CO₂ has a good solubility in the majority of organic solvents at elevated pressures. Dissolution of CO₂ in a solvent is often referred as gas expansion.^[32] Application of a gas antisolvent, such as CO₂, could potentially alleviate the problem of solvent-antisolvent separation; the dissolved CO₂ will readily boil out from the solution after reducing the pressure.

5.3.1 Conclusions

An experimental set-ups were built, which allowed the visual observation of phase behaviour during CO₂ exposure, and also the separation of the precipitated solid under pressure became possible (Appendix - I). The phase behaviour of numerous solute-solvent pairs were qualitatively tested during expansion by CO₂ (4.17, p131). A noteworthy disadvantage was the operation at high pressure. Lower temperatures allowed operating at lower pressures, which would significantly alleviate equipment design on scale. A significant solvent dependency was also observed. The solubility decreased more dramatically in tetramethyl urea compared to DMF, for instance. The qualitative observations of phase behaviour allowed the development of preparative solute-solvent separations at elevated pressures (4.18, p141).

The change of solubility induced by CO₂ highly depended on the chemical structure of the solute and varied on a wide range. This could be exploited for separations, namely, if the target solute, of which solubility decreased more dramatically during expansion, could be separated from other solutes with less sensitive solubility characteristics. The separation was demonstrated on the example of Pymetazole **41** and Omeprazole **21** (4.20, p146).

5.3.2 Potential upgrade of visual phase behaviour investigations

An upgrade of the available experimental setup could greatly contribute to more efficient data acquirement. The current setup allowed the visual observation of phase behaviour during gas expansion. The gross composition within the cell was known because the composition and amount of solution, and also the amount of injected CO₂ were known. However, properties of co-existing phases, such as composition, volume or density were not accurately known, and could only be roughly estimated. Consequently, the distribution of species between light and heavy phases were not accurately know. The distribution also depended on the amount of sample loaded initially into the cell. Moreover, certain properties could not be manipulated independently. For instance, the pressure could be increased by addition of CO₂ into the system, but this also changed the composition.

Application of a VVVC, variable volume view cell, would greatly enhance accuracy and reproducibility. A VVVC could be conveniently used to monitor phase changes of a previously synthesised mixtures by manipulating the pressure.^[130] However, there are certain limitations of using a VVVC. Namely, it is only the phase behaviour that can be observed, which could be precipitation. If a complex mixture with multiple components is studied, it is not known which of the many components is actually precipitating.

5.3.3 Potential upgrades of the solid separation experiments

Using a filter compartment and a back pressure regulator, the separation of the precipitated solid became possible under pressure. The typical amount of solute in the system was about 100 mg. Most of the precipitated solid accumulated in the filter compartment, allowing convenient separation. However, another portion covered the large surface of the inner cavity area of the experimental device. The removal of the solid from the cavities could not be carried out perfectly, and it is also hard to estimate the efficiency of the removal. The efficiency could also be hugely affected by the consistency of the precipitate. A possibility to overcome the accuracy and reproducibility problems of the solid removal approach could be sampling the liquid phase. Instead of solid isolation, the composition of the saturated liquid phase would give information about the amount of precipitate after gas expansion. The rate of data acquiring could also be greatly enhanced by sampling. However, the complexity of the experimental setup would increase significantly. A sampling system within the pressurised system would be necessary. The sampling system would need to be able to transfer the taken sample directly to an assaying device, such as GC or HPLC. The quick screening with such analytical method would help optimising the conditions of separation, such as temperature, pressure and CO₂ concentration, and allow a design of an optimised preparative procedure.

The developed procedures, including CO₂ aided aqueous extraction, CO₂ aided crystallisation *via* adduct formation and application of pressurised CO₂ as an antisolvent could potentially be useful for the synthesis of AstraZeneca drug candidate SB-214857-A.

Chapter - 6

Experimental

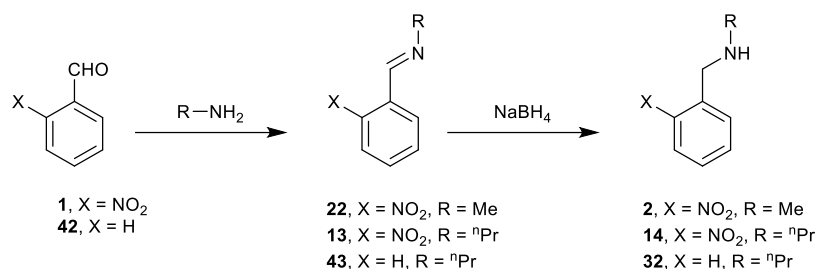
6.1 Instrumentation

Nuclear magnetic resonance (NMR) spectra were recorded for ^1H and ^{13}C at 300 and 75 MHz on Bruker DPX300 spectrometer, and at 500 and 125 MHz on a Bruker Avance 500 spectrometer. Chemical shifts are expressed in parts per million (ppm) downfield of tetramethylsilane internal standard (TMS singlet at 0 ppm). The proton coupling constants were reported as corrected. Multiplicities were abbreviated as follows: s singlet, bs broad singlet, d doublet, t triplet, q quartet, pent pentet, sex sextet and m multiplet. Fourier transform infrared (FTIR) spectroscopy were recorded on a Perkin Elmer Spectrum One spectrometer on thin film sample. Ultraviolet/visible (UV/Vis) spectra and absorbances were recorded on a Cary 100 dual beam spectrometer in quartz cuvettes with 10 mm beam pathway. Electrospray MS were recorded on a Bruker Daltonix HCTultra spectrometer. An Agilent 1200 series HPLC system was used for chromatographic analysis, equipped with a diode array detector. Elemental analyses were done on a Carlo Erba 1108 elemental analyser (C, H, N), and with Schöniger oxygen flask combustion and titration for halogens. Melting points were measured on a Griffin apparatus in glass capillaries and are uncorrected. Thin layer chromatography (TLC) was carried out on Merck pre-coated glass silica gel 60 F₂₅₄ plates with fluorescent indicator 254 nm, and were visualised using ultraviolet light. A Büchi rotary evaporator evacuated by a diaphragm pump was used to remove solvents at 15 mmHg. X-ray diffraction data were collected on a Bruker X8 Apex diffractometer using Mo-K α source with graphite monochromator. Hydrogen atoms were placed into idealised geometric positions. Thermogravimetric analysis (TGA) was carried out on a Mettler Toledo SDTA851e analyser, equipped with a TS0801R0 auto sampler. The equipment was calibrated by $\text{CuSO}_4 \cdot 5\text{H}_2\text{O}$ standard. Gas flowrates were measured by Caché variable area flowmeters with an accuracy of $\pm 2.5\%$. The *pH* was measured by a Jenway 3540 *pH* meter using a glass electrode (Electrolyte: 3.5 M KCl).

6.2 Materials

Carbon dioxide was supplied by BOC Gases UK ($\text{CO}_2 > 99.9\%$; $\text{H}_2\text{O} < 20$ ppm; $\text{O}_2 < 30$ ppm) Chemicals used in organic syntheses, in distribution experiments or in high pressure experiments were obtained from commercial sources and used without further purification. If bases were available only as salts, the free bases were obtained by a neutralisation with aqueous sodium hydroxide, extraction by organic solvent (MTBE or EtOAc), drying (MgSO_4), and concentration *in vacuo*. Omeprazole **21** and Pymetazole **41** were synthesised within our research group by Judith Spence.

6.3 Organic syntheses



6.3.1 *O*-Nitrobenzyl methylamine **2**^[12]

O-Nitrobenzaldehyde **1** (10.0 g, 66.2 mmol) was dissolved in ethanol (40 ml). While being stirred at room temperature, a solution of methylamine (2.46 g, 79.4 mmol, 1.20 equiv.) in ethanol (60 ml) was added within 10 minutes. Having stirred for 1 hour, TLC showed the formation of imine **22** intermediate product. Ground NaBH₄ (3.00 g, 79.4 mmol, 1.20 equiv.) was added portionwise. Evolution of H₂ gas, a temperature increased to 30 °C and darkening of the reaction mixture was observed. Having stirred for one hour at room temperature, TLC showed only product. The system was diluted with water (200 ml) and the ethanol was removed *in vacuo*. The residues were diluted with water (100 ml), extracted into ethyl acetate (3×80 ml), dried (MgSO₄) and concentrated to give the crude product *O*-Nitrobenzyl methylamine **2** as brown oil (10.85 g, 62.2 mmol, 94%). The concentration of by-product *o*-nitrobenzylalcohol **15** in the crude was 4.7wt%, estimated by ¹H-NMR integration of benzyl protons at 3.87 and 4.93 ppm. *R*_f 0.11 (75:23:2 EtOAc, hexane, TEA); δ_H (300 MHz, DMSO-*d*6); 7.91 (1H, d, *J*=8.1 Hz, *ArH*), 7.67 (2H, m, *ArH*), 7.49 (1H, m, *ArH*), 3.87 (2H, s, *ArCH*₂), 2.24 (3H, s, *CH*₃); δ_C (75 MHz, DMSO-*d*6); 149.50, 135.73, 133.58, 131.71, 128.39, 125.17, 53.15, 36.50; *m/z* (ESI) 167.1 (100%, 1+M⁺); ν_{max}/cm⁻¹ (film); 3334 (w, br.), 3071 (w), 2937 (m), 2849 (m), 2795 (m), 1610 (m), 1577 (m), 1525 (s), 1346 (s), 730 (s).

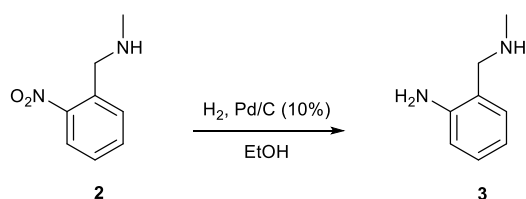
6.3.2 *O*-Nitrobenzyl *n*-propylamine **14**^[161]

O-Nitrobenzaldehyde **1** (15.0 g, 100 mmol) was dissolved in ethanol (50 ml). While being stirred at room temperature, a solution of *n*-propylamine (7.18 g, 120 mmol, 1.20 equiv.) in ethanol (40 ml) was added in 15 minutes. Having stirred for 15 minutes, ground NaBH₄ (5.00 g, 133 mmol, 1.33 equiv.) was added portionwise. Evolution of H₂ gas, slight increase of temperature and darkening of the reaction mixture was observed. After three hours of stirring at room temperature, the system was diluted with water (400 ml), and the ethanol was removed *in vacuo*. The aqueous residues were diluted with water (100 ml) and extracted into ethyl acetate (3×70 ml). The combined organic phase was washed with water (2×50 ml), dried (MgSO₄) and concentrated to give the crude product

O-Nitrobenzyl *n*-propylamine **14** as brown oil (18.66 g, 93.9 mmol, 94%). The concentration of by-product *o*-nitrobenzylalcohol **15** in the crude was 2.4wt%, estimated by ¹H-NMR integration of benzyl protons at 4.03 and 4.93 ppm. *R*_f 0.25 (75:23:2 EtOAc, hexane, TEA); δ_H (300 MHz, CDCl₃); 7.94 (1H, d, *J*=9.0 Hz, *ArH*), 7.60 (2H, m, *ArH*), 7.40 (1H, t, *J*=7.5 Hz, *ArH*), 4.03 (2H, s, *Ar-CH*₂), 2.60 (2H, t, *J*=7.2 Hz, *NCH*₂), 1.54 (1H, bs, *NH*), 1.53 (2H, sex, *J*=7.2 Hz, *CH*₂), 0.93 (3H, t, *J*=7.5 Hz, *CH*₃); δ_C (75 MHz, CDCl₃); 149.49, 136.30, 133.55, 131.64, 128.24, 125.10, 124.99, 51.87, 51.29, 23.65; *m/z* (ESI) 195.1 (100%, *MH*⁺); ν_{max}/cm⁻¹ (film); 3349 (m, br.), 3069 (m), 2959 (m), 1610 (m), 1525 (s), 1348 (s), 1123 (m).

6.3.3 Benzyl *n*-propylamine **32**

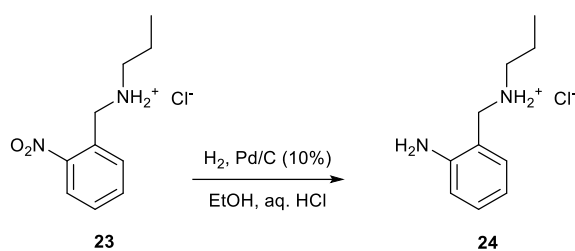
A solution of *n*-propylamine (5.50 g, 100 mmol, 1.33 equiv.) in dichloromethane (10 ml) was added into a solution of benzaldehyde **42** (7.90 g, 75 mmol) in dichloromethane (20 ml). ¹H-NMR spectroscopy showed no aldehyde present after refluxing for 3 hours. The system was diluted with methanol (80 ml) and ground NaBH₄ (4.25 g, 112 mmol, 1.50 equiv.) was added portionwise. Evolution of H₂ gas was observed. Having stirred under reflux for 30 minutes, TLC showed no starting material. The reaction mixture was concentrated, diluted with water (100 ml), extracted into ethyl acetate (3×80 ml). The combined organic phase was washed with water (3×80 ml), dried (MgSO₄) and concentrated to give crude product as pale yellow oil. The crude was distilled *in vacuo* to yield *o*-benzyl propylamine **32** as colourless oil (7.32 g, 49 mmol, 65%). *R*_f 0.50 (75:23:2 EtOAc, hexane, TEA); b.p. 43-49 °C at 0.125 mmHg; δ_H (300 MHz, CDCl₃); 7.21-7.33 (5H, m, *ArH*-1), 3.79 (2H, s, *Ar-CH*₂), 2.60 (2H, t, *J*=7.5 Hz, *NCH*₂), 1.53 (2H, sex, *J*=7.5 Hz, *CH*₂), 1.30 (1H, bs, *NH*), 0.92 (3H, t, *J*=7.5 Hz, *CH*₃); δ_C (75 MHz, CDCl₃); 141.01, 128.85, 128.65, 127.28, 54.51, 51.78, 23.64, 12.21; ν_{max}/cm⁻¹ (film); 3303 (m, br.), 3027 (m), 2959 (s), 2874 (s), 2383 (m), 1604 (m), 1494 (s), 1454 (s).



6.3.4 Synthesis of *o*-aminobenzyl methylamine **3** by the reduction of *o*-nitrobenzyl methylamine **2**

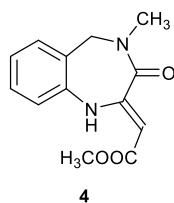
O-Nitrobenzyl methylamine **2** (2.0 g, 12.0 mmol) was dissolved in ethanol (120 ml) and catalyst (10% Pd on charcoal, 120 mg) was added. The system was evacuated and hydrogen gas was introduced. The purging procedure was repeated twice. After stirring

for 30 minutes at room temperature in H₂ gas atmosphere, the catalyst was filtered off on Celite and the reaction mixture was concentrated *in vacuo* to give aniline **3** as light brown oil (1.55 g, 11.4 mmol, 95%). *R*_f 0.09 (75:23:2 EtOAc, hexane, TEA); δ_H (300 MHz, DMSO-*d*6); 6.93 (2H, m, *ArH*), 6.62 (1H, d, *J*=7.5 Hz, *ArH*), 6.50 (1H, dd, *J*=7.5, 4.0 Hz, *ArH*), 5.22 (2H, bs, *ArNH*₂), 3.56 (2H, s, *ArCH*₂), 2.26 (3H, s, *CH*₃); δ_C (75 MHz, DMSO-*d*6); 147.82, 129.65, 127.87, 123.65, 116.10, 114.95, 54.16, 36.00; *m/z* (ESI) 136.2 (100%, *M*⁺); ν_{max}/cm⁻¹ (NaCl); 3418 (s, br.), 3318 (s, br.), 3023 (m), 2936 (s), 2842 (s), 2792 (s), 1615 (s), 1495 (s), 1460 (s), 751 (s).



6.3.5 *O*-Aminobenzyl *n*-propylamine hydrochloride **24**

O-Nitrobenzyl propylamine **14** (0.52 g, 2.70 mmol) was dissolved in methanol (30 ml). Aqueous HCl (37%, 0.68 ml, 3.3 equiv.) and catalyst (10% Pd on charcoal, 30 mg) were added. The system was evacuated and hydrogen gas was introduced. The purging procedure was repeated two more times. After stirring for one hour the catalyst was filtered off on Celite and the reaction mixture was concentrated *in vacuo*. The resulting colourless salt was suspended in ether (15 ml), filtered and washed with ether-methanol mixture. After drying, *o*-aminobenzyl propylamine hydrochloride **24** was obtained as colourless needles (0.39 g, 2.40 mmol, 90%). M.p. 191-195 °C; δ_H (300 MHz, D₂O); 7.55 (3H, m, *ArH*), 7.41 (1H, d, *J*=6.5 Hz, *ArH*), 4.29 (2H, s, *ArCH*₂), 3.09 (2H, t, *J*=7.5 Hz, *NCH*₂), 1.67 (2H, sex, *J*=7.8 Hz, *CH*₂), 0.91 (3H, t, *J*=7.5 Hz, *CH*₃); δ_C (75 MHz, D₂O); 132.45, 131.90, 130.35, 130.00, 124.86, 124.78, 49.99, 46.25, 19.68, 10.59; *m/z* (ESI) 165.2 (100%, *M*⁺¹); ν_{max}/cm⁻¹(film); 2777 (m, br.), 2528 (m, br.), 1986 (m, br.), 1626 (m), 1502 (s), 1445 (s), 1319 (m).



6.3.6 Synthesis of benzodiazepine **4** from free amine **3** starting material

Solution of dimethyl acetylenedicarboxylate, DMAD **37**, (2.10 g, 14.7 mmol, 1 equiv.) in methanol (4.5 ml) was introduced dropwise into the solution of *o*-aminobenzyl methylamine **3** (2.00 g, 14.7 mmol, 1 equiv.) in methanol (11 ml) while being cooled by ice (0-5 °C). After 90 minutes of stirring (0-5 °C), TLC did not indicate aniline starting material **3**. Glacial acetic acid (118 mg, 2.0 mmol, 0.13 equiv.) was added, and the reaction mixture was heated under reflux for 3 hours. After cooling to 50 °C, a solution of CH₃ONa (5.26 mmol, 0.95 ml 30wt%, 0.36 equiv.) was added and the resulting solution was stirred under reflux for 2 hours. The reaction mixture was cooled to 50 °C, and glacial acetic acid (315 mg, 5.26 mmol, 0.36 equiv.) and water (20 ml) was added. Having stirred for one hour, the reaction mixture cooled down to 0-5 °C by ice bath, and stirred for 5 hours. The precipitated colourless solid was filtered out, washed with aqueous methanol (w:m=3:2), and dried in air to give benzodiazepine **4** as pale yellow needles (1.86 g, 7.56 mmol, 51.4%). M.p.: 113-115 °C; *R*_f 0.51 (49:49:2 EtOAc, hexane, TEA); δ_H (300 MHz, CDCl₃); 10.62 (1H, bs, NH), 7.31 (1H, td, *J*=8.0, 2 Hz, ArH), 7.18 (1H, d, *J*=8.0 Hz, ArH), 7.06 (2H, m, ArH), 5.43 (1H, s, CCH), 4.27 (2H, bs, ArCH₂), 3.74 (3H, s, OCH₃), 3.09 (3H, s, NCH₃); δ_C (75 MHz, CDCl₃); 170.87, 162.68, 153.74, 139.33, 129.72, 128.40, 127.59, 123.78, 120.75, 89.53, 51.01, 50.96, 34.74; ν_{max}/cm⁻¹ (film); 3242 (s), 2949 (s), 1656 (s), 1615 (s), 1584 (s), 1270 (s.). Analytical data obtained was in accordance with published data.^[12]

6.4 UV/Vis spectroscopy and HPLC calibrations

Calibrating solution of *o*-nitrobenzyl methylamine **2**, Propranolol **18**, Prilocaine **19** and Lidocaine **20** were prepared using alkalified aqueous ethanol (ethanol:water 4:6 vol, 0.01 M NaOH in water). The absorbance was measured with a dual beam Cary 100 spectrometer at room temperature (Table 6.1-6.4, Figure 6.1-6.4). SBW: Spectral bandwidth.

Table 6.1. Calibration data for *o*-nitrobenzyl methylamine **2**. λ : 261.0 nm, SBW: 3 nm, measurement time: 3 s.

| Entry | Concentration /M | Absorbance |
|-------|-----------------------|------------|
| 1 | 4.13×10^{-4} | 2.188 |
| 2 | 8.65×10^{-5} | 0.461 |
| 3 | 5.41×10^{-5} | 0.295 |
| 4 | 1.09×10^{-5} | 0.060 |
| 5 | 5.45×10^{-6} | 0.029 |

Calibration curve for *o*-nitrobenzyl methylamine

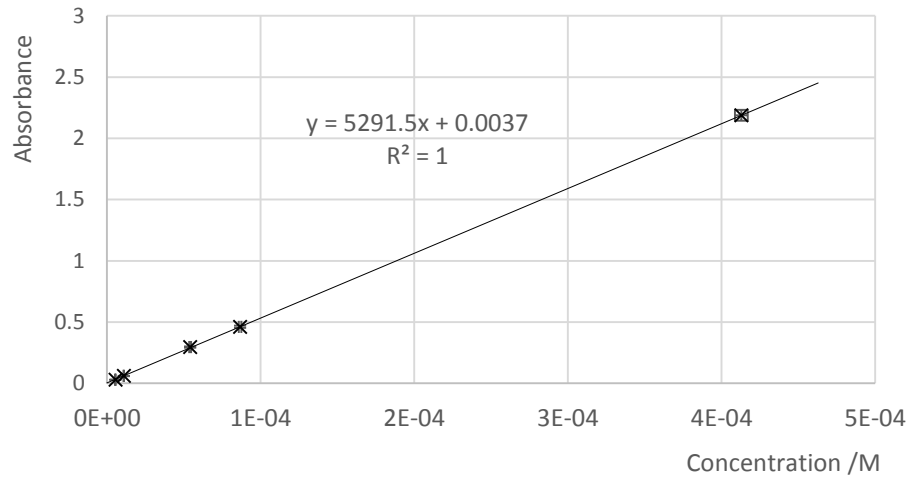


Figure 6.1. Calibration curve for *o*-nitrobenzyl methylamine **2**. λ : 261.0 nm, SBW: 3 nm, measurement time: 3 s.

Table 6.2. Calibration data for Propranolol **18**. λ : 291.9 nm, SBW: 2 nm, measurement time: 3 s.

| Entry | Concentration /M | Absorbance |
|-------|-----------------------|------------|
| 1 | 2.91×10^{-4} | 1.718 |
| 2 | 1.35×10^{-4} | 0.799 |
| 3 | 8.46×10^{-5} | 0.489 |
| 4 | 1.71×10^{-5} | 0.097 |
| 5 | 8.53×10^{-6} | 0.048 |

Calibration curve for Propranolole

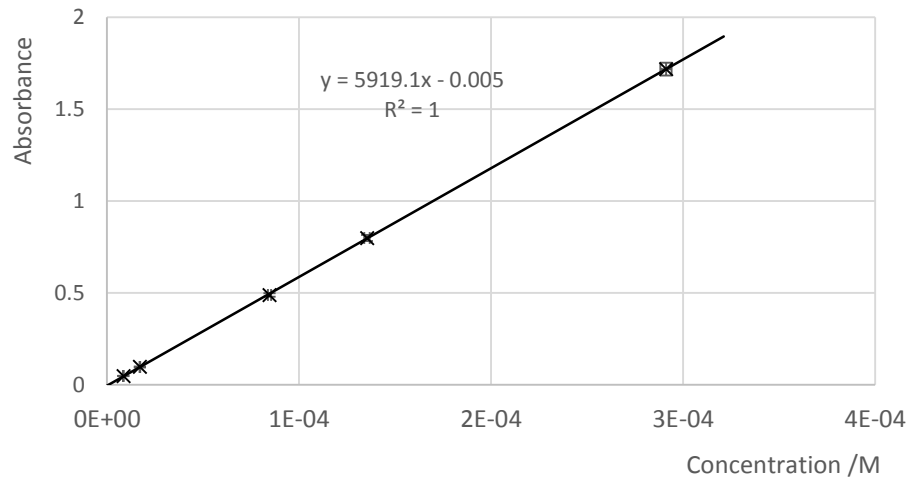


Figure 6.2. Calibration curve for Propranolol **18**. λ : 291.9 nm, SBW: 2 nm, measurement time: 3 s.

Table 6.3. Calibration data for Prilocaine **19**. λ : 230.6 nm, SBW: 2 nm, measurement time: 3 s.

| Entry | Concentration /M | Absorbance |
|-------|-----------------------|------------|
| 1 | 3.15×10^{-4} | 2.011 |
| 2 | 1.59×10^{-4} | 1.025 |
| 3 | 9.92×10^{-5} | 0.648 |
| 4 | 2.00×10^{-5} | 0.132 |
| 5 | 1.00×10^{-5} | 0.063 |

Calibration curve for Prilocaine

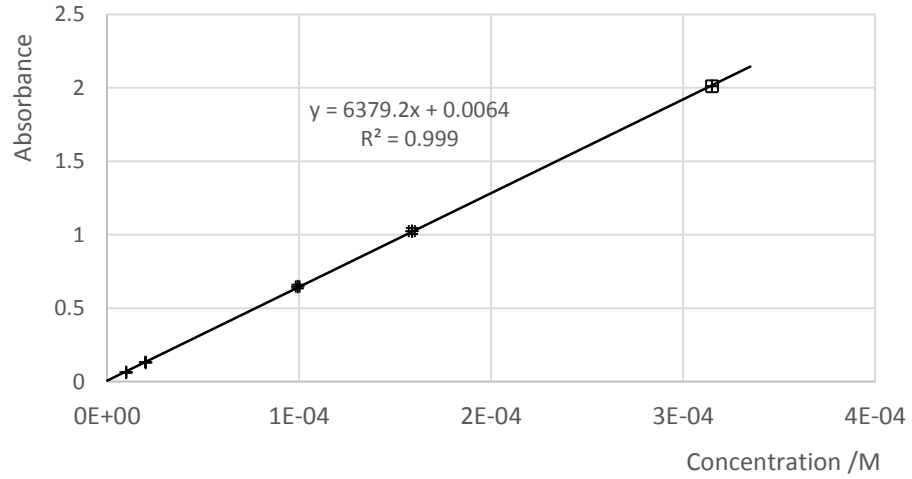


Figure 6.3. Calibration curve for Prilocaine **19**. λ : 230.6 nm, SBW: 2 nm, measurement time: 3 s.

Table 6.4. Calibration data for Lidocaine **20**. λ : 214.5 nm, SBW: 2 nm, measurement time: 3 s.

| Entry | Concentration /M | Absorbance |
|-------|-----------------------|------------|
| 1 | 6.37×10^{-3} | 2.276 |
| 2 | 4.88×10^{-4} | 0.171 |
| 3 | 2.25×10^{-4} | 0.079 |
| 4 | 1.27×10^{-4} | 0.041 |
| 5 | 7.97×10^{-5} | 0.026 |

Calibration curve for Lidocaine

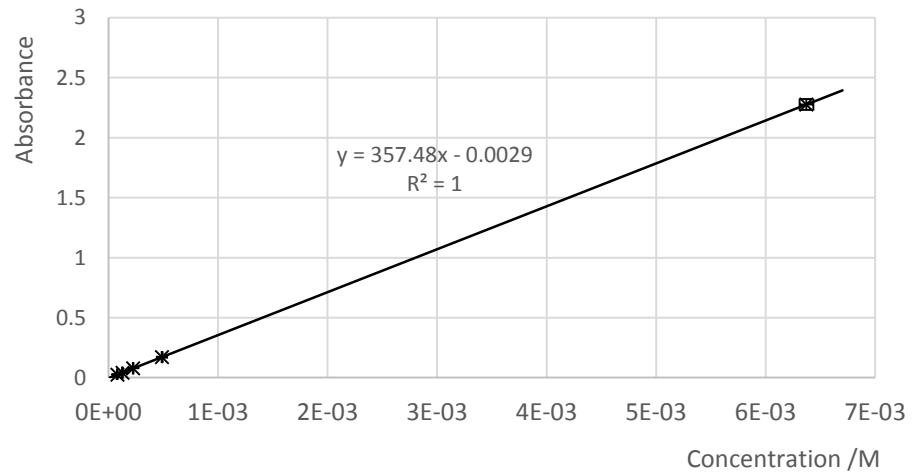


Figure 6.4. Calibration curve for Lidocaine **20**. λ : 214.5 nm, SBW: 2 nm, measurement time: 3 s.

The composition of *o*-nitrobenzyl propylamine **14** was measured by HPLC. Eluent: aqueous ammonia (0.1wt%) + acetonitrile. Eluent flow: 0.5 ml/min; Gradient: 5 to 95% acetonitrile in 5.0 min. Retention time: 2.65 min on a C18 column (Ascentis express, 50×2.1 mm; 2.7 μm). Temperature: 20 °C. Detector channel: DAD signal A (220 nm) (Figure 6.5). A calibration curve for *o*-nitrobenzyl methylamine **2** was also recorded. The eluent system, column, temperature and detector channel were the same as for the analysis of propyl derivative **14**. The retention time was 1.82 min (Figure 6.6).

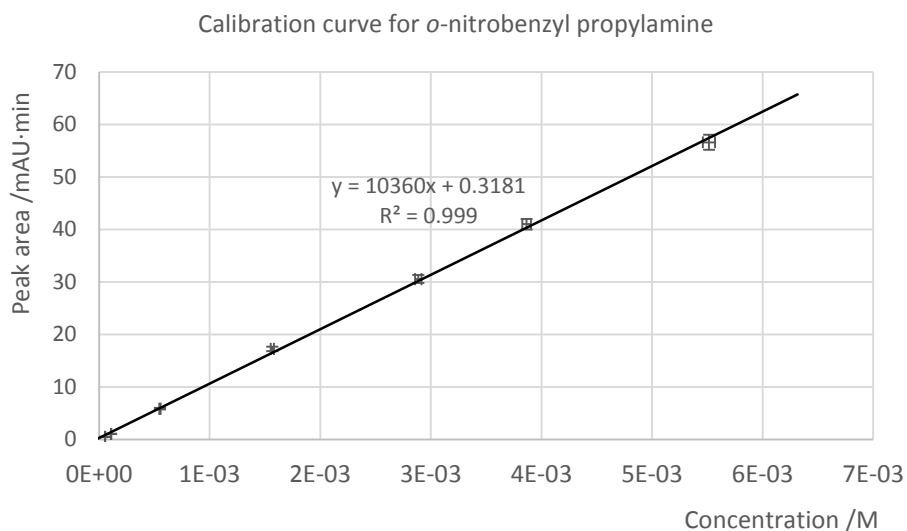


Figure 6.5. HPLC calibration curve for *o*-nitrobenzyl propylamine **14**.

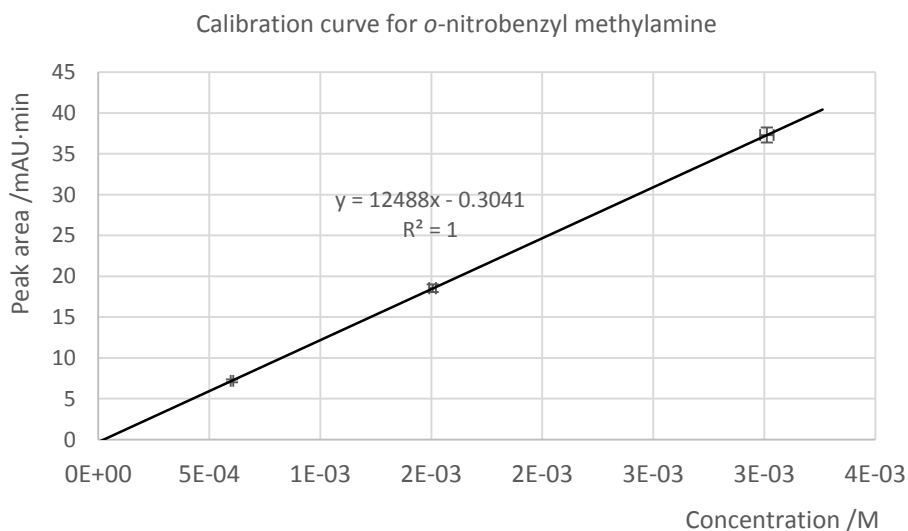


Figure 6.6. HPLC calibration curve for *o*-nitrobenzyl methylamine **2**.

6.5 Experiments with CO₂ adducts

6.5.1 Qualitative carbamate formation tests of benzylamines at ambient pressure

CO₂ was streamed through the solutions of benzyl amines in MTBE for 30 minutes at room temperature and atmospheric pressure, while phase changes were monitored. The volume of the reaction mixture was maintained by a continuous substitution of the evaporated solvent. If formation of precipitate was not observed, the experiments were repeated using diethyl ether and hexane solutions (Table 6.5).

Table 6.5. Qualitative CO₂ adduct formation tests of benzylamines, under atmospheric conditions.

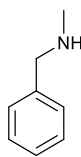
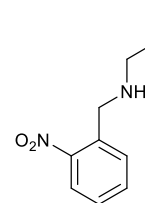
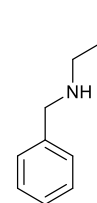
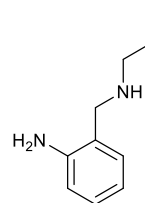
| Entry | Amine | Amine in system /g | Amine in system /mmol | Solvent | Observation |
|-------|---------------|-----------------------|--------------------------|--|-------------------------------------|
| 1 | 2 | 1.00 | 6.02 | MTBE (5 ml) | Precipitation of pale yellow solid |
| 2 | | | | MTBE (5 ml) | |
| 3 | 17 | 1.00 | 8.26 | (C ₂ H ₅) ₂ O (5 ml) | Precipitation of solid not observed |
| 4 | | | | Hexane (5 ml) | |
| 5 | 3 | 1.00 | 7.35 | MTBE (5 ml) | Precipitation of pale yellow solid |
| 6 | | | | MTBE (5 ml) | |
| 7 | 14 | 1.00 | 8.26 | (C ₂ H ₅) ₂ O (5 ml) | Precipitation of solid not observed |
| 8 | | | | Hexane (5 ml) | |
| 9 | | | | MTBE (5 ml) | |
| 10 | 32 | 1.00 | 8.26 | (C ₂ H ₅) ₂ O (5 ml) | Precipitation of solid not observed |
| 11 | | | | Hexane (5 ml) | |
| 12 | | | | MTBE (5 ml) | |
| 13 | 33 | 1.00 | 8.26 | (C ₂ H ₅) ₂ O (5 ml) | Precipitation of solid not observed |
| 14 | | | | Hexane (5 ml) | |

6.5.2 Qualitative carbamate formation tests of benzylamines at elevated pressures

The tested benzylamine was loaded into a high pressure view cell. The cell was purged with CO₂ (2.0 MPa) three times in order to remove the traces of air. Half of the reactor volume was loaded with liquid CO₂ and agitated by means of magnetic stirrer at 5.8 MPa and room temperature (24 °C) for 30 minutes, while phase changes were monitored. After 1 hour the cell was vented (Table 6.6). The showed pressures are gauge pressures. Detailed information can be found about the experimental set-up in Appendix - I.

The experiments were repeated at 10.0 MPa and 40 °C (Table 6.6).

Table 6.6. Qualitative CO₂ adduct formation tests of benzylamines at elevated pressures.

| | |  | |  | |  | |  | |
|-----------------|-------------------|---|------|---|------|---|------|---|------|
| | | 17 | | 14 | | 32 | | 33 | |
| Amine in system | /g /mmol | 0.50 4.13 | | 0.50 2.58 | | 0.50 3.36 | | 0.50 3.05 | |
| Pressure | /MPa | 5.8 | 10.0 | 5.8 | 10.0 | 5.8 | 10.0 | 5.8 | 10.0 |
| Temperature | /°C | 24 | 40 | 24 | 40 | 24 | 40 | 24 | 40 |
| Observation | | I.V. | I.V. | I.V. | T.G. | I.V. | I.V. | I.V. | T.G. |
| New IR peaks at | /cm ⁻¹ | 1547 ^a | | 1746 ^b | | 1675 ^a , 1619 ^c , 1406 ^a , 1307 ^c | | 1650 ^a | |

I.V.: Product increased in viscosity

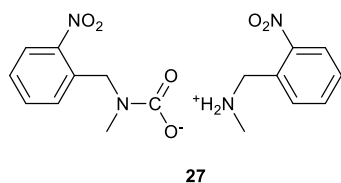
T.G.: Formation of thick gum was observed

^acarbamate absorption

^bcarbamic acid absorption

^cbicarbonate acid absorption

The amines regained their consistency within a day after exposure to air after venting.



6.5.3 *O*-Nitrobenzyl methylamine carbamate salt **27**; Synthesis by exposure to continuous flow of CO₂

Carbon dioxide was bubbled through the solution of *o*-nitrobenzyl methylamine **2** (2.00 g, 12.0 mmol) in MTBE (10 ml) for one hour. The amount of evaporated organic solvent was compensated to keep the volume near constant. Due to the evaporation of solvent and expansion of CO₂, the temperature of the reaction mixture decreased to

0 °C. Carbamate salt **27** precipitated as a pale yellow solid (1.40 g, 3.72 mmol, 62%). M.p.: 70-73 °C; found: C, 54.55; H, 5.35; N, 15.00%; C₁₇H₂₀N₄O₆ requires C, 54.25; H, 5.36; N, 14.89%; HMBC NMR spectrum can be seen below (Figure 6.7). *m/z* (ESI) 167.1 (100%, 1+M⁺); $\nu_{\max}/\text{cm}^{-1}$ (neat); 3333 (w, br.), 3071 (w), 2937 (m), 2850 (m), 2796 (m), 1644 (w), 1610 (w), 1577 (s), 1524 (s), 729 (s).

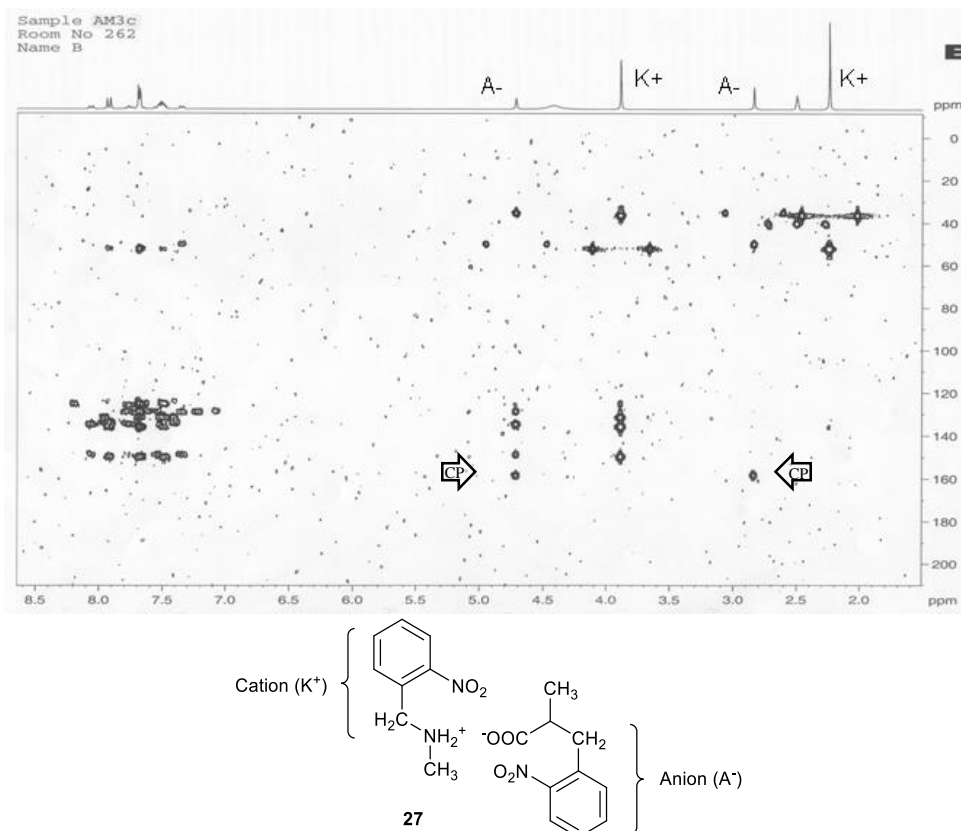


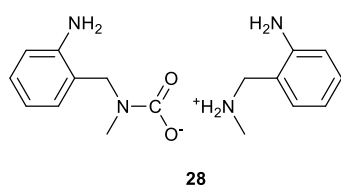
Figure 6.7. HMBC NMR spectrum of carbamate salt **27** (300/75 MHz, DMSO-*d*₆). Methyl and methylene hydrogen atoms of carbamate anion (A⁻) formed cross peaks with low field carbons.

6.5.4 *O*-Nitrobenzyl methylamine carbamate salt **27**; Synthesis by stirring in CO₂ atmosphere

Crude *o*-nitrobenzyl methylamine **2** (48.2 g crude, amount of **2**, assayed by HPLC: 95.1%, 45.8 g, 276 mmol) was dissolved in MTBE (243 ml). The solution was loaded into the experimental vessel. Having evacuated and rinsed with CO₂ three times, the reaction mixture was stirred in CO₂ atmosphere under atmospheric conditions. Precipitation of pale yellow solid occurred after 5 hours of stirring. The reaction was stopped after 16 hours. After filtration and drying in CO₂ enriched atmosphere, pale yellow solid was obtained (38.2 g, 101.6 mmol, 73.6%). Analytical data was identical to the above (6.5.3).

6.5.5 Synthesis of *o*-aminobenzyl methylamine **3** by the reduction of *o*-nitrobenzyl methylamine carbamate salt **27** starting material

Carbamate salt **27** (566 mg, 1.5 mmol) was dissolved in ethanol (30 ml) and catalyst (10% Pd on charcoal, 30 mg) was added. The system was evacuated and hydrogen gas was introduced. The purging procedure was repeated two more times. After stirring for 30 minutes the reaction mixture was filtered through Celite and concentrated *in vacuo* to give *o*-aminobenzyl methylamine **3** as light brown oil in nearly quantitative yield (384 mg, 2.82 mmol, 98%). The analytical data were identical to the data of alternative synthesis (6.3.4).



6.5.6 *O*-Aminobenzyl methylamine carbamate **28**

O-Aminobenzyl methylamine **3** (3.9 g, 28.7 mmol) was dissolved in MTBE (22 ml). The solution was loaded into the experimental vessel. Having evacuated and rinsed with CO₂ three times, the reaction mixture was stirred in CO₂ atmosphere under atmospheric conditions. Precipitation of colourless solid occurred within minutes while the temperature of reaction mixture slightly increased. The reaction was stopped after 1 hour. After filtration and drying, *o*-aminobenzyl methylamine carbamate salt **28** was obtained as colourless prisms (2.85 g, 9 mmol, 63%). M.p. 88-92 °C; found: C, 61.20; H, 7.80; N, 16.85%; C₁₇H₂₆N₄O₃ requires C, 61.06; H, 7.84; N, 16.76%; HMBC NMR can be seen below (Figure 6.8). *m/z* (ESI) 136.2 (100%, M⁺); $\nu_{\max}/\text{cm}^{-1}$ (NaCl); 3390 (s, br.), 3328 (s, br.), 3215 (s), 1642 (m), 1602 (m), 1497 (s), 1391 (m), 1272 (m), 741 (s); Crystal structure: Figure 6.9.

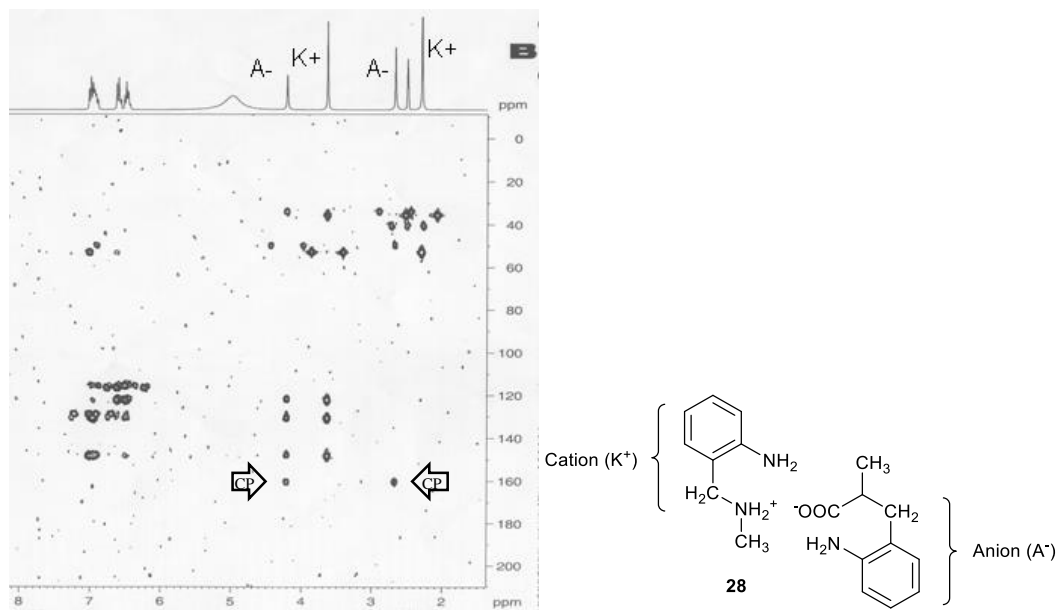


Figure 6.8. HMBC NMR spectrum of carbamate salt **28** (300/75 MHz, DMSO-*d*₆). Methyl and methylene hydrogen atoms of carbamate anion (A⁻) formed cross peaks with low field carbons.

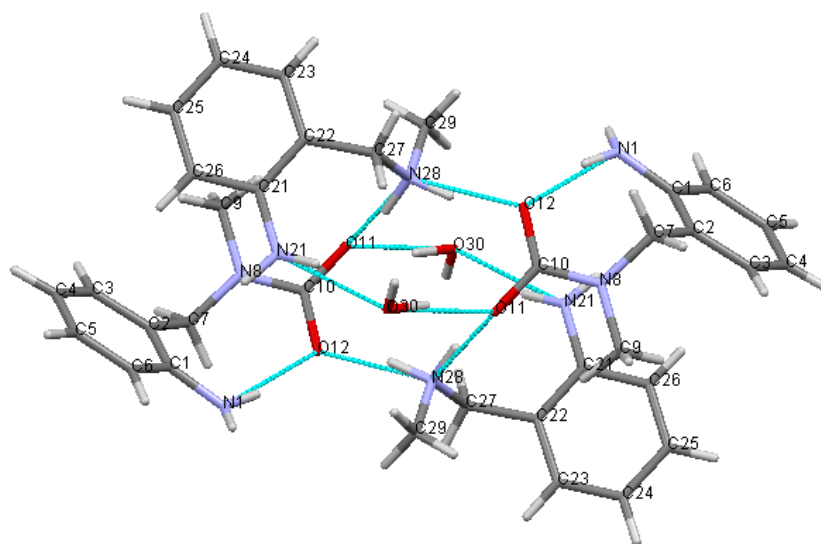
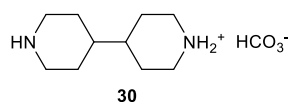


Figure 6.9. Crystal structure of *o*-aminobenzyl methylamine carbamate monohydrate **28**, crystallised as a monohydrate dimer. Further information about the X-ray crystallographic measurement is included in Appendix - II.



6.5.7 Bipiperidine bicarbonate **30**

A solution of bipiperidine **11** (286 mg, 1.70 mmol) in chloroform (5 ml) was exposed to a stream of CO₂ gas (0.25 l/min). Decrease of temperature was observed because of solvent evaporation, which was compensated by continuous addition of solvent. Precipitation of colourless solid was observed within minutes. The streaming of CO₂ was

stopped after 30 minutes. The solid was filtered off and washed with a small amount of solvent. The obtained piperidine bicarbonate **30** salt was dried in air (230 mg, 1.00 mmol, 58.8%). M.p. 170-172 °C; found: C, 57.05; H, 9.60; N, 12.10%; $C_{11}H_{22}N_2O_3$ requires C, 57.33; H, 9.63; N, 12.16%; HMBC NMR can be seen below (Figure 6.10). $\nu_{\max}/\text{cm}^{-1}$ (film); 3202 (m, br.), 1637 (s), 1560 (s, br.), 1408 (s), 1266 (s).

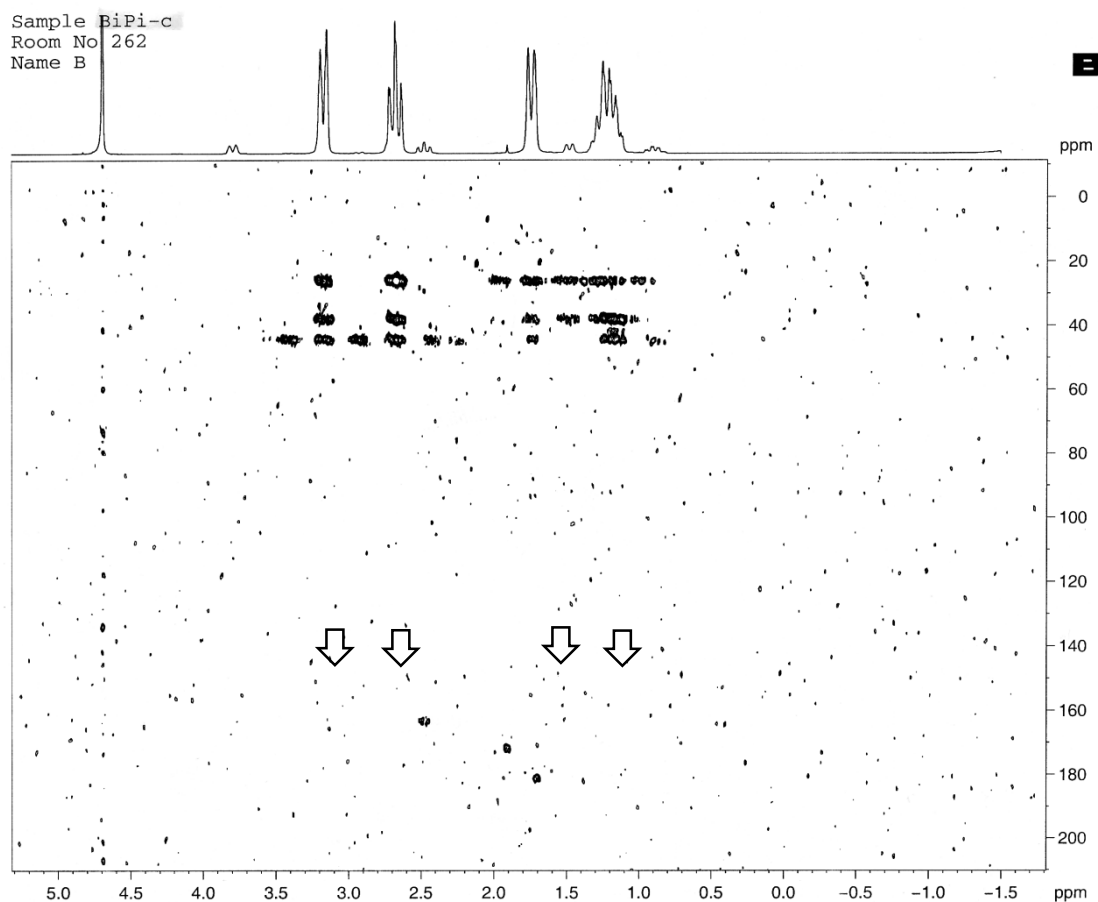


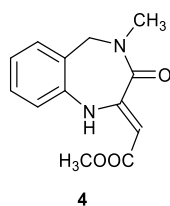
Figure 6.10. HMBC NMR spectrum of bipiperidine - CO₂ adduct. Main hydrogen atoms did not form cross peaks with low field carbon atoms.

6.5.8 Quantitative solubility test of *o*-nitrobenzyl methylamine **2** in MTBE + CO₂

O-Nitrobenzyl methylamine **2** (2.00 g) was dissolved in MTBE (6 ml). A stream of CO₂ saturated by solvent was bubbled through the solution. After five minutes, the solution turned opaque, and precipitation of pale yellow solid, *o*-nitrobenzyl methylamine carbamate salt **27**, started. The flow of CO₂ was stopped after 30 minutes, and the saturated liquid phase was sampled for analysis. The reaction mixture was diluted with MTBE (4 ml), saturated with CO₂ (15 minutes) and sampled. Another dilution with MTBE (17 ml) took place, and the procedure was repeated. The experiment was repeated at 0 °C using ice-bath. Experimental results are summarised (Table 6.7).

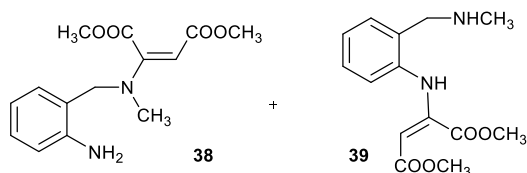
Table 6.7. Solubility *o*-nitrobenzyl methylamine carbamate **27** in MTBE at two different temperatures. The concentration of samples was measured by UV/Vis spectroscopy after dilution with alkaline aqueous ethanol (water:ethanol 6:4 vol, 0.01 M NaOH, $\lambda = 261$ nm, SBW = 3 nm). Barometer: 101.2 kPa.

| Temperature | Composition /wt% | Absorbance | Dilution | C _{sample} /M | C _{solution} /M | g/l |
|-------------|------------------|------------|----------|------------------------|--------------------------|-------|
| 0 °C | 10 | 0.456 | 417 | 8.56×10^{-05} | 0.027 | 4.44 |
| | 20 | 0.560 | 417 | 1.05×10^{-04} | 0.033 | 5.46 |
| | 30 | 0.666 | 417 | 1.25×10^{-04} | 0.039 | 6.50 |
| 24 °C | 10 | 1.576 | 315 | 2.97×10^{-04} | 0.124 | 20.56 |
| | 20 | 1.668 | 315 | 3.15×10^{-04} | 0.131 | 21.75 |
| | 30 | 1.729 | 315 | 3.26×10^{-04} | 0.136 | 22.54 |



6.5.9 Synthesis of benzodiazepine **4** from carbamate salt **28** starting material

A solution of DMAD **37** (0.90 g, 6.32 mmol, 2 equiv.) in methanol (2.0 ml) was introduced dropwise into the solution of *o*-aminobenzyl methylamine carbamate salt **28** (1.00 g, 3.16 mmol, 1 equiv.) in methanol (5 ml) while being cooled by ice bath (0-5 °C). After 90 minutes of stirring (0-5 °C), glacial acetic acid (50 mg, 0.85 mmol, 0.26 equiv.) was added, and the reaction mixture was heated under reflux for 3 hours. After cooling to 50 °C, a solution of CH₃ONa (2.26 mmol, 0.40 ml 30wt% solution, 0.72 equiv.) was added and the resulting solution was stirred under reflux for 2 hours. The reaction mixture was cooled to 50 °C, and glacial acetic acid (135 mg, 2.26 mmol, 0.72 equiv.) and water (8 ml) was added. Having stirred for one hour, the reaction mixture cooled down to 0-5 °C by ice bath, and stirred for 5 hours. The precipitated colourless solid was filtered out, washed with aqueous methanol (w:m=3:2), and dried in air to give benzodiazepine **4** as pale yellow needles (200 mg, 0.81 mmol, 13%). Analytical data obtained was identical with the product of the alternative synthesis (6.3.6).^[12]



6.5.10 Synthesis of the mixture of anilines **38** and **39** using *o*-aminobenzyl methylamine **3** starting material.

A solution of DMAD **37** (689 mg, 4.85 mmol, 1 equiv.) in methanol-*d*₄ (1.5 ml) was introduced into a solution of *o*-aminobenzyl methylamine **3** (660 mg, 4.85 mmol, 1 equiv.) in methanol-*d*₄ (3.5 ml) while being cooled by ice (0-5 °C). After 90 minutes the stirring was stopped, and sample was taken for NMR analysis. The ratio of isomers **38** and **39** was 1:0.75, according to ¹H-NMR integration of the benzyl protons at 4.25 ppm (**38**) and 4.31 ppm (**39**).^[12]

6.5.11 Synthesis of the mixture of anilines **38** and **39** using *o*-aminobenzyl methylamine carbamate salt **28** starting material, in CO₂ atmosphere.

A solution of DMAD **37** (689 mg, 4.85 mmol, 2 equiv.) in methanol-*d*₄ (1.5 ml) was introduced into a reaction vessel, cooled by ice bath (0-5 °C). The vessel was evacuated and filled with CO₂ three times. A solution of *o*-aminobenzyl methylamine carbamate **28** (766 mg, 2.43 mmol, 1 equiv.) in methanol-*d*₄ (3.5 ml) was added, and stirred in CO₂ atmosphere while being cooled by an ice bath (0-5 °C). After 90 minutes of stirring was stopped, and sample was taken for NMR analysis. The ratio of isomers **38** and **39** was 1:0.81, according to ¹H-NMR integration of the benzyl protons at 4.25 ppm (**38**) and 4.31 ppm (**39**).^[12] Multiplication of proton peaks was observed, indicating carbamate or bicarbonate salt of anilines **38** and **39** were present.^[83]

6.6 Carbamate stability tests

6.6.1 Qualitative stability experiments

O-Nitrobenzyl methylamine carbamate **27** (4×125 mg), prepared in procedure 6.5.4, was loaded into four sample vials.

Sample 1 left opened in a vial and exposed to air at room temperature. The pale yellow solid decomposed in 24 hours and formed a light brown oil which was identified as *o*-nitrobenzyl methylamine **2** by ¹H-NMR spectroscopy.

Sample 2 left in a closed vial at room temperature. It remained solid for longer than five days.

Sample 3 left in a closed vial at room temperature with a smaller vial filled with water. It remained solid for more than three days.

Sample 4 left in an evacuated vial at room temperature. The pale yellow solid decomposed in 48 hours and formed a light brown oil which was identified as *o*-nitrobenzyl methylamine **2** by $^1\text{H-NMR}$ spectroscopy.

6.6.2 Quantitative stability tests of *o*-nitrobenzyl methylamine carbamate salt **27**

O-Nitrobenzyl methylamine carbamate salt **27** (110 mg) was put on a scale in a Petri dish. A data recording system collated on-line data through the measurement, continuously recording and storing the actual weight (Figure 6.11). A constant flow of dry N_2 gas was applied to remove the evolving CO_2 . The instrument was constructed within our research group by Dr Guillaume Raynel.

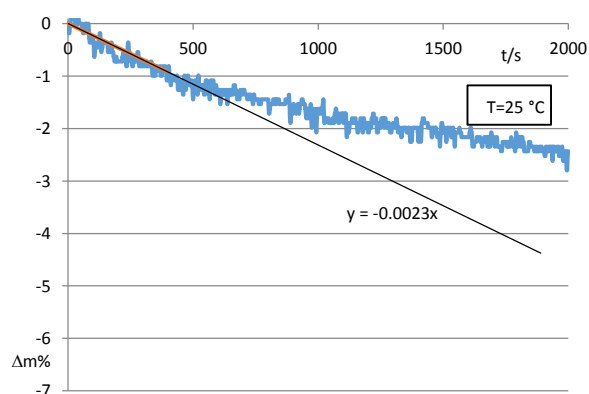


Figure 6.11. $\Delta\text{m}\%$ - t diagram of *o*-nitrobenzyl methylamine carbamate salt **27** at room temperature.

The weight loss of *o*-nitrobenzyl methylamine carbamate salt **27** (150 mg sample) was recorded at 30, 40 and 50 °C with a TGA instrument. The experimental results are shown below (Figure 6.13-6.14).

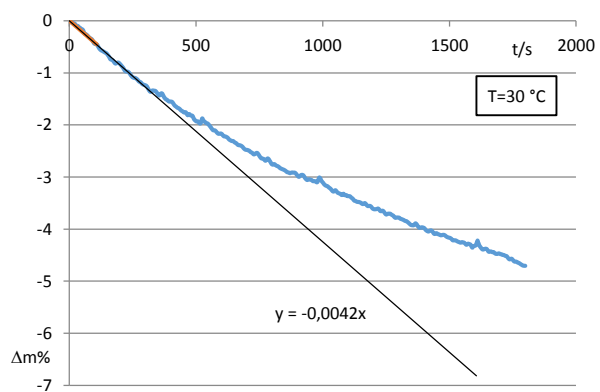


Figure 6.12. TGA trace of *o*-nitrobenzyl methylamine carbamate salt **27** at 30 °C.

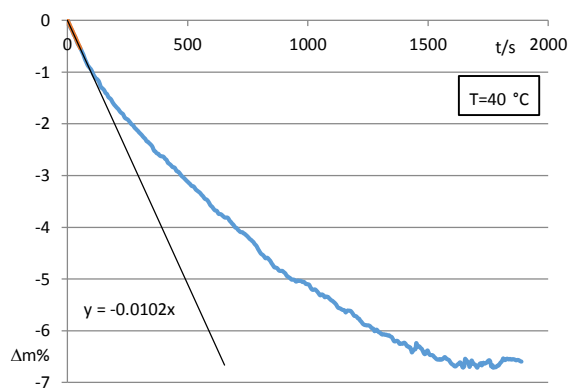


Figure 6.13. TGA trace of *o*-nitrobenzyl methylamine carbamate salt **27** at 40 °C.

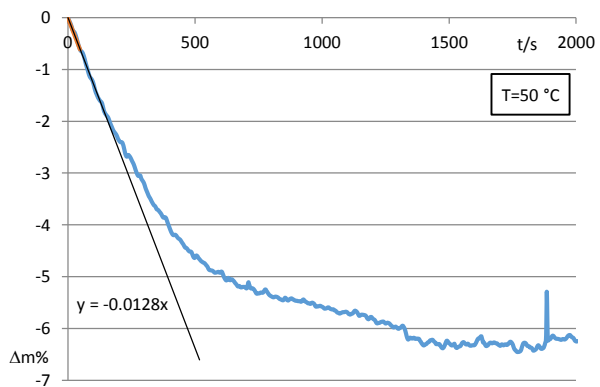


Figure 6.14. TGA trace of *o*-nitrobenzyl methylamine carbamate salt **27** at 50 °C.

6.7 Distribution tests of bases between organic and aqueous phases by preparative procedures - Screening

Preparation of stock solution

A stock solution of the tested bases was made as per Table 6.8-6.13. The primary solvent was MTBE. If the solubility was below 2wt%, other solvent was used, as noted.

Extraction with water

The stock solution (10 ml) was extracted into water (10 ml) by shaking in a separation funnel. The phases were allowed to separate, and the organic phase was dried (MgSO_4), filtered and concentrated, and the mass of recovered material was measured. The initial solute mass was calculated from the concentration and the mass of the used stock solution. The difference between the initial solute mass and the recovered mass is shown (Table 6.8-6.13).

Extraction with water + CO_2

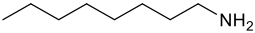
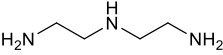
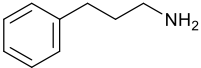
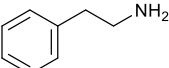
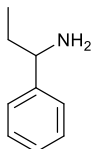
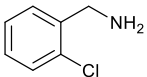
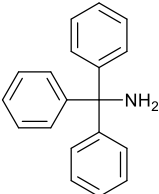
The stock solution (10 ml) was extracted into water (10 ml) while CO_2 was bubbled through the system for 15 minutes with a flowrate of 0.5 l/min. The flow of CO_2 was stopped, and the phases were allowed to separate. The organic phase was dried (MgSO_4), filtered and concentrated, and the mass of recovered material was measured. The initial solute mass was calculated from the concentration and the mass of the used stock solution. The difference between the initial solute mass and the recovered mass is shown (Table 6.8-6.13).

Extraction with aqueous HCl

The weight of the stock solution (10 ml) was measured, and mass of solute was calculated with the concentration of the stock solution. One equivalent of HCl was diluted to 10 ml, and used for the extraction of the stock solution by shaking in a separation funnel. The phases were allowed to separate, and the organic phase was dried (MgSO_4), filtered and concentrated, and the mass of recovered material was measured. The difference between the initial solute mass and the recovered mass is shown (Table 6.8-6.13).

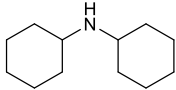
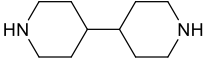
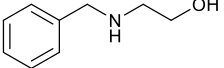
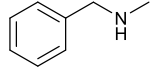
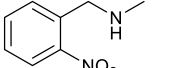
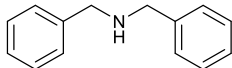
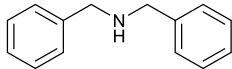
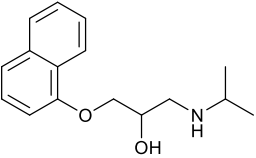
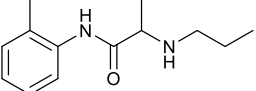
The experiments were carried out at room temperature and ambient pressure.

Table 6.8. Used solvents and stock solution concentrations of the tested primary amines, along with the results of the extraction experiments.

| Entry | Compound | Solvent | Conc. /wt% | Extracted by | | |
|-------|---|---------|------------|--------------|-------------------------|------------------|
| | | | | Water | Water + CO ₂ | Aq. HCl 1 equiv. |
| 1 |  <i>n</i> -octylamine | MTBE | 2.5 | 42% | 68% | 68% |
| 2 |  diethylenetriamine | MTBE | 2.5 | >95% | n.t. | n.t. |
| 3 |  3-phenylpropylamine | MTBE | 2.5 | 30% | >95% | >95% |
| 4 |  2-phenylethylamine | MTBE | 2.5 | 28% | >95% | >95% |
| 5 |  1-phenylpropan-1-amine | MTBE | 2.5 | 10% | 74% | >95% |
| 6 |  2-chlorobenzylamine | MTBE | 2.5 | <5% | 50% | 56% |
| 7 |  tritylamine | MTBE | 2.5 | <5% | 6% | >95% |

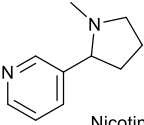
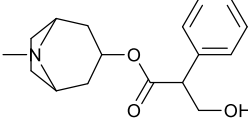
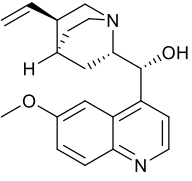
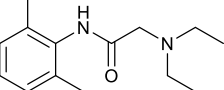
n.t.: not tested because of too high aqueous solubility

Table 6.9. Used solvents and stock solution concentrations of the tested secondary amines, along with the results of the extraction experiments.

| Entry | Compound | Solvent | Conc. /wt% | Extracted by | | |
|-------|--|-------------------|------------|--------------|-------------------------|------------------|
| | | | | Water | Water + CO ₂ | Aq. HCl 1 equiv. |
| 1 |  dicyclohexylamine | MTBE | 2.5 | 10% | 68% | >95% |
| 2 |  biperidine 11 | CHCl ₃ | 3.0 | 33% | >95% | n.t. |
| 3 |  N-benzylethanolamine | MTBE | 2.5 | 37% | >95% | >95% |
| 4 |  methyl benzylamine | MTBE | 2.5 | 26% | 74% | 74% |
| 5 |  methyl nitrobenzylamine 2 | MTBE | 5.0 | 36% | 87% | 94% |
| 6 |  dibenzylamine | MTBE | 2.5 | <5% | <5% | 53% |
| 7 |  dibenzylamine | Hex | 2.5 | <5% | <5% | 67% |
| 8 |  Propranolol 18 | MTBE | 2.6 | 23% | 84% | >95% |
| 9 |  Prilocaine 19 | MTBE | 2.6 | 41% | 52% | >95% |

n.t.: not tested because of high extraction with water +CO₂

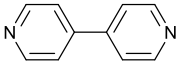
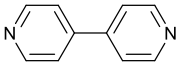
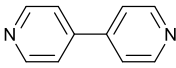
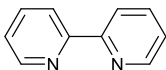
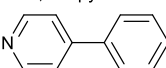
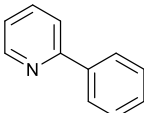
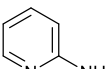
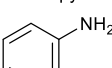
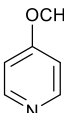
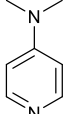
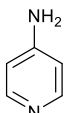
Table 6.10. Used solvents and stock solution concentrations of the tested tertiary amines, along with the results of the extraction experiments.

| Entry | Compound | Solvent | Conc. /wt% | Extracted by | | |
|-------|--|---------------------------------|------------|--------------|-------------------------|------------------|
| | | | | Water | Water + CO ₂ | Aq. HCl 1 equiv. |
| 1 |  Quinuclidine | MTBE | 5.0 | 61% | >95% | >95% |
| 2 |  DABCO | MTBE | 2.5 | >95% | n.t. | n.t. |
| 3 |  Nicotine | MTBE | 2.6 | 53% | >95% | >95% |
| 4 |  Atropine | EtOAc | 2.9 | 28% | >95% | >95% |
| 5 |  Quinine | CH ₂ Cl ₂ | 5.3 | 12% | precip. | 14% |
| 6 |  Lidocaine 20 | MTBE | 2.4 | 31% | 60% | >95% |

n.t.: not tested because of too high aqueous solubility

precip.: precipitation of colourless solid was observed; experiment halted

Table 6.11. Used solvents and stock solution concentrations of the tested pyridines, along with the results of the extraction experiments.

| Entry | Compound | Solvent | Conc. /wt% | Extracted by | | |
|-------|--|-------------------|------------|--------------|-------------------------|------------------|
| | | | | Water | Water + CO ₂ | Aq. HCl 1 equiv. |
| 1 |  4,4'-bipyridine 9 | MTBE | 2.5 | Precip. | | >95% |
| 2 |  4,4'-bipyridine 9 | EtOAc | 2.5 | 17% | 17% | >95% |
| 3 |  4,4'-bipyridine 9 | CHCl ₃ | 2.5 | 5% | 27% | >95% |
| 4 |  2,2'-bipyridine | MTBE | 2.5 | 16% | 16% | >95% |
| 5 |  4-phenylpyridine | MTBE | 2.5 | 5% | 5% | >95% |
| 6 |  2-phenylpyridine | MTBE | 2.5 | 5% | 5% | 74% |
| 7 |  <i>o</i> -aminopyridine | MTBE | 2.5 | 44% | 55% | >95% |
| 8 |  <i>m</i> -aminopyridine | MTBE | 2.5 | 58% | 63% | >95% |
| 9 |  <i>o</i> -methoxypyridine | MTBE | 2.6 | 73% | 73% | >95% |
| 10 |  <i>p</i> -dimethylaminopyridine | EtOAc | 3.6 | <5% | >95% | 84% |
| 11 |  aminopyridine | EtOAc | 0.9 | 76 | >95% | >95% |

precip.: precipitation of colourless solid was observed, experiment halted

Table 6.12. Used solvents and stock solution concentrations of the tested anilines, along with the results of the extraction experiments.

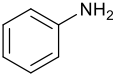
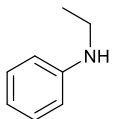
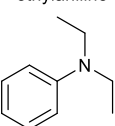
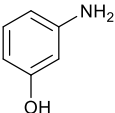
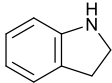
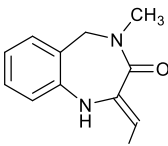
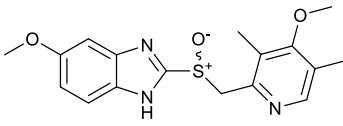
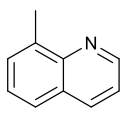
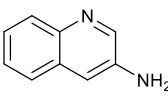
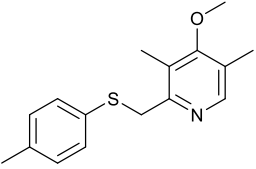
| Entry | Compound | Solvent | Conc. /wt% | Extracted by | | |
|-------|--|---------|------------|--------------|-------------------------|------------------|
| | | | | Water | Water + CO ₂ | Aq. HCl 1 equiv. |
| 1 |  aniline | MTBE | 5.0 | 10% | 10% | >95% |
| 2 |  ethylaniline | MTBE | 2.0 | <5% | 13% | 73% |
| 3 |  diethylaniline | MTBE | 2.0 | <5% | <5% | 53% |
| 4 |  <i>m</i> -aminophenol | MTBE | 2.0 | 47% | 54% | 93% |

Table 6.13. Used solvents and stock solution concentrations of the tested heterocycles, along with the results of the extraction experiments.

| Entry | Compound | Solvent | Conc. /wt% | Extracted by | | |
|-------|---|-------------------|------------|--------------|-------------------------|------------------|
| | | | | Water | Water + CO ₂ | Aq. HCl 1 equiv. |
| 1 |  Indoline | MTBE | 10.0 | <5% | <5% | 68% |
| 2 |  benzodiazepine 4 | MTBE | 2.3 | 21% | 20% | 26% |
| 3 |  Omeprazole 21 | CHCl ₃ | 2.5 | 9% | 9% | 88% |
| 4 |  8-methylquinoline | MTBE | 4.0 | <5% | <5% | >95% |
| 5 |  3-aminoquinoline | MTBE | 5.0 | 34% | 21% | >95% |
| 6 |  sulfanylmethylpyridine | MTBE | 2.5 | 10% | 10% | 79% |

6.8 Distribution tests of bases between organic and aqueous phases under ambient conditions – Detailed studies

Unless stated otherwise, the experiments were carried out at room temperature and ambient pressure. The taken samples were diluted with alkalified aqueous ethanol (ethanol:water 4:6 vol, 0.01 M NaOH in water).

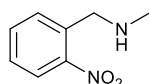
6.8.1 Distribution before CO₂ exposure

Solution of base in MTBE was prepared, and stirred vigorously with the same volume of water. The phases were allowed to separate, and samples were taken from the co-existing phases. The samples were diluted and assayed by UV/Vis spectroscopy or HPLC.

The distribution was also tested in more dilute systems. The two phase system was diluted by the addition of water and MTBE, and the procedure was repeated at several concentrations. The experimental vessels were 10, 25, 50, 100, 250, and 500 ml measuring cylinders for the experiments at 30, 20, 10, 5, 2.5 and 1wt% nominal concentrations, respectively. A *K* partitioning coefficient was calculated with Eq.28 (Table 6.14-6.18).

$$K = \frac{c_{org}}{c_{aq}} \quad \text{Eq.28}$$

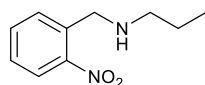
Table 6.14. Distribution data of *o*-nitrobenzyl methylamine **2** between water and MTBE under ambient conditions at various concentrations are presented below. The amount of amine in the system was 1.00 g (6.02 mmol). The amount of solvent in the system (MTBE and water) is shown. The samples taken from the phases in equilibrium were diluted, and an absorbance was measured by UV/Vis spectroscopy ($\lambda = 261$ nm, SBW = 3 nm, measurement time: 3 s).



o-nitrobenzyl methylamine **2**

| Nominal concentration: /wt% | | 30 | 20 | 10 | 5 | 2.5 | 1 |
|-----------------------------|-------------------|------------------------|------------------------|------------------------|------------------------|------------------------|------------------------|
| Organic phase | Volume: /ml | 3 | 5 | 12 | 26 | 53 | 133 |
| | Absorbance: | 1.470 | 1.480 | 1.571 | 1.762 | 1.587 | 1.001 |
| | Dilution: | 5000 | 3333 | 1667 | 833 | 417 | 167 |
| | Concentration: /M | 1.385 | 0.930 | 0.494 | 0.277 | 0.125 | 0.031 |
| Aqueous phase | Volume: /ml | 3 | 5 | 12 | 26 | 53 | 133 |
| | Absorbance: | 0.085 | 1.092 | 1.073 | 1.012 | 0.873 | 0.359 |
| | Dilution: | 500 | 333 | 167 | 83.3 | 50 | 50 |
| | Concentration: /M | 7.82×10 ⁻⁰³ | 6.86×10 ⁻⁰² | 3.37×10 ⁻⁰² | 1.59×10 ⁻⁰² | 8.22×10 ⁻⁰³ | 3.37×10 ⁻⁰³ |
| | <i>K</i> (Eq.28): | 177.07 | 13.56 | 14.66 | 17.44 | 15.17 | 9.34 |

Table 6.15 Distribution data of *o*-nitrobenzyl propylamine **14** between water and MTBE under ambient conditions at various concentrations are presented below. The amount of amine in the system was 1.00 g (5.15 mmol). The amount of solvent in the system (MTBE and water) is shown. The samples taken from the phases in equilibrium were diluted, and assayed by HPLC (eluent: aq. ammonia (0.1wt%) + acetonitrile; gradient: 5 to 95% in 5.00 min; retention time: 2.65 min, detector channel: DAD signal A, 220 nm).

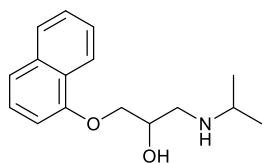


o-nitrobenzyl propylamine **14**

| Nominal concentration: /wt% | | 30 | 20 | 10 | 5 |
|-----------------------------|-------------------------|------------------------|------------------------|------------------------|------------------------|
| Organic phase | Volume: /ml | 3 | 5 | 12 | 26 |
| | Area: /mAU·min | 23.19 | 19.03 | 25.05 | 10.68 |
| | Dilution ^a : | 500 | 333 | 200 | 200 |
| | Concentration: /M | 1.111 | 0.608 | 0.48 | 0.205 |
| Aqueous phase | Volume: /ml | 3 | 5 | 12 | 26 |
| | Area: /mAU·min | 1.67 | 1.14 | 1.49 | 0.76 |
| | Dilution ^a : | 50 | 50 | 25 | 25 |
| | Concentration: /M | 7.98×10^{-03} | 5.45×10^{-03} | 3.57×10^{-03} | 1.82×10^{-03} |
| <i>K</i> (Eq.28): | | 139.1 | 111.5 | 134.4 | 112.6 |

^aDiluted with absolute ethanol

Table 6.16. Distribution data of Propranolol **18** between water and MTBE under ambient conditions at various concentrations are presented below. The amount of amine in the system was 640 mg (2.47 mmol). The amount of solvent in the system (MTBE and water) is shown. The samples taken from the phases in equilibrium were diluted, and an absorbance was measured by UV/Vis spectroscopy ($\lambda = 291.9$ nm, SBW = 2 nm, measurement time: 3 s).

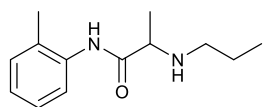


Propranolol **18**

| Nominal concentration: /wt% | | 30 | 20 | 10 | 5 | 2.5 | 1 |
|-----------------------------|-------------------|-------------------|-------------------|------------------------|------------------------|------------------------|------------------------|
| Organic phase | Volume: /ml | | | 8 | 17 | 35 | 89 |
| | Absorbance: | n.t. ^a | n.t. ^a | 0.765 | 0.857 | 0.934 | 0.971 |
| | Dilution: | | | 1250 | 625 | 333 | 133 |
| | Concentration: /M | | | 0.162 | 0.091 | 0.053 | 0.022 |
| Aqueous phase | Volume: /ml | | | 8 | 17 | 35 | 89 |
| | Absorbance: | n.t. ^a | n.t. ^a | 0.012 | 0.010 | 0.007 | 0.006 |
| | Dilution: | | | 1250 | 625 | 333 | 133 |
| | Concentration: /M | | | 3.05×10^{-03} | 1.31×10^{-03} | 5.70×10^{-04} | 2.01×10^{-04} |
| <i>K</i> (Eq.28): | | | | 53.32 | 69.30 | 92.77 | 109.40 |

^anot tested because of low solubility

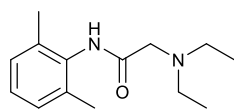
Table 6.17. Distribution data of Prilocaine **19** between water and MTBE under ambient conditions at various concentrations are presented below. The amount of amine in the system was 649 mg (2.95 mmol). The amount of solvent in the system (MTBE and water) is shown. The samples taken from the phases in equilibrium were diluted, and an absorbance was measured by UV/Vis spectroscopy ($\lambda = 230.6$ nm, SBW = 2 nm, measurement time: 3 s).



Prilocaine **19**

| Nominal concentration: /wt% | | 30 | 20 | 10 | 5 | 2.5 | 1 |
|-----------------------------|-------------------|----------------------------|----------------------------|----------------------------|----------------------------|----------------------------|----------------------------|
| Organic phase | Volume: /ml | 2 | 3.5 | 8 | 17 | 35 | 89 |
| | Absorbance: | 1.479 | 1.992 | 1.746 | 1.834 | 1.780 | 1.522 |
| | Dilution: | 4000 | 2500 | 1250 | 625 | 333 | 133 |
| | Concentration: /M | 0.923 | 0.778 | 0.341 | 0.179 | 0.093 | 0.032 |
| Aqueous phase | Volume: /ml | 2 | 3.5 | 8 | 17 | 35 | 89 |
| | Absorbance: | 0.020 | 0.025 | 0.043 | 0.071 | 0.051 | 0.049 |
| | Dilution: | 4000 | 2500 | 1250 | 625 | 333 | 133 |
| | Concentration: /M | 1.06× 10 ⁻⁰² | 8.76× 10 ⁻⁰³ | 7.76× 10 ⁻⁰³ | 6.69× 10 ⁻⁰³ | 2.52× 10 ⁻⁰³ | 9.65× 10 ⁻⁰⁴ |
| <i>K</i> (Eq.28): | | 86.81 | 88.81 | 43.91 | 26.77 | 36.72 | 32.81 |

Table 6.18. Distribution data of Lidocaine **20** between water and MTBE under ambient conditions at various concentrations are presented below. The amount of amine in the system was 660 mg (2.82 mmol). The amount of solvent in the system (MTBE and water) is shown. The samples taken from the phases in equilibrium were diluted, and an absorbance was measured by UV/Vis spectroscopy ($\lambda = 214.5$ nm, SBW = 2 nm, measurement time: 3 s).



Lidocaine **20**

| Nominal concentration: /wt% | | 30 | 20 | 10 | 5 | 2.5 | 1 |
|-----------------------------|-------------------|----------------------------|----------------------------|----------------------------|----------------------------|----------------------------|----------------------------|
| Organic phase | Volume: /ml | 2 | 3.5 | 8 | 17 | 35 | 89 |
| | Absorbance: | 0.848 | 0.804 | 0.860 | 0.637 | 0.673 | 0.247 |
| | Dilution: | 500 | 333 | 178.57 | 100 | 50 | 50 |
| | Concentration: /M | 1.190 | 0.752 | 0.431 | 0.179 | 0.094 | 0.035 |
| Aqueous phase | Volume: /ml | 2 | 3.5 | 8 | 17 | 35 | 89 |
| | Absorbance: | 0.008 | 0.010 | 0.016 | 0.017 | 0.015 | 0.008 |
| | Dilution: | 500 | 333 | 178.57 | 100 | 50 | 50 |
| | Concentration: /M | 1.50× 10 ⁻⁰² | 1.11× 10 ⁻⁰² | 9.14× 10 ⁻⁰³ | 5.26× 10 ⁻⁰³ | 2.45× 10 ⁻⁰³ | 1.46× 10 ⁻⁰³ |
| <i>K</i> (Eq.28): | | 79.48 | 67.76 | 47.09 | 34.02 | 38.59 | 23.94 |

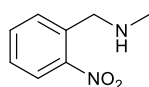
6.8.2 Distribution after CO₂ exposure

A solution of base in MTBE was stirred vigorously with water. CO₂ was introduced into the system through a sparger. The stream of CO₂ was saturated with organic solvent before entering the reaction vessel. The sparger was immersed into the aqueous phase.

The flow of CO₂ was kept constant for 15 minutes (0.5 l/min), and stopped. The phases were allowed to separate, and samples were taken from the co-existing phases. The samples were diluted and assayed by UV/Vis spectroscopy or HPLC.

The distribution was also tested in more dilute systems. The two phase system was diluted by the addition of water and MTBE, and the procedure was repeated at several concentrations. A *K* partitioning coefficient was calculated Eq.28 (Table 6.19-6.23).

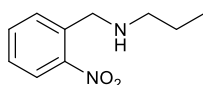
Table 6.19. Distribution data of *o*-nitrobenzyl methylamine **2** between water and MTBE after CO₂ saturation under ambient conditions at various concentrations are presented below. The amount of amine in the system was 1.00 g (6.02 mmol). The amount of solvent in the system (MTBE and water) is shown. The samples taken from the phases in equilibrium were diluted, and an absorbance was measured by UV/Vis spectroscopy ($\lambda = 261$ nm, SBW = 3 nm, measurement time: 3 s).



o-nitrobenzyl methylamine **2**

| Nominal concentration: /wt% | | 30 | 20 | 10 | 5 | 2.5 | 1 |
|-----------------------------|-------------------|----------------------------|----------------------------|----------------------------|----------------------------|----------------------------|----------------------------|
| Organic phase | Volume: /ml | 3 | 5 | 12 | 26 | 53 | 133 |
| | Absorbance: | 1.541 | 2.134 | 2.276 | 1.931 | 1.154 | 0.309 |
| | Dilution: | 500 | 333 | 179 | 100 | 50 | 50 |
| | Concentration: /M | 1.45× 10 ⁻⁰¹ | 1.34× 10 ⁻⁰¹ | 7.15× 10 ⁻⁰² | 3.04× 10 ⁻⁰² | 1.09× 10 ⁻⁰² | 2.89× 10 ⁻⁰³ |
| Aqueous phase | Volume: /ml | 3 | 5 | 12 | 26 | 53 | 133 |
| | Absorbance: | 1.158 | 1.272 | 1.098 | 0.957 | 1.029 | 1.178 |
| | Dilution: | 5000 | 3333 | 1667 | 833 | 417 | 167 |
| | Concentration: /M | 1.091 | 0.799 | 0.345 | 0.150 | 0.081 | 0.037 |
| <i>K</i> (Eq.28): | | 0.133 | 0.168 | 0.207 | 0.202 | 0.135 | 0.078 |

Table 6.20. Distribution data of *o*-nitrobenzyl propylamine **14** between water and MTBE after CO₂ saturation under ambient conditions at various concentrations are presented below. The amount of amine in the system was 1.00 g (5.15 mmol). The amount of solvent in the system (MTBE and water) is shown. The samples taken from the phases in equilibrium were diluted, and assayed by HPLC (eluent: aq. ammonia (0.1wt%) + acetonitrile; gradient: 5 to 95% in 5.00 min; retention time: 2.65 min, detector channel: DAD signal A, 220 nm).

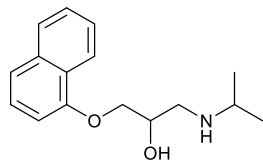


o-nitrobenzyl propylamine **14**

| Nominal concentration: /wt% | | 30 | 20 | 10 | 5 | 1 |
|-----------------------------|-------------------------|----------------------------|----------------------------|----------------------------|----------------------------|----------------------------|
| Organic phase | Volume: /ml | 2 | 3.5 | 8 | 17 | 35 |
| | Area: /mAU·min | 168.52 | 104.67 | 38.31 | 25.22 | 2.98 |
| | Dilution ^a : | 50 | 50 | 50 | 25 | 25 |
| | Concentration: /M | 0.807 | 0.501 | 0.183 | 0.06 | 0.007 |
| Aqueous phase | Volume: /ml | 2 | 3.5 | 8 | 17 | 35 |
| | Area: /mAU·min | 4.85 | 6.52 | 9.38 | 4.89 | 4.29 |
| | Dilution ^a : | 500 | 333 | 200 | 200 | 50 |
| | Concentration: /M | 2.32× 10 ⁻⁰¹ | 2.08× 10 ⁻⁰¹ | 1.80× 10 ⁻⁰¹ | 9.37× 10 ⁻⁰² | 2.05× 10 ⁻⁰² |
| <i>K</i> (Eq.28): | | 3.473 | 2.408 | 1.021 | 0.645 | 0.347 |

^aDiluted with absolute ethanol

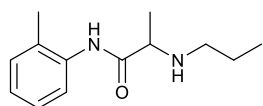
Table 6.21. Distribution data of Propranolol **18** between water and MTBE after CO₂ saturation under ambient conditions at various concentrations are presented below. The amount of amine in the system was 642 mg (2.48 mmol). The amount of solvent in the system (MTBE and water) is shown. The samples taken from the phases in equilibrium were diluted, and an absorbance was measured by UV/Vis spectroscopy ($\lambda = 291.9$ nm, SBW = 2 nm, measurement time: 3 s).



Propranolol **18**

| Nominal concentration: /wt% | | 30 | 20 | 10 | 5 | 2.5 | 1 |
|-----------------------------|-------------------|----------------------------|----------------------------|----------------------------|----------------------------|----------------------------|----------------------------|
| Organic phase | Volume: /ml | 2 | 3.5 | 8 | 17 | 35 | 89 |
| | Absorbance: | 0.138 | 0.144 | 0.263 | 0.348 | 0.285 | 0.161 |
| | Dilution: | 4000 | 2500 | 1250 | 625 | 333 | 133 |
| | Concentration: /M | 9.53× 10 ⁻⁰² | 6.22× 10 ⁻⁰² | 5.61× 10 ⁻⁰² | 3.71× 10 ⁻⁰² | 1.62× 10 ⁻⁰² | 3.69× 10 ⁻⁰³ |
| Aqueous phase | Volume: /ml | 2 | 3.5 | 8 | 17 | 35 | 89 |
| | Absorbance: | 0.908 | 1.116 | 1.021 | 0.847 | 0.826 | 0.895 |
| | Dilution: | 4000 | 2500 | 1250 | 625 | 333 | 133 |
| | Concentration: /M | 0.617 | 0.473 | 0.217 | 0.090 | 0.047 | 0.020 |
| <i>K</i> (Eq.28): | | 0.866 | 0.884 | 0.794 | 0.708 | 0.742 | 0.846 |

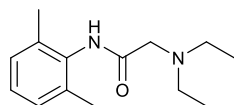
Table 6.22. Distribution data of Prilocaine **19** between water and MTBE after CO₂ saturation under ambient conditions at various concentrations are presented below. The amount of amine in the system was 643 mg (2.92 mmol). The amount of solvent in the system (MTBE and water) is shown. The samples taken from the phases in equilibrium were diluted, and an absorbance was measured by UV/Vis spectroscopy ($\lambda = 230.6$ nm, SBW = 2 nm, measurement time: 3 s).



Prilocaine **19**

| Nominal concentration: /wt% | | 30 | 20 | 10 | 5 | 2.5 | 1 |
|-----------------------------|-------------------|-------|-------|-------|-------|-------|-------|
| Organic phase | Volume: /ml | 2 | 3.5 | 8 | 17 | 35 | 89 |
| | Absorbance: | 1.055 | 0.910 | 0.821 | 0.718 | 0.684 | 0.526 |
| | Dilution: | 4000 | 2500 | 1250 | 625 | 333 | 133 |
| | Concentration: /M | 0.658 | 0.355 | 0.160 | 0.070 | 0.036 | 0.011 |
| Aqueous phase | Volume: /ml | 2 | 3.5 | 8 | 17 | 35 | 89 |
| | Absorbance: | 0.191 | 0.251 | 0.344 | 0.484 | 0.590 | 0.680 |
| | Dilution: | 4000 | 2500 | 1250 | 625 | 333 | 133 |
| | Concentration: /M | 0.118 | 0.097 | 0.067 | 0.047 | 0.031 | 0.014 |
| <i>K</i> (Eq.28): | | 5.592 | 3.649 | 2.396 | 1.486 | 1.160 | 0.773 |

Table 6.23. Distribution data of Lidocaine **20** between water and MTBE after CO₂ saturation under ambient conditions at various concentrations are presented below. The amount of amine in the system was 660 mg (2.82 mmol). The amount of solvent in the system (MTBE and water) is shown. The samples taken from the phases in equilibrium were diluted, and an absorbance was measured by UV/Vis spectroscopy ($\lambda = 214.5$ nm, SBW = 2 nm, measurement time: 3 s).



Lidocaine **20**

| Nominal concentration: /wt% | | 30 | 20 | 10 | 5 | 2.5 | 1 |
|-----------------------------|-------------------|-------|-------|-------|-------|-------|-------|
| Organic phase | Volume: /ml | 2 | 3.5 | 8 | 17 | 35 | 89 |
| | Absorbance: | 0.667 | 0.588 | 0.540 | 0.499 | 0.491 | 0.141 |
| | Dilution: | 500 | 333 | 179 | 100 | 50 | 50 |
| | Concentration: /M | 0.936 | 0.550 | 0.271 | 0.140 | 0.069 | 0.020 |
| Aqueous phase | Volume: /ml | 2 | 3.5 | 8 | 17 | 35 | 89 |
| | Absorbance: | 0.076 | 0.104 | 0.143 | 0.170 | 0.198 | 0.114 |
| | Dilution: | 500 | 333 | 179 | 100 | 50 | 50 |
| | Concentration: /M | 0.109 | 0.099 | 0.072 | 0.048 | 0.028 | 0.016 |
| K (Eq.28): | | 0.105 | 0.153 | 0.211 | 0.256 | 0.289 | 0.448 |

6.9 Distribution tests of bases between aqueous and organic phases during the course of N₂ gas induced decarboxylation

Unless stated otherwise, the experiments were carried out at room temperature and ambient pressure. The taken samples were diluted with alkalified aqueous ethanol (ethanol:water 4:6 vol, 0.01 M NaOH in water).

Distribution before CO₂ exposure

Solution of base in MTBE (13 ml) was stirred vigorously with water (13 ml) in the experimental vessel at room temperature. The phases were allowed to separate, and samples were taken from the co-existing phases. The samples were diluted and assayed by UV/Vis spectroscopy or HPLC (Entry 1, Table 6.24-6.35).

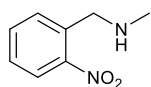
Distribution after CO₂ saturation

CO₂ was introduced into the amine-MTBE-water system through a sparger at ambient pressure and temperature. The stream of CO₂ was saturated with organic solvent before entering the reaction vessel. The sparger was immersed into the aqueous phase. The flow of CO₂ was kept constant (0.5 l/min) for 15 minutes, and stopped. The phases were allowed to separate, and samples were taken from the co-existing phases. The samples were diluted assayed by UV/Vis spectroscopy or HPLC (Entry 2, Table 6.24-6.35).

Distribution during the course of N₂ gas induced decarboxylation

N₂ gas was introduced into the experimental vessel through a sparger at ambient pressure and temperature. The stream of N₂ gas was saturated with organic solvent before entering the reaction vessel. The sparger was immersed into the aqueous phase. The flow of N₂ gas was kept constant. After a certain period of time, the introduction of N₂ gas was suspended by removal of the sparger. The phases were allowed to separate, and samples were taken from the co-existing phases. The flow of N₂ gas was resumed after sampling. The collected samples were diluted, and assayed by UV/Vis spectroscopy or HPLC (Entries 3-7, Table 6.24-6.35).

| | | |
|-------------|-------------------------------|--------------------|
| Table 6.24. | Amount of amine: | 245 mg (1.48 mmol) |
| | Amount of water & MTBE: | 13 + 13 ml |
| | Characteristic concentration: | 2.5wt% |
| | N ₂ gas flowrate: | 0.14 l/min |
| | Dilution after sampling: | 417 |
| | Wavelength: | 261 nm |
| | SBW: | 3 nm |
| | Measurement time: | 3 s |



o-nitrobenzyl methylamine 2

| Entry | N ₂ gas bubbling time /min | A _{org} | C _{org} /M | A _{aq} | C _{aq} /M | K Eq.28 |
|-------|---------------------------------------|------------------|---------------------|-----------------|--------------------|---------|
| 1 | Before CO ₂ saturation | 1.421 | 0.112 | 0.091 | 0.007 | 16.060 |
| 2 | CO ₂ saturation | 0.105 | 0.008 | 1.003 | 0.079 | 0.102 |
| 3 | 5 | 0.374 | 0.029 | 0.789 | 0.062 | 0.472 |
| 4 | 15 | 0.618 | 0.048 | 0.561 | 0.044 | 1.102 |
| 5 | 30 | 0.822 | 0.064 | 0.377 | 0.029 | 2.191 |
| 6 | 60 | 0.960 | 0.075 | 0.241 | 0.019 | 4.024 |
| 7 | 120 | 1.020 | 0.080 | 0.153 | 0.012 | 6.770 |

Table 6.25.

Amount of amine: 499 mg (3.01 mmol)

Amount of water & MTBE: 13 + 13 ml

Characteristic concentration: 5wt%

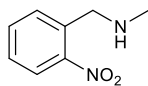
N₂ gas flowrate: 0.14 l/min

Dilution after sampling: 1667

Wavelength: 261 nm

SBW: 3 nm

Measurement time: 3 s



o-nitrobenzyl methylamine 2

| Entry | N ₂ gas bubbling time /min | A _{org} | C _{org} /M | A _{aq} | C _{aq} /M | K Eq.28 |
|-------|---------------------------------------|--------------------|---------------------|--------------------|--------------------|---------|
| 1 | Before CO ₂ saturation | 1.354 ^a | 0.213 | 0.952 ^b | 0.015 | 14.231 |
| 2 | CO ₂ saturation | 1.877 ^b | 0.029 | 1.062 ^a | 0.167 | 0.177 |
| 3 | 5 | 0.259 | 0.081 | 0.572 | 0.179 | 0.449 |
| 4 | 15 | 0.464 | 0.145 | 0.383 | 0.120 | 1.213 |
| 5 | 30 | 0.586 | 0.184 | 0.255 | 0.079 | 2.316 |
| 6 | 60 | 0.682 | 0.214 | 0.177 | 0.055 | 3.907 |
| 7 | 120 | 0.707 | 0.222 | 0.111 | 0.034 | 6.501 |

^aDilution: 833

^bDilution: 83

Table 6.26.

Amount of amine: 1.00 g (6.02 mmol)

Amount of water & MTBE: 12 + 12 ml

Characteristic concentration: 10wt%

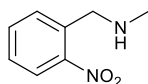
N₂ gas flowrate: 0.14 l/min

Dilution after sampling: 2500

Wavelength: 261 nm

SBW: 3 nm

Measurement time: 3 s



o-nitrobenzyl methylamine 2

| | N ₂ gas bubbling time /min | A _{org} | C _{org} /M | A _{aq} | C _{aq} /M | K Eq.28 |
|---|---------------------------------------|--------------------|---------------------|--------------------|--------------------|---------|
| 1 | Before CO ₂ saturation | 1.731 ^a | 0.544 | 0.941 ^b | 0.030 | 18.416 |
| 2 | CO ₂ saturation | 2.841 ^b | 0.089 | 1.439 ^a | 0.452 | 0.198 |
| 3 | 5 | 0.661 | 0.311 | 1.075 | 0.507 | 0.614 |
| 4 | 15 | 1.003 | 0.472 | 0.708 | 0.333 | 1.418 |
| 5 | 30 | 1.199 | 0.565 | 0.490 | 0.230 | 2.456 |
| 6 | 60 | 1.276 | 0.601 | 0.295 | 0.138 | 4.359 |
| 7 | 120 | 1.207 | 0.569 | 0.175 | 0.081 | 6.981 |

^aDilution: 1667

^bDilution: 167

Table 6.27.

Amount of amine: 3.00 g (mmol)

Amount of water & MTBE: 10 + 10 ml

Characteristic concentration: 30wt%

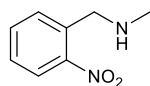
N₂ gas flowrate: 0.14 l/min

Dilution after sampling: 5000

Wavelength: 261 nm

SBW: 3 nm

Measurement time: 3 s



o-nitrobenzyl methylamine 2

| Entry | N ₂ gas bubbling time /min | A _{org} | C _{org} /M | A _{aq} | C _{aq} /M | K Eq.28 |
|-------|---------------------------------------|--------------------|---------------------|--------------------|--------------------|---------|
| 1 | Before CO ₂ saturation | 1.589 | 1.498 | 0.784 ^a | 0.074 | 20.305 |
| 2 | CO ₂ saturation | 1.873 ^a | 0.177 | 1.216 | 1.146 | 0.154 |
| 3 | 5 | 0.475 | 0.446 | 1.093 | 1.030 | 0.433 |
| 4 | 15 | 0.669 | 0.629 | 0.947 | 0.892 | 0.706 |
| 5 | 30 | 0.840 | 0.790 | 0.718 | 0.676 | 1.169 |
| 6 | 60 | 1.090 | 1.027 | 0.414 | 0.388 | 2.646 |
| 7 | 120 | 1.029 | 0.969 | 0.172 | 0.160 | 6.051 |

^aDilution: 500

Table 6.28.

Amount of amine: 253 mg (1.52 mmol)

Amount of water & MTBE: 13 + 13 ml

Characteristic concentration: 2.5wt%

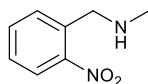
N₂ gas flowrate: 0.30 l/min

Dilution after sampling: 417

Wavelength: 261 nm

SBW: 3 nm

Measurement time: 3 s



o-nitrobenzyl methylamine 2

| Entry | N ₂ gas bubbling time /min | A _{org} | C _{org} /M | A _{aq} | C _{aq} /M | K Eq.28 |
|-------|---------------------------------------|------------------|---------------------|-----------------|--------------------|---------|
| 1 | Before CO ₂ saturation | 1.436 | 0.113 | 0.097 | 0.007 | 15.165 |
| 2 | CO ₂ saturation | 0.147 | 0.011 | 1.137 | 0.089 | 0.127 |
| 3 | 5 | 0.528 | 0.041 | 0.854 | 0.067 | 0.617 |
| 4 | 15 | 0.829 | 0.065 | 0.557 | 0.044 | 1.492 |
| 5 | 30 | 0.857 | 0.067 | 0.376 | 0.029 | 2.287 |
| 6 | 60 | 0.863 | 0.068 | 0.234 | 0.018 | 3.725 |
| 7 | 120 | 0.826 | 0.065 | 0.136 | 0.010 | 6.193 |

Table 6.29.

Amount of amine: 253 mg (1.52 mmol)

Amount of water & MTBE: 13 + 13 ml

Characteristic concentration: 2.5wt%

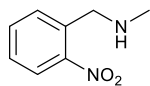
N₂ gas flowrate: 0.40 l/min

Dilution after sampling: 417

Wavelength: 261 nm

SBW: 3 nm

Measurement time: 3 s



o-nitrobenzyl methylamine 2

| Entry | N ₂ gas bubbling time /min | A _{org} | C _{org} /M | A _{aq} | C _{aq} /M | K Eq.28 |
|-------|---------------------------------------|------------------|---------------------|-----------------|--------------------|---------|
| 1 | Before CO ₂ saturation | 1.329 | 0.104 | 0.098 | 0.007 | 13.946 |
| 2 | CO ₂ saturation | 0.129 | 0.010 | 1.006 | 0.079 | 0.126 |
| 3 | 5 | 0.415 | 0.032 | 0.701 | 0.055 | 0.591 |
| 4 | 15 | 0.556 | 0.044 | 0.437 | 0.034 | 1.275 |
| 5 | 30 | 0.673 | 0.053 | 0.306 | 0.024 | 2.208 |
| 6 | 60 | 0.685 | 0.054 | 0.184 | 0.014 | 3.765 |
| 7 | 120 | 0.658 | 0.052 | 0.110 | 0.008 | 6.083 |

Table 6.30.

Amount of amine: 249 mg (1.50 mmol)

Amount of water & MTBE: 13 + 13 ml

Characteristic concentration: 2.5wt%

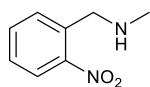
N₂ gas flowrate: 0.14 l/min

Dilution after sampling: 417

Wavelength: 261 nm

SBW: 3 nm

Measurement time: 3 s



o-nitrobenzyl methylamine 2

| Entry | N ₂ gas bubbling time /min | A _{org} | C _{org} /M | A _{aq} | C _{aq} /M | K Eq.28 |
|-------|---------------------------------------|------------------|---------------------|-----------------|--------------------|---------|
| 1 | Before CO ₂ saturation | 1.337 | 0.105 | 0.099 | 0.008 | 13.875 |
| 2 | CO ₂ saturation | 0.147 | 0.011 | 1.106 | 0.087 | 0.131 |
| 3 | 5 | 0.461 | 0.036 | 0.835 | 0.065 | 0.551 |
| 4 | 10 | 0.720 | 0.056 | 0.653 | 0.051 | 1.102 |
| 5 | 15 | 0.815 | 0.064 | 0.522 | 0.041 | 1.564 |
| 6 | 20 | 0.950 | 0.075 | 0.413 | 0.032 | 2.308 |
| 7 | 25 | 0.931 | 0.073 | 0.358 | 0.028 | 2.614 |

Table 6.31.

Amount of amine: 255 mg (1.54 mmol)

Amount of water & MTBE: 13 + 13 ml

Characteristic concentration: 2.5wt%

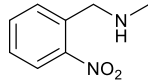
N₂ gas flowrate: 0.30 l/min

Dilution after sampling: 417

Wavelength: 261 nm

SBW: 3 nm

Measurement time: 3 s



o-nitrobenzyl methylamine 2

| Entry | N ₂ gas bubbling time /min | A _{org} | C _{org} /M | A _{aq} | C _{aq} /M | K Eq.28 |
|-------|---------------------------------------|------------------|---------------------|-----------------|--------------------|---------|
| 1 | Before CO ₂ saturation | 1.352 | 0.106 | 0.097 | 0.007 | 14.354 |
| 2 | CO ₂ saturation | 0.161 | 0.012 | 1.039 | 0.082 | 0.153 |
| 3 | 5 | 0.503 | 0.039 | 0.802 | 0.063 | 0.626 |
| 4 | 10 | 0.636 | 0.050 | 0.612 | 0.048 | 1.038 |
| 5 | 15 | 0.655 | 0.051 | 0.443 | 0.035 | 1.481 |
| 6 | 20 | 0.789 | 0.062 | 0.389 | 0.030 | 2.034 |
| 7 | 25 | 1.079 | 0.085 | 0.345 | 0.027 | 3.141 |

Table 6.32.

Amount of amine: 249 mg (1.50 mmol)

Amount of water & MTBE: 13 + 13 ml

Characteristic concentration: 2.5wt%

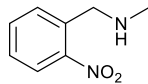
N₂ gas flowrate: 0.40 l/min

Dilution after sampling: 417

Wavelength: 261 nm

SBW: 3 nm

Measurement time: 3 s



o-nitrobenzyl methylamine 2

| Entry | N ₂ gas bubbling time /min | A _{org} | C _{org} /M | A _{aq} | C _{aq} /M | K Eq.28 |
|-------|---------------------------------------|------------------|---------------------|-----------------|--------------------|---------|
| 1 | Before CO ₂ saturation | 1.350 | 0.106 | 0.097 | 0.007 | 14.355 |
| 2 | CO ₂ saturation | 0.145 | 0.011 | 1.041 | 0.082 | 0.137 |
| 3 | 5 | 0.479 | 0.037 | 0.802 | 0.063 | 0.596 |
| 4 | 10 | 0.641 | 0.050 | 0.612 | 0.048 | 1.047 |
| 5 | 15 | 0.867 | 0.068 | 0.478 | 0.037 | 1.818 |
| 6 | 20 | 0.876 | 0.069 | 0.414 | 0.032 | 2.124 |
| 7 | 25 | 0.991 | 0.078 | 0.360 | 0.028 | 2.770 |

Table 6.33.

Amount of amine: 500 mg (2.58 mmol)

Amount of water & MTBE: 13 + 13 ml

Characteristic concentration: 5wt%

N₂ gas flowrate: 0.15 l/min

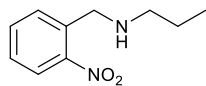
Dilution after sampling^b: Aqueous phase: 50^a;
Organic phase: 100

Eluent: aq. ammonia (0.1wt%) + acetonitrile
5 to 95% in 5.00 min

Column: C18

Retention time: 2.65 min

Detector channel: DAD signal A (220 nm)



o-nitrobenzyl propylamine 14

| Entry | N ₂ gas bubbling time /min | Area _{org} /mAU·min | C _{org} /M | Area _{aq} /mAU·min | C _{aq} /M | K Eq.28 |
|-------|---------------------------------------|------------------------------|------------------------|-----------------------------|------------------------|---------|
| 1 | Before CO ₂ saturation | 21.32 | 2.04×10 ⁻⁰¹ | 20.24 | 1.94×10 ⁻⁰³ | 105.298 |
| 2 | CO ₂ saturation | 7.29 | 6.98×10 ⁻⁰² | 29.72 | 1.42×10 ⁻⁰¹ | 0.49 |
| 3 | 5 | 11.74 | 1.12×10 ⁻⁰¹ | 23.36 | 1.12×10 ⁻⁰¹ | 1.006 |
| 4 | 15 | 13.00 | 1.25×10 ⁻⁰¹ | 14.40 | 6.89×10 ⁻⁰² | 1.806 |
| 5 | 30 | 16.59 | 1.59×10 ⁻⁰¹ | 8.36 | 4.00×10 ⁻⁰² | 3.968 |
| 6 | 60 | 21.33 | 2.04×10 ⁻⁰¹ | 3.72 | 1.78×10 ⁻⁰² | 11.484 |
| 7 | 120 | 19.81 | 1.90×10 ⁻⁰¹ | 1.36 | 6.53×10 ⁻⁰³ | 29.036 |

^aThe aqueous phase was measured without dilution after CO₂ saturation.

^bDiluted with absolute ethanol

Table 6.34.

Amount of amine: 248 mg (0.96 mmol)

Amount of water & MTBE: 13 + 13 ml

Characteristic concentration: 2.5wt%

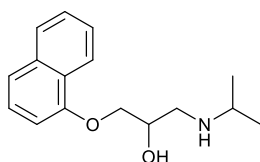
N₂ gas flowrate: 0.14 l/min

Dilution after sampling: 333

Wavelength: 291.9 nm

SBW: 2 nm

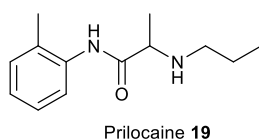
Measurement time: 3 s



Propranolol 18

| Entry | N ₂ gas bubbling time /min | A _{org} | C _{org} /M | A _{aq} | C _{aq} /M | K Eq.28 |
|-------|---------------------------------------|------------------|------------------------|-----------------|------------------------|---------|
| 1 | Before CO ₂ saturation | 1.428 | 8.07×10 ⁻⁰² | 0.007 | 5.25×10 ⁻⁰⁴ | 153.796 |
| 2 | CO ₂ saturation | 0.250 | 1.42×10 ⁻⁰² | 0.785 | 4.44×10 ⁻⁰² | 0.321 |
| 3 | 5 | 0.651 | 3.69×10 ⁻⁰² | 0.581 | 3.29×10 ⁻⁰² | 1.119 |
| 4 | 15 | 1.058 | 5.98×10 ⁻⁰² | 0.277 | 1.58×10 ⁻⁰² | 3.788 |
| 5 | 30 | 1.104 | 6.24×10 ⁻⁰² | 0.141 | 8.08×10 ⁻⁰³ | 7.726 |
| 6 | 60 | 1.233 | 6.97×10 ⁻⁰² | 0.059 | 3.46×10 ⁻⁰³ | 20.155 |
| 7 | 120 | 1.220 | 6.90×10 ⁻⁰² | 0.025 | 1.53×10 ⁻⁰³ | 44.941 |

| | | |
|-------------|-------------------------------|--------------------|
| Table 6.35. | Amount of amine: | 252 mg (1.15 mmol) |
| | Amount of water & MTBE: | 13 + 13 ml |
| | Characteristic concentration: | 2.5wt% |
| | N ₂ gas flowrate: | 0.14 l/min |
| | Dilution after sampling: | 333 |
| | Wavelength: | 230.6 nm |
| | SBW: | 2 nm |
| | Measurement time: | 3 s |



| Entry | N ₂ gas bubbling time /min | A _{org} | C _{org} /M | A _{aq} | C _{aq} /M | K Eq.28 |
|-------|---------------------------------------|------------------|------------------------|-----------------|------------------------|---------|
| 1 | Before CO ₂ saturation | 1.712 | 8.91×10 ⁻⁰² | 0.0378 | 1.82×10 ⁻⁰³ | 48.983 |
| 2 | CO ₂ saturation | 1.000 | 5.20×10 ⁻⁰² | 0.664 | 3.45×10 ⁻⁰² | 1.508 |
| 3 | 5 | 1.390 | 7.23×10 ⁻⁰² | 0.3246 | 1.68×10 ⁻⁰² | 4.312 |
| 4 | 15 | 1.571 | 8.17×10 ⁻⁰² | 0.1355 | 6.91×10 ⁻⁰³ | 11.824 |
| 5 | 30 | 1.842 | 9.59×10 ⁻⁰² | 0.0788 | 3.96×10 ⁻⁰³ | 24.233 |
| 6 | 60 | 1.741 | 9.06×10 ⁻⁰² | 0.0587 | 2.91×10 ⁻⁰³ | 31.152 |
| 7 | 120 | 1.784 | 9.29×10 ⁻⁰² | 0.0404 | 1.95×10 ⁻⁰³ | 47.507 |

6.10 Monitoring of *pH*

6.10.1 Monitoring of *pH* during the CO₂ saturation of the *o*-nitrobenzyl methylamine **2** + water + MTBE system

Stock solution of *o*-nitrobenzyl methylamine **2** (5 ml, 2.5wt%, in MTBE) was stirred with distilled water (5 ml). The stirring was stopped after 5 min, and a *pH* was measured using a glass *pH* electrode (t=0). The two phase system was loaded into a measuring cylinder, and CO₂ was streamed through (0.5 l/min). The CO₂ was previously saturated with MTBE. The *pH* was measured by immersion of the *pH* electrode into the aqueous phase with 5 min frequency. The stream of CO₂ was suspended during the *pH* measurement. The experiment was carried out at room temperature and ambient pressure (Table 6.36).

Table 6.36. Measured *pH* during the CO₂ saturation of the *o*-nitrobenzyl methylamine **2** + water + MTBE system at room temperature and atmospheric pressure.

| Time /min | <i>pH</i> |
|--------------|-----------|
| 0 | 10.01 |
| 5 | 6.94 |
| 10 | 6.92 |
| 15 | 7.29 |
| 20 | 7.45 |
| 25 | 6.94 |

6.10.2 Monitoring of *pH* during the N₂ gas induced decarboxylation of the CO₂ saturated *o*-nitrobenzyl methylamine **2** + water + MTBE system

A mixture of stock solution of *o*-nitrobenzyl methylamine **2** (5 ml, 2.5wt%, in MTBE) and distilled water (5 ml) was saturated by CO₂ by streaming the gas (0.5 l/min, 10 min) in a measuring cylinder. The *pH* of the CO₂ saturated system was measured using a glass *pH* electrode (t=0). N₂ gas (0.15 l/min) was streamed through the system, and the *pH* was measured by immersion of the *pH* electrode into the aqueous phase (Table 6.37). The stream of N₂ was suspended during the *pH* measurement. The experiment was carried out at room temperature and ambient pressure. The stream of gases was previously saturated with MTBE.

Table 6.37. Measured *pH* during the N₂ gas induced decarboxylation of the CO₂ saturated *o*-nitrobenzyl methylamine **2** + water + MTBE system at room temperature and atmospheric pressure.

| Time /min | <i>pH</i> |
|--------------|-----------|
| 0 | 6.90 |
| 5 | 7.72 |
| 15 | 8.04 |
| 30 | 8.21 |
| 60 | 8.52 |
| 120 | 8.77 |

6.11 Application of CO₂ as antisolvent at elevated pressures

6.11.1 Qualitative precipitation tests at room temperature or above

The solution to test was introduced into a stainless steel view cell (17 cm³ in volume) through a borehole of 1/16" diameter with a syringe. The loaded cell was rinsed three times with CO₂ (0.2 MPa) in order to remove any traces of air. Agitation was turned on and the heating was set to the desired temperature. The system was stirred (30 min) until the temperature of the sample and the temperature of the reactor body reached equilibrium. CO₂ was loaded into the cell *via* a syringe pump. The amount of consumed CO₂ was monitored using the syringe pump controller. The measured pressure and observed phase transitions were noted. The approximate expansion of the solution was also noted. The used vessel did not have a calibration. The volume reading was done qualitatively, based on the estimation of volume occupied by the liquid phase of the reactor volume (17 cm³). The stirring was suspended during the estimation of expansion and observation of phase change (Table 6.38-6.68).

The showed pressures are gauge pressures. Detailed information can be found about the experimental set-up in Appendix - I.

Abbreviations

| | |
|------------------|------------------------|
| g | gas |
| lq | liquid |
| V _{lqh} | volume of heavy liquid |
| V _{lql} | volume of light liquid |

Table 6.38. Expansion of the tritylamine + TMU system with CO₂.

| Entry | Injected CO ₂ /g | P/MPa | Approx. Expansion /% | Observation |
|-------|-----------------------------|-------|----------------------|--|
| 1 | 14.3 | 7.94 | 750% | Single heavy phase |
| 2 | 16.2 | 8.11 | 1033% | Precipitation of large amount of solid |
| 3 | 20.7 | 11.65 | 1600% | Large amount of solid + single fluid phase |

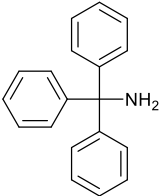
| | | | | |
|--|---|-----|---|-----------|
|  <p>tritylamine</p> | + | TMU | Tested solution: volume/concentration 1 ml 0.39 M | T = 40 °C |
|--|---|-----|---|-----------|

Table 6.39. Expansion of the tritylamine + DMSO system with CO₂.

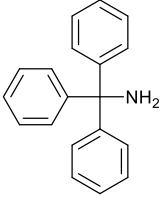
|  tritylamine | | + | DMSO | Tested solution: volume/concentration | | T = 40 °C |
|--|-----------------------------|-------|----------------------|--|--------|-----------|
| | | | | 1 ml | 0.39 M | |
| Entry | Injected CO ₂ /g | P/MPa | Approx. Expansion /% | Observation | | |
| 1 | 14.6 | 8.17 | 466-750% | lq. + lq. + g. | | |
| 2 | 17.4 | 8.39 | 1033% | lq. + lq. + g.; V _{lqh} << V _{lql} | | |
| 3 | 21.2 | 11.82 | 1600% | Single fluid phase; no solid | | |

Table 6.40. Expansion of the Ibuprofen + DMSO system with CO₂.

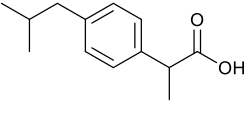
|  Ibuprofen | | + | DMSO | Tested solution: volume/concentration | | T = 40 °C |
|--|-----------------------------|-------|----------------------|--|--------|-----------|
| | | | | 1 ml | 0.49 M | |
| Entry | Injected CO ₂ /g | P/MPa | Approx. Expansion /% | Observation | | |
| 1 | 16.4 | 8.22 | 750% | lq. + lq. + g.; V _{lqh} << V _{lql} | | |
| 2 | 21.9 | 12.68 | 1600% | Single fluid phase; no solid | | |

Table 6.41. Expansion of the Ibuprofen + TMU system with CO₂.

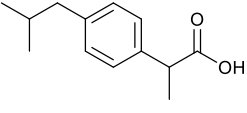
|  Ibuprofen | | + | TMU | Tested solution: volume/concentration | | T = 40 °C |
|--|-----------------------------|-------|----------------------|---------------------------------------|--------|-----------|
| | | | | 1 ml | 0.49 M | |
| Entry | Injected CO ₂ /g | P/MPa | Approx. Expansion /% | Observation | | |
| 1 | 11.0 | 7.58 | 467% | lq. + g. | | |
| 2 | 15.4 | 8.13 | 750% | lq. + g. | | |
| 3 | 20.8 | 13.20 | 1600% | Single fluid phase; no solid | | |

Table 6.42. Expansion of the Ibuprofen + EtOH system with CO₂.

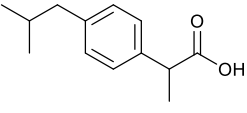
|  Ibuprofen | | + | EtOH | Tested solution: volume/concentration | | T = 40 °C |
|--|-----------------------------|-------|----------------------|---------------------------------------|--------|-----------|
| | | | | 1 ml | 0.49 M | |
| Entry | Injected CO ₂ /g | P/MPa | Approx. Expansion /% | Observation | | |
| 1 | 13.6 | 7.82 | 750% | lq. + g. | | |
| 2 | 20.6 | 13.30 | 1600% | Single fluid phase; no solid | | |

Table 6.43. Expansion of the Amlodipine + DMSO system with CO₂.

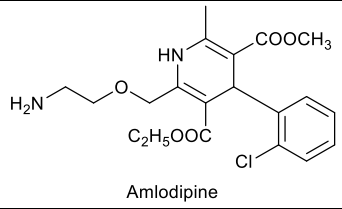
|  Amlodipine | | | + DMSO | Tested solution: volume/concentration 1 ml 0.24 M | T = 40 °C |
|---|-----------------------------|-------|----------------------|---|-----------|
| Entry | Injected CO ₂ /g | P/MPa | Approx. Expansion /% | Observation | |
| 1 | 14.7 | 8.08 | 466-750% | lq. + lq. + g.; V _{lqh} << V _{lql} | |
| 2 | 21.5 | 11.13 | 1600% | Small amount of solid + Single fluid phase | |

Table 6.44. Expansion of the Amlodipine + TMU system with CO₂.

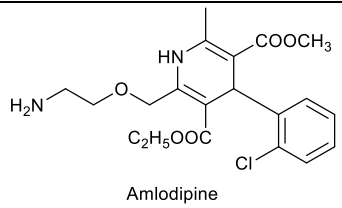
|  Amlodipine | | | + TMU | Tested solution: volume/concentration 1 ml 0.24 M | T = 40 °C |
|---|-----------------------------|-------|----------------------|---|-----------|
| Entry | Injected CO ₂ /g | P/MPa | Approx. Expansion /% | Observation | |
| 1 | 8.6 | 6.61 | 183% | Precipitation started | |
| 2 | 14.1 | 7.95 | 750% | Solid + lq. + g. | |
| 3 | 22.6 | 12.51 | 1600% | Solid + single fluid phase | |

Table 6.45. Expansion of the Amlodipine + EtOH system with CO₂.

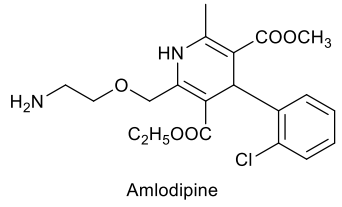
|  Amlodipine | | | + EtOH | Tested solution: volume/concentration 1 ml 0.24 M | T = 40 °C |
|---|-----------------------------|-------|----------------------|---|-----------|
| Entry | Injected CO ₂ /g | P/MPa | Approx. Expansion /% | Observation | |
| 1 | 11.8 | 7.68 | 467% | lq. + lq. + g.; V _{lqh} << V _{lql} | |
| 2 | 19.8 | 12.86 | 1600% | lq. + g.; V _{lq} < V _{sc} | |

Table 6.46. Expansion of the benzodiazepine 4 + DMSO system with CO₂.

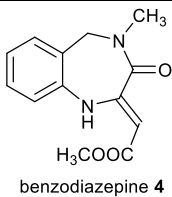
|  benzodiazepine 4 | | + DMSO | Tested solution: volume/concentration 1 ml 0.41 M | | T = 40 °C |
|---|-----------------------------|--------|---|--------------------------------------|-----------|
| Entry | Injected CO ₂ /g | P/MPa | Approx. Expansion /% | Observation | |
| 1 | 15.8 | 8.24 | 750% | lq. + g. | |
| 2 | 21.8 | 12.79 | 1600% | Single fluid phase; no precipitation | |

Table 6.47. Expansion of the benzodiazepine 4 + TMU system with CO₂.

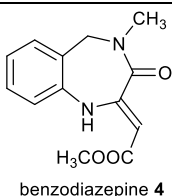
|  benzodiazepine 4 | | + TMU | Tested solution: volume/concentration 1 ml 0.41 M | | T = 40 °C |
|---|-----------------------------|-------|---|--------------------------------------|-----------|
| Entry | Injected CO ₂ /g | P/MPa | Approx. Expansion /% | Observation | |
| 1 | 14.5 | 7.88 | 750% | lq. + g. | |
| 2 | 21.0 | 12.86 | 1600% | Single fluid phase; no precipitation | |

Table 6.48. Expansion of the Quinine + DMSO system with CO₂.

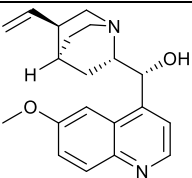
|  Quinine | | + DMSO | Tested solution: volume/concentration 1 ml 0.31 M | | T = 40 °C |
|--|-----------------------------|--------|---|---|-----------|
| Entry | Injected CO ₂ /g | P/MPa | Approx. Expansion /% | Observation | |
| 1 | 14.07 | 8.17 | 467 | lq. + lq. + g.; V _{lqh} > V _{lql} | |
| 2 | 17.20 | 8.37 | 1033 | lq. + lq. + g.; V _{lqh} << V _{lql} | |
| 3 | 21.73 | 13.20 | 1600 | Minimal amount of solid lq. + g.; V _{lq} << V _{sc} | |

Table 6.49. Expansion of the Quinine + TMU system with CO₂.

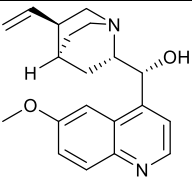
|  Quinine | | + | TMU | Tested solution: volume/concentration 1 ml 0.31 M | | T = 40 °C |
|--|-----------------------------|-------|----------------------|---|--|-----------|
| Entry | Injected CO ₂ /g | P/MPa | Approx. Expansion /% | Observation | | |
| 1 | 5.8 | 5.97 | 100 | Precipitation of solid started | | |
| 2 | 11.9 | 7.81 | 467 | Precipitation; quick sedimentation of solid | | |
| 3 | 16.5 | 8.28 | 1033 | Large amount of solid | | |
| 4 | 20.7 | 12.67 | 1600 | Solid + single fluid phase | | |

Table 6.50. Expansion of the Quinine + DMF system with CO₂.

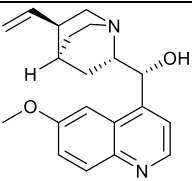
|  Quinine | | + | DMF | Tested solution: volume/concentration 1 ml 0.31 M | | T = 40 °C |
|--|-----------------------------|-------|----------------------|---|--|-----------|
| Entry | Injected CO ₂ /g | P/MPa | Approx. Expansion /% | Observation | | |
| 1 | 13.66 | 7.79 | 750% | Precipitation of solid started | | |
| 2 | 20.38 | 12.51 | 1600% | Small amount of precipitate + Single fluid phase | | |

Table 6.51. Expansion of the Quinine + EtOH system with CO₂.

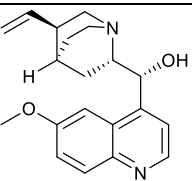
|  Quinine | | + | EtOH | Tested solution: volume/concentration 1 ml 0.31 M | | T = 40 °C |
|--|-----------------------------|-------|----------------------|---|--|-----------|
| Entry | Injected CO ₂ /g | P/MPa | Approx. Expansion /% | Observation | | |
| 1 | 12.1 | 7.82 | 467% | lq. + lq. + g.; V _{lqh} << V _{lq} | | |
| 2 | 15.0 | 8.11 | 750% | lq. + lq. + g.; V _{lqh} << V _{lq} | | |
| 3 | 19.9 | 11.50 | 1600% | lq. + g.; V _{lq} << V _{sc} | | |

Table 6.52. Expansion of the Quinine + CH₃COOH system with CO₂.

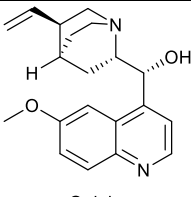
|  Quinine | | + CH ₃ COOH | Tested solution: volume/concentration | | T = 40 °C |
|--|-----------------------------|------------------------|---------------------------------------|--|-----------|
| | | | 1 ml | 0.31 M | |
| Entry | Injected CO ₂ /g | P/MPa | Approx. Expansion /% | Observation | |
| 1 | 13.5 | 7.58 | 750% | lq. + lq. + g.; V _{lqh} << V _{lql} | |
| 2 | 16.4 | 7.89 | 1033% | lq. + lq. + g.; V _{lqh} << V _{lql} | |
| 3 | 21.9 | 12.65 | 1600% | lq. + g.; V _{lq} << V _{sc} | |

Table 6.53. Expansion of the Lidocaine **20** + DMSO system with CO₂.

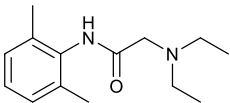
|  Lidocaine 20 | | + DMSO | Tested solution: volume/concentration | | T = 40 °C |
|--|-----------------------------|--------|---------------------------------------|--------------------------------------|-----------|
| | | | 1 ml | 0.43 M | |
| Entry | Injected CO ₂ /g | P/MPa | Approx. Expansion /% | Observation | |
| 1 | 8.9 | 6.99 | 30% | Apparent expansion started | |
| 2 | 16.1 | 8.37 | 750% | Expansion | |
| 3 | 20.2 | 13.20 | 1600% | Single fluid phase; no precipitation | |

Table 6.54. Expansion of the Lidocaine **20** + DMF system with CO₂.

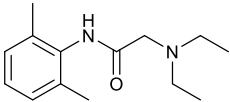
|  Lidocaine 20 | | + DMF | Tested solution: volume/concentration | | T = 40 °C |
|--|-----------------------------|-------|---------------------------------------|--------------------------------------|-----------|
| | | | 1 ml | 0.43 M | |
| Entry | Injected CO ₂ /g | P/MPa | Approx. Expansion /% | Observation | |
| 1 | 5.7 | 5.82 | 30% | Apparent expansion started | |
| 2 | 15.6 | 8.06 | 750% | Expansion | |
| 3 | 19.8 | 10.36 | 1600% | Single fluid phase; no precipitation | |

Table 6.55. Expansion of the Lidocaine **20** + TMU system with CO₂.

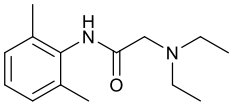
|  Lidocaine 20 | | + TMU | Tested solution: volume/concentration | | T = 40 °C |
|--|-----------------------------|-------|---------------------------------------|--------------------------------------|-----------|
| | | | 1 ml | 0.43 M | |
| Entry | Injected CO ₂ /g | P/MPa | Approx. Expansion /% | Observation | |
| 1 | 14.7 | 8.03 | 750% | Expansion | |
| 2 | 21.6 | 11.82 | 1600% | Single fluid phase; no precipitation | |

Table 6.56. Expansion of the Omeprazole + TMU system with CO₂.

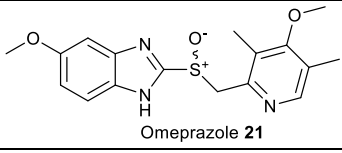
|  Omeprazole 21 | | | + | TMU | Tested solution: volume/concentration 1 ml 0.29 M | | T = 40 °C |
|--|-----------------------------|-------|----------------------|----------------------------|---|--|-----------|
| Entry | Injected CO ₂ /g | P/MPa | Approx. Expansion /% | Observation | | | |
| 1 | 6.9 | 6.15 | 30% | Apparent expansion started | | | |
| 2 | 10.7 | 7.37 | 467% | Precipitation of solid | | | |
| 3 | 16.4 | 8.08 | 1033% | Solid + Single fluid phase | | | |

Table 6.57. Expansion of the Pyrimetazole + TMU system with CO₂.

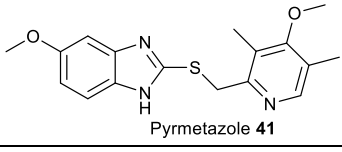
|  Pyrimetazole 41 | | | + | TMU | Tested solution: volume/concentration 1 ml 0.30 M | | T = 40 °C |
|--|-----------------------------|-------|----------------------|--|---|--|-----------|
| Entry | Injected CO ₂ /g | P/MPa | Approx. Expansion /% | Observation | | | |
| 1 | 5.3 | 5.83 | 30% | Apparent expansion started | | | |
| 2 | 14.3 | 7.93 | 750% | lq. + lq. + g.; V _{lqh} << V _{lql} | | | |
| 3 | 17.6 | 8.28 | 1600% | lq. + g.; V _{lq} << V _{sc} | | | |

Table 6.58. Expansion of the Pyrimetazole + TMU system with CO₂ at room temperature.

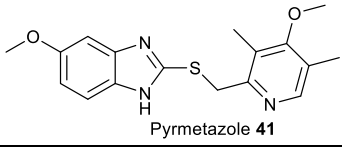
|  Pyrimetazole 41 | | | + | TMU | Tested solution: volume/concentration 1 ml 0.30 M | | T = 25 °C |
|--|-------|----------------------|--|-----|--|--|-----------|
| Entry | P/MPa | Approx. Expansion /% | Observation | | | | |
| 1 | 5.68 | 750% | Precipitation of oil | | | | |
| 2 | 5.82 | 1033% | lq. + lq. + g.; V _{lqh} << V _{lql} | | | | |
| 3 | 12.86 | 1600% | Oily droplets in single fluid phase | | | | |

Table 6.59. Expansion of the Benzimidazole + TMU system with CO₂.

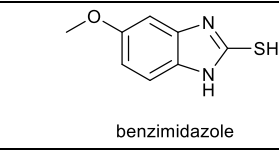
|  benzimidazole | | | + | TMU | Tested solution: volume/concentration 1 ml 0.56 M | | T = 40 °C |
|--|-----------------------------|-------|----------------------|------------------------------------|---|--|-----------|
| Entry | Injected CO ₂ /g | P/MPa | Approx. Expansion /% | Observation | | | |
| 1 | 6.9 | 6.29 | 30% | Apparent expansion started | | | |
| 2 | 14.4 | 7.85 | 750% | Precipitation of solid | | | |
| 3 | 17.5 | 8.06 | 1600% | Solid present + Single fluid phase | | | |

Table 6.60. Expansion of the *p*-aminobenzoic acid + TMU system with CO₂.

| | | | | | | |
|----------|--|---|-----|---------------------------------------|--------|-----------|
| PABA | | + | TMU | Tested solution: volume/concentration | | T = 40 °C |
| | | | | 1 ml | 0.73 M | |

| Entry | Injected CO ₂ /g | P/MPa | Approx. Expansion /% | Observation |
|-------|-----------------------------|-------|----------------------|---|
| 1 | 7.4 | 6.31 | 30% | Apparent expansion started |
| 2 | 12.2 | 7.75 | 467% | lq. + lq. + g.; V _{lqh} << V _{lql} |
| 3 | 17.9 | 8.37 | 750% | lq. + lq. + g.; V _{lqh} << V _{lql} |
| 4 | 21.2 | 11.24 | 1600% | Slow precipitation of small amount of solid + Single fluid phase |

Table 6.61. Expansion of the *p*-aminobenzoic acid + DMSO system with CO₂.

| | | | | | | |
|----------|--|---|------|---------------------------------------|--------|-----------|
| PABA | | + | DMSO | Tested solution: volume/concentration | | T = 40 °C |
| | | | | 1 ml | 0.73 M | |

| Entry | Injected CO ₂ /g | P/MPa | Approx. Expansion /% | Observation |
|-------|-----------------------------|-------|----------------------|--|
| 1 | 4.5 | 5.48 | 30% | Apparent expansion started |
| 2 | 14.5 | 8.22 | 750% | lq. + lq. + g.; V _{lqh} << V _{lql} |

Table 6.62. Expansion of the *p*-aminobenzoic acid + EtOH system with CO₂.

| | | | | | | |
|----------|--|---|------|---------------------------------------|--------|-----------|
| PABA | | + | EtOH | Tested solution: volume/concentration | | T = 40 °C |
| | | | | 1 ml | 0.73 M | |

| Entry | Injected CO ₂ /g | P/MPa | Approx. Expansion /% | Observation |
|-------|-----------------------------|-------|----------------------|--|
| 1 | 2.3 | 5.0 | 30% | Apparent expansion started |
| 2 | 8.7 | 6.0 | 50% | Precipitation of solid started |
| 3 | 12.4 | 7.0 | 750% | Significant amount of solid |
| 4 | 16.5 | 7.2 | 1033% | Significant amount of solid; looked dry, sediment quickly |
| 5 | 20.4 | 8.5 | 1600% | After sedimentation ½ volume of the cell was filled with solid + Single fluid phase |

Table 6.63. Expansion of the Propranolol **18** + TMU system with CO₂.

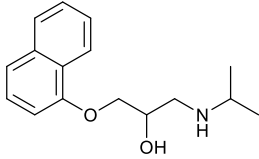
|  Propranolol 18 | | | + | TMU | Tested solution: volume/concentration 1 ml 0.39 M | | T = 40 °C |
|--|-----------------------------|-------|----------------------|-----|---|--|-----------|
| Entry | Injected CO ₂ /g | P/MPa | Approx. Expansion /% | | Observation | | |
| 1 | 3.7 | 5.10 | 30% | | Apparent expansion started | | |
| 2 | 11.3 | 7.45 | 467% | | Precipitation of oil | | |
| 3 | 14.6 | 8.03 | 750% | | lq. + lq. + g.; V _{lqh} << V _{lql} | | |
| 4 | 21.3 | 12.51 | 1600% | | Single fluid phase; no precipitation | | |

Table 6.64. Expansion of the Propranolol **18** + EtOH system with CO₂.

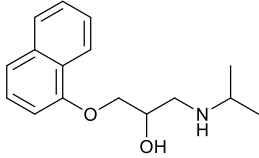
|  Propranolol 18 | | | + | EtOH | Tested solution: volume/concentration 1 ml 0.39 M | | T = 40 °C |
|--|-----------------------------|-------|----------------------|------|---|--|-----------|
| Entry | Injected CO ₂ /g | P/MPa | Approx. Expansion /% | | Observation | | |
| 1 | 11.4 | 7.59 | 467% | | Precipitation of oil | | |
| 2 | 14.3 | 8.56 | 750% | | lq. + lq. + g.; V _{lqh} << V _{lql} | | |
| 3 | 21.2 | 12.72 | 1600% | | Single fluid phase; no precipitation | | |

Table 6.65. Expansion of the Propranolol **18** + DMSO system with CO₂.

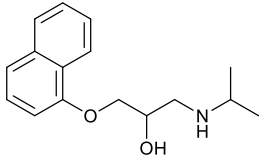
|  Propranolol 18 | | | + | DMSO | Tested solution: volume/concentration 1 ml 0.39 M | | T = 40 °C |
|--|-----------------------------|-------|----------------------|------|---|--|-----------|
| Entry | Injected CO ₂ /g | P/MPa | Approx. Expansion /% | | Observation | | |
| 1 | 14.5 | 7.46 | 467% | | Precipitation of oil | | |
| 2 | 15.1 | 8.03 | 750% | | lq. + lq. + g.; V _{lqh} << V _{lql} | | |
| 3 | 20.8 | 10.44 | 1600% | | Single fluid phase; no precipitation | | |

Table 6.66. Expansion of the Metoprolol + TMU system with CO₂.

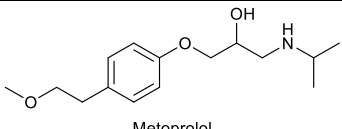
|  Metoprolol | | + | TMU | Tested solution: volume/concentration | | T = 40 °C |
|---|-----------------------------|-------|----------------------|--|--------|-----------|
| | | | | 1 ml | 0.39 M | |
| Entry | Injected CO ₂ /g | P/MPa | Approx. Expansion /% | Observation | | |
| 1 | 10.5 | 7.34 | 467% | Volumetric expansion | | |
| 2 | 14.2 | 7.86 | 750% | lq. + lq. + g.; V _{lqh} << V _{lql} | | |
| 3 | 16.8 | 8.08 | 1033% | lq. + lq. + g.; V _{lqh} << V _{lql} | | |
| 4 | 20.5 | 10.44 | 1600% | Single fluid phase; no precipitation | | |

Table 6.67. Expansion of the Metoprolol + DMSO system with CO₂.

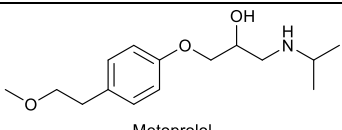
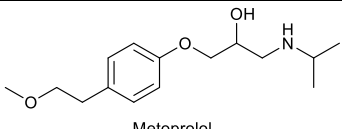
|  Metoprolol | | + | DMSO | Tested solution: volume/concentration | | T = 40 °C |
|---|-----------------------------|-------|----------------------|--|--------|-----------|
| | | | | 1 ml | 0.39 M | |
| Entry | Injected CO ₂ /g | P/MPa | Approx. Expansion /% | Observation | | |
| 1 | 11.6 | 7.86 | 30% | Volumetric expansion | | |
| 2 | 16.8 | 8.24 | 467% | lq. + lq. + g.; V _{lqh} << V _{lql} | | |
| 3 | 21.0 | 10.75 | 750% | Single fluid phase; no precipitation | | |

Table 6.68. Expansion of the Metoprolol + EtOH system with CO₂.

|  Metoprolol | | + | EtOH | Tested solution: volume/concentration | | T = 40 °C |
|---|-----------------------------|-------|----------------------|--|--------|-----------|
| | | | | 1 ml | 0.39 M | |
| Entry | Injected CO ₂ /g | P/MPa | Approx. Expansion /% | Observation | | |
| 1 | 11.4 | 7.59 | 467% | Volumetric expansion | | |
| 2 | 14.2 | 7.84 | 750% | lq. + lq. + g.; V _{lqh} << V _{lql} | | |
| 3 | 16.5 | 7.99 | 1033% | lq. + lq. + g.; V _{lqh} << V _{lql} | | |
| 4 | 21.0 | 13.20 | 1600% | Single fluid phase; no precipitation | | |

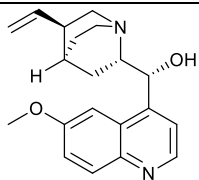
6.11.2 Qualitative precipitation tests below room temperature

The solution to test was introduced into a stainless steel view cell (17 cm³ in volume) through a borehole of 1/16" diameter with a syringe. The loaded cell was rinsed three times with CO₂ (0.3 MPa) in order to remove any traces of air. Agitation was turned on and the cooling was set to the desired temperature. The system was stirred (30 min) until the temperature of the sample and the temperature of the reactor body reached equilibrium. CO₂ was loaded into the cell *via* a syringe pump, until precipitation occurred. The approximate expansion of the solution and the pressure were noted. The

temperature of the system was reduced further by enhancing cooling, and the pressure above the mixture was measured (Table 6.69-6.70).

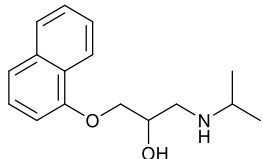
The showed pressures are gauge pressures. Detailed information can be found about the experimental set-up in Appendix - I.

Table 6.69. Expansion of the Quinine + TMU system with CO₂.

|  Quinine | | Tested solution: volume/concentration | | |
|--|--|--|--------|--|
| | | 1 ml | 0.31 M | |

| Entry | Temperature /°C | P/MPa | Approx. Expansion | Observation |
|-------|-----------------|-------|-------------------|---------------------------|
| 1 | -6 | 2.53 | 467% | Solid precipitate present |
| 2 | -16 | 2.10 | 467% | Solid precipitate present |

Table 6.70. Expansion of the Propranolol **18** + TMU system with CO₂.

|  Propranolol 18 | | Tested solution: volume/concentration | | |
|---|--|--|--------|--|
| | | 1 ml | 0.39 M | |

| Entry | Temperature /°C | P/MPa | Approx. Expansion | Observation |
|-------|-----------------|-------|-------------------|-------------------------------------|
| 1 | -5 | 3.20 | 750% | Solution opaque |
| 2 | -13 | 2.28 | 750% | Minimal amount of solid precipitate |
| 3 | -15 | 2.21 | 467% | |
| 4 | -17 | 1.87 | 467% | |

6.12 Antisolvent precipitation tests at elevated pressure with solid isolation

6.12.1 Experiments above the critical temperature of CO₂

Preparation of the equipment

A stainless steel view cell (17 cm³ in volume) was rinsed three times with CO₂ (0.3 MPa) in order to remove any traces of air. The temperature of the cell was set. The cell was pressurised by introduction of CO₂, and stirring was turned on. After 30 minutes of stirring, thermal equilibrium between the load and the reactor body was assumed, and a continuous flow of CO₂ was turned on. The cell was vented through a bottom

withdrawal port with a filter and a back pressure regulator on-line. The pressure of the system was controlled by the back pressure regulator (Table 6.71).

Precipitation of solid after injection

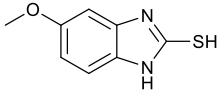
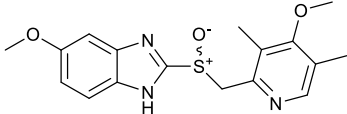
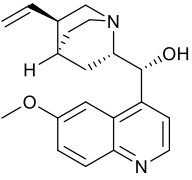
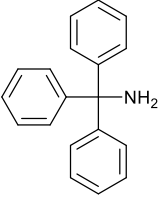
Sample solution was injected into the flow of CO₂ using an injection valve. The point of injection was between the syringe pump and the inlet port of the view cell. Precipitation of solid in the cell was immediately observed after injection and the cell ceased to be transparent. 40 minutes after sample injection the stirring was turned off. At this point the view cell was transparent. 50 minutes after sample injection pumping of CO₂ was turned off, and the cell was vented by a continuous reduction of pressure. The pressure of the system was controlled by the back pressure regulator (Table 6.71).

Disassembly of the equipment and removal of solid

The filter compartment was removed from the bottom port of the cell. The accumulated solid was collected. The cell was opened by removal of the main lid, and further solid precipitate was collected. The collected solid was combined and scaled (Table 6.71).

The showed pressures are gauge pressures. Detailed information can be found about the experimental set-up in Appendix - I.

Table 6.71. Preparative isolation of solutes after precipitation with CO₂, above the critical temperature of CO₂. CO₂ was streamed through the system with a flowrate of 3 ml·min⁻¹ for 40 min while the system was stirred, and further 10 min after the stirring was stopped.

| Entry | Solute | Solvent | V _{sample} /ml | C _{sample} /M | T /°C | P /MPa | Recovery /% |
|----------------|--|---------|-------------------------|------------------------|-------|--------|-------------|
| 1 |  benzimidazole | TMU | 1 | 0.55 | 40 | 10.0 | 70 |
| 2 |  PABA | EtOH | 1 | 0.73 | 40 | 10.0 | 53 |
| 3 ^a |  PABA | EtOH | 1 | 0.73 | 60 | 10.5 | 47 |
| 4 |  Omeprazole 21 | TMU | 1 | 0.29 | 40 | 8.3 | 22 |
| 5 |  Quinine | TMU | 1 | 0.31 | 40 | 10.7 | 21 |
| 6 |  tritylamine | TMU | 1 | 0.39 | 40 | 8.8 | 3 |

^athe flow of CO₂ through the system was 0.25 ml·min⁻¹ for 6 hours

6.12.2 Experiments below the critical temperature of CO₂

Preparation of the equipment

A stainless steel view cell (17 cm³ in volume) was rinsed three times with CO₂ (0.3 MPa) in order to remove any traces of air. The temperature of the cell was set. The cell was loaded up to 1/3 volume with liquid CO₂, and stirring was turned on. After 30 minutes of stirring, thermal equilibrium between the load and the reactor body was assumed (Table 6.72).

Precipitation of solid after injection

A continuous flow of CO₂ was turned on, and the sample solution was injected into the flow immediately using an injection valve. The point of injection was between the syringe pump and the inlet port of the view cell. Precipitation of solid in the cell was

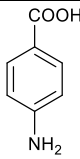
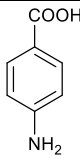
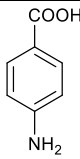
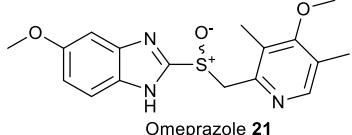
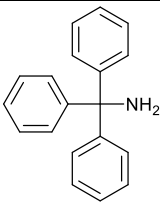
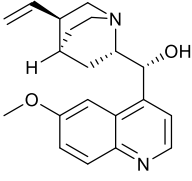
immediately observed. The continuous flow of liquid CO₂ gradually filled the cell, through which the pressure was nearly steady. When the volume of the cell was filled with liquid, pressure steeply rose. When the pressure within the cell reached the BPR's breaking pressure, which had been set previously, flow through the cell started. The pressure of the system was controlled by the back pressure regulator. 30 minutes later the stirring was turned off. At this point the view cell looked transparent. After 10 more minutes of streaming the flow of CO₂ was turned off, and the cell was vented through the bottom withdrawal port (Table 6.72).

Disassembly of the equipment and removal of solid

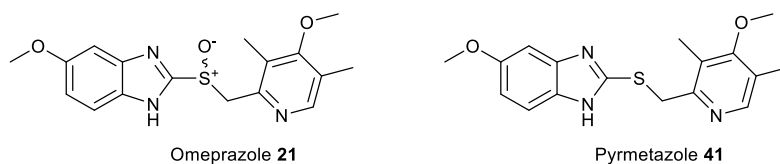
The filter compartment was removed from the bottom port of the cell. The accumulated solid was collected. The cell was opened by removal of the main lid, and further solid precipitate was collected. The collected solid was combined and scaled (Table 6.72).

The showed pressures are gauge pressures. Detailed information can be found about the experimental set-up in Appendix - I.

Table 6.72. Preparative isolation of solutes after precipitation with CO₂, under the critical temperature of CO₂. CO₂ was streamed through the system with a flowrate of 3 ml·min⁻¹ for 40 min while the system was stirred, and further 10 min after the stirring was stopped.

| Entry | Solute | Solvent | V _{sample} /ml | C _{sample} /M | T /°C | P /MPa | Recovery /% |
|-------|--|---------|-------------------------|------------------------|-------|--------|-------------|
| 1 |  PABA | EtOH | 1 | 0.73 | 25 | 8.3 | 54 |
| 2 |  PABA | EtOH | 1 | 0.73 | 0 | 7.3 | 46 |
| 3 |  PABA | EtOH | 1 | 0.73 | -21 | 8.0 | 66 |
| 4 |  Omeprazole 21 | TMU | 1 | 0.29 | 25 | 7.0 | 93 |
| 6 |  tritylamine | TMU | 1 | 0.39 | 25 | 9.0 | 4 |
| |  Quinine | TMU | 1 | 0.31 | 25 | 8.0 | 22.4 |

6.13 Application of CO₂ antisolvent induced precipitation for separation of solutes



A stock solution of Omeprazole **21** (90 g/l) and Pyrimetazole **41** (10 g/l) was created in TMU. The procedure designed for solute precipitation and isolation was used at room temperature (6.12.2). 1 ml sample was injected, the flow of CO₂ was 3 ml/min, and the pressure was 7.0 MPa (gauge). 80 mg sample was removed from the cell (88%). The concentration of Pyrimetazole was reduced to 1.7%, determined by NMR spectra integration of peaks at 7.35 ppm (**21**) and at 4.36 ppm (**41**) in MeOD-*d*₄.

References

- [1] P.T. Anastas, J.C. Warner, *Green Chemistry: Theory and Practice*, Oxford University Press, New York, **1998**.
- [2] R.A. Sheldon, *Chem. Ind.* **1992**, 23, 903.
- [3] I. Vogel, *Textbook of Practical Organic Chemistry*, Longman, London, **1981**.
- [4] S. Arrhenius, *Z. Phys. Chem.* **1889**, 226.
- [5] J. Clayden, N. Greeves, S. Warren *Organic Chemistry*, 2nd ed., Oxford University Press, Oxford, **2012**.
- [6] P. Knochel, *Modern Solvents in Organic Synthesis*, Springer, Heidelberg, **1999**.
- [7] P.G. Jessop, L. Walter, *Chemical Synthesis Using Supercritical Fluids*, Wiley-VCH, Weinheim, **1999**.
- [8] B. Kirchner, *Ionic Liquids*, Springer, Berlin, **2009**.
- [9] R.K. Henderson, C. Jimenez-Gonzalez, D.J.C. Constable, S.R. Alston, G.G.A. Inglis, G. Fisher, J. Sherwood, S.P. Binks, A.D. Curzons, *Green Chem.* **2011**, 13, 854.
- [10] O. Mitsunobu, *Synthesis* **1981**, 1.
- [11] G. Wittig, U. Schollkopf, *Chem. Ber.* **1954**, 87, 1318.
- [12] I.P. Andrews, R.J. Atkins, G.F. Breen, J.S. Carey, M.A. Forth, D.O. Morgan, A. Shamji, A.C. Share, S.A.C. Smith, T.C. Walsgrove, A.S. Wells, *Org. Process Res. Dev.* **2003**, 7, 655.
- [13] R.J. Atkins, A. Banks, R.K. Bellingham, G.F. Breen, J.S. Carey, S.K. Etridge, J.F. Hayes, N. Hussain, D.O. Morgan, P. Oxley, S.C. Passey, T.C. Walsgrove, A.S. Wells, *Org. Process Res. Dev.* **2003**, 7, 663.
- [14] ftp://ftp.cmdl.noaa.gov/ccg/co2/trends/co2_mm_mlo.txt, NOAA, Mauna Loa, Hawaii, USA, viewed Jul. 2013.
- [15] P.M.M. Blauwhoff, B. Kamphuis, W.P.M. van Swaaij, K.R. Westerterp, *Chem. Eng. Process.* **1985**, 19, 1.
- [16] *Bridging the Emissions Gap*, United Nations Environment Programme (UNEP) **2011**, Source: <http://www.unep.org/publications/ebooks>, viewed Aug. 2013.
- [17] J.C. Pales, C.D. Keeling, *J. Geophys. Res.* **1965**, 70, 6053.
- [18] C. Baird, M. Cann, *Environmental Chemistry*, W.H. Freeman, New York, **2012**.
- [19] A.D. Buckingham, R.L. Disch, *Proc. R. Soc. A* **1963**, 273, 275.
- [20] I. Omae, *Coord. Chem. Rev.* **2012**, 256, 1384.
- [21] D. Chaturvedi, S. Ray, *Monatsh. Chem.* **2006**, 137, 127.
- [22] R. Sander, <http://www.henrys-law.org>, *Compilation of Henry's Law Constants for Inorganic and Organic Species of Potential Importance in Environmental Chemistry (Version 3)*, viewed Aug. 2013.
- [23] J.A. Dean, *Lange's Handbook of Chemistry*, McGraw-Hill Inc., New York, **2005**.
- [24] E.J. Beckman, *J. Supercrit. Fluids* **2004**, 28, 121.
- [25] G. Brunner, *Gas Extractions*, Steinkopff, Darmstadt, **1994**.
- [26] <http://www.globalccsinstitute.com/publications/>, viewed Aug. 2013.
- [27] V.J. Krukonis, M.A. McHugh, *Supercritical fluid extraction: principles and practice*, Butterworth-Heinemann, Boston, **1994**.
- [28] S.T. Sie, G.W. Rijnders, *Anal. Chim. Acta* **1967**, 38, 31.
- [29] M.J. Tenorio, M.J. Torralvo, E. Enciso, C. Pando, J.A.R. Renuncio, A. Cabanas, *J. Supercrit. Fluids* **2009**, 49, 369.
- [30] E. Reverchon, C. Della Porta, A. Di Trollo, S. Pace, *Ind. Eng. Chem. Res.* **1998**, 37, 952.
- [31] G.R. Akien, M. Poliakoff, *Green Chem.* **2009**, 11, 1083.
- [32] P.G. Jessop, B. Subramaniam, *Chem. Rev.* **2007**, 107, 2666.
- [33] L.A. Blanchard, Z.Y. Gu, J.F. Brennecke, E.J. Beckman, *Green Industrial Applications of Ionic Liquids, Vol. 92* (Eds.: R. D. Rogers, K. R. Seddon, S. Volkov), Springer, Dordrecht, **2003**, pp. 403.
- [34] Zs. Fonyó, Gy. Fábry, *Vegyipari Műveletani Alapismertek (Chemical Engineering)*, Nemzeti Tankönyvkiadó Zrt., Budapest, **2001**.
- [35] A. Fick, *Ann. Phys.* **1855**, 170, 59.
- [36] P. Atkins, *Physical Chemistry*, 7 ed., Oxford University Press, Oxford, **2002**.

- [37] J.M. Prausnitz, R.N. Lichtenthaler, E.G. de Azavedo, *Molecular Thermodynamics of Fluid-Phase Equilibria*, Prentice-Hall, Englewood Cliffs, N.J., **1986**.
- [38] H.W. Nernst, *Z. Phys. Chem.* **1891**, *8*, 110.
- [39] R. Aveyard, R.W. Mitchell, *Transactions of the Faraday Society* **1970**, *66*, 37.
- [40] www.chemeo.com, viewed Jul. 2013.
- [41] G.X. Ma, A. Jha, *Org. Process Res. Dev.* **2005**, *9*, 847.
- [42] H.J. Lucas, *J. Am. Chem. Soc.* **1930**, *52*, 802.
- [43] A. Torvanger, M.T. Lund, N. Rive, *Mitig. Adapt. Strateg. Glob. Chang.* **2013**, *18*, 187.
- [44] J.P. Bercu, K.L. Dobo, E. Gocke, T.J. McGovern, *Int. J. Toxicol.* **2009**, *28*, 468.
- [45] A.J. Hepburn, A.J. Daugulis, *J. Chem. Technol. Biotechnol.* **2012**, *87*, 42.
- [46] K.L. Toews, R.M. Shroll, C.M. Wai, N.G. Smart, *Anal. Chem.* **1995**, *67*, 4040.
- [47] M.H. Chuang, M. Johannsen, in *International Symposium on Supercritical Fluids*, Arcachon, France, **2009**.
- [48] K.N. West, C. Wheeler, J.P. McCarney, K.N. Griffith, D. Bush, C.L. Liotta, C.A. Eckert, *J. Phys. Chem. A* **2001**, *105*, 3947.
- [49] R.F. Borch, M.D. Bernstein, H.D. Durst, *J. Am. Chem. Soc.* **1971**, *93*, 2897.
- [50] G.T. Balogh, A. Tarcsay, G.M. Keseru, *J. Pharm. Biomed. Anal.* **2012**, *67-68*, 63.
- [51] R.A. Clara, A.C. Gomez Marigliano, D. Morales, H.N. Solimo, *J. Chem. Eng. Data* **2010**, *55*, 5862.
- [52] J.F. Izquierdo, F. Cunill, M. Vila, J. Tejero, M. Iborra, *J. Chem. Eng. Data* **1992**, *37*, 339.
- [53] B. Shaik, J. Singh, I. Ahmad, D.P. Singh, S. Singh, N. Singh, V.K. Agrawal, *J. Indian Chem. Soc.* **2012**, *89*, 1375.
- [54] R. Gonzalez-Olmos, M. Iglesias, *Chemosphere* **2008**, *71*, 2098.
- [55] H. Lumbroso, C. Marschalk, *J. Chim. Phys. Phys.-Chim. Biol.* **1952**, *49*, 385.
- [56] E.C. Ihmels, J. Gmehling, *J. Chem. Eng. Data* **2002**, *47*, 1307.
- [57] C.W. Hoerr, M.R. McCorkle, A.W. Ralston, *J. Am. Chem. Soc.* **1943**, *65*, 328.
- [58] W.M. Haynes, *CRC Handbook of Chemistry and Physics*, 92 ed., CRC press, Florida, **2011**.
- [59] S.L. Shapiro, L. Freedman, E.S. Isaacs, V. Bandurco, *J. Med. Pharm. Chem.* **1962**, *5*, 793.
- [60] M. Canle, I. Demirtas, H. Maskill, *J. Chem. Soc.-Perkin Trans. 2* **2001**, 1748.
- [61] C.C. Price, P.R. Koneru, R. Shibakaw, *J. Med. Chem.* **1968**, *11*, 1226.
- [62] L. Garciarrio, E. Iglesias, J.R. Leis, M.E. Pena, A. Rios, *J. Chem. Soc.-Perkin Trans. 2* **1993**, 29.
- [63] F. Gritti, G. Guiochon, *Anal. Chem.* **2004**, *76*, 4779.
- [64] K. Valko, C.M. Du, C.D. Bevan, D.P. Reynolds, M.H. Abraham, *J. Pharm. Sci.* **2000**, *89*, 1085.
- [65] A.M. Casanovas, C. Labat, P. Courriere, J. Oustrin, *Eur. J. Med. Chem.* **1982**, *17*, 333.
- [66] F. Barbato, M.I. La Rotonda, F. Quaglia, *Pharm. Res.* **1997**, *14*, 1699.
- [67] A.J. Hoefnagel, M.A. Hoefnagel, B.M. Wepster, *J. Org. Chem.* **1981**, *46*, 4209.
- [68] M. Huerta-Fontela, M.T. Galceran, F. Ventura, *Environ. Sci. Technol.* **2008**, *42*, 6809.
- [69] R.D. O'Brien, R.W. Fisher, *J. Econ. Entomol.* **1958**, *51*, 169.
- [70] L.A. Hansch C., *Pomona College Medicinal Chemistry Project*, Claremont, CA 91711, **1987**.
- [71] Y. Mrestani, R.H.H. Neubert, A. Krause, *Pharm. Res.* **1998**, *15*, 799.
- [72] F.A. Chrzanowski, B.A. McGrogan, B.E. Maryanoff, *J. Med. Chem.* **1985**, *28*, 399.
- [73] A.M. Zissimos, M.H. Abraham, M.C. Barker, K.J. Box, K.Y. Tam, *J. Chem. Soc.-Perkin Trans. 2* **2002**, 470.
- [74] K.B. Raj, *Heterocyclic Chemistry*, 3 ed., New Age International, New Delhi, **1999**.
- [75] C. Yamagami, T. Fujita, *J. Pharm. Sci.* **2000**, *89*, 1505.
- [76] S. Xu, L. Li, Y. Tan, J. Feng, Z. Wei, L. Wang, *Bull. Environ. Contam. Toxicol.* **2000**, *64*, 316.
- [77] E.A. Castro, M. Cubillos, J.G. Santos, *J. Org. Chem.* **2004**, *69*, 4802.
- [78] D.L. Yang, G. Zuccarello, B.R. Mattes, *Macromolecules* **2002**, *35*, 5304.
- [79] A. Leo, C. Hansch, D. Elkins, *Chem. Rev.* **1971**, *71*, 525.
- [80] F. Csizmadia, A. Tsantili-Kakoulidou, I. Panderi, F. Darvas, *J. Pharm. Sci.* **1997**, *86*, 865.
- [81] J. Wang, T. Hou, *Comb. Chem. High T. Scr.* **2011**, *14*, 328.
- [82] X.G. Wang, W. Conway, R. Burns, N. McCann, M. Maeder, *J. Phys. Chem. A* **2010**, *114*, 1734.
- [83] K. Masuda, Y. Ito, M. Horiguchi, H. Fujita, *Tetrahedron* **2005**, *61*, 213.
- [84] O. Bayer, *Angew. Chem.* **1947**, *59*, 257.
- [85] D.K. Chattopadhyay, K. Raju, *Prog. Polym. Sci.* **2007**, *32*, 352.
- [86] O. Kreye, H. Mutlu, M.A.R. Meier, *Green Chem.* **2013**, *15*, 1431.
- [87] R.J. Kuhr, W.H. Dorough, *Carbamate Insecticides: Chemistry, Biochemistry, and Toxicology*, CRC Press, Cleveland, **1976**.

- [88] T.W. Greene, P.G.M. Wuts, *Protective Groups in Organic Synthesis*, Wiley, New York, **1991**.
- [89] F. Fichter, B. Becker, *Chem. Ber.* **1911**, *44*, 3473.
- [90] H.B. Wright, M.B. Moore, *J. Am. Chem. Soc.* **1948**, *70*, 3865.
- [91] C. Bosch, W. Meiser, *Process of Manufacturing Urea*, Patent number:1.429.483, USA, **1922**.
- [92] D.B. Dell'Amico, F. Calderazzo, L. Labella, F. Marchetti, G. Pampaloni, *Chem. Rev.* **2003**, *103*, 3857.
- [93] M. Caplow, *J. Am. Chem. Soc.* **1968**, *90*, 6795.
- [94] P.V. Danckwerts, *Chem. Eng. Sci.* **1979**, *34*, 443.
- [95] J.E. Crooks, J.P. Donnellan, *J. Chem. Soc.-Perkin Trans. 2* **1988**, 191.
- [96] J.E. Crooks, J.P. Donnellan, *J. Chem. Soc.-Perkin Trans. 2* **1989**, 331.
- [97] F.G. Bordwell, *Acc. Chem. Res.* **1988**, *21*, 456.
- [98] A. Ion, V. Parvulescu, P. Jacobs, D. De Vos, *Green Chem.* **2007**, *9*, 158.
- [99] E.M. Hampe, D.M. Rudkevich, *Tetrahedron* **2003**, *59*, 9619.
- [100] C. Faurholt, *Z. Anorg. Allg. Chem.* **1921**, *120*, 85.
- [101] B.G. Cox, *Acids and Bases: Solvent Effects on Acid-Base Strength*, Oxford University Press, Oxford, **2013**.
- [102] D.L. Frasco, *J. Chem. Phys.* **1964**, *41*, 2134.
- [103] M. Aresta, E. Quaranta, *Tetrahedron* **1992**, *48*, 1515.
- [104] F.C. Kinross, Ph.D. Thesis, University of Leeds, **2010**.
- [105] G. Raynel, Ph.D. Thesis, University of Leeds, **2004**.
- [106] M. Bartolini, C. Bertucci, R. Gotti, V. Tumiatti, A. Cavalli, M. Recanatini, V. Andrisano, *Journal of Chromatography A* **2002**, *958*, 59.
- [107] M. Remko, K.R. Liedl, B.M. Rode, *J. Chem. Soc. Faraday T.* **1993**, *89*, 2375.
- [108] C.J. Cheng, X.Y. Wang, L.X. Xing, B. Liu, R. Zhu, Y.F. Hu, *Adv. Synth. Catal.* **2007**, *349*, 1775.
- [109] R. Dohrn, S. Peper, J.M.S. Fonseca, *Fluid Phase Equilib.* **2010**, *288*, 1.
- [110] Z. Knez, M. Skerget, L. Ilic, C. Lutge, *J. Supercrit. Fluids* **2008**, *43*, 383.
- [111] C. Crampon, G. Charbit, E. Neau, *J. Supercrit. Fluids* **1999**, *16*, 11.
- [112] B. Kulik, S. Kruse, J. Pelto, *J. Supercrit. Fluids* **2008**, *47*, 135.
- [113] Z. Fang, R.L. Smith, H. Inomata, K. Arai, *J. Supercrit. Fluids* **2000**, *16*, 207.
- [114] J.A. Nighswander, N. Kalogerakis, A.K. Mehrotra, *J. Chem. Eng. Data* **1989**, *34*, 355.
- [115] A.E. Andreatta, L.J. Florusse, S.B. Bottini, C.J. Peters, *J. Supercrit. Fluids* **2007**, *42*, 60.
- [116] A. Kordikowski, A.P. Schenk, R.M. van Nielen, C.J. Peters, *J. Supercrit. Fluids* **1995**, *8*, 205.
- [117] C. Duran-Valencia, A. Valtz, L.A. Galicia-Luna, D. Richon, *J. Chem. Eng. Data* **2001**, *46*, 1589.
- [118] H.S. Byun, N.H. Kim, C. Kwak, *Fluid Phase Equilib.* **2003**, *208*, 53.
- [119] H.S. Byun, C.W. Lee, C.Y. Jung, *J. Chem. Eng. Data* **2004**, *49*, 53.
- [120] Z. Wagner, J. Pavlicek, *Fluid Phase Equilib.* **1994**, *97*, 119.
- [121] T.S. Reighard, S.T. Lee, S.V. Olesik, *Fluid Phase Equilib.* **1996**, *123*, 215.
- [122] F.P. Lucien, N.R. Foster, *Ind. Eng. Chem. Res.* **1996**, *35*, 4686.
- [123] S.M. Walas, *Phase Equilibria in Chemical Engineering*, Butterworth Publishers, Stoneham, MA, **1985**.
- [124] J.A. Nelder, R. Mead, *Comput. J.* **1965**, *7*, 308.
- [125] C.A. Eckert, M.J. Lazzaroni, D. Bush, J.S. Brown, *J. Chem. Eng. Data* **2005**, *50*, 60.
- [126] M. Muller, U. Meier, A. Kessler, M. Mazzotti, *Ind. Eng. Chem. Res.* **2000**, *39*, 2260.
- [127] R. Rajasingam, L. Lioe, Q.T. Pham, F.P. Lucien, *J. Supercrit. Fluids* **2004**, *31*, 227.
- [128] A.P. Abbott, E.G. Hope, R. Mistry, A.M. Stuart, *Green Chem.* **2009**, *11*, 1530.
- [129] M.E. Jones, R.W. Taft, M.J. Kamlet, *J. Am. Chem. Soc.* **1977**, *99*, 8452.
- [130] B. De Gioannis, A. Vega-Gonzalez, P. Subra, *J. Supercrit. Fluids* **2004**, *29*, 49.
- [131] M. Munto, N. Ventosa, S. Sala, J. Veciana, *J. Supercrit. Fluids* **2008**, *47*, 147.
- [132] F.E. Wubbolts, O.S.L. Bruinsma, G.M. van Rosmalen, *J. Supercrit. Fluids* **2004**, *32*, 79.
- [133] D. Suleiman, L.A. Estevez, J.C. Pulido, J.E. Garcia, C. Mojica, *J. Chem. Eng. Data* **2005**, *50*, 1234.
- [134] F.Z. Oumada, C. Rafols, M. Roses, E. Bosch, *J. Pharm. Sci.* **2002**, *91*, 991.
- [135] S. Winiwarter, N.M. Bonham, F. Ax, A. Hallberg, H. Lennernas, A. Karlen, *J. Med. Chem.* **1998**, *41*, 4939.
- [136] F. Barbato, M.I. La Rotonda, F. Quaglia, *J. Pharm. Sci.* **1997**, *86*, 225.
- [137] C.J. Chang, A.D. Randolph, *AIChE J.* **1990**, *36*, 939.
- [138] I. Kikic, N. De Zordi, M. Moneghini, D. Solinas, *J. Supercrit. Fluids* **2010**, *55*, 616.
- [139] J. Jung, M. Perrut, *J. Supercrit. Fluids* **2001**, *20*, 179.
- [140] Y.S. Youn, J.H. Oh, K.H. Ahn, M. Kim, J. Kim, Y.W. Lee, *J. Supercrit. Fluids* **2011**, *59*, 117.

- [141] E. Reverchon, *J. Supercrit. Fluids* **1999**, *15*, 1.
- [142] P. Sencar-Bozic, S. Srcic, Z. Knez, J. Kerc, *Int. J. Pharm.* **1997**, *148*, 123.
- [143] L.H. Horsley, *Azeotropic Data—III*, American Chemical Society, Washington D.C., **1973**.
- [144] H.Z. Kister, *Distillation Design*, McGraw-Hill Inc., New York, **1992**.
- [145] J.D. van der Waals, *Over de Continuïteit van den Gas- en Vloeistofoestand*, A.W. Sijthoff, Leiden, **1873**.
- [146] P.H. van Konynenburg, R.L. Scott, *Philos. T. Roy. Soc. A* **1980**, *298*, 495.
- [147] H.J. Ng, D.B. Robinson, *J. Chem. Eng. Data* **1978**, *23*, 325.
- [148] R.J. Bakker, L.W. Diamond, *Geochim. Cosmochim. Acta* **2000**, *64*, 1753.
- [149] M. Kariznovi, H. Nourozieh, J. Abedi, *J. Chem. Thermodyn.* **2011**, *43*, 1719.
- [150] S. Skjoldjorgensen, *Fluid Phase Equilib.* **1984**, *16*, 317.
- [151] Z.M. Liu, G.Y. Yang, L. Ge, B.X. Han, *J. Chem. Eng. Data* **2000**, *45*, 1179.
- [152] Ciba Holding Inc., *New 2,9-dichloroquinacridone in platelet form*, Patent number:WO2008/55807 A2, USA, **2008**.
- [153] <http://www.sigmaaldrich.com/>, viewed Sept. 2013.
- [154] B.M. Trost, *Science* **1991**, *254*, 1471.
- [155] S.K. Jha, G. Madras, *Fluid Phase Equilib.* **2005**, *238*, 174.
- [156] C.H. Wong, *Enzymes in Synthetic Organic Chemistry*, Elsevier Science Ltd., Oxford, **1994**.
- [157] K. Faber, *Biotransformations in Organic Chemistry*, Springer-Verlag, London, **2011**.
- [158] V. Koehler, K.R. Bailey, A. Znabet, J. Raftery, M. Helliwell, N.J. Turner, *Angew. Chem.-Int. Edit.* **2010**, *49*, 2182.
- [159] W. Kroutil, E.M. Fischereder, C.S. Fuchs, H. Lechner, F.G. Mutti, D. Pressnitz, A. Rajagopalan, J.H. Sattler, R.C. Simon, E. Sirola, *Org. Process Res. Dev.* **2013**, *17*, 751.
- [160] M. Stirling, J. Blacker, M.I. Page, *Tetrahedron Lett.* **2007**, *48*, 1247.
- [161] K. Orito, A. Horibata, T. Nakamura, H. Ushito, H. Nagasaki, M. Yuguchi, S. Yamashita, M. Tokuda, *J. Am. Chem. Soc.* **2004**, *126*, 14342.

Appendix - I

Description of the high pressure equipment

A-I.1 High pressure CO₂ supply system

Operation with high pressure CO₂, either liquid or supercritical, required a safe and reliable solvent supply system. The CO₂ set-up was fitted in the Wolfson CO₂ Laboratory of the University of Leeds. It was designed for the continuous supply of CO₂ at pressures up to 40 MPa for the connected units.

The CO₂ was stored in a liquid withdrawal cylinder. Shut-off valves were installed on-line to allow emergency stop of the flow if leak occurred. The cylinder was connected to a scavenger unit consisting of two packed columns. Alumina packing in one of the columns removed the traces of water, and activated hydrogenation catalyst in the other column removed the traces of oxygen from the CO₂ stream. A filter was also installed after the scavenger unit to protect the pump (Figure A-I.1).

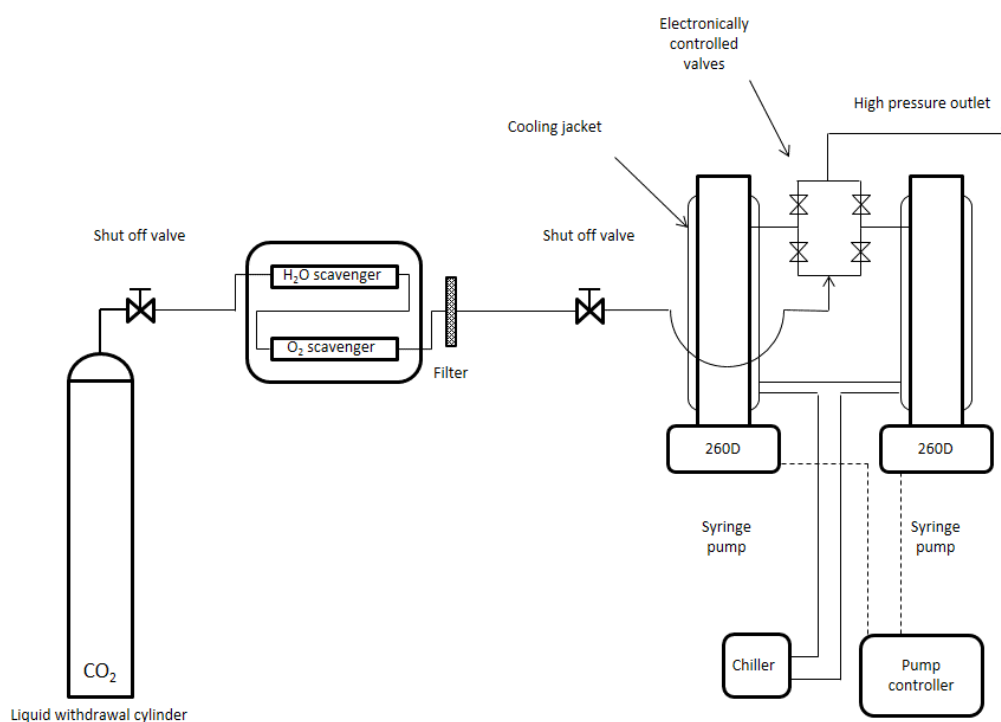


Figure A-I.1. The cylinder-scavenger-pump line of the high pressure system.

The liquid CO₂ was pressurised with a pair of Isco 260D syringe pumps (Figure A-I.3). The pumps were chilled to allow their charging with CO₂. Their temperature during operation was about -5 °C. The pumps were installed for simultaneous operation, therefore they could supply pressurised CO₂ continuously, either in constant pressure mode or constant flow mode.

The outlet of the high pressure pumps was connected to a central control panel (Figure A-I.3), which could supply four CO₂ consumer units if operating in constant

pressure mode. The central control panel was equipped with HPLC ports, which could be used to supply solvents/solutions to the experimental units. To avoid flow from the HPLC pumps into the syringe pumps, check valves were installed (Figure A-I.2).

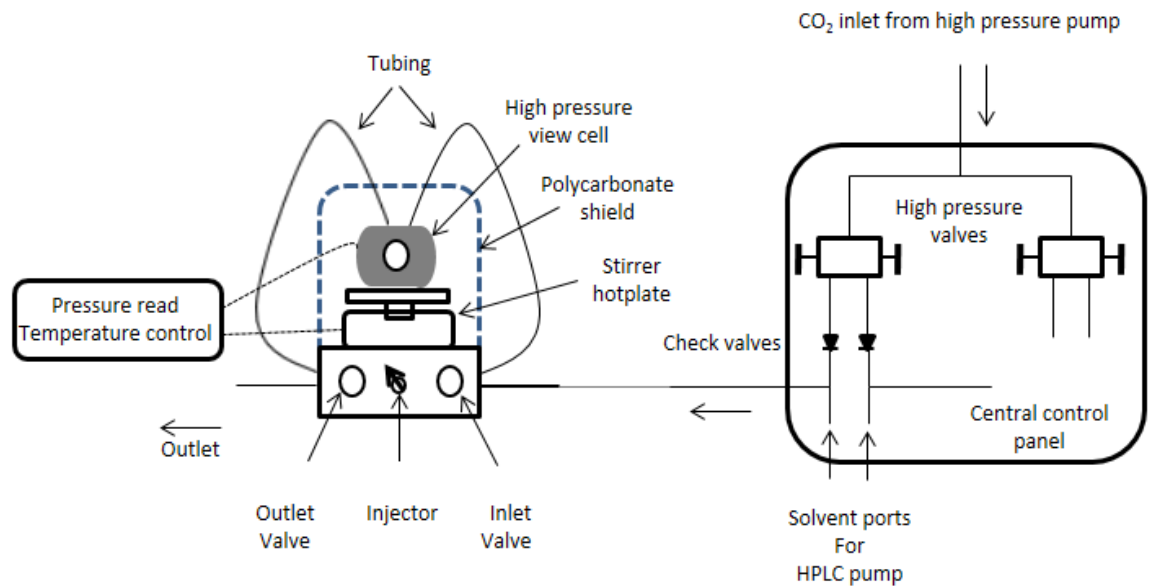


Figure A-I.2. Central control unit – control box – high pressure cell line of the high pressure system



Figure A-I.3. Photo of the high pressure CO₂ supply system. Central control panel (1); high pressure pump (2); chiller (3); HPLC pump (4).

The central control unit was connected to control boxes through 316 stainless steel tubing (o.d.: 1/16"; i.d.: 0.0225"). The control boxes were equipped with SSI valves that allowed loading or venting the pressure cells. They also had a Rheodyne 7125 HPLC injector loop on-line. This allowed injection of 1 ml liquid into an already pressurised reactor. The control boxes had Zook rupture plates built in between the cell and the outlet port, for safety reasons (size: 1/2"; type: PB-ST; material: 316SS; burst pressure: 18.2±10% MPa). An electronic pressure gauge was also installed to the control box, branching from the cell inlet tubing (Omega MMG5.0KV5P5A6T3A5; accuracy: ±0.2%). An electronic pressure transducer displayed the pressure.

A polycarbonate shield was also installed on the top of the control box, for safety reasons. The pressure cell was sitting on a stirrer hotplate unit, within the shield. The temperature of the reactor wall was measured by a K-type (accuracy: ±1 °C) thermocouple inserted into a pre-drilled hole. A PID control unit maintained the set temperature by controlling the heating power of the hot plate. The temperature of the hotplate was also monitored by the controller, and a cascade control mode was

implemented. The heat controller and the pressure transducer were built into the same unit, displaying the actual pressure and temperature (Figure A-I.5).

The system was modified for operation below room temperature. A Peltier module (Custom Thermoelectric 12711-6M31-26CW), cooled by a water block, was installed to cool the cell, and allowed operation as low as -20 °C.

A-I.2 High pressure view cells

A-I.2.1 General design of high pressure cells

The high pressure view cells were designed and built by the research group at Leeds using 316 stainless steel. The diameter of the cylindrical inner cavity of the view cells was 25.5 mm and the length was 35 mm. The test pressure of the cells was 20 MPa. The view cells were the weakest element of the system in terms of pressure rating. The rupture plates limited the pressure of the cells to 16 MPa. The maximum allowed sustained pressure of the cells was 13.5 MPa.

The reactor consisted of a body and a lid. Both body and lid had a 15 mm thick borosilicate glass window, allowing internal viewing. The lid could be routinely removed to allow efficient sample removal or cleaning. In operation, the lid was sealed by a BS218 O-ring, and held in place by four high tensile grade 12.9 bolts with hex socket heads. The reactor body had 1/8" NPT female pipe thread on the top for inlet and outlet, or thermometer connection.

A-I.2.2 High pressure cell, modified for isolation of solid under pressure

A special setup was also designed for solid isolation under pressure (Figure A-I.4). The equipment was built around a cell with a bottom withdrawal port. The port was connected to a spring loaded GO BP66 back pressure regulator through a filter compartment. Continuous flow CO₂ was maintained by the syringe pumps, and the BPR was controlling the pressure. The vessel contents were discharged with the flow, and the solid was collected in the filter compartment (Figure A-I.4-A-I.6).

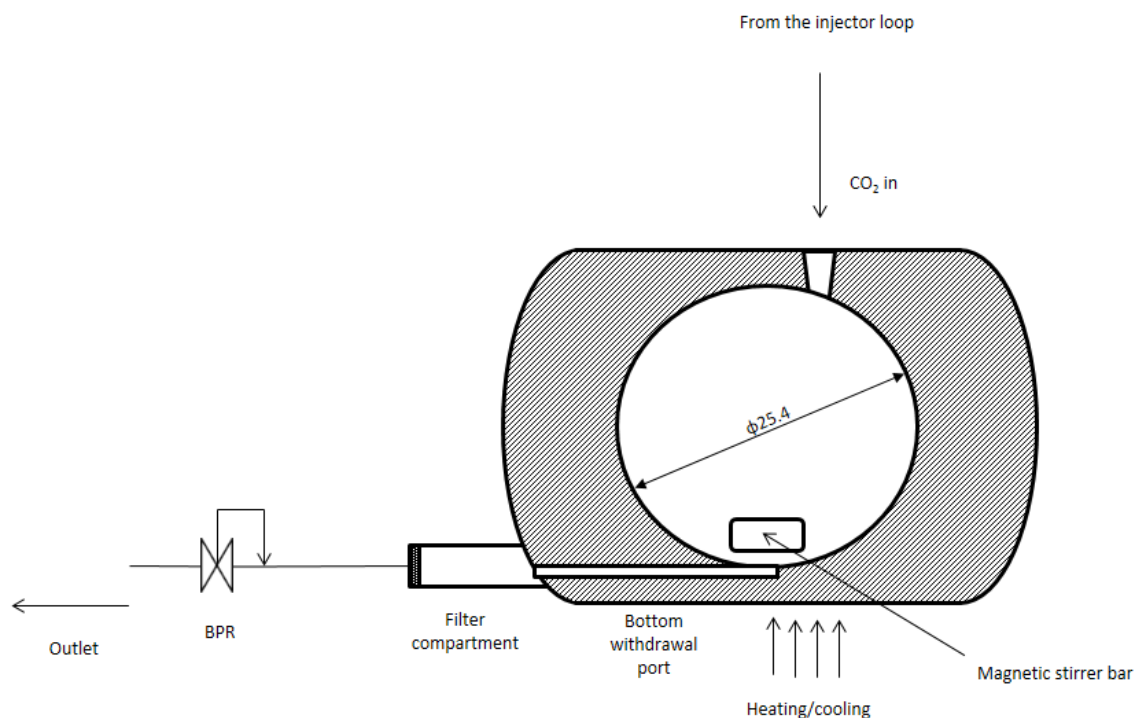


Figure A-I.4. Equipment designed for isolation of solid at high pressures. The CO₂ antisolvent could enter the cell through the inlet, and could continuously dilute the solution. The content of the cell was leaving through the bottom withdrawal port. The solid was accumulated in the filter compartment. The pressure within the cell was controlled by a back pressure regulator.

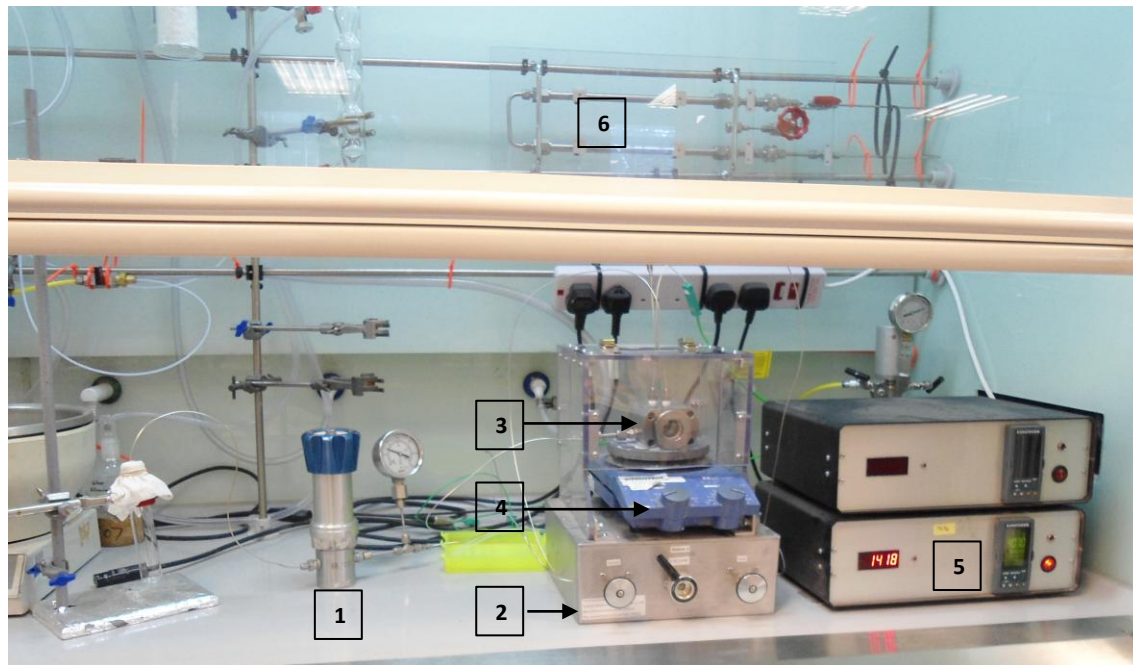
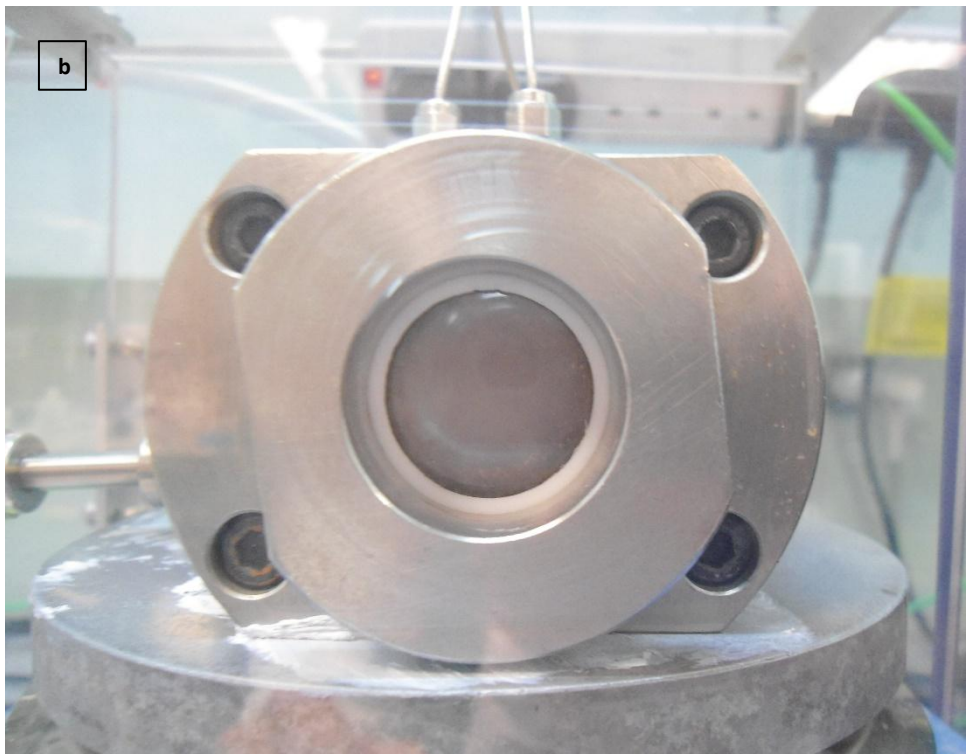
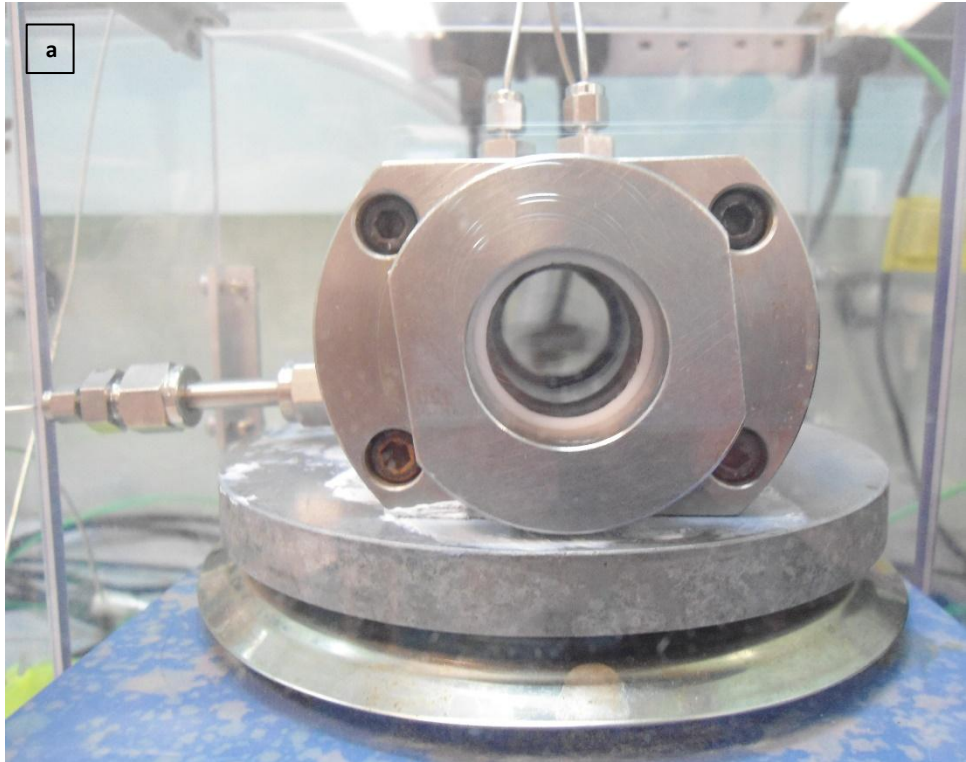


Figure A-I.5. Photo of the experimental set-up. From left to right: back pressure regulator (1); control box (2) with pressure cell equipped with bottom withdrawal port (3) sitting on a hotplate (4); temperature controller and pressure transducer unit (5); the scavenger unit can be seen in the background (6).

A7



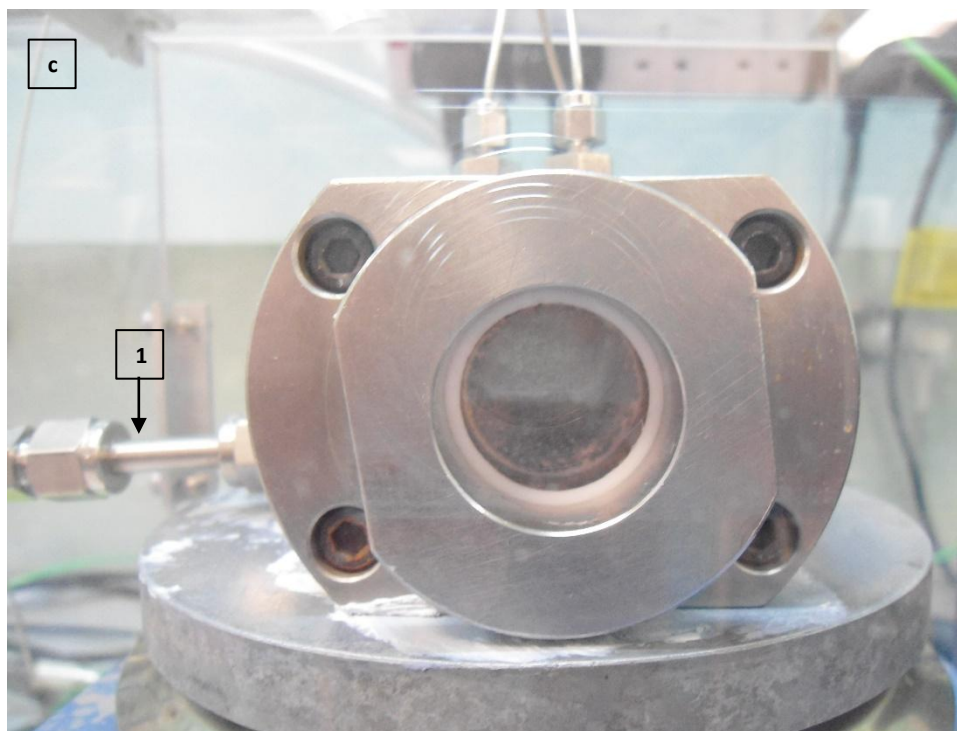


Figure A-I.6a-c. Photo of the high pressure cell with bottom withdrawal in operation for solid isolation; a, before the injection - the cell was loaded with scCO_2 being stirred; b, shortly after injection of 1 ml solution of Omeprazole **21** in tetramethyl urea (100 g/l) - transparency ceased because of solid precipitation; c, after 40 minutes of CO_2 streaming (3 ml/min) through the stirred cell - precipitate was still visible, but the cell became transparent. Most of the precipitate was collected from the filter compartment (1) after venting.

A-I.3 Qualitative determination of volumetric expansion in view cell

The volume of the initial solution was known, it was 1 ml in most expansion experiments. Increasing the CO_2 pressure over the solution caused volumetric expansion. The volume of the expanded solution was estimated from the filled reactor volume. The volume of stirrer bar and possible precipitate were neglected (Figure A-I.7).

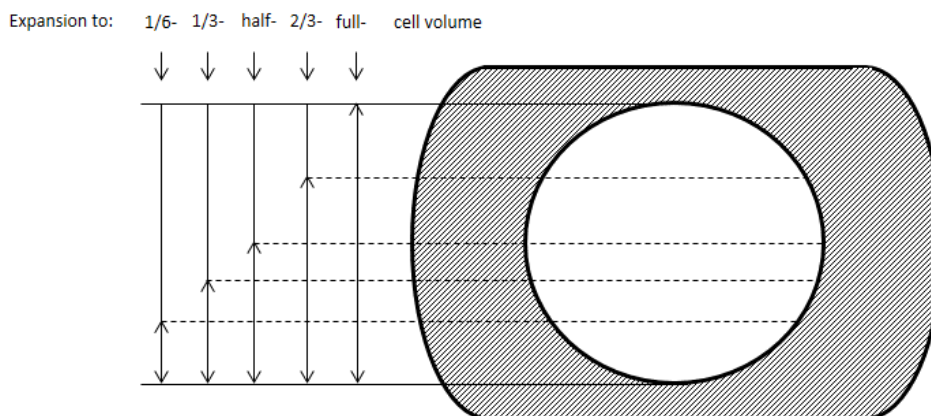


Figure A-I.7. The volumetric expansion caused by CO_2 was qualitatively estimated by the approximate occupied reactor volume. The full volume of the cell was 17 ml.

Appendix - II

X-ray crystallographic data tables and structure refinement

Table A-II.1. X-ray crystallographic analysis of *o*-aminobenzyl methylamine carbamate monohydrate dimer (Figure 6.9).

| | | | |
|----------------------|-----------------------------|---------------------------|-----------------------------|
| Formula | $C_{34}H_{52}N_8O_6$ | | |
| Formula weight | 668 g mol^{-1} | | |
| Wavelength | 0.71073 Å | | |
| Space group | P -1 | | |
| Cell lengths | $a = 7.6470(8)$ Å | $b = 8.9223(9)$ Å | $c = 14.8563(16)$ Å |
| Cell angles | $\alpha = 104.468(5)^\circ$ | $\beta = 94.863(5)^\circ$ | $\gamma = 105.430(5)^\circ$ |
| Cell volume | 933.603 Å ³ | | |
| Reduced cell lengths | $a = 7.647$ | $c = 8.9223$ | $c = 14.8563$ |

Table A-II.2. Atomic co-ordinates and equivalent isotropic displacement parameters (Å²) with standard uncertainties in parentheses for carbon, nitrogen and oxygen atoms. U_{eq} is defined as 1/3 of the trace of the orthogonalised U_{ij} tensor.

| Atom | x | y | z | U_{eq} |
|------|-----------|-----------|-------------|----------|
| C1 | 0.5959(3) | 0.3795(2) | 0.27679(15) | 0.0222 |
| C1 | 1.4041(3) | 1.6205(2) | 0.72321(15) | 0.0222 |
| C10 | 0.6475(3) | 0.8348(2) | 0.36701(15) | 0.0234 |
| C10 | 1.3525(3) | 1.1652(2) | 0.63299(15) | 0.0234 |
| C2 | 0.5006(3) | 0.4433(2) | 0.21576(15) | 0.0232 |
| C2 | 1.4994(3) | 1.5567(2) | 0.78424(15) | 0.0232 |
| C21 | 1.0425(3) | 0.7456(3) | 0.23273(17) | 0.0298 |
| C21 | 0.9575(3) | 1.2544(3) | 0.76727(17) | 0.0298 |
| C22 | 1.1583(3) | 0.9054(3) | 0.24345(16) | 0.0265 |
| C22 | 0.8417(3) | 1.0946(3) | 0.75655(16) | 0.0265 |
| C23 | 1.1805(3) | 0.9642(3) | 0.16387(17) | 0.0342 |
| C23 | 0.8195(3) | 1.0358(3) | 0.83613(17) | 0.0342 |
| C24 | 1.0917(4) | 0.8667(4) | 0.07331(18) | 0.0445 |
| C24 | 0.9083(4) | 1.1333(4) | 0.92669(18) | 0.0445 |
| C25 | 0.9827(4) | 0.7065(4) | 0.06213(19) | 0.0473 |
| C25 | 1.0173(4) | 1.2935(4) | 0.93787(19) | 0.0473 |
| C26 | 0.9583(3) | 0.6467(3) | 0.1399(2) | 0.0408 |
| C26 | 1.0417(3) | 1.3533(3) | 0.8601(2) | 0.0408 |
| C27 | 1.2630(3) | 1.0116(3) | 0.34007(16) | 0.026 |
| C27 | 0.7370(3) | 0.9884(3) | 0.65993(16) | 0.026 |
| C29 | 1.1270(3) | 1.2457(3) | 0.37237(19) | 0.0337 |
| C29 | 0.8730(3) | 0.7543(3) | 0.62763(19) | 0.0337 |
| C3 | 0.4812(3) | 0.3764(3) | 0.11735(16) | 0.0291 |
| C3 | 1.5188(3) | 1.6236(3) | 0.88265(16) | 0.0291 |
| C4 | 0.5543(4) | 0.2508(3) | 0.07759(17) | 0.0328 |
| C4 | 1.4457(4) | 1.7492(3) | 0.92241(17) | 0.0328 |
| C5 | 0.6480(3) | 0.1886(3) | 0.13787(17) | 0.0317 |
| C5 | 1.3520(3) | 1.8114(3) | 0.86213(17) | 0.0317 |
| C6 | 0.6672(3) | 0.2507(3) | 0.23608(16) | 0.0276 |
| C6 | 1.3328(3) | 1.7493(3) | 0.76392(16) | 0.0276 |
| C7 | 0.4226(3) | 0.5826(3) | 0.25623(16) | 0.0247 |

A11

| | | | | |
|-----|-----------|-------------|-------------|--------|
| C7 | 1.5774(3) | 1.4174(3) | 0.74377(16) | 0.0247 |
| C9 | 0.5985(4) | 0.8070(3) | 0.19521(17) | 0.0319 |
| C9 | 1.4015(4) | 1.1930(3) | 0.80479(17) | 0.0319 |
| N1 | 0.6100(3) | 0.4350(2) | 0.37529(13) | 0.0282 |
| N1 | 1.3900(3) | 1.5650(2) | 0.62471(13) | 0.0282 |
| N21 | 1.0047(3) | 0.6876(3) | 0.31080(17) | 0.0377 |
| N21 | 0.9953(3) | 1.3124(3) | 0.68920(17) | 0.0377 |
| N28 | 1.1480(3) | 1.0992(2) | 0.39981(13) | 0.0259 |
| N28 | 0.8520(3) | 0.9008(2) | 0.60019(13) | 0.0259 |
| N8 | 0.5585(3) | 0.7458(2) | 0.27717(13) | 0.0257 |
| N8 | 1.4415(3) | 1.2542(2) | 0.72283(13) | 0.0257 |
| O11 | 0.7655(2) | 0.97396(18) | 0.37908(12) | 0.0304 |
| O11 | 1.2345(2) | 1.02604(18) | 0.62092(12) | 0.0304 |
| O12 | 0.6068(2) | 0.77397(19) | 0.43626(10) | 0.0281 |
| O12 | 1.3932(2) | 1.22603(19) | 0.56374(10) | 0.0281 |
| O30 | 0.7399(2) | 1.2489(2) | 0.50637(12) | 0.0312 |
| O30 | 1.2601(2) | 0.7511(2) | 0.49363(12) | 0.0312 |

Table A-II.3. Hydrogen atom co-ordinates and isotropic displacement parameters (\AA^2) with standard uncertainties in parentheses.

| Atom | x | y | z | U_{eq} |
|------|----------|----------|------------|----------|
| H1A | 0.678(4) | 0.389(3) | 0.4053(19) | 0.032 |
| H1A | 1.322(4) | 1.611(3) | 0.5947(19) | 0.032 |
| H1B | 0.611(3) | 0.537(3) | 0.4024(18) | 0.026 |
| H1B | 1.389(3) | 1.463(3) | 0.5976(18) | 0.026 |
| H21A | 1.101(5) | 0.725(4) | 0.366(2) | 0.058 |
| H21A | 0.899(5) | 1.275(4) | 0.634(2) | 0.058 |
| H21B | 0.937(5) | 0.585(4) | 0.296(2) | 0.052 |
| H21B | 1.063(5) | 1.415(4) | 0.704(2) | 0.052 |
| H23 | 1.261(4) | 1.070(3) | 0.1707(17) | 0.026 |
| H23 | 0.739(4) | 0.930(3) | 0.8293(17) | 0.026 |
| H24 | 1.111(4) | 0.907(4) | 0.018(2) | 0.056 |
| H24 | 0.889(4) | 1.093(4) | 0.982(2) | 0.056 |
| H25 | 0.932(4) | 0.633(4) | -0.002(2) | 0.051 |
| H25 | 1.068(4) | 1.367(4) | 1.002(2) | 0.051 |
| H26 | 0.879(5) | 0.539(5) | 0.130(3) | 0.065 |
| H26 | 1.121(5) | 1.461(5) | 0.870(3) | 0.065 |
| H27A | 1.320(3) | 0.947(3) | 0.3788(18) | 0.028 |
| H27A | 0.680(3) | 1.053(3) | 0.6212(18) | 0.028 |
| H27B | 1.369(4) | 1.091(3) | 0.3326(18) | 0.031 |
| H27B | 0.631(4) | 0.909(3) | 0.6674(18) | 0.031 |
| H28A | 1.210(4) | 1.140(3) | 0.464(2) | 0.038 |
| H28A | 0.790(4) | 0.860(3) | 0.536(2) | 0.038 |
| H28B | 1.032(4) | 1.029(4) | 0.399(2) | 0.038 |
| H28B | 0.968(4) | 0.971(4) | 0.601(2) | 0.038 |

A12

| | | | | |
|------|----------|----------|------------|-------|
| H29A | 1.074(4) | 1.215(3) | 0.308(2) | 0.035 |
| H29A | 0.926(4) | 0.785(3) | 0.692(2) | 0.035 |
| H29B | 1.046(4) | 1.296(4) | 0.413(2) | 0.05 |
| H29B | 0.954(4) | 0.704(4) | 0.587(2) | 0.05 |
| H29C | 1.258(4) | 1.327(3) | 0.3817(18) | 0.03 |
| H29C | 0.742(4) | 0.673(3) | 0.6183(18) | 0.03 |
| H3 | 0.412(4) | 0.417(3) | 0.0759(19) | 0.032 |
| H3 | 1.588(4) | 1.583(3) | 0.9241(19) | 0.032 |
| H30A | 0.624(5) | 1.229(4) | 0.519(2) | 0.06 |
| H30A | 1.376(5) | 0.771(4) | 0.481(2) | 0.06 |
| H30B | 0.747(5) | 1.143(5) | 0.466(3) | 0.07 |
| H30B | 1.253(5) | 0.857(5) | 0.534(3) | 0.07 |
| H4 | 0.539(4) | 0.200(4) | 0.010(2) | 0.051 |
| H4 | 1.461(4) | 1.800(4) | 0.990(2) | 0.051 |
| H5 | 0.698(4) | 0.096(3) | 0.1091(18) | 0.03 |
| H5 | 1.302(4) | 1.904(3) | 0.8909(18) | 0.03 |
| H6 | 0.724(4) | 0.201(3) | 0.281(2) | 0.038 |
| H6 | 1.276(4) | 1.799(3) | 0.719(2) | 0.038 |
| H7A | 0.374(3) | 0.572(3) | 0.3146(18) | 0.024 |
| H7A | 1.626(3) | 1.428(3) | 0.6854(18) | 0.024 |
| H7B | 0.318(4) | 0.573(3) | 0.2096(18) | 0.03 |
| H7B | 1.682(4) | 1.427(3) | 0.7904(18) | 0.03 |
| H9A | 0.614(4) | 0.719(3) | 0.1418(19) | 0.034 |
| H9A | 1.386(4) | 1.281(3) | 0.8582(19) | 0.034 |
| H9B | 0.500(5) | 0.846(4) | 0.174(2) | 0.054 |
| H9B | 1.500(5) | 1.154(4) | 0.826(2) | 0.054 |
| H9C | 0.724(5) | 0.896(5) | 0.216(3) | 0.074 |
| H9C | 1.276(5) | 1.104(5) | 0.784(3) | 0.074 |

Table A-II.4. Anisotropic displacement parameters (\AA^2). The anisotropic displacement factor exponent takes the form: $-2\pi^2[h^2a^*{}^2U_{11} + \dots + 2hka^*b^*U_{12}]$.

| Atom | U11 | U22 | U33 | U12 | U13 | U23 |
|------|--------|--------|--------|--------|---------|---------|
| C1 | 0.019 | 0.0207 | 0.0255 | 0.0025 | 0.0027 | 0.0078 |
| C10 | 0.0209 | 0.0222 | 0.0284 | 0.0101 | 0.0057 | 0.0052 |
| C2 | 0.0205 | 0.0213 | 0.026 | 0.0044 | 0.002 | 0.0058 |
| C21 | 0.021 | 0.0299 | 0.0387 | 0.0116 | 0.0043 | 0.0059 |
| C22 | 0.0211 | 0.0306 | 0.0284 | 0.0101 | 0.0038 | 0.0067 |
| C23 | 0.0296 | 0.045 | 0.032 | 0.0151 | 0.0091 | 0.0125 |
| C24 | 0.0428 | 0.071 | 0.0272 | 0.0297 | 0.0092 | 0.0122 |
| C25 | 0.0377 | 0.063 | 0.0327 | 0.0272 | -0.0055 | -0.0108 |
| C26 | 0.0262 | 0.0376 | 0.0484 | 0.0126 | -0.0036 | -0.0062 |
| C27 | 0.0199 | 0.0284 | 0.0286 | 0.0048 | 0.0041 | 0.0084 |
| C29 | 0.0295 | 0.0319 | 0.0414 | 0.0092 | 0.0062 | 0.0134 |
| C3 | 0.0312 | 0.0278 | 0.0256 | 0.0054 | -0.0002 | 0.008 |
| C4 | 0.0441 | 0.0277 | 0.0243 | 0.0084 | 0.0083 | 0.0048 |
| C5 | 0.0376 | 0.0234 | 0.0355 | 0.0098 | 0.013 | 0.0076 |
| C6 | 0.0279 | 0.0246 | 0.0336 | 0.0086 | 0.0065 | 0.0126 |
| C7 | 0.0212 | 0.0266 | 0.0254 | 0.008 | -0.0005 | 0.0061 |
| C9 | 0.0428 | 0.0309 | 0.0301 | 0.0174 | 0.0102 | 0.0149 |
| N1 | 0.0338 | 0.0265 | 0.0242 | 0.0104 | 0.0003 | 0.0067 |
| N21 | 0.0279 | 0.032 | 0.052 | 0.0022 | 0.0047 | 0.0176 |
| N28 | 0.0223 | 0.0274 | 0.0254 | 0.003 | 0.0036 | 0.0075 |
| N8 | 0.0293 | 0.0237 | 0.0266 | 0.0105 | 0.0038 | 0.0088 |
| O11 | 0.0257 | 0.0225 | 0.0408 | 0.0063 | 0.0093 | 0.0048 |
| O12 | 0.0286 | 0.0291 | 0.0241 | 0.0072 | 0.0047 | 0.0046 |
| O30 | 0.0318 | 0.0288 | 0.0343 | 0.0099 | 0.0083 | 0.0093 |

Table A-II.5. Interatomic distances (Å) with standard uncertainties in parentheses.

| Atom1 | Atom2 | Length | Atom1 | Atom2 | Length |
|-------|-------|----------|-------|-------|----------|
| N1 | C1 | 1.407(3) | N21 | H21A | 0.98(3) |
| N1 | H1A | 0.90(3) | N21 | H21B | 0.88(3) |
| N1 | H1B | 0.90(3) | C21 | C22 | 1.426(3) |
| C1 | C2 | 1.430(3) | C21 | C26 | 1.426(3) |
| C1 | C6 | 1.423(3) | C22 | C23 | 1.414(4) |
| C2 | C3 | 1.413(3) | C22 | C27 | 1.524(3) |
| C2 | C7 | 1.531(3) | C23 | H23 | 0.96(2) |
| C3 | H3 | 0.97(3) | C23 | C24 | 1.405(3) |
| C3 | C4 | 1.406(4) | C24 | H24 | 0.98(3) |
| C4 | H4 | 0.98(3) | C24 | C25 | 1.410(4) |
| C4 | C5 | 1.405(4) | C25 | H25 | 0.99(3) |
| C5 | H5 | 1.02(3) | C25 | C26 | 1.395(5) |
| C5 | C6 | 1.405(3) | C26 | H26 | 0.96(4) |
| C6 | H6 | 1.02(3) | C27 | N28 | 1.524(3) |
| C7 | N8 | 1.487(3) | C27 | H27A | 1.05(3) |
| C7 | H7A | 0.99(3) | C27 | H27B | 0.96(3) |
| C7 | H7B | 0.98(3) | N28 | C29 | 1.506(4) |
| N8 | C9 | 1.477(3) | N28 | H28A | 0.96(3) |
| N8 | C10 | 1.380(3) | N28 | H28B | 0.94(3) |
| C9 | H9A | 1.01(3) | C29 | H29A | 0.95(3) |
| C9 | H9B | 0.97(4) | C29 | H29B | 1.01(3) |
| C9 | H9C | 1.03(3) | C29 | H29C | 1.04(3) |
| C10 | O11 | 1.286(2) | O30 | H30A | 0.90(4) |
| C10 | O12 | 1.301(3) | O30 | H30B | 1.00(4) |
| N21 | C21 | 1.405(4) | | | |

Table A-II.6. Angles between interatomic vectors (°) with standard uncertainties in parentheses.

| Atom1 | Atom2 | Atom3 | Angle | Atom1 | Atom2 | Atom3 | Angle |
|-------|-------|-------|----------|-------|-------|-------|----------|
| C1 | N1 | H1A | 112(2) | C21 | N21 | H21B | 114(2) |
| C1 | N1 | H1B | 120(2) | H21A | N21 | H21B | 117(3) |
| H1A | N1 | H1B | 119(2) | N21 | C21 | C22 | 121.7(2) |
| N1 | C1 | C2 | 121.2(2) | N21 | C21 | C26 | 120.1(2) |
| N1 | C1 | C6 | 120.0(2) | C22 | C21 | C26 | 118.1(2) |
| C2 | C1 | C6 | 118.7(2) | C21 | C22 | C23 | 120.0(2) |
| C1 | C2 | C3 | 118.8(2) | C21 | C22 | C27 | 120.2(2) |
| C1 | C2 | C7 | 120.6(2) | C23 | C22 | C27 | 119.7(2) |
| C3 | C2 | C7 | 120.6(2) | C22 | C23 | H23 | 120(2) |
| C2 | C3 | H3 | 119(2) | C22 | C23 | C24 | 121.0(2) |
| C2 | C3 | C4 | 122.2(2) | H23 | C23 | C24 | 119(2) |
| H3 | C3 | C4 | 119(2) | C23 | C24 | H24 | 121(2) |
| C3 | C4 | H4 | 124(2) | C23 | C24 | C25 | 119.0(3) |
| C3 | C4 | C5 | 118.8(2) | H24 | C24 | C25 | 120(2) |
| H4 | C4 | C5 | 117(2) | C24 | C25 | H25 | 119(2) |
| C4 | C5 | H5 | 119(2) | C24 | C25 | C26 | 120.8(3) |
| C4 | C5 | C6 | 120.4(2) | H25 | C25 | C26 | 120(2) |
| H5 | C5 | C6 | 121(2) | C21 | C26 | C25 | 121.0(2) |
| C1 | C6 | C5 | 121.1(2) | C21 | C26 | H26 | 120(3) |
| C1 | C6 | H6 | 117(2) | C25 | C26 | H26 | 118(3) |
| C5 | C6 | H6 | 122(2) | C22 | C27 | N28 | 113.4(2) |
| C2 | C7 | N8 | 113.6(2) | C22 | C27 | H27A | 113(1) |
| C2 | C7 | H7A | 111(1) | C22 | C27 | H27B | 109(2) |
| C2 | C7 | H7B | 107(2) | N28 | C27 | H27A | 109(1) |
| N8 | C7 | H7A | 108(1) | N28 | C27 | H27B | 109(2) |
| N8 | C7 | H7B | 110(2) | H27A | C27 | H27B | 103(2) |
| H7A | C7 | H7B | 107(2) | C27 | N28 | C29 | 113.4(2) |
| C7 | N8 | C9 | 116.1(2) | C27 | N28 | H28A | 109(2) |
| C7 | N8 | C10 | 122.8(2) | C27 | N28 | H28B | 112(2) |
| C9 | N8 | C10 | 121.1(2) | C29 | N28 | H28A | 105(2) |
| N8 | C9 | H9A | 111(2) | C29 | N28 | H28B | 110(2) |
| N8 | C9 | H9B | 111(2) | H28A | N28 | H28B | 108(3) |
| N8 | C9 | H9C | 107(2) | N28 | C29 | H29A | 110(2) |
| H9A | C9 | H9B | 109(3) | N28 | C29 | H29B | 110(2) |
| H9A | C9 | H9C | 107(3) | N28 | C29 | H29C | 108(2) |
| H9B | C9 | H9C | 113(3) | H29A | C29 | H29B | 110(3) |
| N8 | C10 | O11 | 119.1(2) | H29A | C29 | H29C | 109(2) |
| N8 | C10 | O12 | 118.1(2) | H29B | C29 | H29C | 111(2) |
| O11 | C10 | O12 | 122.8(2) | H30A | O30 | H30B | 105(3) |
| C21 | N21 | H21A | 118(2) | | | | |

Table A-II.7. Torsion angles (°) with standard uncertainties in parentheses.

| Atom1 | Atom2 | Atom3 | Atom4 | Torsion | Atom1 | Atom2 | Atom3 | Atom4 | Torsion |
|-------|-------|-------|-------|-----------|-------|-------|-------|-------|-----------|
| H1A | N1 | C1 | C2 | -177(2) | H21A | N21 | C21 | C26 | 149(2) |
| H1A | N1 | C1 | C6 | 7(2) | H21B | N21 | C21 | C22 | -176(2) |
| H1B | N1 | C1 | C2 | -30(2) | H21B | N21 | C21 | C26 | 6(2) |
| H1B | N1 | C1 | C6 | 154(2) | N21 | C21 | C22 | C23 | -174.6(2) |
| N1 | C1 | C2 | C3 | -176.3(2) | N21 | C21 | C22 | C27 | 7.2(4) |
| N1 | C1 | C2 | C7 | 4.3(3) | C26 | C21 | C22 | C23 | 2.8(4) |
| C6 | C1 | C2 | C3 | -0.2(3) | C26 | C21 | C22 | C27 | -175.4(2) |
| C6 | C1 | C2 | C7 | -179.6(2) | N21 | C21 | C26 | C25 | 175.0(3) |
| N1 | C1 | C6 | C5 | 177.3(2) | N21 | C21 | C26 | H26 | -2(3) |
| N1 | C1 | C6 | H6 | 2(2) | C22 | C21 | C26 | C25 | -2.4(4) |
| C2 | C1 | C6 | C5 | 1.2(3) | C22 | C21 | C26 | H26 | -180(3) |
| C2 | C1 | C6 | H6 | -175(2) | C21 | C22 | C23 | H23 | -178(2) |
| C1 | C2 | C3 | H3 | 178(2) | C21 | C22 | C23 | C24 | -0.8(4) |
| C1 | C2 | C3 | C4 | -0.8(3) | C27 | C22 | C23 | H23 | 0(2) |
| C7 | C2 | C3 | H3 | -3(2) | C27 | C22 | C23 | C24 | 177.4(2) |
| C7 | C2 | C3 | C4 | 178.6(2) | C21 | C22 | C27 | N28 | -83.0(3) |
| C1 | C2 | C7 | N8 | 85.4(3) | C21 | C22 | C27 | H27A | 41(2) |
| C1 | C2 | C7 | H7A | -37(2) | C21 | C22 | C27 | H27B | 156(2) |
| C1 | C2 | C7 | H7B | -153(2) | C23 | C22 | C27 | N28 | 98.8(3) |
| C3 | C2 | C7 | N8 | -94.0(3) | C23 | C22 | C27 | H27A | -137(2) |
| C3 | C2 | C7 | H7A | 144(2) | C23 | C22 | C27 | H27B | -23(2) |
| C3 | C2 | C7 | H7B | 27(2) | C22 | C23 | C24 | H24 | -178(2) |
| C2 | C3 | C4 | H4 | 178(2) | C22 | C23 | C24 | C25 | -1.6(4) |
| C2 | C3 | C4 | C5 | 0.7(4) | H23 | C23 | C24 | H24 | -1(3) |
| H3 | C3 | C4 | H4 | -1(3) | H23 | C23 | C24 | C25 | 176(2) |
| H3 | C3 | C4 | C5 | -178(2) | C23 | C24 | C25 | H25 | -173(2) |
| C3 | C4 | C5 | H5 | 179(2) | C23 | C24 | C25 | C26 | 2.0(4) |
| C3 | C4 | C5 | C6 | 0.3(4) | H24 | C24 | C25 | H25 | 4(3) |
| H4 | C4 | C5 | H5 | 1(3) | H24 | C24 | C25 | C26 | 178(2) |
| H4 | C4 | C5 | C6 | -177(2) | C24 | C25 | C26 | C21 | 0.1(4) |
| C4 | C5 | C6 | C1 | -1.2(4) | C24 | C25 | C26 | H26 | 177(3) |
| C4 | C5 | C6 | H6 | 174(2) | H25 | C25 | C26 | C21 | 175(2) |
| H5 | C5 | C6 | C1 | -179(2) | H25 | C25 | C26 | H26 | -8(4) |
| H5 | C5 | C6 | H6 | -4(3) | C22 | C27 | N28 | C29 | -78.1(2) |
| C2 | C7 | N8 | C9 | 76.7(3) | C22 | C27 | N28 | H28A | 165(2) |
| C2 | C7 | N8 | C10 | -101.5(2) | C22 | C27 | N28 | H28B | 47(2) |
| H7A | C7 | N8 | C9 | -160(2) | H27A | C27 | N28 | C29 | 155(1) |
| H7A | C7 | N8 | C10 | 22(2) | H27A | C27 | N28 | H28A | 39(2) |
| H7B | C7 | N8 | C9 | -43(2) | H27A | C27 | N28 | H28B | -80(3) |
| H7B | C7 | N8 | C10 | 139(2) | H27B | C27 | N28 | C29 | 44(2) |
| C7 | N8 | C9 | H9A | -44(2) | H27B | C27 | N28 | H28A | -73(3) |
| C7 | N8 | C9 | H9B | 77(2) | H27B | C27 | N28 | H28B | 169(3) |
| C7 | N8 | C9 | H9C | -159(2) | C27 | N28 | C29 | H29A | 57(2) |
| C10 | N8 | C9 | H9A | 135(2) | C27 | N28 | C29 | H29B | 178(2) |

A17

| | | | | | | | | | |
|------|-----|-----|-----|-----------|------|-----|-----|------|--------|
| C10 | N8 | C9 | H9B | -104(2) | C27 | N28 | C29 | H29C | -61(2) |
| C10 | N8 | C9 | H9C | 19(2) | H28A | N28 | C29 | H29A | 176(3) |
| C7 | N8 | C10 | O11 | 178.9(2) | H28A | N28 | C29 | H29B | -63(3) |
| C7 | N8 | C10 | O12 | -1.6(3) | H28A | N28 | C29 | H29C | 58(2) |
| C9 | N8 | C10 | O11 | 0.8(3) | H28B | N28 | C29 | H29A | -68(3) |
| C9 | N8 | C10 | O12 | -179.7(2) | H28B | N28 | C29 | H29B | 52(3) |
| H21A | N21 | C21 | C22 | -34(2) | H28B | N28 | C29 | H29C | 173(3) |